MAILLARD REACTION–BASED ROUTES FOR STABLE FOOD EMULSIONS

JILU FENG

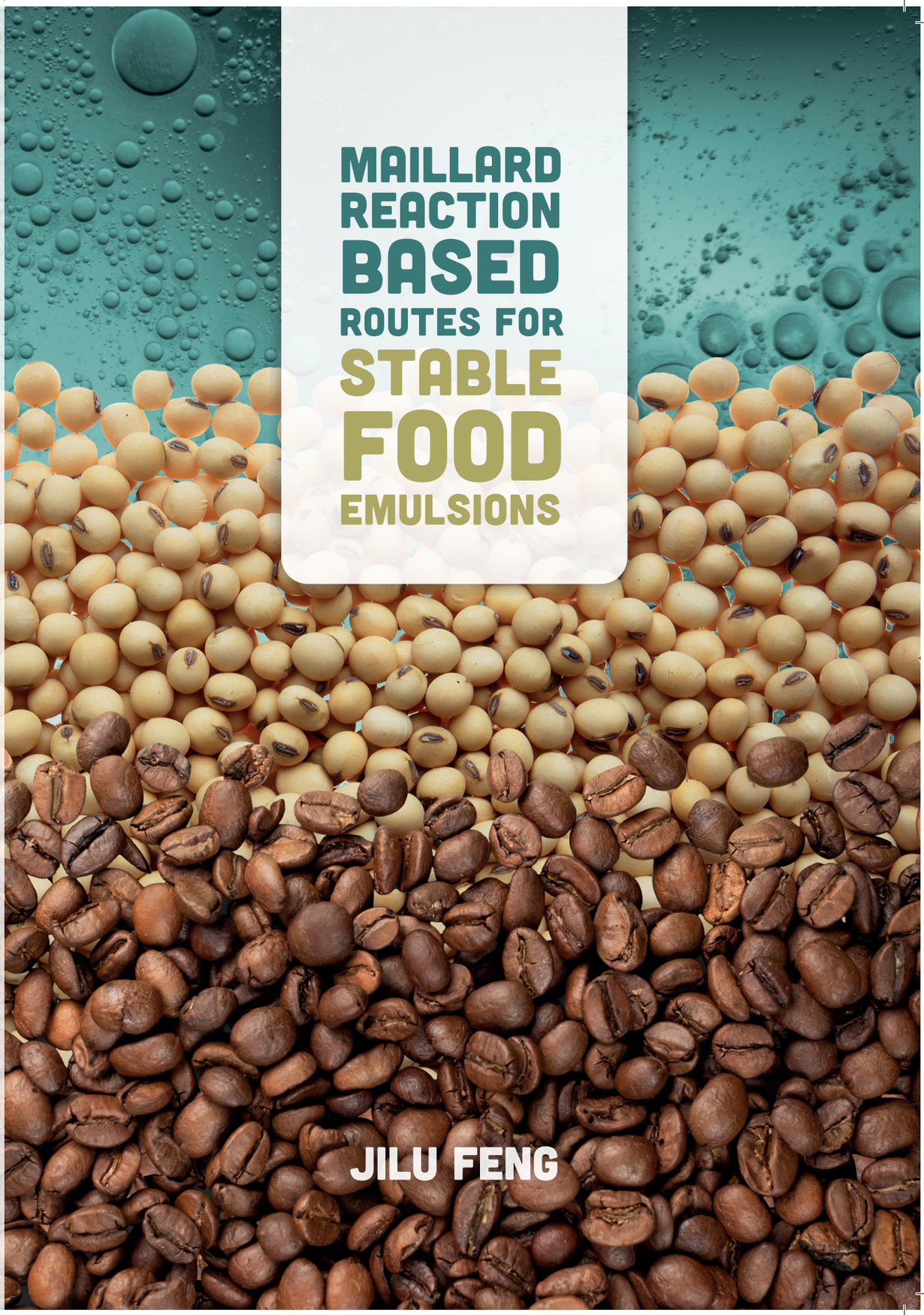

MAILLARD REACTION BASED ROUTES FOR STABLE FOOD EMULSIONS

JILU FENG

Propositions

1. Interfacial antioxidants in multiphase systems mitigate oxidative rancidity.
   (this thesis)

2. The oxidative stability of emulsions is intricately related to their physical stability.
   (this thesis)

3. Dietary change to “natural” foods goes against millennia of human evolution.

4. Acceptance of meat analogues is highest when they resemble what they replace.

5. The balance between homesickness and sick-of-home determines the level of a culture shock.

6. Working from home during the pandemic suits introverted people.

Propositions belonging to the thesis, entitled

Maillard reaction-based routes for stable food emulsions

Jilu Feng
Wageningen, 1 April 2022

Maillard reaction-based routes for stable food emulsions

Jilu Feng

Thesis committee

Promotors

Prof. Dr V. Fogliano
Professor of Food Quality and Design
Wageningen University & Research

Prof. Dr C.G.P.H. Schroën
Personal chair at the Food Process Engineering Group
Wageningen University & Research

Co-promotor

Dr C.C. Berton-Carabin
Associate professor, Food Process Engineering Group
Wageningen University & Research

Other members

Prof. Dr H.A. Schols, Wageningen University & Research
Dr M. Hennebelle, Wageningen University & Research
Dr A. Madadlou, Norwegian University of Science and Technology, Trondheim, Norway
Dr C. van der Ven, Danone Nutricia Research, Utrecht

This research was conducted under the auspices of the Graduate School VLAG (Advanced studies in Food Technology, Agrobiotechnology, Nutrition, and Health Sciences).

Maillard reaction-based routes for stable food emulsions

Jilu Feng

Thesis

submitted in fulfilment of the requirements for the degree of doctor

at Wageningen University

by the authority of the Rector Magnificus,

Prof. Dr A.P.J. Mol,

in the presence of the

Thesis Committee appointed by the Academic Board

to be defended in public

on Friday 1 April 2021

at 1:30 p.m. in the Aula.

Jilu Feng
Maillard reaction-based routes for stable food emulsions
246 pages

Ph.D. thesis, Wageningen University, Wageningen, the Netherlands (2022)
With references, with summaries in English

ISBN: 978-94-6447-063-5
DOI: https://doi.org/10.18174/560278

Contents

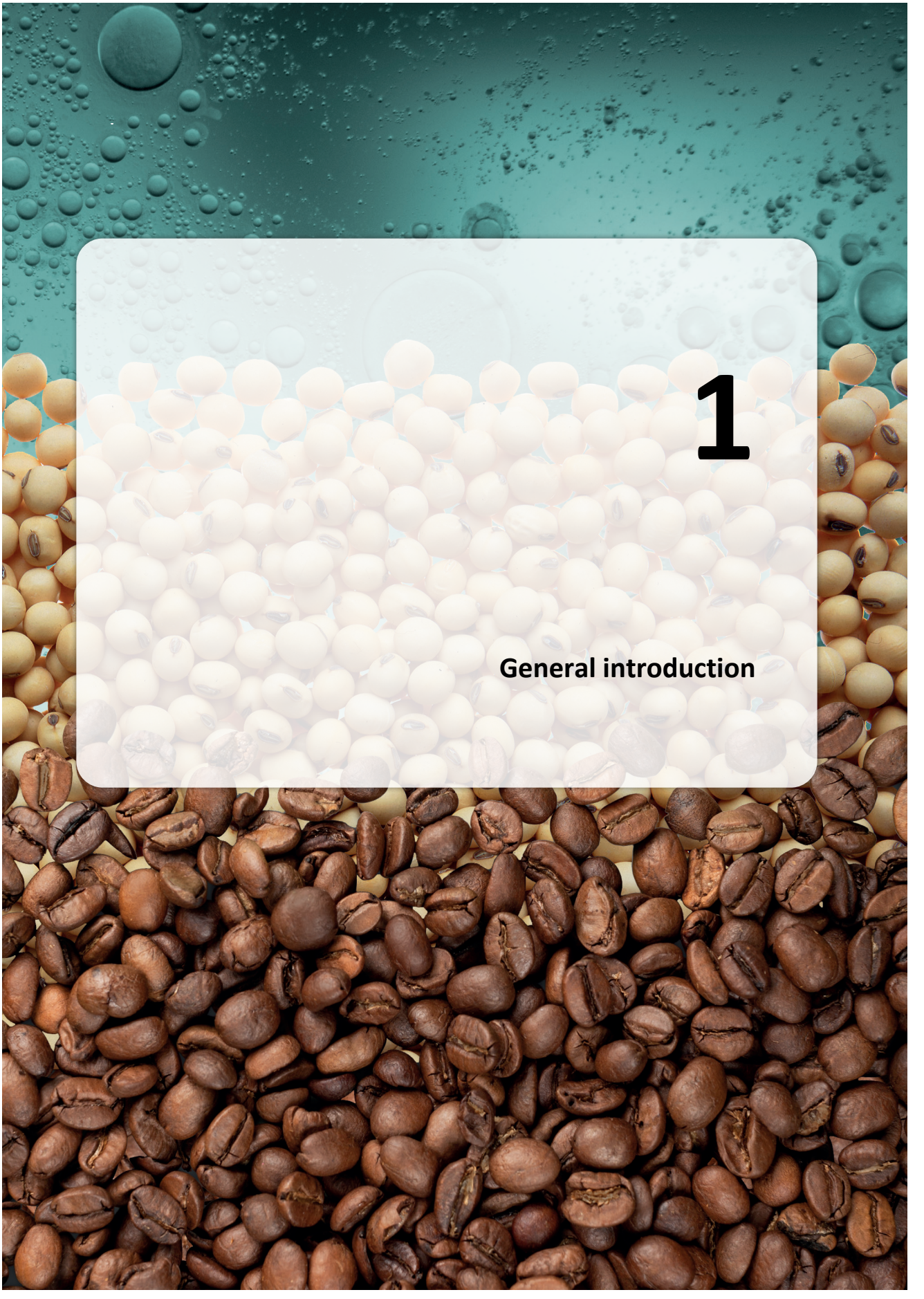

1

General introduction

1.1 Shelf-life of food products

In order to be able to feed a growing world population with sufficient food, the stability of these foods is of great importance, since it determines their shelf-life, and through that also the amount of food that is wasted. Often, the shelf-life is determined by microbial effects, which are mostly controlled through heat treatment to reduce the total bacterial load, and that of pathogens. The next effects that start hitting in are physical and chemical instability, leading to loss of structure and development of off-flavors that make the food unacceptable from a consumer point of view.

A special class of food products that are susceptible to both physical and chemical instabilities are those that contain oil droplets dispersed in a continuous phase, i.e., oil-in-water (O/W) emulsions. There is a large range of natural or processed food products that fall within this class. In such systems, droplets tend to cream or sediment depending on the density ratio used, to flocculate, to coalesce, and in very specific cases they may be prone to Ostwald ripening. Some of those physical destabilization phenomena can be prevented with the use of emulsifiers, of which common examples in foods include surfactants and animal-derived proteins.

Chemical destabilization, in particular oxidative deterioration of lipids, is another major concern in food emulsions, especially when they contain health-promoting polyunsaturated fatty acids. To mitigate lipid oxidation, synthetic antioxidants, such as butylated hydroxytoluene, butylated hydroxyanisole, ethylenediaminetetraacetic acid, and ascorbyl palmitate, are often used. However, in the past decade, a strong tendency toward using food ingredients that are natural and sustainable has emerged. This has led to the use of plant-based ingredients that unfortunately are not as functional as components that were standardly used till 10 years ago, especially when subjected to heat treatment during food processing.

Still, plant proteins are an interesting class of components to consider, both for physical and chemical stability issues, especially because they can be modified using mild methods that can be applied either prior to, or during food production. In this thesis, we focus on the potential of Maillard reaction products (MRPs) from plant proteins and carbohydrates that are either prepared in model systems or stem from coffee. As described later, if these components nest in the oil-water interface they may act as emulsion stabilizers, and if they have antioxidant properties, this may lead to a dual functionality imparting both physical and oxidative stability to emulsions.

1.2 Physical stability of emulsions and emulsion stabilizers

Emulsions are usually formed by homogenization, leading to very fast droplet generation. To facilitate droplet formation, emulsifiers are used that amongst others decrease the interfacial tension. Food emulsifiers include low molecular weight emulsifiers (often referred to as surfactants) and amphiphilic biopolymers (**Figure 1.1**). Surfactants are small molecules consisting of a hydrophilic head and a hydrophobic tail, which can rapidly adsorb to the surface of the newly formed droplets and form a monolayer interface with a high surface load. Amphiphilic biopolymers (e.g., proteins and some polysaccharides) have both polar and nonpolar groups distributed along their backbone. After adsorbing to the interface, they generate steric and electrostatic repulsion between droplets, and form elastic layers by intermolecular interactions, when given sufficient time.

Dairy proteins have been successfully and extensively used as emulsifiers; however, due to their impact on the planet (water usage, greenhouse gas emissions), there is a need to partly or fully replace them e.g., with plant proteins (e.g., soy proteins and pea proteins), or with particles that are known to be able to very effectively stabilize oil-water interfaces, by nesting at the interface when they have appropriate wettability that keeps them in that position, and opposes Brownian diffusion that would carry them away from the surface (Berton-Carabin & Schroën, 2015; McClements, 2015).

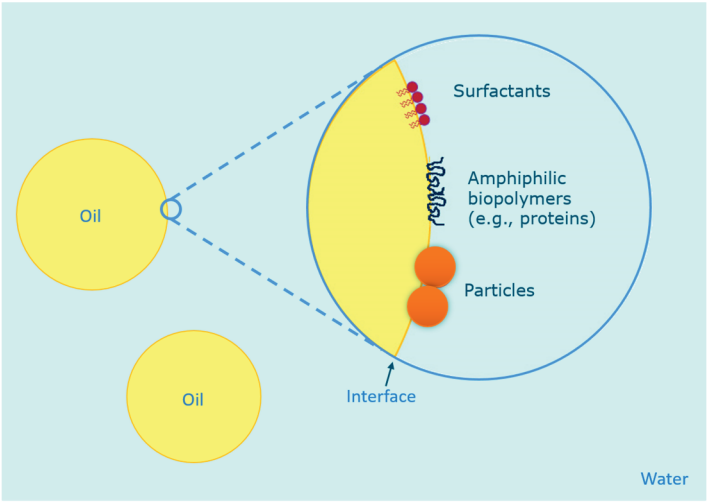

Figure 1.1. Schematic representation of adsorbed surfactants, amphiphilic biopolymers, and particles at the oil-water interface (not to scale).

All emulsions are prone to physically destabilize when given sufficient time (**Figure 1.2**). In brief, emulsions tend to separate gravitationally (creaming or sedimentation) because of the density differences between the oil and water phases. The viscosity of the continuous phase can be modified by the use of thickening agents, thus slowing down droplet creaming /sedimentation or even forming a gel (gelling agent) that effectively puts a hold on creaming/sedimentation. Flocculation occurs when attractive forces exceed repulsive forces between droplets. In contrast with flocculation where droplets do not merge, coalescence occurs when the interfacial films between two droplets break due to insufficient surface coverage. The speed of surface coverage is determined by the mass transfer conditions in the device, which are co-determined by amongst other the shear rate and viscosity of the continuous phase. In general, surface active components reduce or even prevent coalescence by steric and electrostatic effects. A higher continuous phase viscosity has opposite effects; it reduces mass transfer to the interface, and at the same time reduces film thinning and thus the chance of film rupture leading to coalescence. To be complete, Ostwald ripening usually does not occur in food O/W emulsions because the solubility of triacylglycerols in water is negligible (McClements, 2005).

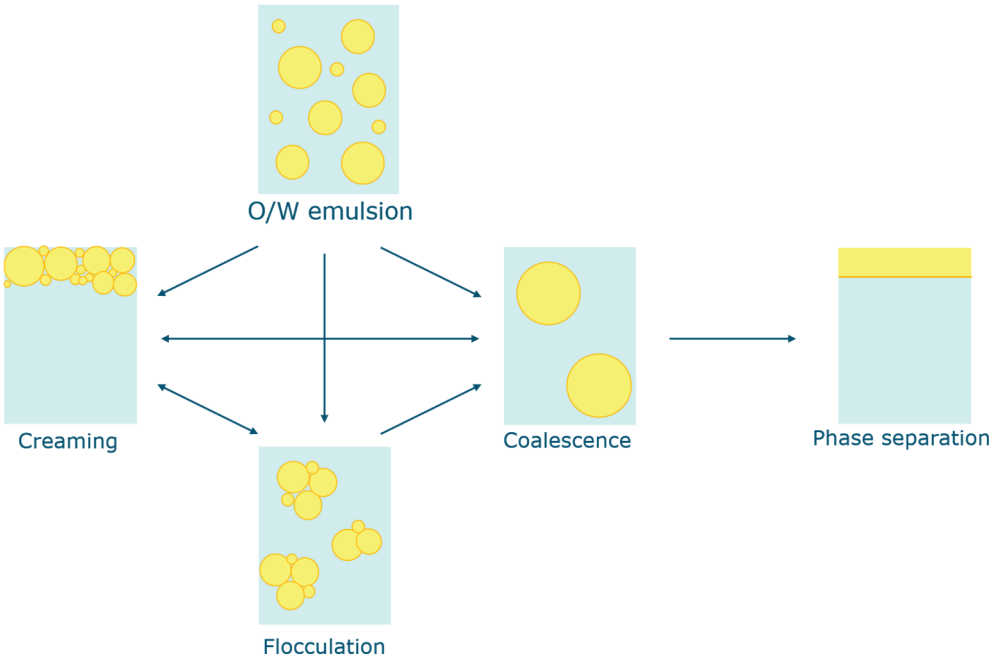

Figure 1.2. Schematic representation of different physical destabilization phenomena in oil-in-water emulsions.

1.3 Oxidative stability and the role of emulsifiers in lipid oxidation

Lipid oxidation is a cascaded radical reaction consisting of initiation, propagation, and termination (see **Figure 2.2** in the next chapter), which causes quality deterioration in food emulsions. It is generally described as a free radical chain reaction that involves unsaturated lipids (or trace hydroperoxides), oxygen, and hydrophilic pro-oxidants (e.g., transition metals, free radicals) in O/W emulsions. It is generally accepted that lipid oxidation is initiated at the oil-water interface (Berton-Carabin et al., 2014; Laguerre et al., 2020). For this reason, food scientists have been interested in using the interface to improve the oxidative stability of emulsions, and in doing so, also opportunities to create physical stability may arise.

An effective strategy is the use of antioxidant emulsifiers that adsorb at the oil-water interface (McClements & Decker, 2018). Proteins (such as whey proteins, soy proteins, and egg proteins) that possess antioxidant activities (e.g., free radicals scavenging and transition metals chelating activities) are interesting components, since they comply with clean-label requirements (Gu et al., 2017; Shao & Tang, 2014; Villiere et al., 2005). Furthermore, recently, a number of Pickering particles with antioxidant activity have been successfully used; examples include milled red rice particles, matcha tea powder, spinach leaf powder, kafirin nanoparticles, and colloidal lipid particles (Lu & Huang, 2020; Schröder et al., 2020, 2021; Xiao et al., 2015).

In this thesis, we make use of another alternative: chemically linked compounds that can either be made on purpose, or inherently present in certain foods. For instance, glycated proteins formed by conjugating proteins to carbohydrates via the Maillard reaction can be used to stabilize emulsions, and do this better than proteins alone (Karbasi & Madadlou, 2018; Nooshkam et al., 2019). Examples of such Maillard reaction products to act as dual-functional ingredients in emulsions are reviewed in **Chapter 2**. Later in the thesis, we use these components not only as interface stabilizers, but also add them to the continuous phase to thus influence either chemical or physical emulsion stability, and in some cases even both.

Unadsorbed emulsifiers in the continuous phase play an important role in lipid oxidation (Berton-Carabin et al., 2014). It has been suggested that unadsorbed surfactants form micelles or small droplets containing small amounts of lipids or lipid hydroperoxides, thus protecting them against (further) oxidation (Donnelly et al., 1998; Nuchi et al., 2002; Ponginebbi et al., 1999). Furthermore, unadsorbed proteins have been shown to protect lipids from oxidation through other mechanisms including metal chelation, scavenging free radicals, and binding secondary lipid oxidation products (Berton-Carabin et al., 2014; Elias et al., 2005; Faraji et al., 2004; Gumus et al., 2017). Alternatively, it has been suggested that the oxidation may be increased by micellar transport between droplets (Laguerre et al., 2017).

1.4 The Maillard reaction

The Maillard reaction (MR) is an important reaction responsible for color and flavor formation in a variety of foods. It is a cascade of successive non-enzymatic chemical reactions between the free amino groups from amino acids, peptides, or proteins and the carbonyl groups from reducing sugars. The MR comprises three stages: initial, intermediary, and final, and the schematic representation of the Maillard reaction can be found in **Figure 2.1** (in the next chapter).

Among all the Maillard reaction products (MRPs), initial stage MRPs (glycated proteins) and final stage MRPs (melanoidins) have attracted great interest as functional food ingredients because of their positive effects on the functionality (e.g., emulsifying, foaming, gelation, and encapsulating properties) and/or biological properties (e.g., antioxidant activity, antimicrobial activity) when applied in of food products (de Oliveira et al., 2016; Lee et al., 2017; Nooshkam et al., 2020; Nooshkam & Varidi, 2020; Oliver et al., 2006; Troise & Fogliano, 2013).

1.4.1 Glycated soy proteins

The most extensively used plant proteins are currently soy proteins that have interesting functional properties such as emulsifying, foaming, and gelling abilities. Modification of proteins via the early stage of the MR has been shown to improve these properties (Deng, 2021; Zhang et al., 2019); see **Table S1** for an overview of publications related to improved emulsification properties and/or physical stability of emulsions. It has been suggested that the Maillard reaction could unfold the globular structure of soy proteins and expose formerly buried hydrophobic groups, which increases their affinity towards the oil phase in emulsions. Besides, the covalently linked polysaccharides could form a thick layer at the interface which improves the physical stability of emulsions.

1.4.2 Coffee melanoidins

Compared to the amount of work on MRPs prepared in model systems (i.e., using carbohydrates and proteins as starting materials), relatively little work has focused on the emulsifying properties of MRPs inherently present in certain foods (such as coffee, beer, and bakery products). Coffee is one of the most widely consumed beverages, and during roasting, the Maillard reaction takes place to a large extent. The high temperature and low water activity favor the formation of melanoidins, which account for ~29% of the dry matter in coffee brew (Ludwig, Clifford, et al., 2014).

The chemical structure of melanoidins is still not completely clear, but model studies have shed some light on this matter (Ludwig, Mena, et al., 2014; Moreira et al., 2012). It has been suggested that melanoidins are polymers consisting of repeating units of low molecular weight MRPs (e.g., furans and pyrroles) (Hayase et al., 2006; Tressl, Wondark, et al., 1998; Tressl, Wondrak, et al., 1998). Alternatively, it has been mentioned that melanoidins are formed by cross-linking of LMW colored MRPs to proteins through the reactive side chains of amino acids (e.g., lysine, arginine, and cysteine) (Hofmann, 1998a, 1998b, 1998c). Furthermore, it has been mentioned that the melanoidin skeleton mainly consists of sugar degradation products polymerized via aldol-type condensation (Cämmerer & Kroh, 1995; Cämmerer et al., 2002; Kroh et al., 2008).

Unlike model systems where reactions take place under controlled conditions, the situation during coffee bean roasting is much more complex, and the structure and composition of coffee melanoidins are therefore different from those of melanoidins prepared in model systems (Nunes & Coimbra, 2010). In addition to the small sugars and proteins, polysaccharides and phenolic compounds are also involved, accounting for ~50 and 10 wt% of coffee melanoidins, respectively (Moreira et al., 2017). Studies carried out in the past decades enable us to partially reveal some of their structural features **(Figure 1.3)**.

During coffee roasting, galactomannans and type II arabinogalactans (that are normally covalently linked to proteins: arabinogalactan–proteins (AGPs)), undergo depolymerization and debranching; galactomannans and arabinose side chains of arabinogalactans could

undergo transglycosylation, the reducing end of galactomannans could be modified by several reactions (e.g., isomerization, oxidation, and MR), and AGPs could lose their protein moiety. These reaction products, together with galactomannans and AGPs, are able to combine into melanoidins via covalent linkage. In addition, proteins could undergo denaturation, depolymerization during roasting, of which the products could then be integrated into the polymeric structure of melanoidins. Furthermore, the coffee roasting process may promote oxidation, degradation, decarboxylation, isomerization, and polymerization of the phenolic compounds (predominantly chlorogenic acids (CGAs)), which could then be incorporated into melanoidins through covalent or non-covalent linkages. The most likely linkage site was suggested to be the arabinose from the arabinogalactan side chains or protein fragments (Bekedam, 2008; Bekedam et al., 2006; Coelho et al., 2014; Moreira et al., 2013, 2014, 2015, 2017; Nunes et al., 2012; Shaheen et al., 2021; Wang et al., 2021).

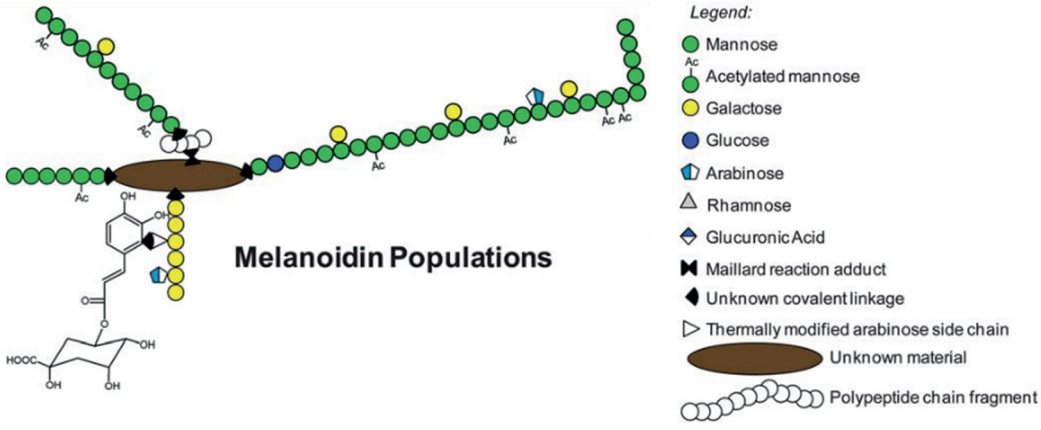

Figure 1.3. Example of the structure of coffee melanoidins (Moreira et al., 2012).

Given the composition of coffee melanoidins, it can be assumed that some of the compounds might be able to physically stabilize emulsions, due to their amphiphilic nature (e.g., furan and pyrrole-like hydrophobic fractions and negatively-charged hydrophilic fractions (Bekedam et al., 2007; Gniechwitz et al., 2008)), or due to their 'particle-like' behavior. Besides, AGPs are believed to predominantly determine the emulsifying

properties of the widely used emulsifier gum Arabic (Dickinson, 2003); galactomannans as such (e.g., from locust bean gum, fenugreek gum, guar gum, and tara gum) exhibit some surface activity and emulsifying capacity (Garti & Reichman, 1994; Wu et al., 2009). On the other hand, it has been reported that melanoidins have strong antioxidant potential, as reviewed in **Chapter 2**. Briefly, this includes breaking the radical chain by hydrogen donation, chelating metal to form inactive complexes, and decomposing hydroperoxides into non-radical products (Delgado-Andrade et al., 2005; Echavarría et al., 2012; Mesías & Delgado-Andrade, 2017). Even though the antioxidant activity of coffee melanoidins has been studied, their ability to act as antioxidants or stabilizers in emulsions has not been investigated yet, which is why we elaborate on this in **Chapters 5 and 6**.

1.5 Research aim and outline of the thesis

In this thesis, we investigate the potential of MRPs, either prepared in model systems or inherently present in foods, to act as dual-function ingredients (i.e., physical stabilizers and antioxidants) in food emulsions. A graphical representation of the outline of this thesis is given in **Figure 1.4**. **Chapter 2** gives a literature review on the use of MRPs as interfacial stabilizers and/or antioxidants in O/W emulsions. In **Chapter 3**, we characterize the chemical and structural features of various glycated soy proteins, leading to a comprehensive understanding of the functionality of Maillard reaction products. In **Chapter 4**, we assess the ability of early-stage MRPs (glycated soy proteins with dextran) added to the continuous phase of pre-formed O/W emulsions to prevent lipid oxidation. In **Chapter 5**, we explore the potential of final stage MRPs (coffee melanoidins) as ingredients to physically stabilize emulsions. In **Chapter 6**, we further investigate the efficiency of these components to physically and oxidative stabilize O/W emulsions when present at the interface or in the continuous phase. Finally, we summarize the thesis and put our findings in a future perspective in (**Chapter 7)**.

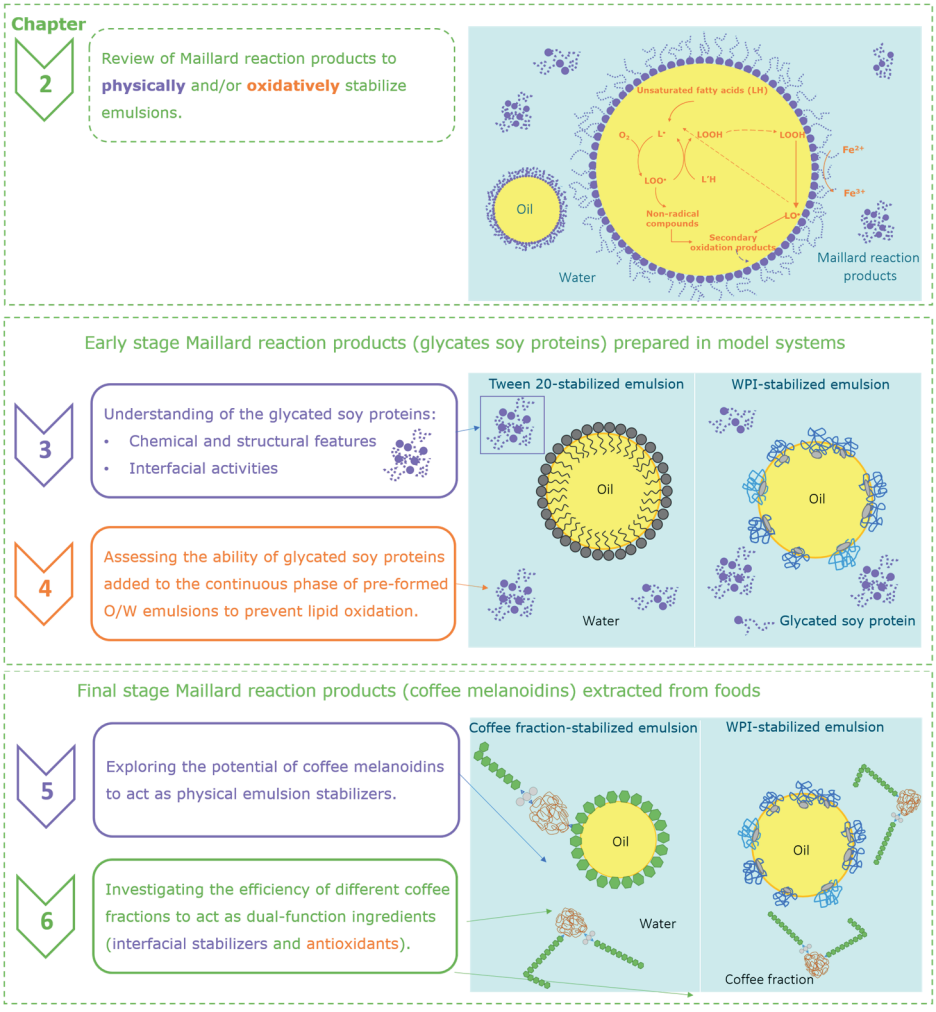

Figure 1.4. Graphical outline of the chapters in this thesis (not to scale).

Supplementary materials

Table S1. Lists of studies using glycated soy proteins to improve emulsifying properties.

Emulsifier	Glycation conditions	Main Conclusions	References
Soy protein isolate (SPI)-acacia gum (AG)	Wet heating (80 °C, 0-48 h, pH 7.5)	Emulsions prepared with SPI-AG conjugates showed smaller droplet size and higher creaming stability than those prepared with SPI alone.	Mu, Zhao, Zhao, Cui, & Liu, 2011
SPI-dextran, or soy protein hydrolysates -dextran	Wet heating (95 °C, 1.5 h, pH 7.0)	Limited hydrolysis combined with protein glycation improved freeze-thaw stability of emulsions.	Yu et al., 2018
SPI-dextran	Dry heating (40 °C, 0-12 d; 60 °C, 0-8 d; 80 °C, 0-48 h; 79% relative humidity (RH), pH 7 and 8.5)	1. SPI-dextran conjugates exhibited higher emulsifying activity index (EAI) than SPI. 2. Emulsions prepared with SPI-dextran had smaller droplet size than those prepared with SPI.	Boostani, Aminlari, Moosavi-nasab, Niakosari, & Mesbahi, 2017
SPI-dextran	Ultrasound or microwave	SPI-dextran conjugates improved the freeze-thaw stability of SPI emulsions.	Zhang et al., 2017
SPI-dextran	Dry heating (60 °C, 1 week, 79% RH, pH 7)	Droplet aggregation upon heating was prevented due to SPI-dextran adsorption, which increased the droplet surface hydrophilicity and steric hindrance.	Diftis & Kiosseoglou, 2006
SPI-dextran	Dry heating (60 °C, 1 and 3 weeks, 79% RH, pH 7)	Adsorbed SPI-dextran created repulsive steric force that slowed cream separation.	Diftis, Biliaderis, & Kiosseoglou, 2005
SPI-AG	Dry heating (60 °C, 3, 6, 9d, 79% RH, pH 7)	1. SPI-AG conjugates had higher EAI and emulsifying stability index (ESI) than SPI. 2. Emulsions prepared with SPI-AG conjugates had smaller droplet size and higher apparent viscosity than those prepared with SPI/AG mixture.	Li et al., 2015

SPI-gum karaya	Dry heating (60 °C, 3 d, 75% RH, pH 7)	1. Emulsions containing SPI-gum karaya conjugates had higher viscosity than those containing gum karaya. 2. Emulsion with the conjugates had smaller droplet size and lower polydispersity than those with gum karaya.	Shekarforoush, Mirhosseini, & Islam, 2016
SPI-maltodextrin (MD)	Dry heating (90 °C, 2 h; 115 °C, 2 h; 140 °C, 2 h; 79% RH, pH 6.8)	Emulsions stabilized with SPI-MD conjugates (prepared at 140 °C) were stable against pH, ionic strength, and thermal treatment.	Zhang, Wu, Lan, & Yang, 2013
SPI-soy hull hemi-celluloses (SHH)	Dry heating (60 °C, 7 d)	The average droplet size of SPI-SHH conjugate-stabilized emulsions was smaller than SPI- and SHH-stabilized emulsions when prepared freshly and during the whole storage period at pH 7.0 and 60℃.	Wang, Wu, & Liu, 2017
SPI-soy soluble poly-saccharide	Dry heating (55, 60 or 65 °C, 36–96 h, 75% RH, pH 7)	The droplet size of emulsions stabilized with SPI-soy soluble polysaccharide conjugates remained similar for up to 70 days during storage at 25℃, upon thermal treatment at 95℃ for 30 min, or under simulated gastric conditions for 2 h.	Yang, Cui, Gong, Miller, et al., 2015

2

Maillard reaction products as functional components in oil-in-water emulsions: A review highlighting interfacial and antioxidant properties

This chapter has been submitted as Feng, J., Berton-Carabin, C. C., Fogliano, V., & Schroën, K. (2022). Maillard reaction products as functional components in oil-in-water emulsions: A review highlighting interfacial and antioxidant properties. Trends in Food Science & Technology, 121, 129–141. https://doi.org/https://doi.org/10.1016/j.tifs.2022.02.008

Abstract

Background: Lipid oxidation gives rise to the formation of off-flavors and is therefore a major concern for food quality. When present in food emulsions (e.g., milk, yogurts, salad dressings), labile polyunsaturated lipids usually oxidize faster than in bulk oil, which can be mitigated by antioxidants. However, the use of synthetic antioxidants is not desired from a "clean-label" point of view. Therefore, we focus on the potential of Maillard reaction products (MRPs), which are biobased molecules that are formed during heating and that may possess excellent antioxidant and emulsifying properties.

Scope and approach: The *in situ* antioxidant activity of MRPs in emulsion systems is reviewed; effects occurring in the continuous phase and at the interface of oil-in-water (O/W) emulsions are distinguished. A dedicated section of the review focuses on the MRPs that are intrinsically present in various foods.

Key findings and conclusions: MRPs may partition between the continuous phase and the oil-water interface in emulsions, which allows them to counteract lipid oxidation by various physicochemical mechanisms, including metal chelation and free radical scavenging. MRPs intrinsically present in foods are promising components to achieve food products with high oxidative stability, while complying with consumer points of view.

2.1 Introduction

Oxidative deterioration of lipids is a major concern since it gives rise to undesirable changes in flavor, taste, and appearance of foods, which shorten the shelf life of food products (Chaiyasit et al., 2007; Sun et al., 2011). In addition, it generates compounds with questionable metabolic effect (e.g., hydroperoxides and reactive aldehydes) (Schaich, 2020b), which might damage the nutritional quality of foods, thus making the application of healthy polyunsaturated (PUFA) lipids in foods a challenge (Genot et al., 2013; Jacobsen et al., 2008). Probing the mechanisms of lipid oxidation and antioxidation in multiphase foods is especially relevant because lipids commonly exist as dispersions in foods, such as milk, yogurts, infant formula, dips, salad dressing and so on (Decker et al., 2017). These systems consist of lipids dispersed as small droplets in an aqueous phase, called oil-in-water (O/W) emulsions. In such emulsions, lipids normally oxidize faster than in bulk oil due to the large oil-water interfacial area, as well as the emulsification process which may promote oxidation (Genot et al., 2013; Jacobsen et al., 2013).

The use of antioxidants is an effective strategy to counteract lipid oxidation in emulsions. Addition of synthetic antioxidants (such as butylated hydroxytoluene (BHT) and tertiary butylhydroquinone (TBHQ)) to foods is a common practice owing to their high efficiency and low cost. However, the safety of these antioxidants becomes more and more part of public discussions. Some synthetic antioxidants in high dose may exert potential harmful effects (e.g., tumor-promotion) as shown in animal models, and thus low acceptable daily intake (ADI) values have been established by European Food Safety Authority (EFSA) (e.g., 0.25 and 0.7 mg/kg bw/day for BHT and TBHQ, respectively) (EFSA, 2004, 2012). Due to the lack of complete and accurate information on these synthetic preservatives, consumers have been raising doubts about their consumption (Lorenzo et al., 2017). There is a clear drive toward more natural and label-friendly alternatives.

A category of components that may comply with sustainability and naturalness trends and can be applied in O/W emulsions are Maillard reaction products (MRPs) that are formed

during heating. They have been reported to hold high potential for antioxidant activity and emulsifying properties (de Oliveira et al., 2016; Manzocco et al., 2000; Nooshkam et al., 2019). From an optimal activity perspective, surface-active antioxidants are particularly relevant, since they would accumulate at the oil-water interface, the location at which lipid oxidation initiates (McClements & Decker, 2000; McClements & Decker, 2018). Therefore, in the present review, we report on the potential of these compounds for developing food emulsions with high oxidative and physical stability.

MRPs are formed by the glycation of amino-bearing compounds with reducing sugars. This may alter the protein structure and thus lead to the exposure of hydrophobic groups that have affinity for the oil-water interface, whereas hydrophilic sugar moieties extend into the continuous water phase and act as a physical barrier ideally preventing droplet aggregation (Liu et al., 2011; O'Mahony et al., 2018; Zhang et al., 2019). Furthermore, MRPs are capable of binding metal ions and scavenging free radicals and can thereby improve the oxidative stability of emulsions (Nooshkam et al., 2019). In emulsions, if MRPs are used as emulsifiers, they would most likely partition between the interface and the continuous phase, which are both environments where the presence and activity of antioxidant molecules are of high importance (Berton-Carabin et al., 2014; Faraji et al., 2004; Genot et al., 2013). All these features make MRPs promising components for use in food emulsions, although it is good to point out that in literature the various effects as they would occur in different physical locations in food products have not been segmented (mostly an overall effect is reported).

MRPs are inherently present in certain foods (such as coffee, beer, and bakery products) but can also be specifically targeted, using proteins and polysaccharides as starting materials. Great efforts have been made to study the antioxidant activity of these components that is after isolation using specific assays. For more information, we refer through to the following reviews (Hidalgo & Zamora, 2017; Lee & Shibamoto, 2002; Manzocco et al., 2000; Namiki, 1988; Nooshkam et al., 2019). Yet, the antioxidant activity (e.g., radical scavenging and metal chelating activity) of MRPs when measured using indirect methods in the absence of an oxidizable substrate does not necessarily reflect the

mechanisms involved when it pertains to lipid oxidation in food systems (Echavarría et al., 2012), as is the case for many antioxidants (Laguerre et al., 2007). It is therefore extremely important to investigate antioxidant effects of MRPs in systems that do justice to the complexity of the food matrix, which has only very recently become part of the research in this field.

In the present paper, we review the interfacial properties as well as the mechanisms of antioxidant activity of MRPs in O/W emulsions. We start by defining the playing field (emulsions, lipid oxidation, and MRPs). Next, we focus on the properties of the MRPs, both from a physical (emulsifying properties) and chemical (antioxidant activity) point of view. In the next section, we connect this to effects reported for food emulsions stabilized by MRPs. We wrap up with a brief outlook on the future application of MRPs in foods to achieve products that are intrinsically more stable both from physical and oxidative points of view.

2.2 Emulsions, oxidation, and MR products

2.2.1 Food emulsions

Emulsions are multiphase systems that consist of at least one polar phase (usually water) and one nonpolar phase (usually oil), with one phase being dispersed as droplets in the other phase. The emulsions we consider in this review are oil-in-water (O/W) emulsions, thus containing small oil droplets dispersed in a water phase. Emulsions are thermodynamically unstable systems that tend to minimize their interfacial area, and therewith, their free energy (ΔG, J) (Eq. 2.1).

$$\Delta G = \gamma \, \Delta A \tag{2.1}$$

where γ (N/m) is the interfacial tension between the oil and water, and ΔA (m^2) is the difference in interfacial area. To avoid phase separation, surface-active compounds (generally referred to as emulsifiers) are used to lower the interfacial tension and provide electrostatic and/or steric repulsion between droplets. Yet, all emulsions are prone to

gravitational separation, flocculation, and coalescence depending on the time scale of observation (McClements, 2005).

2.2.2 *Lipid oxidation in emulsions*

Lipid oxidation is generally described as a complex sequence of chemical reactions starting from unsaturated fatty acids and oxygen-active species. It takes place through a free radical chain mechanism for which we refer through to numerous comprehensive reviews (see e.g., Frankel, 1980; Schaich, 2013; Schaich, 2020); here, we will limit ourselves to a general description of the basic mechanisms. Lipid autoxidation can be divided into three stages: initiation, propagation, and termination (Farmer et al., 1942). In the initiation stage, in the presence of an initiator, unsaturated fatty acids (LH) lose a hydrogen atom at an allylic methylene group whereby alkyl radicals ($L^{\bullet}$) are formed. These highly reactive alkyl radicals ($L^{\bullet}$) can quickly react with triplet oxygen to form lipid peroxyl radicals ($LOO^{\bullet}$). Since these radicals have higher energy than alkyl radicals ($L^{\bullet}$), they can abstract hydrogen atoms from another unsaturated fatty acid (LH) to produce hydroperoxides (LOOH) and new alkyl radicals (see also **Figure 2.2**). Hydroperoxides are primary oxidation products that can be quantified using various methods (Gheysen et al., 2019; Merkx et al., 2018; Uluata et al., 2021). Hydroperoxides can decompose via different pathways (e.g., cyclization, rearrangement, hydrogen abstraction, scission and condensation) to form secondary oxidation products (such as aldehydes, alcohols, hydrocarbons, ketones and volatile organic acids). These products may be quantified by different analyses, such as the ρ-anisidine value (pAV, quantifying total aldehydes), thiobarbituric acid-reactive substances (TBARS, quantifying various compounds including malondialdehyde) (Viau et al., 2016), and volatile compounds (e.g., propanal and hexanal) (Jacobsen et al., 2021). In the termination stage, two radicals react with each other to form stable non-radical compounds, which will terminate the radical chain reaction. In addition to this classic scheme, “hydroperoxide initiation” has been proposed recently: decomposition of (pre-existing) traces of hydroperoxides at the oil-water interface has been hypothesized as a crucial reaction for the initiation of lipid radicals (Laguerre et al., 2020).

O/W emulsions comprise three main regions: the interior of the oil droplets, the continuous water phase, and the interface between these two phases. Molecules will partition between these three regions based on polarity and surface activity. Hydrophobic substances (e.g., tocopherols, oil-soluble pigments) are predominantly located in the oil phase, hydrophilic substances (e.g., salts and metal ions) in the continuous water phase, and amphiphilic compounds (e.g., emulsifiers) at the interface (McClements & Decker, 2000). The location of these substances will largely impact lipid oxidation, (systematically reviewed by Berton-Carabin et al., 2014), since lipid oxidation initiation in emulsions is considered to take place at the oil-water interface where pro-oxidants (e.g. transition metals and oxygen) and unsaturated fatty acids (or trace hydroperoxides) come into contact (Berton-Carabin et al., 2014; Laguerre et al., 2020). The large interfacial area could thus promote the initiation of lipid oxidation, although it is good to keep in mind that the actual course of the reaction is a result of reaction kinetics, in combination with diffusion, and advection effects taking place (McClements & Decker, 2000). For instance, hydroperoxides may diffuse to the interface, which can favor their contact with pro-oxidants thereby accelerating lipid oxidation.

2.2.3 *Maillard reaction*

The Maillard reaction was first detected by Louis Camille Maillard in 1912 (Maillard, 1912) and comprises of a complex series of chemical reactions between carbonyl groups (in reducing sugars) and free amino groups in proteins, peptides, or amino acids that lead to non-enzymatic browning. Only in 1953, the first consolidated scheme of the MR was proposed (Hodge, 1953), which comprises of three stages termed: initial, intermediary, and final (**Figure 2.1**), although in practice these phases can occur simultaneously and are interrelated (Silván et al., 2011).

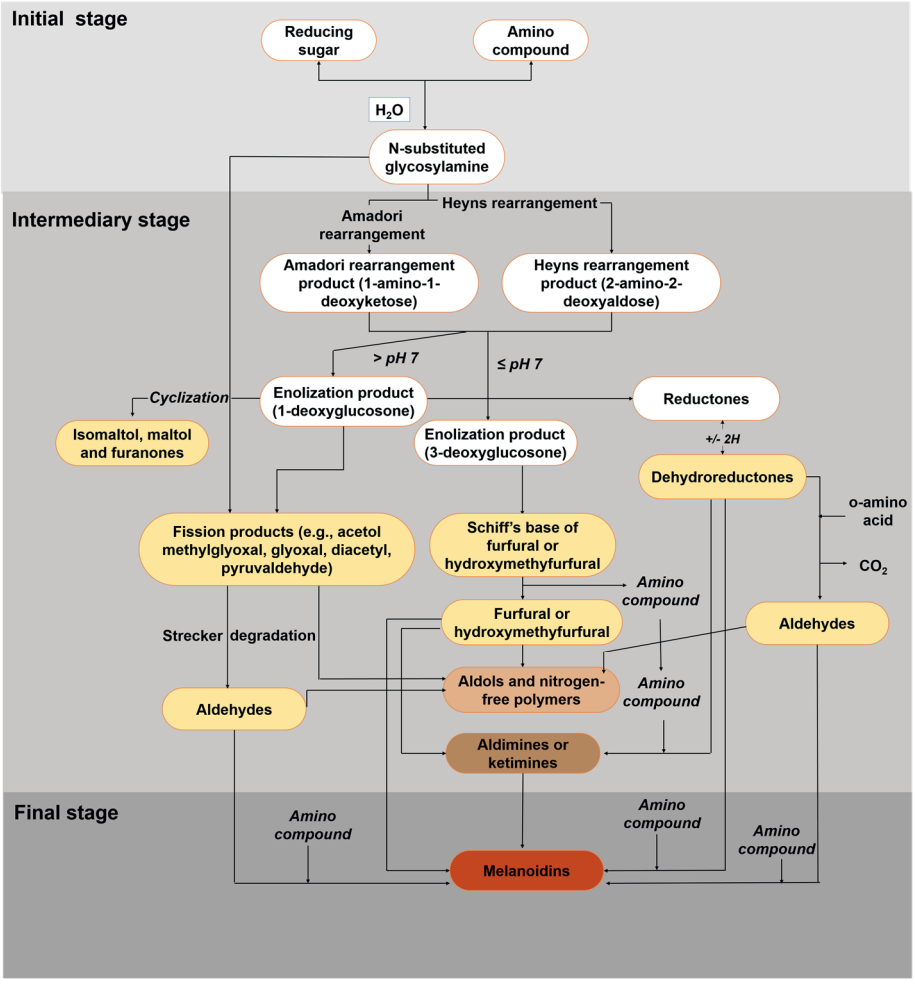

Figure 2.1. Schematic representation of the Maillard 'reaction'. Adapted with permission from Hodge (1953). Copyright 2011 American Chemical Society.

In the initial stage, condensation reactions take place between carbonyl groups and free amino groups (mainly ε-amino groups) to form unstable Schiff base compounds (O'Brien & Morrissey, 1989) that undergo cyclization and in turn form reversible *N*-substituted glycosylamines (O'Brien & Morrissey, 1989). *N*-glycosylamines from aldose generate Amadori compounds (1-amino-1-deoxyketoses), whereas those from ketose generate Heyns compounds (2-amino-2-deoxyaldoses) (Davidek & Davidek, 2004). Both components

do not lead to brown color, but the nutritional value might be reduced due to the decrease in amino acid availability (de Oliveira et al., 2016).

The intermediary stage starts with the decomposition of Amadori and Heyns compounds via different routes (Hellwig & Henle, 2010). At acidic pH, they undergo 1,2-enolization to generate furfural or hydroxymethylfurfural (HMF), whereas at alkaline pH, they undergo 2,3-enolization to generate reductones (e.g., 4-hydroxy-5-methyl-2,3-dihydrofuran-3-one (HMF_{one})) and fission products (e.g., acetol, glyoxal, and methylglyoxal). The dicarbonyl compounds formed can react with amino acids leading to aldehydes and aminoketones via Strecker degradation (Yaylayan, 2003), or react with arginyl and lysyl residues to yield advanced glycation end-products (AGEs), such as N^{ε}-(carboxy-methyl)lysine (CML) and N^{ε}-(carboxyethyl)lysine (CEL) (Han et al., 2013). In this stage, a yellowish color, flavor formation, and increased reducing power are observed (Nooshkam et al., 2019).

In the final stage, the reactive compounds from the intermediary stage may undergo different reactions (including retro-aldolization, isomerization, rearrangement, and condensation), resulting in the formation of brown-colored, nitrogen-containing and high-molecular-weight polymerized products, called melanoidins (Martins et al., 2001). The chemical structure and formation mechanism of these compounds are still not fully understood. The final phase of MR is mainly responsible for color and flavor formation in most thermally processed foods.

Based on the stage of the Maillard reaction, MRPs with different features may be created, although it is intrinsically complex to control the reaction. A few studies have tried to limit the Maillard reaction to the initial stage to preserve emulsification properties of proteins and prevent the formation of advanced glycosylation end-products (dAGEs) of which the intake has controversial physiological consequences (Delgado-Andrade & Fogliano, 2018; Oliver et al., 2006; Sedaghat Doost et al., 2019). Other researchers have focused on e.g., antioxidant, antimicrobial, and anti-inflammatory activity, of melanoidins using them as functional food ingredients (Martinez-Gomez et al., 2020; Mesías & Delgado-Andrade, 2017).

2.2.4 *Emulsifying properties of Maillard reaction products*

The emulsifying properties of some MRPs were first demonstrated by Kato and co-workers (Kato et al., 1988, 1990). It is generally accepted that both the protein and carbohydrate parts of the MRPs contribute to the reported emulsifying properties (Liu et al., 2011; O'Mahony et al., 2018; Zhang et al., 2019). The Maillard reaction results in (partial) protein unfolding, and exposure of hydrophobic groups which increases their affinity for the oil phase. Besides, the hydrophilic carbohydrate moieties extend into the continuous phase, which can prevent droplet aggregation through steric hindrance and/or electrostatic repulsion. Recently, Li and co-workers found that glycation could increase the flexibility of soy protein isolate (i.e., conformational rearrangement of the tertiary protein structure upon external environment changes), thereby facilitating adsorption at the oil-water interface (Li, Cui, et al., 2019; Li, Wang, et al., 2019). Publications related to the physical stability of emulsions with MRPs are summarized in **Table S2.1**.

Emulsions stabilized with MRPs have been reported to resist various environmental stresses better than those stabilized with proteins alone. For example, Drapala, Auty, Mulvihill, & Mahony (2016) found that whey protein hydrolysate-maltodextrin MRPs stabilized infant formula emulsions exhibited excellent thermal stability (resistant to bridging flocculation due to the increased steric hindrance of maltodextrin). Emulsions stabilized with MRPs made from soy whey protein isolate and fenugreek gum did not show a significant change in average droplet size after 21 days of storage at 25 °C in the presence of 0.5 M NaCl, or at pH close to the isoelectric point (~pH 4.0) (Kasran, Cui, & Goff, 2013; Kasran et al., 2013). In addition, soy protein isolate-soy soluble polysaccharide MRPs were able to protect citral in emulsions during exposure to simulated gastric and intestinal fluids (Yang et al., 2015).

The emulsifying properties of MRPs are affected by several parameters, such as reaction time, structure and molecular weight of carbohydrates and proteins, protein:carbohydrate ratio, overall net charge, etc. Miralles, Martínez-Rodríguez, Santiago, van de Lagemaat, & Heras (2007) found that the emulsifying capacity of β-lactoglobulin-chitosan MRPs (formed at 40 °C and 79% relative humidity) increased with reaction time up to 2 days, after which

the capacity decreased. Likewise, the freeze-thaw stability of emulsions stabilized with soy protein hydrolysate-dextran MRPs increased and then decreased for MRPs prepared at increasing incubation time during their production. This may indicate that early stage MRPs facilitate emulsification, and emulsion stability, and later stage MRPs lose these capacities. Delahaije, Gruppen, Van Nieuwenhuijzen, Giuseppin, & Wierenga (2013) showed that steric stabilization of oil droplets depends greatly on the molecular weight of the carbohydrates attached to patatin, a protein purified from potato, with beneficial effects found for Mw > 500 Da. Similarly, Wong, Day, & Augustin (2011) prepared MRPs from soluble wheat proteins and dextrans D10 or D65 (Mw 6400 Da or 41000 Da, respectively), and found that the larger dextran D65 that is conjugated at the N-terminal domain of the protein leads to additional interfacial layer thickness around the oil droplets (around 6 nm) compared to the smaller dextran D10 that conjugates with the C-terminal domain.

2.3 Antioxidant activity of the Maillard reaction products

2.3.1. *Standard assays*

The antioxidant activity exerted by MRPs is based on a wide variety of mechanisms, including free radical scavenging (e.g., hydroxyl, superoxide, and peroxyl radicals), chelation of metal ions, and breakdown of radical chain reactions (Echavarría et al., 2012; Langner & Rzeski, 2014; Nooshkam et al., 2019; Vhangani & Wyk, 2016). All these effects can be measured using the assays summarized in **Table 2.1** which includes their potential antioxidant mechanisms.

The reducing power and/or ferric-reducing/antioxidant power (FRAP) is used to evaluate the electron donating activity that enables MRPs to convert reactive radicals to a stable form (Hamdani et al., 2018). MRPs have substantial reducing activity, probably because (i) the Maillard reaction alters the protein structure leading to exposure of certain amino acids (e.g., tryptophan, tyrosine, and methionine) that possess electron donating ability (Hamdani et al., 2018); (ii) Amadori products formed in the initial stages and the hydroxyl and pyrrole groups of MRPs formed in the advanced stage of Maillard reaction might act as

Table 2.1 Antioxidant activities of the Maillard reaction products

Antioxidant assay	Principle of method	Possible antioxidant compounds	Mechanisms	Reference
Reducing power	Antioxidants reduce ferric chloride/ferricyanide complexes to ferrous form (Perl's Prussian blue color). Medium: phosphate buffer, pH 6.6.	1. Reductones 2. Hydroxyl and pyrrole groups of advanced MRPs (e.g. melanoidins) 3. Exposed amino acids	1. Hydrogen transfer 2. Reducing activity 3. Electron donation	Gu 2010; Hamdani 2018; Wang 2013
Ferric-reducing/antioxidant power (FRAP)	Antioxidants can reduce ferric iron to ferrous iron. Medium: acetate buffer, pH 3.6.	1. Heterocyclic products 2. Amadori products and thermolysis compounds 3. Reductones 4. Hydroxyl groups of MRPs	1. Reducing activity 2. Reducing activity 3. Hydrogen transfer 4. Reducing activity (electron donation)	Karnjanapratum 2017; Kim, 2013
DPPH or ABTS radical scavenging activity*	Antioxidants can convert $DPPH^{\bullet}$ or $ABTS^{\bullet+}$ to stable molecules. Medium: ethanol or methanol ($DPPH^{\bullet}$) or water ($ABTS^{\bullet+}$).	1. Intermediate or final MRPs 2. Exposed hydrophobic amino acids	1. Hydrogen donation 2. Electron donation	Nasrollahzadeh 2017; Sproston & Akoh, 2016, Khadidja 2017; Liu 2014
Metal chelating activity	Antioxidants can chelate metal ions. Medium: aqueous solution.	1. Hydroxyl, ketone, or pyrrole groups of e.g., Amadori products and melanoidins 2. Thiol groups in MRPs	1. Reducing activity and chelating activity 2. Chelating activity	Gu 2010; Morales 2005; Sproston & Akoh, 2016
Hydroxyl radical scavenging activity	Suppressed malondialdehyde formation by scavenging radicals from Fenton reaction. Medium: aqueous solution.	Hydroxyl groups of the MRPs (e.g., melanoidins)	Chelating activity	Han 2017

*DPPH is 1,1-Diphenyl-2-picrylhydrazyl, ABTS is 2,2'-Azinobis (3-ethylbenzothiazoline-6-sulphonic acid) diammonium salt.

electron donors (Fiore et al., 2012; Pawar et al., 2012; Vhangani & Wyk, 2016), and heterocyclic products that are also then formed could provide reducing activity (Karnjanapratum et al., 2017); (iii) reductones are able to donate a hydrogen atom to break the radical chain reaction (Wang et al., 2013).

The metal chelation ability of MRPs can be attributed to hydroxyl, pyrrole or ketone groups (Gu et al., 2010; Morales et al., 2005), anionic melanoidins binding positively charged metals (Morales et al., 2005), and thiol-derived MRPs binding metals in general (Sproston & Akoh, 2016).

Free radical scavenging activity of MRPs has been extensively studied, using 1,1-diphenyl-2-picrylhydrazyl (DPPH), 2,2'-azinobis (3-ethylbenzothiazoline-6-sulphonic acid) diammonium salt (ABTS), hydroxyl, peroxyl, and superoxide anion radical scavenging activity. The DPPH and ABTS scavenging activities are predominantly attributed to hydrogen donation by intermediate or final MRPs and electron donation by exposed amino groups (e.g., tryptophan, tyrosine, valine, and phenylalanine) (Khadidja et al., 2017; Liu et al., 2014; Nasrollahzadeh et al., 2017; Sproston & Akoh, 2016). It is relevant to point out that the DPPH assay is normally carried out with relatively high ethanol or methanol concentrations, which may not be fully representative of the antioxidant activity of MRPs when present in an emulsion. MRPs also interfere with the Fenton reaction owning to their ability to chelate metal ions (Han, Yi, Wang, & Huang, 2017). Other antioxidant activities (including hydroxyl radical scavenging activity, superoxide anion radical scavenging activity, oxygen radical absorbing capacity, and (2,3-bis(2-methoxy-4-nitro-5-sulpho-phenyl)-2H-tetrazolium-5-carboxanilide) tetrazolium salt reducibility) of MRPs have also been studied and confirmed (Nooshkam et al., 2019).

From the above, we can expect that some MRPs may have the potential to improve the oxidative stability of labile molecules when tested under model conditions. However, the fact that some MRPs are reducing agents could also promote oxidation by the regeneration of Fe^{2+} from Fe^{3+}. For example, melanoidins from barley malt could reduce Fe^{3+} to Fe^{2+} in a Fenton system, resulting in an increase of hydroxyl radicals, and thus induce a pro-oxidant

effect. Therefore, whether MRPs can slow down lipid oxidation in food emulsions is a question that still needs to be answered, as we try to do later.

2.3.2. *Maillard reaction products and the oxidative stability of O/W emulsion*

The antioxidant activity of a compound in foods is influenced not only by its chemical antioxidative capacities (e.g., metal chelating and free radical scavenging capacity) but also by its physical location and partitioning, interactions with other components, and environmental conditions (Decker et al., 2005). To properly evaluate this, O/W model emulsions have been used for various MRPs, as listed in **Tables 2.2 and 2.3**.

Partitioning of antioxidants in emulsions is one of the key factors influencing the susceptibility of lipids to oxidation. For instance, negatively charged compounds attract cationic metal ions; when such an attraction occurs at the surface of the oil droplets, this might favor lipid oxidation, whereas binding of metal cations by continuous phase components tends to retard lipid oxidation. For clarity, we first review the effects of MRPs present in the continuous phase (**Table 2.2**) and later at the interface (**Table 2.3**), and finally bring them together for full emulsion systems (**Figure 2.2**).

MRPs in the continuous phase of emulsions

Unadsorbed compounds (located in the continuous phase) have been shown to affect the oxidation of emulsified lipids, and their contribution may be substantial and even overrule the effect of adsorbed compounds (Berton-Carabin et al., 2014). Riisom, Sims, & Fioriti (1980) applied lysine-dextrose MRPs (1% level basis lysine) in safflower O/W emulsions, and they found that these emulsions were only slightly more oxidatively stable (as measured through oxygen uptake) than control emulsions (with lysine only). Similarly, limited effect of lysine-honey MRPs (reacted for 4 and 8 h) was observed when added to linoleic acid model emulsions (at 1% level of addition) (Antony et al., 2000). However, when these MRPs were heated for 12 – 20 h and added at 5 - 20%, a strong antioxidant effect was observed. Apparently, the antioxidant effect of MRPs depends on the extent of the reaction. Strong antioxidant effect was also reported for milk protein–carbohydrate MRPs added to krill O/W

emulsions, which reduced oxidation of eicosapentaenoic acid (EPA) and docosahexaenoic acid (DHA) and lowered propanal concentrations (Shen et al., 2014). This was attributed to the antioxidant activity of MRPs, although it is good to mention that the intrinsic antioxidant activity of unreacted compounds was not measured.

The antioxidant effect of MRPs added in the continuous phase of emulsions is probably related to their ability to act as metal chelators and free radical scavengers. Wijewickreme & Kitts (1997) found that lysine-fructose MRPs could bind copper ions significantly less compared to lysine-glucose MRPs, which was related to high antioxidant activity of the latter, whereas the former showed a pro-oxidant effect in O/W emulsions. Binding of metal ions may decrease their availability for chemical reactions and thus inhibit the decomposition of lipid hydroperoxides (Berton-Carabin et al., 2014). This effect is largely influenced by the pH; for instance, casein peptides-glucose MRPs had lower antioxidant activity at pH 3.0 than at pH 7.0 in Tween 20-stabilized emulsions, which could be due to the positive charge of the MRPs at pH 3.0 which may repel the cationic metal ions (Dong, Wei, Chen, McClements, & Decker, 2011).

Unadsorbed MRPs can scavenge free radicals produced in the continuous phase and/or from oxidizing lipids excreted to the continuous phase. For instance, the DPPH and ABTS radical scavenging activity of MRPs prepared from chito-oligomer increased as their preparation time increased, which led to less lipid oxidation in linoleic acid model emulsions (Jung et al., 2014), and when reacted at 80 °C for 240 min, MRPs (800 μg/mL) even delayed lipid oxidation more strongly than ascorbic acid (800 μg/mL) in linoleic acid emulsions after storage at 40 °C for 4 days (Jung et al., 2014).

Also, combined effects of radical scavenging and metal binding activities have been reported. Casein peptide-glucose MRPs produced at longer reaction time had increased DPPH radical scavenging activity, whereas their ability to chelate metals decreased, overall resulting in an increase in lipid oxidation (Dong et al., 2011). These combined effects may form an explanation for apparently contradictory results in the literature; i.e., the intrinsic antioxidant ability of MRPs does not always correlate with their propensity to limit lipid

oxidation in emulsions. For instance, the antioxidant capacity of lysine-glucose MRPs as measured through TBARS formation in an emulsion increased with reaction time up to 60 min and then leveled off, but no correlation was found with lipid oxidation rate (Ruiz-Roca et al., 2008). Similarly, MRPs prepared from hydrolyzed β-lactoglobulin and glucose showed increased antioxidant activities as a function of heating time but lipid oxidation was not influenced accordingly (Dong et al., 2012).

There are several other effects that may contribute to the complexity of lipid oxidation in such systems, and that we mention here to make the image complete. First, emulsifiers in the continuous phase may interact with MRPs, therewith altering the conformation of the protein moieties in MRPs (Donnelly et al., 1998). This may expose amino acids with antioxidant activity, thus retarding lipid oxidation (Feng et al., 2020). Second, prolonging the heating time of the MRPs could lead to protein aggregation (Zhou, Wu, Zhang, & Wang, 2017), and the large aggregates in the continuous phase of emulsions may lead to depletion flocculation. Also, a change in physical stability of emulsions (e.g., change in the interfacial area) may affect the oxidation of emulsified lipids. However, most studies did not measure the physical stability (e.g., droplet size) of model emulsions, making it difficult to evaluate the actual effect of MRPs on lipid oxidation. Third, environmental conditions (e.g., solvent, pH, and concentration) can be rather different between emulsions and assays used to investigate antioxidant behavior (e.g., DPPH radical scavenging ability is measured in organic solutions). Fourth, the interfacial composition is generally far from equilibrium and changes during storage (Berton-Carabin et al., 2014), and MRPs in the continuous phase may partly replace or adsorb on top of initially adsorbed emulsifiers. This is shown in studies of Browdy & Harris (1997) and Vhangani & Wyk (2016), who used MRPs and Tween 20 (the former study) or MRPs and egg yolk (the latter study), which stresses the importance of (dynamic) interfacial composition.

Table 2.2 Effects of Maillard reaction products in the continuous phase on the oxidative stability of O/W emulsions (MR conditions).

Reference	Highlights	Maillard reaction			Emulsions	
		Starting materials	Reaction conditions	MRP properties	Composition and physical properties	Lipid oxidation
Riisom, Sims, & Fioriti, 1980	Emulsions with MRPs were slightly more stable to lipid oxidation as compared to control emulsions (with lysine only).	Lysine, dextrose	Wet heating (WH): 50 °C, 15, 4, 8, 17, and 24 h		Safflower oil (25%), sodium stearoyl lactylate (1%), distilled monoglycerides (1%) *MRPs (1% level basis lysine) were added after emulsification.	Oxygen absorption rates
Wijewickreme & Kitts, 1997	1. Antioxidant activity (AA) glucose-lysine MRPs > fructose-lysine MRPs. 2. Various *in vitro* methods to evaluate oxidative behavior.	Lysine, glucose or fructose	WH: different reaction time, temperature, initial a_w & pH		Tween 80 (0.2 w/v%), linoleic acid (0.75 w/v%), 0.1 M Potassium phosphate buffer (pH 6.8) *MRPs (0.04 w/v%) were added after emulsification.	Oxygen consumption TBARS
Antony, Han, Rieck, & Dawson, 2000	1. AA increased with reaction time. 2. AA highest between 10-15% MRP.	Lysine, honey (expressed as percent glucose)	WH: reflux condenser, 4, 8, 12, 16, and 20 h	Absorbance (450 nm), pH, reducing sugar (refractometry), volatiles	Tween 20 (1%), linoleic acid (10 v%), 0.1 M potassium phosphate buffer (pH 6.2) *MRPs (1-20 v%) were added after emulsification.	Conjugated dienes (CD)
Romero, Doval, Sturla, & Judis, 2005	Soluble MRP high reduction power, and low DPPH and superoxide scavenging. Conjugate good AA in emulsion system.	Sarcoplasmic protein, malondialdehyde (secondary lipid oxidation product)	WH: 80 °C, 4 h, pH 7.6; sol. fraction	Color, protein carbonyl content, AA: reducing power, DPPH, superoxide radical scavenging, total phenolic content	Linoleic acid (0.570 w/v%), Tween 20 (0.578 w/v%), Phosphate buffer (pH 7.17) *MRPs (0, 1 and 10 w/v%) were added after emulsification.	CD, PV, TBARS
Ruiz-Roca, Navarro, & Seiquer, 2008	Severe heat treatment kept lipid peroxidation intact but decreased free radical scavenging activity.	Lysine, glucose	WH: oven, 150 °C, 15, 30, 60, 90 min	Weight loss, absorbance (280 and 420 nm), pH, free lysine content, AA: DPPH radical scavenging, copper and iron chelation	Tween 80 (0.2 w/v%), linoleic acid (0.75 w/v%), 0.1 M potassium phosphate buffer (pH 6.8) *MRPs (0.04 w/v%) were added after emulsification.	TBARS
Giroux, Houde, & Britten, 2010	Low amount of MRPs added to dairy beverages reduced oxidation of ω-3 polyunsaturated fatty acids during sterilization.	Milk protein concentrate, sucrose, glucose-fructose (1:1) mixture, glucose-galactose (1:1) mixture	Autoclave: 110 °C, 10 min	Color, redox potential (Pt-ring electrode), hydroxymethylfurfural (HMF)	Milk protein concentrate (3.6 wt%), $FeSO_4$ (0.001 wt%), linseed oil (2 wt%), pH 6.7 *Final concentration protein and lactose, 3.5 and 2.0 wt%. *MRPs (5 v%) were added after emulsification.	Propanal and hexanal

Dong et al 2011	MRPs did not dramatically alter the antioxidant activity of casein peptides.	Hydrolyzed sodium caseinate, glucose	WH: 80 °C, 12 h, pH 8	Browning, degree of conjugation, AA: DPPH, metal chelating, bitterness evaluation	Tween 20 (1.0 wt%), fish oil (10 wt%) *MRPs (0.001 w/v%) were added after emulsification. Zeta-potential, droplet size, creaming stability	PV, TBARS
Dong et al., 2012	The extent of Maillard reaction affected the AA of MRPs (increased and then decreased).	Hydrolyzed beta-lactoglobulin, glucose	WH: 90 °C, up to 18 h, pH 8	Absorbance & fluorescence, size, free amino group content, AA: FRAP, DPPH, metal chelating	Tween 20 (1.0 wt %), menhaden oil (10 wt%) *MRPs (0.001 w/v%) were added after emulsification. Zeta-potential, droplet size, creaming stability	PV, propanal
Jung, Park, Ahn, & Je, 2014	DPPH, ABTS, and reducing power increased significantly with heating time. Effective lipid peroxidation inhibition.	Chitooligomer	WH: 80 °C, 0-240 min	UV absorbance and browning, molecular weight (GPChrom), AA: DPPH and ABTS, reducing power	Linoleic acid emulsion *MRPs solution (50 v%) were added to emulsions.	TBARS
Shen, Bhail, Sanguansri& Augustin, 2014	MRPs added to the aqueous phase of phospholipid stabilized emulsion increased EPA and DHA stability.	Whey protein isolate (WPI) and Sodium caseinate (7:3), glucose and dried glucose syrup (1:1)	WH: 100 °C, 50 min, pH 7.5		Krill oil (20 wt%) *MRPs (3.0 wt%) or fish gelatin were added to emulsions at pH 8.0.	Fatty acid methyl ester analysis, propanal
Browdy & Harris, 1997	MRPs suppress hydroperoxide and thiobarbituric acid-reactive substance formation, and lowered oxygen.	Low-lactose sweet whey solutions	WH: 65 °C, 12-48 h, pH 8.0	Fluorescence, browning	Tween 20 (3.3 v%), soybean oil (40 v%), whey solution (10-50 w/v%), cuprous sulfate (10 µM, 3.3 v%), phosphate buffer (pH 8.0)	PV, TBARS, oxygen uptake
Sproston & Akoh, 2016	Prevention of lipid oxidation.	L-cysteine, glucose	Dry heating: 85 °C, 2, 4, 6h, 77% relative humidity	Browning, HMF, AA: ABTS/H_2O_2/HRP decolorization, metal chelation	Non-fat dry milk, α-lactalbumin-enriched WPC, lactose, locust bean gum, carrageenan, lecithin, monoacylglycerol, structured lipid	PV, pAV
Vhangani & Wyk, 2016	Inhibition of lipid oxidation.	Amino acids (Glycine and lysine), sugars (Fructose and ribose)	WH: 60 or 80 °C, or autoclave: 121 °C, 15, 60 and 120 min	Browning, AA: DPPH & peroxyl radical scavenging	MRPs (0.5 wt%), egg yolk (49.5 wt%), sunflower oil (50 wt%)	PV, TBARS, pAV

AA, antioxidant activity; CD, conjugated dienes; PV, peroxide value; TBARS, thiobarbituric acid-reactive substances; pAV, p-anisidine value.

MRPs at the interface

Although protein glycation by the Maillard reaction has been used to improve the physical stability of emulsions for about three decades, the use of such MRPs as interfacial antioxidants started only recently (**Table 2.3**). Consoli et al. (2018) found that when MRPs prepared from sodium caseinate and maltodextrin or dried glucose syrup were heated for a longer time (from 0 to 24 h), the MRP solutions displayed greater antioxidant activities (FRAP and DPPH radical scavenging activity), and MRP-stabilized emulsions had higher oxidative stability compared to systems containing the starting protein and carbohydrate mixture. This was attributed to the formation of advanced MRPs with antioxidant properties. Wang et al. (2019) and Wang et al. (2020) reported that proteins glycated with carbohydrates enhanced the antioxidant activity in aqueous media (DPPH and ABTS radical scavenging activity, oxygen radical absorption capacity) and in emulsions (peroxide value (PV) or thiobarbituric acid-reactive substances (TBARS)). They claimed that the dense and thick interfacial layers created by the MRPs may protect oil droplets from oxidation through physical effects. In the work of Zha and co-workers, this was linked to the physical barrier effect of MRPs to inhibit the decomposition of hydroperoxides (Zha, Dong, et al., 2019; Zha, Yang, et al., 2019). However, such physical barrier effects are questionable given the size of the reactive species involved in oxidation, and the lack of direct experimental evidence for such an effect. First, the thickness or density of the interfacial layers was not tested in these studies, whereas in general, an oil-water interface formed by biopolymers is porous at the scale of pro-oxidant molecules (Berton-Carabin et al., 2021). Second, the physical effect of the adsorbed glycated proteins was not distinguished from their chemical effects (e.g., metal chelating activity) nor from the effect of the glycated proteins remaining in the continuous phase.

In the work by Cermeño et al. (2019), conjugating carrageenan with whey protein concentrate (WPC) led to an enhanced generation of secondary lipid oxidation products (as measured by TBARS) in emulsions, compared to WPC emulsions. However, it was difficult to assess the involved mechanisms, as some physical destabilization of the emulsions

occurred upon incubation (coalescence and flocculation). Additional investigations would be needed to elucidate the relationship between the physical and oxidative stability in emulsions, which is probably multifactorial and therefore difficult to decipher.

The effects of MRPs in O/W emulsions are summarized in **Figure 2.2**. In the initiation stage of lipid oxidation, MRPs and proteins can scavenge radicals, therewith delaying the free radical chain propagation process (**Figure 2.2**, arrow A). MRPs and proteins can bind transition metals therewith preventing them from initiating radical formation and decomposing surface-active hydroperoxides (LOOH) (arrow B). When free radicals and unbound metal ions reach the interface to react with unsaturated fatty acids (LH), adsorbed MRPs can quench free radicals and chelate metal ions. It is important to realize that unadsorbed and adsorbed MRPs may contribute synergistically to the oxidative stability of emulsions.

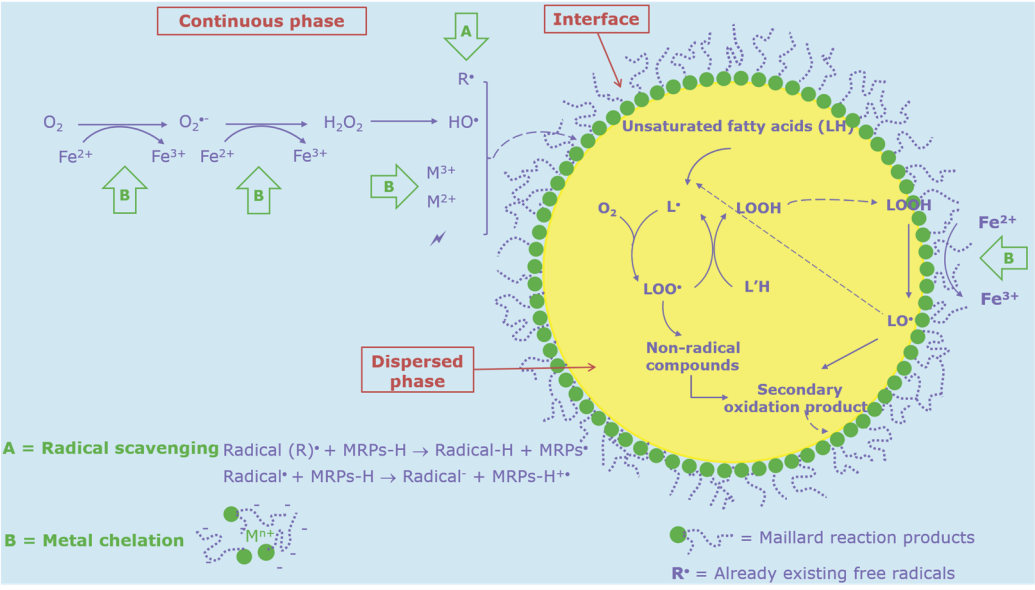

Figure 2.2. Antioxidant mechanisms of Maillard reaction products (MRPs) in oil-in-water emulsions.

Table 2.3 Maillard reaction products as emulsifiers on the oxidative stability of O/W emulsions.

Reference	Highlights	Maillard reaction			Emulsions		
		Starting materials	Reaction conditions	MRP properties	Composition	Physical properties	Lipid oxidation
Consoli et al., 2018	Higher physical stability and lower oxidation than sodium caseinate emulsions.	Sodium caseinate, maltodextrin, dried glucose syrup	Wet heating (WH): 75 °C, 3 - 24 h, pH 7.5	Color, rheology, interfacial tension, SDS-PAGE, size exclusion chromatography (SEC), AA: DPPH radical scavenging, FRAP	MRPs 30 wt%, palm oil 4.5 wt%, resveratrol 0.02 wt%, pH 7.5	DS 0.72 -1.03 µm, ZP -54 to -51 mV, rheology microstructure, creaming index	DPPH, FRAP
Cermeño et al., 2019	MRPs had antioxidant and emulsifying activity.	Whey protein concentrate /hydrolysate, carrageenan	Dry heating (DH): 60 °C, 6-48 h, 79% RH	Molecular mass distribution (GP-HPLC), color, extent of conjugation (TNBS method), AA: oxygen radical absorbance capacity	MRPs 1 w/v%, corn oil 30 wt%, pH 4.0	DSD, coalescence/ flocculation index, microstructure, rheology	TBARS
Wang et al., 2019	Stable against aggregation during storage and oxidation stability due to antioxidant activity and adsorption of modified protein.	Egg white proteins, isomalto-oligo-saccharide	DH: 60 °C, 3 d, 79% RH; sol. fraction: 90 °C, 30 min, pH 6.0-9.0	Surface hydrophobicity, particle size, zeta-potential, grafting degree, AA: DPPH and ABTS	MRPs 1 w/v%, Arowana sunflower oil 10 v%	DSD, ZP -60 to -30 mV, protein content at the interface, microstructure	PV
Zha, Dong, Rao, & Chen, 2019	High physical and oxidative stability. MRPs prevented hydroperoxide transition metal interaction, rather than scavenge free radicals.	Pea protein isolate, gum Arabic	DH: 60 °C, 0, 1, 3 and 5 d, 79% RH, pH 7.0	Color, SDS-PAGE, relative solubility, SEM, free Amadori compounds and melanoidins (UV–Vis), free amino groups	MRP supernatant 0.20 wt%, corn oil 2 wt%, phosphate buffer (10 mM, pH 7.0)	DS (D[4,3] 0.75 - 20.7 µm), ZP -70 to 10 mV	PV, hexanal
Zha, Yang, Rao, & Chen, 2019	Maillard-reaction leads to cross-linked PPH-GA MRPs; chemical stability enhanced by increased surface hydrophilicity and steric hindrance.	Pea protein hydrolysate, gum Arabic	DH: 60 °C, 0, 0, 1, 3 and 5 d, 79% RH, pH 7.0	Color, SDS-PAGE, FTIR, SEM, SEC, light scattering, relative solubility, free Amadori compounds and melanoidins UV–Vis, free amino groups, volatiles (GC-MS)	MRP supernatant, 0.20 wt%, corn oil 2 wt%, phosphate buffer (10 mM, pH 7.0)	DS 0.6 - 1.3 µm, ZP -70 to 10 mV	PV, hexanal
Shi et al., 2019	Synergetic effects absorbed and unabsorbed MRPs in lipid oxidation.	WPI, dextran	DH: 60 °C, 1-14 d, 79% RH	Grafting degree, AA: DPPH, metal chelating	MRPs 1 w/v%, soybean oil 10 wt%	DS 330-580 nm, ZP -35 to -20 mV, protein adsorption	PV
Wang, Wang, Chen, Fu, & Liu, 2020	MRPs lead to smaller droplets, better storage and oxidative stability than whey protein.	WPI, mulberry fruit poly-saccharide	DH: 60 °C, 0, 48, and 72 h, 79% RH	Surface hydrophobicity, intrinsic fluorescence spectroscopy, SDS-PAGE, emulsion foaming capacity /stability, glycation degree AA: DPPH, oxygen radical absorption	MRPs 1% w/v, fish oil 10%, pH 4.0	DS 300 to 550 nm, ZP -39 to -20 mV, rheology, protein adsorption	TBARS

AA, antioxidant activity; DPPH, 1,1-Diphenyl-2-picrylhydrazyl; FRAP, Ferric-reducing/antioxidant power; PV, peroxide value; TBARS, thiobarbituric acid-reactive substances; DS(D), droplet size (distribution); ZP, zeta-potential; SDS-PAGE, sodium dodecyl sulfate polyacrylamide gel electrophoresis; SEM, scanning electron microscopy; FTIR, Fourier-transform infrared spectroscopy.

2.3.3. Maillard reaction products inherently present in foods

MRPs inherently occur in certain foods (e.g., coffee, cocoa, dairy and bakery products) as a result of processing. Although the antioxidant capacity of model MRPs has been already well studied (section 2.3.2), research regarding the effects of MRPs derived from such foods is still scarce. Therefore, in this section, we review their antioxidant activity and explore their potential for application in emulsions.

Endogenous formation of MRPs in foods has been reported as an antioxidant source. High temperatures applied during food processing often favor the formation of MRPs, which affects the antioxidant profile of the products. Michalska et al. (2008) evaluated the development of MRPs during rye bread baking and their contribution to the overall antioxidant activity of bread. They reported that early MRPs formed in bread did not exhibit antioxidant activity, whereas the advanced MRPs formed in bread crust had strong peroxyl and ABTS radical scavenging activities. Likewise, Anese et al. (1999) studied the effect of drying temperature on the formation of MRPs in pasta. Results showed that antioxidant potential was associated with the formation of advanced MRPs, but early stage MRPs seemed to have pro-oxidant properties, which may be due to the formation of some highly reactive radicals in the early stages of the MR and the degradation of natural antioxidants (Calligaris et al., 2004). In addition, Serpen & Gökmen (2009) reported that there was a reasonable correlation between color, total antioxidant capacity and acrylamide levels in potato crisps; they revealed that potato crisps had high antioxidant activity, which was the result of the formation of MRPs during the frying process. Lin et al. (2015) incorporated ground roasted coffee in ground top round beef and found that roasted coffee was able to lower lipid oxidation (TBARS) to the same or even greater extent than rosemary (containing phenolic antioxidants). Later, Patrignani et al. (2016) investigated the *in vivo* antioxidant effect of MRPs in biscuits on rats and concluded that rats fed with higher amounts of MRPs had higher serum antioxidant activity (FRAP, ABTS) and lower oxidation damage (TBARS). These findings suggest that MRPs developed in foods have strong antioxidant activity, and therefore, when extracted may be used as functional ingredients (e.g., antioxidants). For

example, fructosyl arginine [N-α-(1-deoxy-D-fructos-1-yl)-L-arginine; Fru-Arg], a low molecular weight MRP that can be isolated from aged garlic extract, exhibits antioxidant activity *in vitro* (Ide et al., 1999; Ryu et al., 2001) through hydrogen peroxide scavenging, at a related activity comparable to ascorbic acid (Ryu et al., 2001). Positive effects were also found in Cu^{2+}-induced LDL (low density lipoprotein) oxidation systems for rat pulmonary artery endothelial cells (lower formation of TBARS and inhibited the release of lactate dehydrogenase), and murine macrophages (inhibited release of peroxides) (Ide et al., 1999). The oxidative cleavage of Fru-Arg in these systems may proceed via metal complexing and reducing properties (O'Brien & Morrissey, 1997).

Melanoidins, the final stage MRPs that contain anionic, brown-colored, high-molecular-weight and nitrogen-containing compounds, have also been studied in relation to their strong antioxidant effect. Studies have mainly focused on melanoidins extracted from real foods, including coffee (Bekedam, Schols, Van Boekel, & Smit, 2006; Borrelli, Visconti, Mennella, Anese, & Fogliano, 2002; Delgado-Andrade & Morales, 2005; Morales & Jiménez-Pérez, 2004; Zhang et al., 2019; Zhang et al., 2019), vinegar (Liu et al., 2016; Xu et al., 2007), cocoa (Summa et al., 2008; Quiroz-Reyes & Fogliano, 2018), and beer (Morales & Jiménez-Pérez, 2004). For these compounds, the actual antioxidant mechanisms are unclear because their chemical structures are still largely unknown (Mesías & Delgado-Andrade, 2017; Wang et al., 2011). Researchers have suggested the ability of melanoidins to chelate metals, quench radicals, or act as reducing agents (Echavarría et al., 2012; Wang et al., 2011). The metal chelating ability of melanoidins could be ascribed to their anionic nature, which was shown to allow them to form stable complexes with metals similar to anionic hydrophilic polymers (Gomyo & Horikoshi, 1976). Ćosović, Vojvodić, Bošković, Plavšić, & Lee (2010) reported that nitrogen atoms may be responsible for complexing copper ions, and hydroxyl and ketone groups of pyridone or pyranone serve as chelating agents (Wang et al., 2011). Furthermore, melanoidins can scavenge a variety of radicals, such as ABTS, DPPH, and N,N-dymethyl-*p*-phenylenediamine (DMPD) (Borrelli et al., 2002; Morales & Babbel, 2002). For certain melanoidins from pasta and tomato puree, a linear correlation between radical quenching activity and color was found, whereas more complex relations have been

suggested for coffee melanoidins (Manzocco et al., 2000). The actual composition is responsible for the different behaviors, but unfortunately, not well understood. In addition, melanoidins exhibit reducing activity, which may be due to the hydroxyl groups on their heterocyclic regions (Vhangani & Wyk, 2016). Apart from this, for melanoidins from coffee, polyphenols and low molecular weight MRPs non-covalently bound to the melanoidins contribute to overall antioxidative ability (Delgado-Andrade et al., 2005; Delgado-Andrade & Morales, 2005; Morales & Jiménez-Pérez, 2004; Rufián-Henares & Morales, 2007; Tagliazucchi et al., 2010), and may exceed the activity of the melanoidins themselves (Morales & Jiménez-Pérez, 2004).

Melanoidins may be surface-active and thus adsorb at the air-water interface (and overview is in **Table 2.4**). Lusk et al. (1987) isolated a high molecular weight (6-20 kDa) melanoidin fraction from beer that lowered surface tension to 66.0 mN/m (the surface tension at the air-water interface is 72 mN/s). It should be noted that this decrease is somewhat limited compared e.g., proteins (Hinderink et al., 2020), especially considering the fact that the concentration used was 5 times higher than in beer. Later, melanoidins isolated from beer foam liquid were shown to form stable other foams independently of the presence of beer proteins, therewith highlighting a more prominent role than previously recognized (Lusk et al., 1995).

Melanoidins from coffee foam were also investigated (D'Agostina et al., 2004; Piazza et al., 2008). The total foaming fraction (TFF) from espresso coffee was separated into a carbohydrate-like and a melanoidin-like fraction, and the foaming properties were studied (**Figure 2.3**). D'Agostina et al. (2004) reported that the melanoidin-like fraction exhibited higher foaming capacity and antioxidant activity than the carbohydrate-like fraction, and Piazza et al. (2008) observed stronger viscoelastic interfacial properties in melanoidin-like fraction than the carbohydrate-like fraction.

The potential of certain food melanoidins to stabilize emulsions has also been described in a few patents. Roasted coffee particles (10 – 20 wt% dry matter melanoidins proteinous part) have been found to remarkably stabilize emulsions against coalescence, while

exhausted roasted coffee particles (aqueous extraction at 110 and 180 °C) showed slightly less good droplet stabilization than roasted coffee, which was ascribed to the loss of surface-active materials (melanoidins) during extraction (Pipe et al., 2014). In another patent, plant-derived starting materials (containing reducing monosaccharides, phenolic compounds, free amino acids, and pectin) were heated, which resulted in a mixture with emulsification properties (Da Fonseca Selgas Martins et al., 2014). It was claimed that the heating conditions employed led to the formation of substantial quantities of melanoidins, as evidenced by browning and absorbance at 405 nm. When using model melanoidins produced with arginine, glutamine, fructose, and glucose, it was found that these components were not that effective as emulsifiers, leading to a wide range of oil droplet sizes (20 to 60 µm), and a free oil layer on top of the emulsions within 24 hours after emulsification, and complete phase separation after 6 months of storage at 5°C (Da Fonseca Selgas Martins et al., 2014). The low molecular weight and purity of the 'model melanoidins' compared to melanoidins isolated from real foods is expected to have been the cause of the differences observed. To the best of our knowledge, no information regarding lipid oxidation in these emulsion systems is available.

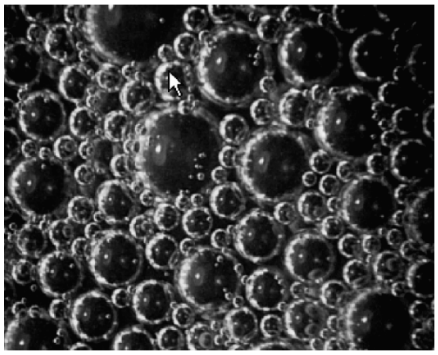

Figure 2.3. Stereo-microscope picture (enlargement: 200x) of the foam surface created by stirring non-defatted melanoidin-like foaming fraction under standard conditions. Reprinted from Journal of Food Engineering, 84, Piazza, L., Gigli, J., & Bulbarello, A, Interfacial rheology study of espresso coffee foam structure and properties, 420-429, Copyright (2021), with permission from Elsevier.

Table 2.4 Literature data on surface-active melanoidins extracted from foods.

Reference	Source	Extraction method	Characterization	Applied in	Characterization of systems	Antioxidant results	Antioxidant mechanism
Lusk et al., 1987	Beer	Size-exclusion and ion-exchange chromatography of 10-50 kDa proteins.	Isoelectric focusing, protein/carbohydrate concentration, absorption and fluorescence spectra		Dynamic surface tension		
Lusk, Goldstein, & Ryder, 1995	Beer foam liquid	Carbohydrates, melanoidins, and 10, 12, 40 kDa proteins prepared by cation-exchange, anion-exchange, and/or preparative HPLC.	Fourier transform infrared spectroscopy	Model beers	Foam quality, reducing sugars, protein assay including Kjeldahl, dynamic surface tension		
D'Agostina, Boschin, Bacchini, & Arnoldi, 2004	Brown polymers (foaming fractions) of freshly prepared espresso coffee	Isolation of total foaming fraction (TFF) from espresso coffee, 2-propanol/water extraction to obtain an insoluble and soluble fraction. Soluble fraction further fractionated with solid-phase extraction.	Size exclusion chromatography (SEC), color (Color dilution analysis), flavor & taste (sensory evaluation), foamability, foam persistence			Melanoidin-rich fractions showed antioxidant properties. More hydrophobic compounds have higher antioxidant capacity.	Nitrogen-containing moieties or polyphenol residues in polymers not polysaccharides. Some antioxidants in the green seed (chlorogenic acids, phenolics), are destroyed by roasting, but overall AA is preserved due to melanoidin formation.
Piazza, Gigli, & Bulbarello, 2008	Foaming fractions from ground dark roasted coffee blend	Isolation of TFF and fractionation in carbohydrate-like, and melanoidin-like components.	Interfacial rheology, viscosity, image analysis				
Pipe et al., 2014	Particles of roasted or green coffee and mixtures thereof	Grinding coffee beans in liquid nitrogen, aqueous extraction, filtration and drying the solid part.	Particle size	Emulsions	Droplet size, optical microscopy		
Da Fonseca Selgas Martins et al., 2014	Plant-derived material with reducing monosaccharides, phenolics, and pectin	Heating to at least 60°C for at least one minute.	Optical absorbance at 405 nm (A_{405})	Emulsions	Visual inspection, optical microscopy		

2.4 Conclusions and perspectives

MRPs can locate both in the continuous phase and at the interface of O/W emulsions, where they may retard lipid oxidation by various physicochemical mechanisms, including metal chelation and free radical scavenging. Melanoidins isolated from certain food products may have a strong antioxidant effect and have the ability to act as surface-active compounds, so they have a great potential to act as interfacial antioxidants. However, to the best of our knowledge, this has hardly been explored yet.

Although MRPs represent a promising class of interfacial antioxidants with potential use in foods, some challenges remain. First, the compositions and structures of MRPs, especially melanoidins, are not that well known, and the underlying reactions cannot be controlled that easily. Thus, it is difficult to directly link antioxidant effects to molecular or supramolecular structures. There is therefore a great demand for advanced analytical methods that still need to be developed. By identifying the exact compositions and structures, in combination with information on their location in an emulsion, antioxidant efficiency may be predicted. Second, the impact of certain MRPs on human health remains a concern. For instance, acrylamide and its metabolite glycidamide have been shown to be genotoxic and carcinogenic. The Benchmark Dose Lower Confidence Limit ($BMDL_{10}$) was selected as 0.17 and 0.43 mg/kg bw/day for tumors and other effects (EFSA, 2015). Therefore, minimizing the level of harmful compounds through strict control of the MR process is of essence. Third, the feasibility of MRPs in industrial applications needs further evaluation, which includes the design of sustainable preparation processes and evaluation of economic profitability.

Overall, the knowledge gained from this review would allow food scientists to design foods with enhanced oxidative and physical stability by employing MRPs in foods making use of effects taking place at different physical locations (interface or continuous phase).

Supplementary materials

Table S2.1 *An overview of Maillard reaction products (MRPs)-stabilized emulsions*

Reference	Maillard reaction					Emulsions				
	Starting materials		Reaction conditions	MRP characterization		Composition	Buffer (pH, I)	Homogenization method	Emulsion properties	
	Protein	Carbohydrate		Physical	Chemical				Physical	Chemical
Animal-based proteins										
Golkar, Nasirpour, Keramat, & Desobry, 2015	β-lactoglobulin (BLG)	Angum gum	Dry heating (60 °C, 1-14 d, 75% relative humidity (RH))	Sodium dodecyl sulphate-polyacrylamide gel electrophoresis (SDS-PAGE)	Amadori and browning compounds by spectrophotometry	MRPs (1.5 wt%), soybean oil (40 v%)		Rotor-stator (12,000 rpm, 2 min)	Droplet size, viscosity, light microscope	
Lesmes & McClements, 2012	BLG	Dextran	Dry heating (60 °C, 24 h, 76% RH, pH 7.0)			MRPs (1 wt% protein), corn oil (5 wt%)		High-speed blender (60 s), Microfluidizer (82 MPa, 3x)	Zeta-potential, droplet size	Upper gastro-intestinal conditions, free fatty acid release (pH-STAT)
Wooster & Augustin, 2006	BLG	Dextran	Dry heating (60 °C, 36 h, 76% RH, pH 7.5)	Size exclusion and anion exchange chromatography, steric layer thickness, protein surface coverage	Free amino groups (o-phthalaldehyde (OPA) method), enzymatic digestion	MRPs (1 wt% BLG), canola oil (20 wt%)		Rotor-stator (13,500 rpm, 2 min), valve homogenizer (8 MPa, 5x)	Zeta-potential, droplet size	
Dunlap & Côté, 2005	BLG	Dextran	Dry heating (55 or 75 °C, 1-7 d), purification by anionic exchange chromatography	SDS-PAGE		MRPs (0.1 wt% protein), sunflower oil (20 wt%)	Phosphate (10 mM, pH 7.0)	Tissue Tearor hand-held homogenizer (15,000 rpm, 1 min), emulsiflex C5 homogenizer (150 MPa, 5x)	Droplet size, creaming, protein surface load	
Bi, Yang, Fang, Nishinari, & Phillips, 2017	BLG	Gum *Acacia Seyal*	Dry heating (60 °C, 12 h, 79% RH, pH 7.0)	Browning index, SDS-PAGE, gel permeation chromatography multi-angle laser light scattering, differential scanning calorimetry (DSC)	Degree of conjugation (2,4,6-trinitrobenzenesulfonic acid (TNBS) method)	Medium chain triglyceride (MCT, 0.5 wt%)		High-speed Polytron PT-MR2100 shear mixer (26,000 rpm, 3 min, ice bath)	Droplet size, light microscopy	
Medrano, Abirached, Moyna, Panizzolo, & Añón, 2012	BLG	Glucose or lactose	Dry heating (50 °C, 51 and 96 h, 65% RH, pH 7.0)		ε-N-2-(furoylmethyl)-l-lysine (furosine) content (HPLC)	Protein or MRPs (0.1 wt% protein), sunflower oil (25 v%)		Rotor-stator (20,000 rpm, 1 min)	Droplet size, protein adsorption, interfacial tension and rheology, stability by vertical scan analyzer	
Cheetangdee & Fukada, 2014	BLG	D-glucose, D-allose, D-fructose, and D-psicose	Dry heating (50 °C, 31% RH, pH 7.0)	Color (Spectrophotometer), GPC, interfacial tension	Free amino group content (OPA method)	n-hexadecane		Rotor-stator homogenizer (20,000 rpm, 1 min)	Zeta-potential, droplet size, emulsion stability (Dispersion stability analyzer)	
Yadav, Parris, Johnston, Onwulata, & Hicks, 2010	BLG, whey protein isolate (WPI)	Corn fiber gum	Dry heating (75 °C, 2 h, 1-4 d and 7 d, 79% RH)	SDS-PAGE		Valencia orange oil (5 wt%)		Polytron homogenizer (20,000 rpm, 1 min), high pressure homogenizer (HPH) (68.95 MPa, 3x)	Emulsion turbidity, droplet size	
Wooster & Augustin, 2007	BLG	Maltose, maltodextrin	Dry heating (60 °C, 36 h, 76% RH, pH 7.5)	SEC, steric layer thickness, protein surface coverage	Free amino group content (OPA method), enzymatic digestion	Canola oil (20 wt%)		Rotor-stator (13,500 rpm, 2 min), valve homogenizer (8 MPa, 5x)	Droplet size, zeta-potential	
Wang, Liu, Xu, Yin, & Yao, 2016	Bovine serum albumin (BSA)	Dextran	Dry heating (60 °C, 48 h, 79% RH, pH 8.0)			MRPs: 1.5% BSA. Oil phase (20 or 40%): 90% MCT and 10 v% ethanol with (1.2-1.5 w/v%) curcumin		Homogenizer (10,000 rpm, 1 min), HPH (90 MPa, 4 min), heat treatment (90 °C, 1 h)	Droplet size, zeta-potential, microstructure (Transmission electron microscopy (TEM))	Curcumin loading efficiency (HPLC), animal experiments

Kim, Choi, Shin, & Moon, 2003	BSA	Galactomannan	Dry heating (60 °C, 3 d, 79% RH), filtered	SDS-PAGE, SEC, fluorescence, Circular Dichroism (CD), emulsifying activity index (EAI), emulsion stability index (ESI)		MRPs (0.1 w/v%), n-tetradecane (20 v%)	Phosphate buffer (10 mM, pH 7.4)		Protein load	
Chen et al., 2016	BSA	Sugar beet pectin (SBP)	Dry heating (85 °C, 5 h, 79% RH, pH 3.8)	Thermogravimetric analysis (DTA-TGA equipment), Fourier-transform infrared spectroscopy (FTIR)	Formation of MRPs (Spectrometry)	MRPs (1 w/v%), soybean oil (10 wt%)		Rotor-stator (19,000 rpm, 3 min), HPH (50 MPa, 1x)	Droplet size, zeta-potential	
Rangsansarid, Cheetangdee, Kinoshita, & Fukuda, 2008	BSA	Aldohexose (D-glucose or D-allose. Sugar ester (6-O-octanoyl-D-glucose)	Dry heating (50 °C, 31% RH, pH 7.0)	GPC, interfacial tension	Free amino group content (OPA method)			Sonicaton (Duty cycle 40%, 1 min)	Droplet size, zeta-potential	
Darewicz & Dziuba, 2001	Beta-casein	Glucose	Wet heating (37 °C, 24 h, pH 7.4)	CD, adsorption isotherms	MALDI-TOF MS	MRPs (0.44 w/v% protein), tricaprylin oil (10 v%)	pH 6.7 Ionic strength of 75 mM	Polytron PT-MR-3000 homogenizer (10,000 rpm, 1 min), HPH (6 MPa, 2x)	Droplet size	
Hou, Wu, Xia, Phillips, & Cui, 2017	Casein hydrophobic peptide	*A. seyal* polysaccharide	Dry heating (60 °C, 3 d)	HPSEC	Degree of conjugation (TNBS)	MRPs (0.2–2 wt%), canola oil (10 wt%)	Acetate (0.1 M, pH 4.0)	High-speed homogenizer (10,000 rpm, 5 min), HPH (35 MPa, 3x)	Droplet size, light microscopy	
Al-Hakkak & Al-Hakkak, 2010	Egg white proteins	High methoxyl pectin	Dry heating (60 °C, 6-48 h, 79% RH)	Rheology, SDS-PAGE, solubility	Free amino group content (TNBS)	MRPs (2 wt%), sunflower oil (10 wt%)		Rotor-stator (24,000 rpm, 3 min), two stage valve HPH (70 MPa, 3x)	Droplet size	
Lin et al., 2012	Gelatin hydrolysates	Glucose	Wet heating (50-60 °C, 6 h, pH 10.0) *Insoluble products extraction with MTBE.	FTIR, surface tension, contact angle (FACE CA-5 contact angle meter), emission spectra		Soybean oil (10 wt%)		Rotor-stator (12,000 rpm, 5 min)	Droplet size, zeta-potential	
Regan & Mulvihill, 2013	Hydrolyzed sodium caseinate	Maltodextrin	Dry heating (60 °C, 96 h or 48 h, 79% RH)	SDS-PAGE, GPC, Color (Colorimeter)	Degree of conjugation (TNBS), available reducing groups on conjugation (Chloramine-T assay)	MRPs (0.8 or 0.7 wt% protein), soy oil (20 wt%)		Rotor-stator (10,000 rpm, 15 s), two-stage laboratory homogenizer (20 and 5 MPa, 5x)	Droplet size	
Chen et al., 2014	Phosvitin	Dextran	Wet heating (100 °C, 6 h)	Solubility, intrinsic (Trp) and extrinsic (ANS) fluorescence emission spectra, CD, EAI, ESI,		MRPs (0.5 w/v% protein), rapeseed oil (1/3 v/v)	Phosphate (10 mM, pH 7.0)	High-speed homogenizer (17,400 rpm, 1 min)	Droplet size, zeta-potential, interfacial layer thickness measurement	
Decourcelle, Sabourin, Dauer, & Guérard, 2010	Shrimp hydrolysate	Xylose	Wet heating (65 °C, 4 h, pH 6.5)	SEC, EAI	Free amino group content (OPA)	MRPs (1.5 wt%), sunflower oil (50 wt%)		Rotor-stator (18,000 rpm, 90 s)	Rheology, creaming	
O'Regan & Mulvihill, 2009	Sodium caseinate	Maltodextrin	Dry heating (60 °C, 96 h, 79% RH)	SDS-PAGE, color (Colorimeter), GPC	Free amines (TNBS), reducing groups (Chloramine-T assay)	MRPs (0.8% w/w protein), soybean oil (20 wt%)		Rotor-stator (10,000 rpm, 15 s), two-stage homogenizer (20 MPa, 5 MPa)	Droplet size	

Ekin, Davidov-pardo, & Julian, 2016	Sodium caseinate	Dextran	Dry heating (60 °C, 48 h, 76% RH)		Degree of conjugation (OPA), AA (ABTS radical scavenging activity)	MRPs (1 wt%), corn oil (10 wt%, containing 2.5 wt% lutein)	Phosphate (5 mM, pH 7.0)	High-speed mixer (10,000 rpm, 2 min), microfluidizer (137.9 MPa, 3x)	Droplet size, zeta-potential	Chemical stability of lutein (colorimeter), free fatty acids, bioaccessibility lutein
Corzo-Martínez et al., 2011	Sodium caseinate	Galactose, lactose, dextran (10 kDa)	Dry heating (different T/time, a_w 0.67, pH 7.0)	Particle size (Delsa Nano C particle analyzer), EAI		Sunflower oil (20 v%)	Phosphate (0.1 M, pH 7.0)	450 digital sonifier (20 kHz, 400 W full power)		
Sabik et al., 2014	Sodium caseinate or hydrolyzed sodium caseinate	Lactose	Wet heating (80 °C, 20 min, pH 7.5) or Dry heating (50 °C, 24 h, 65% RH)	Solubility (Bradford), Colorimetry, EAI	AA (DPPH radical scavenging activity)	MRPs (1.0 wt% protein), oil (10 wt%)	pH 3.0 and 6.8	PT 2100 Polytron Homogenizer (8000 rpm, 1 min), valve homogenizer (20.68 MPa, 3x + 6.89 MPa, 1x)		Degradation lemon oil (headspace solid-phase micro-extraction with gas chromatography-mass spectrometry (HS-SPME-GC/MS))
Perrechil, Santana, Lima, Polastro, & Cunha, 2014	Sodium caseinate	Locust bean gum	Dry heating (54-96 °C, 1, 3, 24 h, 79% RH)	SDS-PAGE, color (Colorimeter)		MRPs (1 w/v%), soybean oil (30 v%)	pH 3.5	Rotor-stator (14,000 rpm, 4 min)	Creaming index (CI), light microscopy, rheology	
Xu, Yuan, Gao, McClements, & Decker, 2013	Whey protein isolate (WPI)	Beet pectin	Dry heating (80 °C, 5 h, 79% RH, pH 7.0)	SDS-PAGE		MRPs (0.5 wt% protein, 1.0 wt% beet pectin), MCT (5 wt%), β-carotene (0.075 wt%)	Phosphate (10 mM, pH 7.0)	Two-speed hand-held homogenizer (3 min), microfluidizer (62 MPa, 3x) Washed emulsions	Droplet size, zeta-potential	β-carotene content (spectrophotometer)
Xu, Wang, Jiang, Yuan, & Gao, 2012	WPI	Beet pectin	Dry heating (80, 90, 100 °C, 1, 3, 5, 7, 9 h, 79% RH, pH 7.0)	SDS-PAGE		MRPs (0.5 wt% protein concentration) MCT (5 wt%), β-carotene (0.075 wt%)	Phosphate buffer (10 mM, pH 7.0)	Rotor-stator (10,000 rpm, 3 min), microfluidizer (50 MPa, 3x)	Droplet size, physical stability (LUMiSizer), freeze–thaw stability (Turbiscan), microstructure microscopy, rheology	β-carotene content (spectrophotometer)
Yi, Liu, Zhang, & Gao, 2018	WPI	Dextran	Dry heating (60 °C, 12, 24, and 48 h, 79% RH, pH 7.0)	SDS-PAGE, Conformation (CD, Fluorescence Spectra Trp)	Degree of conjugation (OPA)	MRPs (1 wt% protein), corn oil (10 wt%), β-carotene (0.2 wt%)		Rotor-stator (13,000 rpm, 2 min), microfluidizer (56 MPa, 2 min)	Droplet size, zeta-potential	
Diah, Vermeir, Martins, Meulenaer, & Meeren, 2016	WPI	Low-methoxyl pectin	Dry heating (60 °C, 4, 8, 16 d, 74% RH, pH 7.0)	pH and absorbance, SDS-PAGE, high resolution pfg-NMR diffusometry	Degree of conjugation (TNBS)	MRPs (0.5%), sunflower oil (10 wt%)		Rotor-stator (24,000 rpm, 1 min), AH-2010 homogenizer (80 MPa, 5x)	Droplet size	
Wefers, Bindereif, Karbstein, & Schaaf, 2018	WPI	Pectin	Dry heating (80 °C, 6 – 168 h, 79% RH)	Solubility, SDS-PAGE, HPSEC, protein content (Kjeldahl), NMR	Degree of conjugation (TNBS), amino acid composition HPLC, Liquid chromatography mass spectrometry (LC-MS)	MRPs (0.5 wt%), rapeseed oil (30 wt%)	pH 5	Rotor-stator (10,000 rpm, 1 min), microfluidizer (40 MPa, 60 MPa)	Droplet size (Laser diffraction particle size analyzer)	
Schmidt et al., 2016	WPI	Pectin	Dry heating (80 °C, 1.5 – 72 h, 79% RH, pH 7.0)	SDS-PAGE, fluorescence spectroscopy, zeta-potential		MRPs (2 wt%), rapeseed oil (30 wt%)		Rotor-stator (10,000 rpm, 1 min), HPH (40 MPa, 80 MPa)	Droplet size (Laser diffraction particle size analyzer)	
Guo, Guo, Yu, & Kong, 2018	WPI	SBP	Dry heating (80 °C, 5 h, 79% RH)	SDS-PAGE, conformation (Fluorescence Spectra), interfacial tension (Optical contact angle)	Degree of conjugation (TNBS method)	MRPs (1.5 wt%), medium chain triglyceride (15 wt%)	Phosphate (10 mM, pH 7.0)	Homogenizer (26,000 rpm, 3 min), HPH (50 MPa, 2x)	Viscosity, droplet size	
Qi, Xiao, & Wickham, 2017	WPI	SBP	Dry heating (60 °C, 72 h, 79% RH)	Total powder and protein solubility, SDS-PAGE	Soluble sulfhydryl and disulfide bond contents, soluble primary and secondary amine content (Ninhydrin reagent)	MRPs, Valencia orange oil	Phosphate buffer (33 mM, pH 6.75)	Polytron bench top homogenizer (20,000 rpm, 30s), EmulsiFlex-B3 HPH (13 MPa, 3x)	Droplet size (HORIBA Laser Scattering Particle Size Distribution Analyzer LA-950)	

Ding, Valicka, Akhtar, & Ettelaie, 2017	WPI	Maltodextrin	Dry heating (80 °C, 3 h, 79% RH)		Degree of conjugation (OPA)	MRPs (2 w/v% protein concentration), sunflower oil (20 v%)	Ionic strength 0.1 M, pH 2.9	Jet homogenizer (35 MPa)	Droplet size, rheological flow properties, Confocal laser scanning microscopy (CLSM)	
Drapala, Auty, Mulvihill, & Mahony, 2016	WPI or Whey protein hydrolysate (WPH)	Maltodextrin	Wet heating (90 °C, 8 h, pH 8.2)		Free thiol groups	1.55, 3.50 and 7.00% of protein, oil and carbohydrate, respectively		Rotor-stator (710 g, 2 min), valve homogenizer (15 MPa, 3 MPa)	Color, fat globule size distribution, zeta-potential, viscosity, CLSM	Protein, fat, moisture, ash and carbohydrate content of emulsions
Plant-based proteins										
Guo & Xiong, 2013	Buckwheat protein	xylose, fructose, glucose, dextran, and maltodextrin	Wet heating (60 °C, 12, 24, and 48 h, pH 6.5)	Difference UV spectroscopy, solubility, SDS-PAGE, intrinsic fluorescence (Trp), DSC, EAI, ESI	Free amines (TNBS)	soybean oil and the protein solution = 1:3, v:v	pH 7.0	Polytron homogenizer (13,500 g, 2 min)	Microstructure (Phase contrast microscopy)	
Pirestani, Nasirpour, Keramat, & Desobry, 2017	Canola protein isolate	Gum Arabic	Wet heating (90 °C, 15 min, pH 7.0)	Zeta-potential, protein solubility, EAI, ESI		MRPs (0.7% protein), sunflower oil (40 v%)	Sodium phosphate (0.01 M, pH 7.0)	Rotor-stator (20,000 rpm, 1 min)	Droplet size, light microscopy, CI, rheology	
Wang, Gan, Li, Nirasawa, & Cheng, 2019	Deamidated wheat gluten (DWG)	Maltodextrin or citrus pectin	Dry heating (80 °C, 0, 3, 6, 9, 12, and 24 h, 79% RH)	SDS-PAGE, FTIR, CD, Surface hydrophobicity, Atomic force microscopy	Degree of conjugation (OPA)	MRPs (0.67 wt%), soybean oil (10 wt%)		Rotor-stator (13,000 rpm, 1 min), two-stage homogenizer (60 MPa, 40 s)	Stability under different NaCl concentrations and pH by droplet size	In-vitro digestion of β-carotene emulsion
Yin, Wang, Liu, & Yao, 2017	Deamidated zein peptide	Dextran or maltodextrin	Dry heating (60 °C, 48 h, 79% RH, pH 8.8)	SDS-PAGE, GPC, conformation (FTIR), zeta-potential	Amino acid composition, amine content (OPA)	MRPs (0.5% peptide),MCT (10 v%)		Homogenizer (10,000 rpm, 1 min), HPH (80 MPa, 4 min)	Droplet size, TEM	
Wong, Day, & Augustin, 2011	Isolated wheat protein	Dextran	Dry heating (60 °C, 5 d, 75% RH), supernatant (10,000 g, 15 min)	SDS-PAGE	Degree of conjugation (OPA), fluorescence emission spectroscopy	MRPs (1 wt% protein), canola oil (20 wt%)	pH 7	Rotor-stator (11,500 rpm, 2 min), valve homogenizer (8 MPa, 2x)	Interfacial layer thickness, enzyme digestion of interfacial layer, droplet size, zeta-potential, CLSM	
Zhang, Guo, Zhu, Peng, & Zhou, 2015	Oat protein isolate	Dextran	Wet heating (90 °C, 0, 20, 40, 60, 80 and 100 min, pH 9.0)	SDS-PAGE	Degree of conjugation (TNBS)	MRPs (0.5% protein), soybean oil (5 v%)		Rotor-stator (13,500 rpm, 2 min), HPH (30, 60 ,90 MPa)	Droplet size, zeta-potential, CLSM	
Chen, Chen, Wu, & Yu, 2016	Peanut protein isolate (PPI)	Maltodextrin	Sonication	SDS-PAGE, zeta potential	Degree of conjugation (OPA), surface hydrophobicity	PPI (2.0 w/v%), sunflower seed oil (20 v%)		High-pressure jet homogenizer (30 MPa)	Droplet size, CLSM	
Tamnak, Mirhosseini, Ping, Mohd, & Muhammad, 2016	Pea protein isolate (PPI)	Pectin	Dry heating (60 °C, 0, 6, 27 and 48 h, 79% RH, pH 7.0)	SDS-PAGE, SEM	Moisture content	MRPs (1 wt%), canola oil (10 wt%)		High shear homogenizer (4000 rpm, 3 min), HPH (25 MPa, 3x)	Viscosity, droplet size, zeta-potential	
Seo, Karboune, & Archelas, 2014	Potato patatin	galactose, galacto-oligosaccharides, galactan	Dry heating (48 °C, 1-7 d, a_w 0.65, pH 7.0). Purification (anion exchange chromatography)	Conformation (FTIR, Fluorescence Spectra)	ε-N-2-(furoylmethyl)-l-lysine (furosine) content (HPLC), free amino groups (TNBS), DPPH radical scavenging activity	Triolein (30 v%)	Acetate (10 mM, pH 3.0) or phosphate (10 mM, pH 7.0)	Ultrasonic liquid processor (20% power (120 W), 3 min), Emulsiflex C5 homogenizer (100 MPa, 3x)	Droplet size, stability (T= 65 °C for 2 h, turbidity at 500 nm after dilution with 0.1 w/v% SDS)	
Delahaije, Gruppen, Van Nieuwenhuijzen, Giuseppin, & Wierenga, 2013	Patatin	Xylose, glucose, maltotriose, or maltopentaose	Dry heating (60 °C, 2.5, 4, 24, and 48 h, 65% RH, pH 7)	Solubility, HPSEC, adsorption Kinetics and Surface Elastic Modulus	Matrix assisted laser desorption/ionization - time of flight mass spectrometry (MALDI-TOF MS), OPA	MRPs (0.5%), sunflower oil (10 v%)	Sodium phosphate (10 mM, pH 7.0)	Rotor-stator (9,500 rpm, 1 min), labhoscope 2.0 laboratory scale HPH (15 MPa, 30x)	Zeta-potential, flocculation (Diffusing wave spectroscopy), light microscopy, critical layer thickness (DLVO theory)	

Du et al., 2013	Rice dreg glutelin	κ-Carrageenan	Dry heating (60 °C, 79% RH)	Solubility, SDS-PAGE, FTIR, CD	Degree of conjugation (OPA), amino acid analysis	MRPs (0.15%), soybean oil (20 v%)	pH 3, 5, 7 or NaCl (0–0.4 M)		CI, droplet size, zeta-potential	
Mu, Zhao, Zhao, Cui, & Liu, 2011	Soy protein isolate (SPI)	Acacia gum	Wet heating (80 °C, 0-48 h, pH 7.5)	SDS-PAGE, solubility	Degree of conjugation (OPA), surface hydrophobicity	MRPs (2 w/v% protein),soy oil (10 wt%)		Continuous agitation, pressure homogenizer (30 MPa, 2x)	Droplet size	
Yu et al., 2018	SPI, or soy protein hydrolysates	Dextran	Wet heating (95 °C, 1.5 h, pH 7.0)	Conformation (FTIR))		MRPs (1.8 w/v%), soy oil (10 wt%)	Phosphate (0.05 mM, pH 7.0)	High shear blender (10,800 rpm, 1 min), HPH (40 MPa, 1x)	Droplet size, flocculation and coalescence by light microscopy, oiling off	
Boostani, Aminlari, Moosavi-nasab, Niakosari, & Mesbahi, 2017	SPI	Dextran	Dry heating (40, 60, 80 °C 0-48 d; 79% RH, pH 7.0 and 8.5)	SDS-PAGE, FTIR, SEM, DSC, EAI, ESI	Degree of conjugation (OPA), DPPH radical scavenging activity	MRP (1%), olive oil (20 wt%)		Homogenizer (10,000 rpm, 5 min), Ultrasonic homogenizer (amplitude 80, cycle 0.7 for 10 min)	Droplet size, zeta-potential	
Zhang et al., 2017	SPI	Dextran	Ultrasound or microwave	Conformation (FTIR), intrinsic fluorescence emission spectroscopy, SEM		MRPs (1.5 w/v% protein), soy oil (20 v%)	Sodium phosphate (0.01 M, pH 7.0)	High-speed blender (11,000 rpm, 1 min), HPH (60 MPa, 2x)	Droplet size, zeta-potential, light microscopy, CI, oiling off	
Diftis & Kiosseoglou, 2006	SPI	Dextran	Dry heating (60 °C, 1 week, 79% RH, pH 7.0)			MRPs (2% protein), corn oil (20 v%)	pH 7.0	Rotor-stator (20,500 rpm, 1 min)	Droplet size	
Diftis, Biliaderis, & Kiosseoglou, 2005	SPI	Dextran	Dry heating (60 °C, 1 and 3 week, 79% RH, pH 7.0)			MRPs (1% Protein), corn oil (50 v%)	Citrate pH 3.8 with 0.3 M NaCl	Rotor-stator (20,500 rpm, 1 min)	Droplet size, rheology	
Li et al., 2015	SPI	Gum acacia	Dry heating (60 °C, 3, 6, 9 d, 79% RH, pH 7.0)	Color, conformation (CD), EAI, ESI	Degree of conjugation (OPA)	MRPs (2 wt%), soy oil (10 v%)	pH 7.5	Pressure homogenizer (30 MPa, 2x)	Droplet size, viscosity	
Shekarforoush, Mirhosseini, & Islam, 2016	SPI	Gum karaya	Dry heating (60 °C, 3 d, 75% RH, pH 7.0)	SDS-PAGE, SEM, ESI		Canola oil (20 wt%)		Stirred for 5 min, HPH (30 MPa, 3x)	Droplet size, rheology	
Zhang et al., 2014	SPI	Maltodextrin	Wet heating (80 °C, 80 min, pH 7.0), enzyme hydrolysis (54 °C, 25 min, pH 7.0)	Surface and interfacial tension	Degree of conjugation (OPA)		pH 7.0	Rotor-stator (10000 rpm, 2 min), HPH (35 MPa, 10 MPa) Freeze-dry emulsions	Emulsions: Advanced Rheometric Expansion System Powder: Thermal analysis, SEM	Powder: Peroxide value, Headspace propanal
Zhang, Wu, Lan, & Yang, 2013	SPI	Maltodextrin	Dry heating (90, 115, 140 °C, 2 h, 79% RH, pH 6.8)	SDS-PAGE	Degree of conjugation (OPA)	MRPs (1 wt%), corn oil (20 v%)	Sodium phosphate (10 mM, pH 7.0)	Rotor-stator (10,000 rpm, 2 min), homogenizer (40 MPa, 2x)	Droplet size, zeta-potential, CI, CLSM	
Wang, Wu, & Liu, 2017	SPI	Soy hull hemicelluloses	Dry heating (60 °C, 7 d)	Color, FTIR, thermogravimetric analysis	Amino acid analysis	MRPs (0.5 wt%), soy oil (20 v%)		High-shear homogenizer (10,000 rpm, 2 min)	Droplet size, light microscopy	
Yang et al., 2015 Yang, Cui, Gong, Miller, et al., 2015	SPI	Soy soluble polysaccharide	Dry heating (55, 60 or 65 °C, 36–96 h, 75% RH, pH 7.0) Super-natant (15,000 g, 30 min)	SDS-PAGE, FTIR, HPSEC		MRPs (3.7 wt%), citral (10 wt%)		Polytron® (20,000 rpm, 3min), jet homogenizer (517.1 MPa, 3x), 90 °C, 30 min, pH 7.0	Droplet size, zeta-potential	Simulated gastrointestinal conditions (citral release measured by GC)
Zhang, Wu, Yang, He, & Wang, 2012	Soy β-conglycinin	Dextran	Dry heating (60 °C, 6 d, 75% RH, pH 6.8) Supernatant (10,000 g, 15 min); Hydrolysis	SDS-PAGE, HPSEC, interfacial tension (OCA20 optical contact angle meter)	Surface hydrophobicity	MRPs (1 w/v%), corn oil (20 v%)	Sodium phosphate buffer (10 mM, pH 7.0)	Rotor-stator homogenizers (10,000 rpm, 1 min), single-pass lab-scale jet homogenizer (~30 MPa, 2x)	Protein adsorption fraction (F_{ads}) and surface load (Γ_{sat}), droplet size, zeta-potential, CI, CLSM	

Xu & Yao, 2009	Acid soluble soy protein	Dextran	Dry heating (60 °C, 75% RH, pH 8.5)	AFM				Homogenizer (10,000 rpm, 1 min), ultrasonication (450 W, 6 min)	Droplet size, zeta-potential, AFM	
Wang & Xiong, 2016	Soy peptides	Polyaldehyde dextran	Wet heating (60 °C, 48 h, pH 6.5) Supernatant (10,000 g, 20 min)	SDS–PAGE	Free amines (TNBS), Schiff base, advanced Maillard reaction product (Fluorescence spectrophotometry, EAI	MRPs (1% protein concentration), soybean oil (5 v%)	Sodium phosphate (10 mM, pH 6.5)	PT10-35 Polytron homogenizer (speed 3, 2 min), HPH (34 MPa)	Morphology (phase contrast microscopy), droplet size	
Li et al., 2016	Soy peptides	Glucose, maltose, MD, and dextran (40 kDa)	Wet heating (60 °C, 3 d, pH 7.0)	FTIR, zeta-potential, surface tension (automated surface tensiometer), ESI	Amino acid (HPLC), surface hydrophobicity	MRPs (0.5 wt% soy peptides), soybean oil (20 v%)		High-speed blender (2 min)	CLSM, interfacial rheology	
Kasran, Cui, & Goff, 2013	Soy whey protein isolate	Fenugreek gum, or partial hydrolysed fenugreek gum	Dry heating (60 °C, 3 d, 75% RH), MRPs (75 or 85 °C 15 min)	SDS–PAGE, HPSEC, solubility		MRPs (0.8 w/v%), canola oil (10 v%)	Acetate buffer (0.1 M, pH 4.0)	Polytron (17,210rpm, 30 min), jet homogenizer (35 MPa, 3x)	Droplet size	

3

Glycation of soy proteins leads to a range of fractions with various supramolecular assemblies and surface activities

This chapter has been published as Feng, J., Berton-Carabin, C. C., Ataç Mogol, B., Schroën, K., & Fogliano, V. (2021). Glycation of soy proteins leads to a range of fractions with various supramolecular assemblies and surface activities. Food Chemistry, 343, 128556. https://doi.org/https://doi.org/10.1016/j.foodchem.2020.128556

Abstract

Dry and subsequent wet heating were used to glycate soy proteins with dextran or glucose, followed by fractionation based on size and solubility. Dry heating led to protein glycation (formation of furosine, Nε-(carboxymethyl)-L-lysine, Nε-(carboxyethyl)-L-lysine, and protein-bound carbonyls) and aggregation (increased particle size); while subsequent wet heating induced partial unfolding and de-aggregation. The measurable free amino group content of soy proteins changed from 0.77 to 0.14, then to 0.62 mmol/g upon dry and subsequent wet heating; this non-monotonic evolution is probably due to protein structural changes, and shows that this content should be interpreted with caution as a glycation marker. After both heating steps, the smaller-sized water- soluble fractions showed higher surface activity than the larger insoluble ones, and dextran conjugates exhibited a higher surface activity than their glucose counterparts. We thereby achieved a comprehensive understanding of the properties of various fractions in plant protein fractions, which is essential when targeting applications.

3.1 Introduction

The Maillard reaction (MR), also known as non-enzymatic browning, is a set of spontaneous and natural chemical reactions between the reducing groups of carbohydrates and the ε-amino groups of amino acids, peptides or proteins (Hodge, 1953). There is extensive evidence that Maillard conjugation (glycated proteins) can improve protein functionality, such as emulsifying, foaming, and gelling properties (Corzo-martínez, Carrera, Moreno, Rodríguez, & Villamiel, 2012; Spotti et al., 2019). Moreover, amphiphilic glycated proteins are able to form submicron particles via self-assembly upon heat treatment above the denaturation temperature of proteins (Feng et al., 2015; Li, Yu, Yao, & Jiang, 2008; Meng, Kang, Wang, Zhao, & Lu, 2018). Such Maillard conjugation-based submicron particles have been used as Pickering stabilizers or delivery vehicles to encapsulate and control release bioactive compounds (Fan, Yi, Zhang, & Yokoyama, 2018; Hernández et al., 2020; Jin et al., 2016; Lin et al., 2019).

Most of the research on Maillard conjugation has been done on animal-derived proteins (e.g., whey protein isolate, β-lactoglobulin, bovine serum albumin, and egg white protein), focusing primarily on characterizing the improved protein functionality (Akhtar & Ding, 2017; Zhang et al., 2019a). Plant proteins are promising alternatives to animal proteins, due to the current trend in using more sustainable food ingredients. Yet, compared to animal proteins, the use of plant-based proteins for Maillard conjugation has been less considered, and limited mainly to soy proteins, pea proteins and wheat proteins (Akhtar & Ding, 2017; Diftis & Kiosseoglou, 2006; Zha, Yang, Rao, & Chen, 2019). Among these, soy protein isolate (SPI) is the most widely used plant protein source owing to its good functional properties such as microencapsulation, emulsification, and gelation properties (Nesterenko, Alric, Silvestre, & Durrieu, 2013). It contains various proteins, with β-conglycinin and glycinin being the predominant ones. β-Conglycinin is a glycoprotein that consists of three subunits α, α' and β, which are randomly linked by non-covalent interactions (Thanh & Shibasaki, 1978). Glycinin is a hexamer, in which acidic and basic subunits are interconnected by a disulphide bond (Shewry, 1995).

Considering the compositional heterogeneity of SPI, as well as the complexity of the MR during which many molecular and supramolecular structure changes may occur, a vast number of components and products are expected to be formed upon glycation. In most studies, proteins are incubated with carbohydrates and the whole reaction mixture is used without any post-reaction purification or fractionation. Some studies did use only the soluble fraction to prepare emulsions, to avoid the clogging of homogenization devices, taking into account the actual concentration after discarding the insoluble compounds (Wefers, Bindereif, Karbstein, & Van Der Schaaf, 2018; Weng et al., 2016). Yet, the insoluble fraction could be interesting for so-called Pickering emulsions or foams, for which insoluble colloidal particles are needed (Berton-Carabin & Schroën, 2015).

On the other hand, many studies have been carried out with limited chemical characterization and control of the extent of the MR and of the molecules and supramolecular structures (protein aggregates) formed. Some studies applied gel electrophoresis to confirm the conjugation between proteins and carbohydrates, although non-quantitatively (Lesmes & McClements, 2012; Xu, Wang, Jiang, Yuan, & Gao, 2012; Yadav, Parris, Johnston, Onwulata, & Hicks, 2010). A few authors attempted to limit the reaction to the initial stages: they estimated the degree of glycation quantifying free amino groups by the o-phthalaldehyde (OPA) or 2,4,6-trinitrobenzenesulfonic acid (TNBS) assays (Akhtar & Ding, 2017). Unfortunately, the free amino groups may be hindered as a result of protein aggregation, and thus prevented from reacting with the involved reagents, leading to an overestimation of the degree of glycation. Therefore, a direct measure of specific Maillard reaction products (MRPs) is mandatory to assess the extent of protein glycation.

The objectives of this study were to characterize the chemical and structural features of various Maillard reaction fractions (e.g., water-soluble vs insoluble, and differently glycated) and ultimately to propose optimal utilization of each fraction to minimize losses of precious materials. To achieve this aim in this paper, we first applied dry heating to induce Maillard conjugation between SPI and glucose or dextran (a large glucose-based polysaccharide), used in different ratios. The reaction products were separated by either centrifugation or

filtration, and a second wet heat treatment was applied, as it was previously shown to alter the structural properties of the products formed in the first heating step, and thereby allow the formation of submicron particles (Feng et al., 2015; Li et al., 2008; Meng et al., 2018). A range of Maillard reaction markers was used to characterize the extent of the reaction (including free amino group, furosine, Nε-(carboxymethyl)-$_L$-lysine, Nε-(carboxyethyl)-$_L$-lysine, and protein-bound carbonyl contents) in all fractions. Surface hydrophobicity and tryptophan fluorescence were used to elucidate conformational changes, and interfacial tension between vegetable oil and water was assessed to prospective functionality in terms of stabilization of multiphase food systems.

3.2 Materials and methods

3.2.1 Materials

Soy protein isolate (SPI, 79.14 ± 0.66 % N; SUPRO® 500E) was obtained from Solae (St Louis, MO, USA). Protein concentration was determined by bicinchoninic acid (BCA) assay (Thermo Scientific, Pierce BCA Protein Assay Kit) or nitrogen determination by the Dumas method (Interscience Flash EA 1112 series, Thermo Scientific, Breda, The Netherlands). Refined rapeseed oil was purchased from a local supermarket (Wageningen, the Netherlands) and stripped with alumina powder (Alumina N, Super I, EcoChrome™, MP Biomedicals, France) to remove impurities and tocopherols (Berton, Genot, & Ropers, 2011). For sodium dodecyl sulphate-gel electrophoresis (SDS-PAGE), Mini-PROTEAN gels (12% TGX™ Gel, 10 well, 30 µL/well), precision plus protein™ standards (dual color), Laemmli sample buffer, Tris/Glycine/SDS buffer, and Bio-safe™ Coomassie G-250 stain were supplied by Bio-Rad (Richmond, CA, USA). D-(+)-Glucose, dextran (average molecular weight 70 kDa), potassium bromide, β-mercaptoethanol, o-phtaldialdehyde, sodium tetraborate decahydrate, sodium dodecyl sulphate (SDS), DL-dithiothreitol (DTT), ammonium formate, 2,4-dinitrophenylhydrazine (DNPH), guanidine hydrochloride, trichloroacetic acid (TCA), and 8-anilino-1-naphthalenesulfonic acid ammonium salt (ANSA) were purchased from Sigma-Aldrich (St. Louis, MO, USA), all at least of analytical grade. Analytical standard l-serine (99%) was supplied by Alfa Aesar (Wardhill, MA, USA), Nε-(2-furoylmethyl)-$_L$-lysine (furosine), Nε-

(carboxymethyl)-$_L$-lysine (CML), Nε-(carboxyethyl)-$_L$-lysine (CEL), Nε-(2-furoyl)-methyl-l-[4,4,5,5-[$^2H_4$]lysine HCl salt (d_4-furosine), Nε-(carboxy[$^2H_2$]methyl)-$_L$-lysine (d_2-CML) were obtained from Polypeptide Group (Strasbourg, France), and Nε-(carboxy[$^2H_4$]ethyl)-$_L$-lysine (d_4-CEL) was purchased from Toronto Research Chemicals Inc. (Ontario, Canada). Hydrochloric acid (37%), ethanol (95%), ethyl acetate (99%), acetonitrile, and formic acid (98-100%) were from Merck Millipore (Merck, Germany). All solutions and dispersions were made using ultrapure water prepared with a Millipore Milli-Q water purification system (Millipore Corporation, Billerica, Massachusetts, US).

3.2.2 Preparation of glycated soy protein isolate

SPI and carbohydrate (glucose or dextran) powder mixtures with a weight ratio of 10:1, 2:1, or 1:1 were dispersed in water and lyophilized, after which the samples were milled with a Fritsch ball mill (Fritsch, Oberstein, Germany). The powder was subsequently incubated at 60 °C for 1 day at a relative humidity of 79% in a desiccator containing a saturated potassium bromide solution for protein glycation to take place, and next stored at -20 °C. Besides, the same procedure was used to make dry heated SPI that served as a control sample.

3.2.3 Fractionation of glycated soy protein isolate

A scheme of the samples prepared for the study is provided in **Figure 3.1**. The glycated SPI samples or dry heated SPI samples were dispersed in water at 5 g/L, and gently stirred at 4 °C overnight to ensure full hydration. These dispersions were fractionated by centrifugation (10,000×*g* at 4 °C for 15 min; Sorvall Lynx 4000 Centrifuge, Thermo Scientific, Agawam, MA, USA) or filtration (Amicon stirred cell, Millipore Co., MA, USA, with Sterlitech polyethersulfone membranes, pore size 0.03 μm). The pellet and retentate were re-dispersed in a volume of water equivalent to the supernatant and filtrate, respectively. The pellet, supernatant, and retentate dispersions were heated in a water bath at 95 °C for 50 min to obtain the corresponding heated samples.

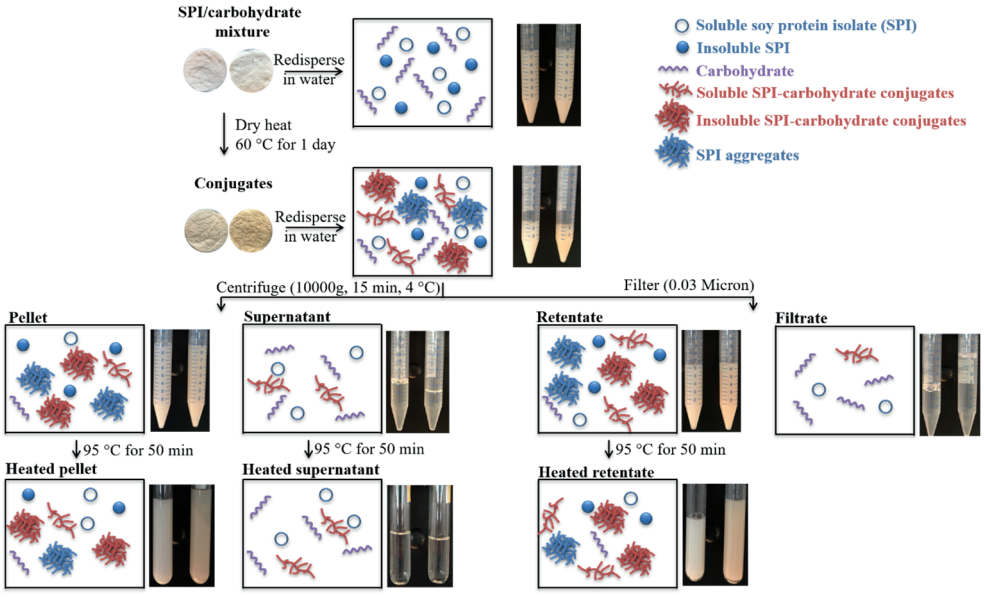

Figure 3.1. Scheme of preparation of the different fractions. Photographs: Visual observations of SPI-dextran (left) and SPI-glucose (right) fractions.

3.2.4 SDS-PAGE

A Mini-PROTEAN^{e} Tetra system (Bio-Rad, Richmond, CA, USA) was used for SDS-PAGE analysis. First, samples (2 mg/mL protein content measured by BCA assay) were diluted 1:1 with Laemmli sample buffer containing 5 v% β-mercaptoethanol and heated at 95 °C for 5 min on an Eppendorf ThermoMixer® C heating block (Eppendorf, Hamburg, Germany). Next, protein standard (10 µL) and sample solutions (20 µL) were loaded in separate wells in Mini-PROTEAN gels. The samples were separated at a constant voltage of 200 V at room temperature for approximately 30 min, after which the gels were stained with Coomassie G-250 for 1 h, and de-stained with water for 12 h. The gels were scanned using a GS-900^{TM} Calibrated densitometer (Bio-rad, USA) and analyzed with Image Lab 5.2.1 software (Bio-Rad, USA).

3.2.5 OPA assay

The free amino group content was estimated using the OPA assay as described by Nielsen, Petersen, and Dambmann (2001) with some modification. Briefly, 200 µL sample (solution or suspension) were added to 1.5 mL of freshly prepared OPA reagent (containing 38.1 g/L sodium tetraborate decahydrate, 0.8 g/L OPA, 1 g/L sodium dodecyl sulfate, and 0.88 g/L DL-dithiothreitol), and mixed on a digital vortex mixer at 2500 rpm for 5 s. The mixture was incubated at room temperature for exactly 3 min, and the absorbance was measured at 340 nm using spectrophotometer DR3900 (Hach Lange, Germany). Calibration curves using L-serine as standard were used to determine the free amino group content expressed as millimole free amino groups per gram of protein (mmol/g protein). The protein concentration was determined with the BCA assay.

3.2.6 Analysis of Maillard reaction markers by LC-MS/MS

Analysis of furosine, CML, and CEL content was conducted on an Ultimate 3000 high-pressure liquid chromatograph (HPLC) (Thermo Scientific, USA) coupled to a Thermo Finnigan TSQ Quantum triple quadrupole mass spectrometer (San Jose, CA, USA) using the method of Troise, Fiore, Wiltafsky, and Fogliano (2015), with modifications. One milliliter of sample solution was mixed with 4 mL of 7.5 M hydrochloric acid (HCl) in a 10 mL heating tube and incubated at 110 °C for 20 h. To prevent oxidation, the heating tubes were saturated with nitrogen and sealed before incubation. Following incubation, the hydrolysates were filtered using syringe filters (PTFE, 0.22 Millipore, Billerica, MA, USA), after which filtrate aliquots (500 µL) were dried under nitrogen. The dried samples were reconstituted in 500 µL water. For SPI and SPI-dextran samples, 100 µL of the reconstituted sample was mixed with 90 µL of acetonitrile spiked with 10 µL internal standard. For SPI-glucose samples, a 10 µL reconstituted sample was mixed with 180 µL 50 v% acetonitrile spiked with 10 µL internal standard. The final concentrations of internal standards in all samples were 500 µg/L furosine, 500 µg/L d_2-CML, and 200 µg/L d_4-CEL. Five microliters of each sample were injected into the LC-MS/MS system.

HPLC separation was performed using a reversed-phase core shell column (Kinetex HILIC 2.6 µm, 100 × 2.1 mm, Phenomenex, Torrance, USA). The mobile phases were: A, aqueous 0.1 v% formic acid; B, 0.1 v% formic acid in acetonitrile; C, 50 mM ammonium formate. The linear gradient elution steps were as follows: 0-0.8 min, 80% B, 10% C; 0.8-3.5 min, 80-40% B, 10% C; 3.5-6.5 min, 40%B, 10% C; 6.5-8 min, 40-80% B, 10% C; 8-10 min, 80% B, 10% C. The flow rate was set at 0.4 mL/min, and detection was achieved by positive electrospray ionization using selected reaction monitoring (SRM). The source parameters were: spray voltage 3.0 kV, vaporizer temperature 250 °C, capillary temperature 310 °C, collision pressure 0.2 Pa, and scan time 100 ms. Data were analyzed with Thermo Xcalibur 4.0.27.19 (Thermo Scientific, USA). The recovery of analytes was determined by spiking the samples with a known amount of analytes (low, middle, and high concentrations, corresponding to 30, 300, and 1000 ppb, respectively). Recovery experiments were repeated six times, and the results were 88.0 ± 7.4%, 91.2 ± 7.0%, and 84.2 ± 6.1% for furosine, CML, and CEL, respectively. Quantification of furosine, CML and CEL was performed by linear regression of the analyte/internal standard peak area ratio against analyte concentration. Protein content of each sample was measured by the Dumas method, and the final results were expressed as mg/g protein. Limit of detection (LOD) and limit of quantification (LOQ) were calculated based on the slope (S) of calibration curve and the standard deviation (SD) of responses according to Eqs. (3.1) and (3.2):

$$\mathrm{LOD} = \frac{3.3 \times SD}{S} \tag{3.1}$$

$$\mathrm{LOQ} = \frac{10 \times SD}{S} \tag{3.2}$$

The LOD were 0.2, 0.3, and 0.8 µg/L for furosine, CML, and CEL, respectively. The LOQ were 0.6, 1, and 2 µg/L for furosine, CML, and CEL, respectively.

3.2.7 Color measurement

The color change of SPI powder upon glycation was measured using a ColorFlex spectrophotometer (Hunter Associates Laboratory, Inc., Reston, VA, USA). Color values

were expressed according to the CIE lab model, in which *L** (lightness), *a** (+a* = red and -a* = green) and *b** (+b* = yellow and -b* = blue) were recorded. The color difference (ΔE) and browning index (BI) were calculated with Eqs. (3.3) and (3.4), respectively (Consoli et al., 2018).

$$\Delta E = \sqrt{(L^* - L_0^*)^2 + (a^* - a_0^*)^2 + (b^* - b_0^*)^2} \quad (3.3)$$

Where L_0^*, a_0^*, and b_0^* are the values before heat treatment, and L^*, a^*, and b^* are the values after dry heat treatment.

$$BI = \frac{x - 0.31}{0.172} \times 100 \quad (3.4)$$

For *x* obtained from Eq (3.5):

$$x = \frac{(a^* + 1.75L^*)}{(5.645L^* + a^* - 3.012b^*)} \quad (3.5)$$

3.2.8 Determination of protein-bound carbonyl content

Protein-bound carbonyl content was measured by derivatization with DNPH following the method described by Duque-Estrada, Kyriakopoulou, de Groot, van der Goot, and Berton-Carabin (2020), with slight modification. Briefly, 0.8 mL of sample was precipitated with 0.8 mL of cold 40 w/v% TCA in 2 mL Eppendorf tubes. The samples were centrifuged at 15,000×*g* for 5 min, the supernatant discarded, and SDS (400 µL, 5 w/v%) was added to the pellet. The sample was then heated at 100 °C for 10 min and ultrasonicated (Elmasonic P 60H, Elma, Germany) at 40 °C for 30 min. For each sample, three aliquots were treated with 0.8 mL DNPH (0.3 w/v% in 3 M HCl), and three with 0.8 mL 3 M HCl (blank). After incubating in the dark at room temperature for 1 h (while vortexing at 2500 rpm for 5 s every 10 min), 400 µL of cold 40 w/v% TCA was added, and the sample was centrifuged as before. The supernatant was removed, and the pellet was washed with 1 mL of ethanol–ethyl acetate (1:1, v:v) solvent, and centrifuged as earlier, which was repeated thrice. The resultant pellet was dissolved in 1.5 mL 6 M guanidine hydrochloride and incubated overnight at 37 °C. Next,

the sample was centrifuged (15,000×*g*, 5 min), and supernatant absorbance was recorded at 370 nm (spectrophotometer DR3900, Hach Lange, Germany). The supernatant protein concentration was measured with the BCA assay, and the protein-bound carbonyl content (mmol/kg soluble protein) was calculated using Eq. (3.6):

$$\text{Carbonyl content} = \frac{Ab_{sample} - Ab_{blank}}{\varepsilon \times l \times protein\ concentration} \quad (3.6)$$

where Ab_{sample} and Ab_{blank} were the absorbances of the sample and blank, respectively, ε is the molar extinction coefficient of carbonyls (22,000 M^{-1} cm^{-1}) and *l* is the cuvette optical path (1 cm).

3.2.9 Surface hydrophobicity

Surface hydrophobicity of proteins in solutions or dispersions was measured by using ANSA as a fluorescence probe (Haskard & Li-Chan, 1998). The sample was diluted to the desired total protein concentration (0.05−0.25 mg/mL, measured with the BCA assay) using 0.01 mol/L phosphate buffer at pH 7.0, after which 40 µL ANSA stock solution (8×10^{-3} mol/L in 0.01 mol/L pH 7.0 phosphate buffer) were added to 2 mL of this diluted sample in a quartz cuvette. The mixtures were stirred with a magnetic bar and stored in the dark for 3 min before measurement. Fluorescence intensity was recorded at 390 (excitation) and 470 nm (emission) using a Shimadzu RF-6000 fluorimeter (Shimadzu, Kyoto, Japan) with slit widths of 5 nm for both excitation and emission. The initial slope of the fluorescence intensity (after blank subtraction) versus protein concentration (mg/mL) was obtained by linear regression analysis and used as an index of surface hydrophobicity.

3.2.10 Intrinsic fluorescence measurements

The intrinsic fluorescence of each sample was determined using the same fluorimeter as in 2.9 and based on the method of Tao et al. (2018). The excitation wavelength was 285 nm, and the intrinsic spectra were recorded between 300 and 400 nm at 60 nm/min scanning speed using slit widths of 5 nm. Prior to analysis, the samples were diluted to a protein

concentration of 1 g/L (measured with the BCA assay) with phosphate buffer (0.01 mol/L, pH 7.0).

3.2.11 Adsorption kinetics

The interfacial tension between stripped rapeseed oil and aqueous solutions (protein concentration 0.1 g/L, measured with the BCA assay) was measured with an automated drop volume tensiometer (Tracker™, Teclis-IT Concept, Longessaigne, France) by analyzing the axial symmetric shape (Laplace profile) of a rising oil drop (40 mm^2) in the aqueous solution. Prior to each experiment, the surface tension between air and water was measured (~ 72 mN/m) to ensure that the syringe, needle, and cuvette were clean. All measurements were conducted for 2 h at 20 °C.

3.2.12 Particle size distribution (PSD)

The size distribution of insoluble fractions was measured by a laser diffraction particle size analyzer (Mastersizer 3000, Malvern Instruments, Worcestershire, UK), by dispersing in water and stirring at 1400 rpm in a dispersion unit (Hydro SM). The refractive indices of protein and water were 1.45 and 1.33, respectively. The absorption index of protein was set to 0.001.

The size distribution of soluble fractions was estimated by dynamic light scattering using a Zetasizer Ultra (Malvern Instruments, Worcestershire, UK). The samples were properly diluted in water to avoid multiple scattering before placing them in a disposable cell (DTS 1080) for analysis. The refractive and absorption indices used for protein were 1.45 and 0.001, respectively.

3.2.13 Statistical analysis

All measurements were done at least in triplicate on samples prepared at least in duplicate in independent experiments. The data were expressed as mean values ± standard deviation. Data were subjected to one-way analysis of variance (ANOVA) using the software package IBM SPSS statistics 23.0.0.2 (SPSS Inc, Chicago, Illinois, USA). The Tukey HSD method was conducted post-hoc for mean comparisons, with $P < 0.05$ being considered as significant.

The lowercase letters in all figures are for comparison of different fractions within one system. The bold italic uppercase letters are for comparison between SPI and SPI-dextran systems, within the same fraction. The normal uppercase letters are for comparison between SPI and SPI-glucose systems within the same fraction.

3.3 Results and discussion

3.3.1 Free amino group content and supramolecular assembly state

At the early stages of the Maillard reaction, ε-amino groups of proteins react with carbonyl groups of reducing sugars to form so-called Amadori compounds (Silván, van de Lagemaat, Olano, & del Castillo, 2006). In SPI-carbohydrate mixtures (**Figure 3.2 A-D & S3.2**), the free amino group contents significantly decreased ($P < 0.05$) after dry heating. Moreover, for SPI-dextran conjugates (**Figure 3.2A, 3.2C & S3.2A**), higher amounts of free amino groups were measured compared to SPI-glucose conjugates (**Figure 3.2B, 3.2D & S3.2B**). The decrease in free amino group content is generally interpreted in literature as a marker for protein glycation (Akhtar & Ding, 2017). The higher free amino group content in SPI-dextran than SPI-glucose conjugates could be explained by (i) at the same SPI-carbohydrate weight ratio, more glucose is present in the mixture than dextran due to its lower molecular weight, which ends up with more reducing end in the mixture, and thus glucose molecules are more likely to react with lysine residues of protein molecules; (ii) dextran is known to react slower than glucose, and (iii) long carbonic chain of dextran may limit protein glycation via steric hindrance (Wang & Ismail, 2012).

However, these results provide additional highlights: first, the second wet heating step applied to the insoluble fractions (i.e., pellet and retentate) increased the concentration of free amino groups (**Figure 3.2 & S3.2**); and second, the apparent loss in free amino groups induced by dry heating is also observed in SPI where heated without carbohydrates (**Figure 3.2E**). These results indicate that other mechanisms (apart from protein glycation) are responsible for the decrease in free amino groups detected by the OPA method. One possible explanation is the protein aggregation determined by thermal treatment as shown

by the particle size of the SPI which dramatically increased upon heating (**Figure 3.2F**). The aggregation determines the burying of amino groups inside the aggregates thus hindering access of the OPA reagent to free amino groups, as already reported for heated proteins (Mulcahy, Fargier-Lagrange, Mulvihill, & O'Mahony, 2017). This is also in line with the observation that the second wet heating increases the free amino group content. The heat treatment above the SPI denaturation temperature makes soy proteins unfold and de-aggregate, as is also clear from the decrease in particle size (**Figure 3.2F**). Such a change in conformation and in supramolecular structure could help free amino groups becoming available again for the OPA reagent, which would thus counteract, at least in part, the effect observed during the first dry heating step.

Lower concentration of free amino groups per gram of protein was observed in all insoluble fractions (i.e., pellet and retentate) compared to soluble fractions (i.e., supernatant and filtrate) (**Figure 3.2**). This is in line with the fact that the number of accessible free amino groups in aggregated protein clusters typical of the insoluble fractions would be lower than in the monomeric proteins present in the soluble fractions.

The outcomes of the OPA method are therefore indicative of a combined effect related not only to the degree of protein glycation, but also to the extent of protein aggregation a known, although too often underestimated, phenomenon, occurring during protein thermal treatment. To understand better the relationship between the extent of the MR and the functional properties of the glycated proteins it is thus important to measure other markers of the Maillard reaction, which is addressed in the next sections.

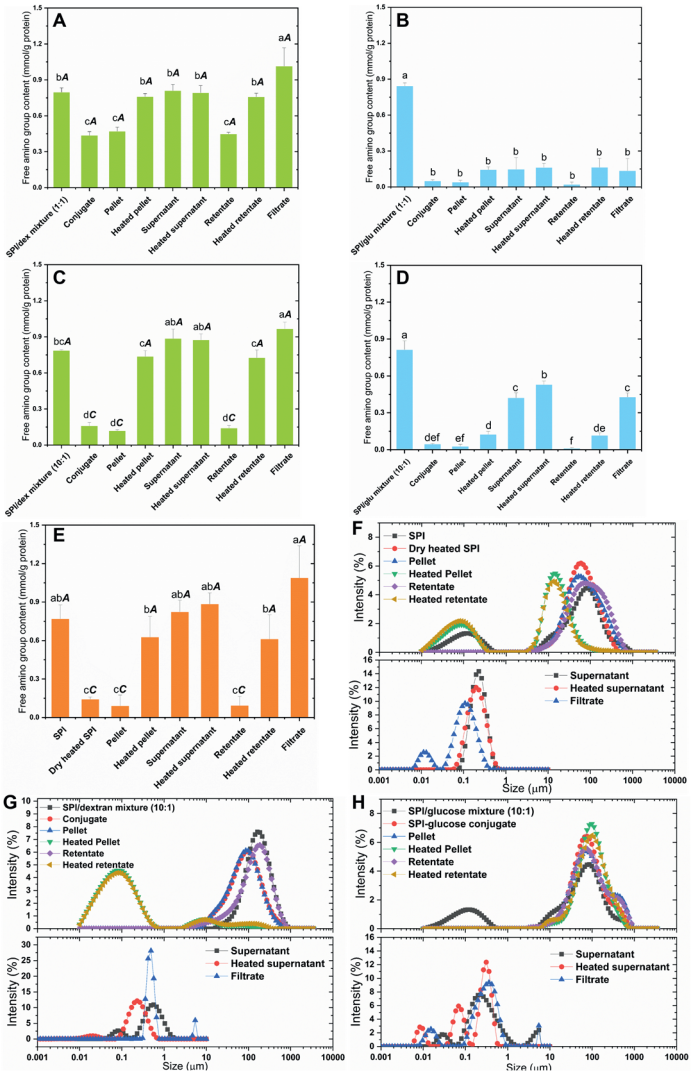

Figure 3.2. (A-E) Free amino group content in different fractions of SPI-dextran (1:1) (A), SPI-glucose (1:1) (B), SPI-dextran (10:1) (C), SPI-glucose (10:1) (D), and SPI (E) systems, as measured by the OPA method. The lowercase letter is for comparison among different fractions in the same system. The uppercase letter is for comparison of SPI and dextran systems within the same fraction. Different letters indicate significant differences ($P < 0.05$). (F-H) Particle size distributions of different fractions of SPI (F), SPI-dextran (10:1) (G), and SPI-glucose (10:1) (H).

3.3.2 Quantification of MRPs as markers of the Maillard reaction

3.3.2.1 Furosine

Furosine [ϵ-N-(furoylmethyl)-l-lysine] is a specific marker for the early stages of the Maillard reaction, being representative of the concentration of the Amadori product glucosyl lysine (Erbersdobler & Somoza, 2007). As shown in **Figure 3.3**, furosine was present (approximately 0.08 mg/g protein) in unheated SPI and unheated SPI/carbohydrate mixture, which is in agreement with Contreras-Calderón, Guerra-Hernández, and García-Villanova (2008), who reported similar values (0.06–0.33 mg/g of soy isolate). The presence of furosine in the starting samples is probably the result of thermal treatment applied during the production of SPI (Zhang et al., 2019b).

The concentration of furosine increased in all conjugates during the initial dry state heating (**Figure 3.3**); the increase being considerably higher in glucose than in dextran conjugates (**Figure 3.3 A-D**). As described earlier, glucose has more reducing ends than dextran and it is more reactive.

For glucose-based systems, no substantial differences in furosine content were found between the different SPI/glucose weight ratios tested (1:1, 2:1 and 10:1), whereas for dextran-based systems, the furosine content increased with decreasing the protein-to-dextran weight ratio (**Figure 3.3 & S3.3**). The molecular weight of SPI is much higher than that of glucose (ranging from around 200 000 to 600 000 g/mol for major SPI fractions (Mohamed & Morris, 1988), and 180.2 g/mol for glucose), and therefore the amount of glucose is already in excess and saturates the reactive sites of protein already at the lowest weight ratio of 10:1. This means that the protein concentration is the limiting factor for the formation of glucose-based Amadori compounds. Conversely, dextran (average molecular weight of 70 000 g/mol) has a molecular weight in the same range as that of SPI, leading to a higher concentration of Amadori compounds at higher dextran concentrations. In accordance with this, because of the large molecular weight and reactivity difference between both carbohydrates, the furosine content in the SPI conjugates was overall much lower with dextran than with glucose.

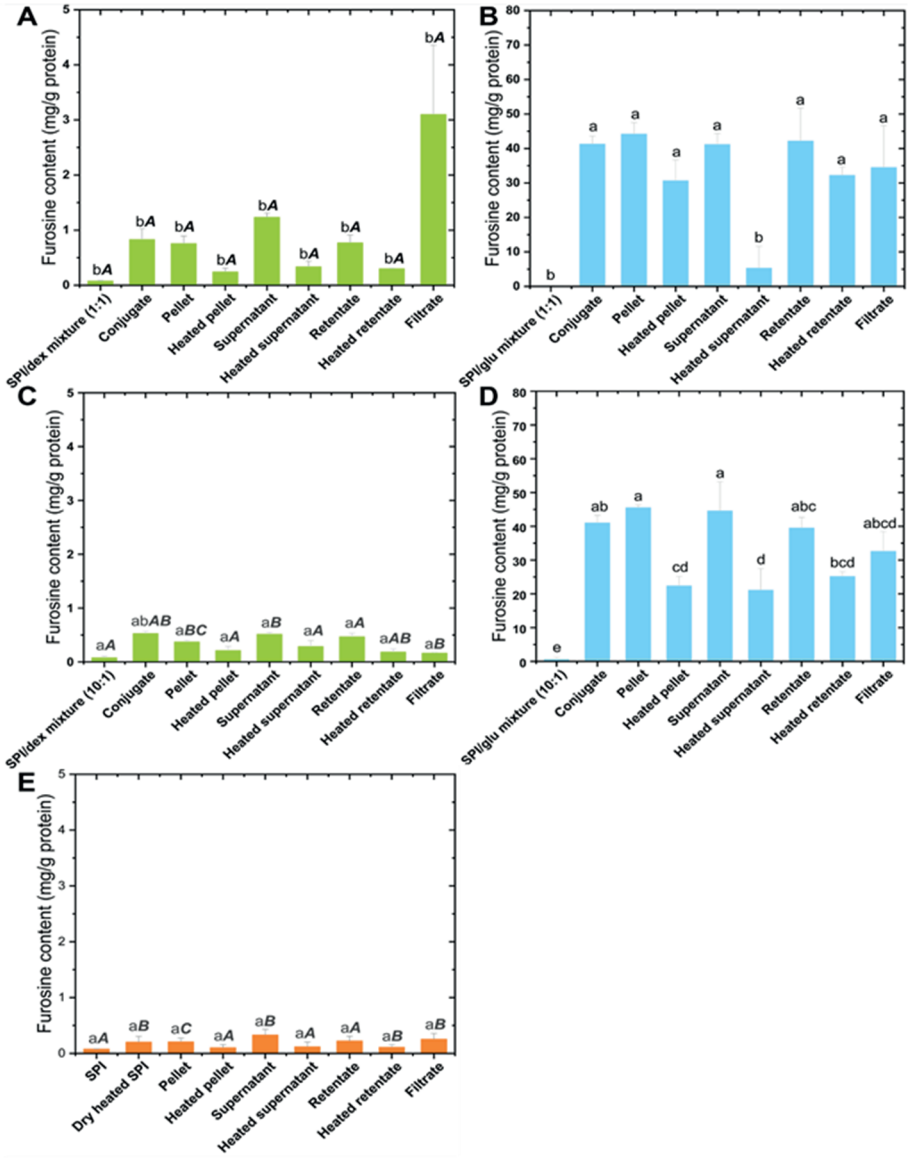

Figure 3.3. Furosine content in different fractions of SPI-dextran (1:1) (A), SPI-glucose (1:1) (B), SPI-dextran (10:1) (C), SPI-glucose (10:1) (D), and SPI (E) systems. The lowercase letter is for comparison among the different fractions in the same system. The uppercase letter is for comparison of SPI and dextran systems within the same fraction. Different letters indicate significant differences ($P < 0.05$).

In glucose-based systems, the furosine content decreased after the second heat treatment (**Figure 3.3 & S3.3**); this indicates that the related Amadori compounds degraded faster to intermediate and end products (Erbersdobler & Somoza, 2007), compared to dextran-based systems. This could be because the Amadori compound Nε-(1-Deoxy-D-fructos-1-yl)-L-lysine (fructosyl-lysine) evolves in intermediate and advanced MRPs, and the glucose present in the system does not have many other lysines to react with, thereby decreasing the overall furosine concentration. In addition, since glucose and dextran are hydrophilic and well soluble in aqueous media, the unreacted sugar molecules could be retained more in the soluble fractions, which could explain that the soluble fractions had a higher reactivity compared to insoluble fractions. It is clear that furosine is a sensitive marker for the early stages of the Maillard reaction, even when carbohydrates with low reducing activity such as dextran are used.

3.3.2.2 CML and CEL contents

The advanced stages of the Maillard reaction can be assessed through advanced glycation end products (AGEs), such as Nε-(carboxymethyl)-$_L$-lysine (CML), and Nε-(carboxyethyl)-$_L$-lysine (CEL). CML is formed mainly via two pathways: oxidation of fructosyl-lysine, and the direct reaction of glyoxal (GO) with lysine. CEL, a homolog of CML, is formed by the reaction of lysine with methylglyoxal (MGO). CEL and CML were present in the starting material (~0.09 and 0.08 mg/g protein, respectively) (**Figure S3.4**), in line with the previously proposed effect due to a thermal treatment applied during the production of commercial SPI.

The concentrations of CML in SPI and SPI-dextran systems ranged from 7.00 to 40.4 mg/100 g of protein, while the values of CEL ranged from 4.80 to 25.0 mg/100 g of protein. CML and CEL contents in SPI-glucose systems were respectively ~10 and 5 times higher than in SPI-dextran systems, respectively. In the SPI-glucose system, CML and CEL contents could reach 396.3 and 138.6 mg/100 g of protein. To the best of our knowledge, there has not been other studies reporting CML and CEL contents in SPI-based systems. However, in powdered soybean-based feed products, CML and CEL contents were found to be 9.94 ± 0.74 and 0.98

± 0.04 mg/100 g of protein, and increased to around 76 and 2.41 mg/100 g of protein, after being incubated at 110 °C for 60 and 45 min, respectively (Troise et al., 2015). This means that the concentrations of CML in SPI and SPI-dextran systems in our study was of the same order of magnitude as the ones reported by Troise and co-workers; while the CML and CEL contents in SPI-glucose systems were much higher than those reported by Troise et al. (2015). Glucose can directly oxidize to generate GO and MGO and further react with lysine to form CML and CEL, whereas dextran has first to be degraded into glucose units, then to be oxidized to induce GO and MGO (**Figure S3.4 A-F**). In addition, dehydration from C3-C4 and C5-C6 of glucose molecules followed by retro-aldol cleavage can also generate GO (Yaylayan & Keyhani, 2000), which would also promote higher CML content in SPI-glucose systems than in SPI-dextran systems.

3.3.2.3 Color

During the final stage of the Maillard reaction, melanoidins, i.e., brown nitrogenous polymers are formed, and hence the color development is often used to get preliminary information on the extent of the reaction in various samples. Color formation is particularly relevant during the first heating step as shown in **Table S3.1** for SPI and various mixtures with carbohydrates. Component b^* that is indicative of yellowness increased in all samples upon heat treatment, though the increase in some dextran-based samples was not significant ($P > 0.05$). Especially in glucose-based systems, L^* values (lightness) decreased and a^* values (redness) increased, together with the results that higher color difference and browning index were found in glucose-based systems than in dextran-based systems, indicating that the Maillard reaction proceeded further in the former ones, in line with the concentration of the various markers presented in sections 3.3.2.1 and 3.3.2.2. These results corresponded with those reported previously where glycation of SPI with gum acacia or soy hull hemicelluloses resulted in an increase in a^* and b^* values and decrease in L^* value, and these authors attributed the development of brown color to the formation of brown polymers at the final stage of Maillard reaction (Li et al., 2015; Wang, Wu, & Liu, 2017).

3.3.2.4 Protein-bound carbonyl content

Maillard reaction generates α-dicarbonyl compounds that can also induce the deamination of amino acids, resulting in the oxidative damage of protein (Estévez, 2011). Protein-bound carbonyls are typically used as biomarkers of protein carbonylation.

The initial carbonyl content in SPI was relatively high, ~12 mmol/kg of protein before heat treatment (**Figure 3.4E**). After the first heat treatment, the protein-bound carbonyl content of SPI-dextran systems was not significantly different ($P > 0.05$) from that of SPI (control), whereas SPI-glucose systems had 3-5 fold higher content than SPI (**Figure 3.4 & S3.5**). Liu, Xiong, and Butterfield (2000) reported a lower carbonyl level (6.4 mmol/kg of protein) for SPI, which is probably due to different processing methods used. In fact, they used freeze-dried SPI whereas the commercial SPI used in this study was prepared by spray drying; the latter being known to induce protein oxidation (Duque-Estrada et al., 2020). Carbonylation of proteins may occur via different pathways: first, oxidative deamination of amino acid side chains (e.g., lysine, arginine, threonine, and proline) via radical-mediation (Estévez, 2011). Second, α-dicarbonyl compounds formed by the Maillard reaction and/or sugar autoxidation may induce oxidative deamination (Akagawa, Sasaki, & Suyama, 2002). In the SPI-glucose systems, the MR was more intense, leading to more Amadori products and α-dicarbonyl compounds (section 3.3.2.), which eventually resulted in more severe protein oxidation.

Furthermore, we observed the simultaneous formation of CML, CEL, and protein-bound carbonyls (**Table S3.2**), which confirms that protein glycation and oxidation are intertwined. α-Aminoadipic semialdehydes (a typical protein oxidation product) can react with lysine residue through Schiff base formation or aldol condensation to form inter- and intra-molecular cross-links (Akagawa et al., 2002), indicating that protein oxidation is important in AGEs formation. Carbonylation of proteins is therefore only partially related to the MR development: therefore, in some food systems it is possible to find a correlation between the extent of protein carbonylation and the concentration of MRPs (like in this study) but in other systems for instance in fat-rich foods the two phenomena are rather separated.

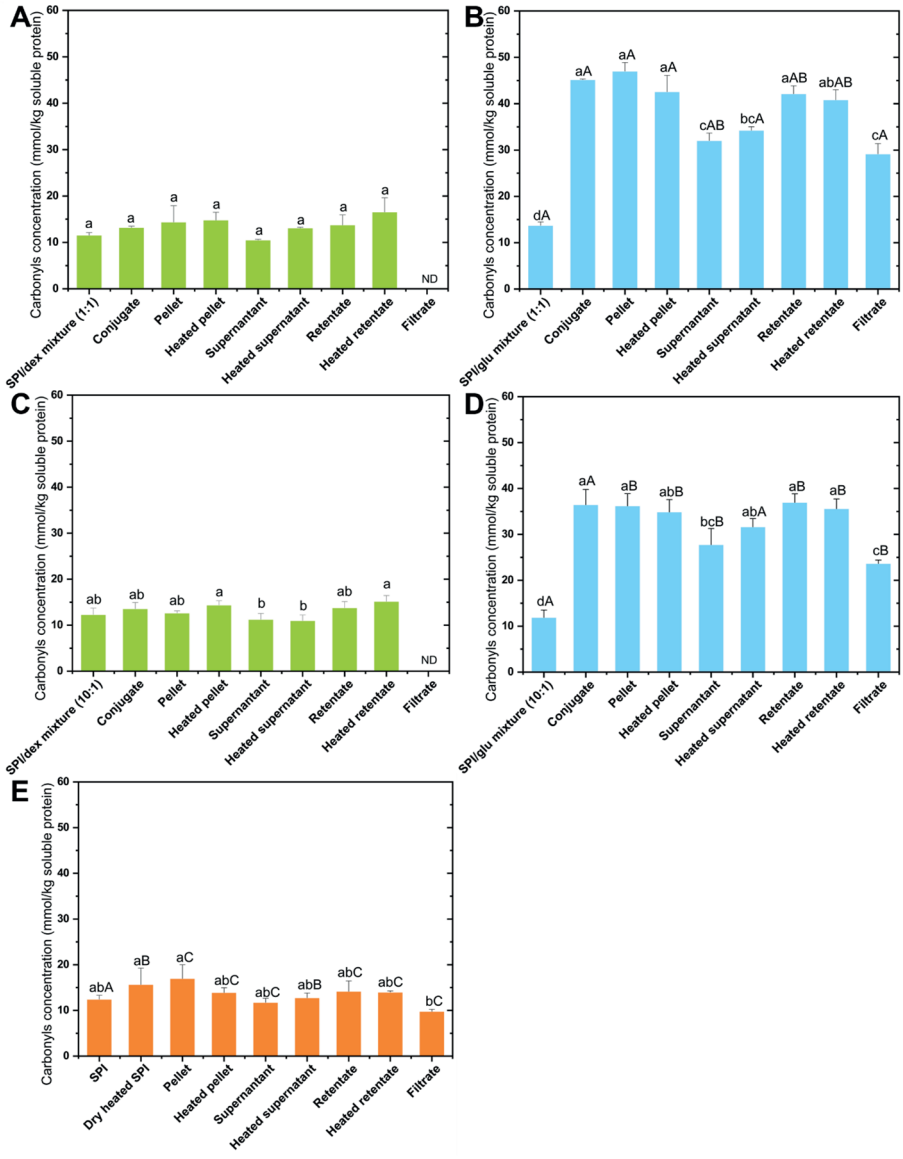

Figure 3.4. Protein-bound carbonyl contents in different fractions of SPI-dextran (1:1) (A), SPI-glucose (1:1) (B), SPI-dextran (10:1) (C), SPI-glucose (10:1) (D), and SPI (E) systems. The lowercase letter is for comparison of different fractions in the same system. The uppercase letter is for comparison of SPI and SPI-glucose systems within the same fractions. Different letters indicate significant differences ($P < 0.05$).

3.3.3 Conformational changes

3.3.3.1 Surface hydrophobicity (H_0) analysis

Protein surface-exposed hydrophobicity is used to identify conformation changes, and is closely related to emulsifying and foaming properties of proteins. Upon dry heating at 60 °C, the surface hydrophobicity of SPI, SPI-dextran (10:1) and SPI-glucose (10:1) samples decreased by around 51%, 54%, and 67%, respectively (**Figure 3.5**). The decrease in surface hydrophobicity could be due to the following reasons. (I) Covalent binding of the hydrophilic carbohydrates (i.e., dextran and glucose) to lysine residues via the Maillard reaction reduced the surface hydrophobicity of proteins; glucose being more potent than dextran because SPI-glucose system contained more hydrophilic AGEs and melanoidins (section 3.3.2.2 and 3.3.2.3) (Chen, Chen, Wu, & Yu, 2016). (II) Glycation influences the isoelectric point of the protein, eliminating one positive charge on the free amino group, which reduces the repulsion among equally charged molecules (Davidov-Pardo, Joye, Espinal-Ruiz, & McClements, 2015). (III) Protein aggregation (see section 3.3.1) that would reduce the exposure of hydrophobic sites on the protein surface.

In contrast with the first dry heating step, the second wet heating step has an opposite effect on surface hydrophobicity; a large increase in surface hydrophobicity was found for insoluble fractions of SPI and SPI-dextran systems (Figure 3.5 A&B). This can be caused by (i) exposure of hydrophobic groups due to partial protein unfolding, and (ii) dissociation of SPI aggregates, therewith exposing hydrophobic groups that were previously hidden inside. These samples also showed relatively high free amino group content as discussed earlier (section 3.3.1).

On the other hand, insoluble SPI-glucose systems did not show a change in surface hydrophobicity after the second heat treatment (Figure 3.5C); most likely their high degree of glycation, and thus advanced, covalently modified reaction products, lead to a system with irreversibly formed protein aggregate (section 3.3.2).

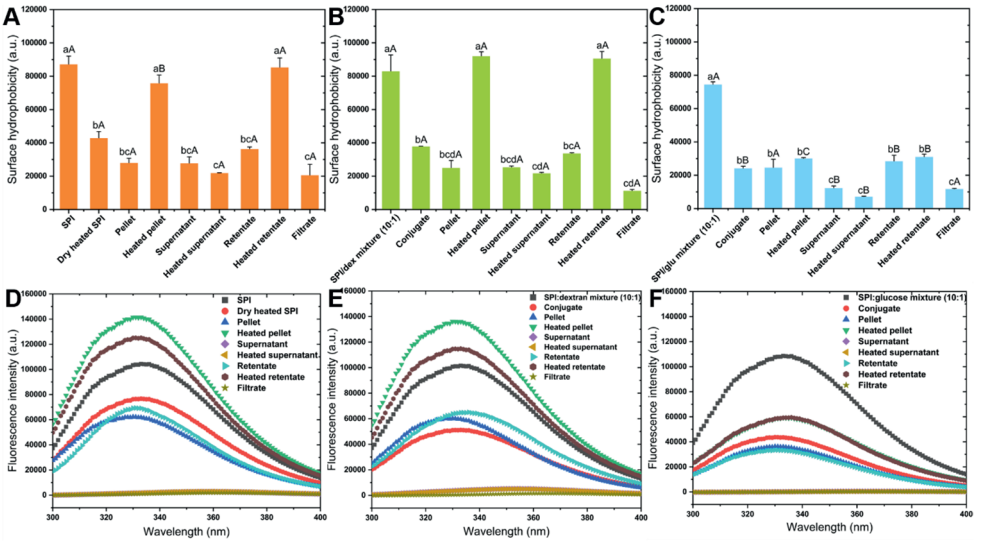

Figure 3.5. (A-C) Protein surface-exposed hydrophobicity of SPI (A), SPI-dextran (10:1) (B), and SPI-glucose (10:1) (C) systems. The lowercase is for comparison among different fractions in the same system. The uppercase is for comparison among different systems with the same fraction. Different letters indicate significant differences ($P < 0.05$). (D-F) Emission fluorescence spectra (λ_{ex}: 285 nm) in aqueous dispersions for SPI (D), SPI-dextran (10:1) (E), and SPI-glucose (10:1) (F) systems.

3.3.3.2 Intrinsic fluorescence analysis

To detect tertiary protein structure changes, the intrinsic fluorescence spectrum was determined. Depending on the microenvironment, the maximum emission (λ_m) can vary from 310 to 360 nm. When λ_m is lower than 330 nm, tryptophan (Trp) is considered to be in a nonpolar environment, while at λ_m >330 nm, it is in a polar environment (Vivian & Callis, 2001). We found a λ_m of SPI of 333 nm (**Figure 3.5D**), which is characteristic of a polar environment; similar results were reported by Shen & Tang (2012) who found 335.6 nm.

Upon the first dry heat treatment, the fluorescence intensity of SPI, SPI-dextran, and SPI-glucose conjugates decreased (**Figure 3.5 & Table S3.3**). The second heat treatment at 95 °C resulted in a huge increase in fluorescence intensity of insoluble fractions (heated pellet

and heated retentate) for SPI and SPI-dextran systems (**Figure 3.5 C&D**), and in a small increase for SPI-glucose systems (**Figure 3.5E**), which is in agreement with the surface hydrophobicity results. The decrease in intensity after the first heat treatment can be attributed to the aggregation of proteins, which shielded Trp residues in all samples. The shielding effect was more prominent in SPI-carbohydrate conjugates than dry heated SPI. It could be because the β-conglycinin and glycinin contain around 8 Trp residues located close to lysine residues (Keerati-u-rai, Miriani, Iametti, Bonomi, & Corredig, 2012), and carbohydrate molecules that react with those lysine residues via the Maillard reaction may block the fluorescent signal. No shift in λ_m was observed indicating that mild heat treatment (60 °C) did not greatly disrupt the protein structure. The second heat treatment may have caused unfolding of proteins and/or aggregate disassociation, thus exposing more hydrophobic groups leading to an increase in fluorescence intensity. Unfolding and dissociation of aggregates are less relevant for SPI-glucose systems, as argued in the previous section.

A slight blue shift of λ_m was observed for the insoluble fractions, indicating that the Trp residues were now present in a more nonpolar environment, for example within the hydrophobic core of aggregates. In the soluble fractions (supernatant, heated supernatant, and filtrate) there was a red shift of λ_m to 363-367 nm (**Figure 3.5 & Table S3.3**) indicative of a more polar environment, although the overall effect was very low compared to that found for insoluble fractions.

3.3.4 Interfacial tension Changes

Changes in the chemical and structural properties of proteins will affect their interfacial properties, herein assessed through interfacial tension measurements at the stripped rapeseed oil-water interface, and presented as semi-log plots (**Figure 3.6**). Protein adsorption can be divided into three stages (Beverung, Radke, & Blanch, 1999): (i) proteins diffuse from the bulk to the interface, and interfacial tension remains constant or decreases slightly during this so-called lag phase; (ii) as the interface gets covered with proteins, the interfacial tension decreases strongly while proteins may undergo conformational changes,

rearrange and reorient; during stage (iii) protein molecules continue to change conformation and form a viscoelastic film, leading to a small decrease in interfacial tension.

The interfacial tension between stripped rapeseed oil and water was first confirmed to be stable at around 30 mN/m; no surface-active species were present (**Figure S3.6**). In the presence of any of the samples (**Figure 3.6**), interfacial tension progressively decreased, but no equilibrium was reached within 7200 s. The soluble fractions (i.e., supernatant, heated supernatant, and filtrate) had a shorter lag phase and decreased the interfacial tension faster than the insoluble fractions (e.g., pellet, retentate), indicating faster adsorption, which is logical given their smaller size (**Figure 3.1 F-H**), and expected ease of orientation at the interface. Conversely, insoluble fractions (pellet and retentate) had a larger particle size (**Figure 3.1 F-H**), and thus diffusion took more time. Furthermore, the insoluble fractions that were subjected to the second heat treatment (i.e., heated pellet and heated retentate) decreased interfacial tension slightly faster than the same samples without this treatment, which may be indicative of improved interfacial orientation due to higher exposed hydrophobicity (section 3.3).

Protein glycation via the Maillard reaction was previously shown to improve the interfacial activity of soy β-conglycinin (Zhang, Wu, Yang, He, & Wang, 2012); however, in the present research, we only found small changes. Conjugation with dextran slightly increased the surface activity of SPI, but this was not the case with glucose (**Figure 3.6 B&C**). Since the extent of MR was high in the SPI-glucose system (section 3.2), a large number of hydrophilic sugars were attached to the protein molecules, which decreased the surface hydrophobicity (**Figure 3.5C**). For the dextran system, less glycation took place, and the molecule was more hydrophobic. This could explain the difference in surface behavior. However, also more protein aggregates appeared in the SPI-glucose systems than in the SPI-dextran systems (section 3.1), which can also have reduced the observed surface activity. The surface activity can be changed using different fractions of glycated SPI results from different treatments (e.g., water-soluble and insoluble, dry and wet heating). This stresses the relevance of our research, and thus the importance of characterizing components used for emulsion

formulation, and that we found to hugely vary depending on the treatment that they received (even as a raw material).

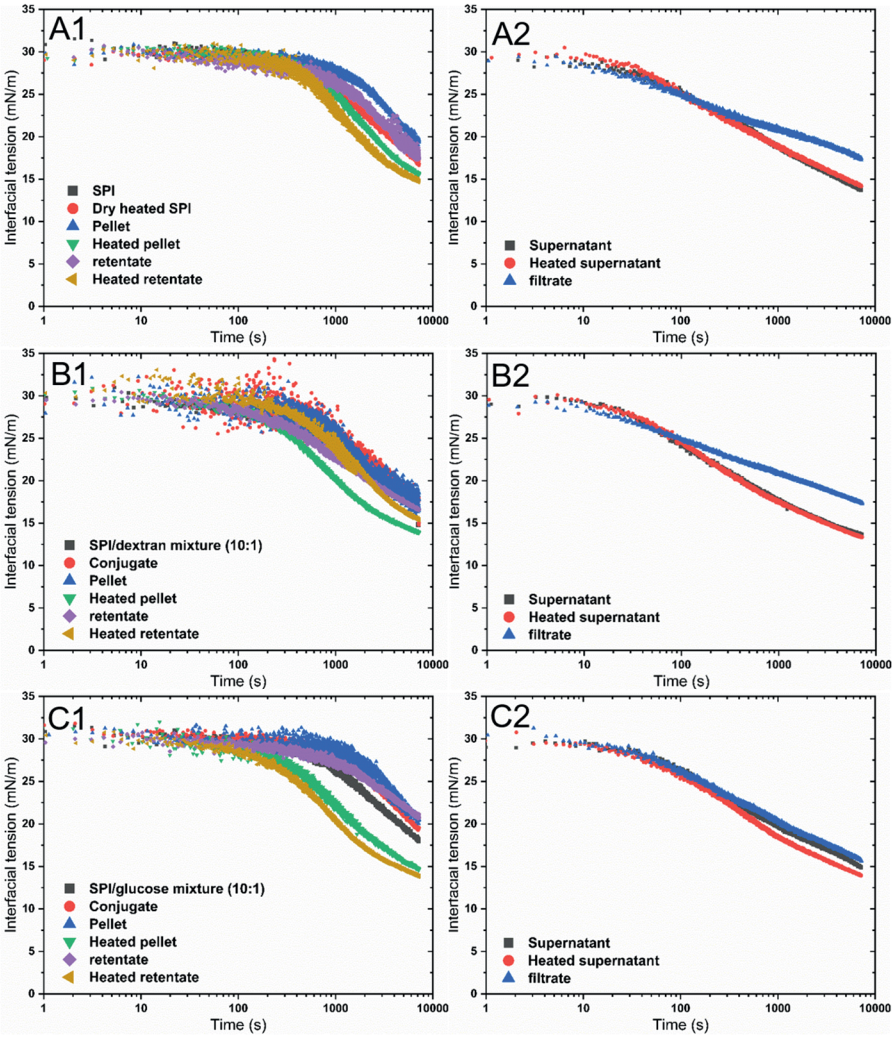

Figure 3.6. Adsorption kinetics of the insoluble fractions (left) and soluble fractions (right) of SPI (A), SPI-dextran (10:1) (B), and SPI-glucose (10:1) (C) systems at the oil-water interface as a function of time (log scale). For clarity, only one representative curve is shown per sample, but similar results were obtained on multiple measurements using independent duplicates.

3.4 Conclusion

The decrease in free amino groups upon protein glycation measured with OPA method was modulated by protein structural changes and should thus be interpreted with caution. Dry and subsequent wet heat treatment differently affect the protein products: dry heating of SPI and carbohydrate led to both protein glycation (as evidenced by the increase in furosine, CML, CEL, and protein-bound carbonyls) and protein aggregation (as evidenced by the decrease in free amino groups in SPI); while the subsequent wet heating above the denaturation temperature of SPI induced proteins to unfold and de-aggregate.

The surface activity of the fractions can be related to the surface hydrophobicity (fluorescence), with water-soluble fractions showing higher activity than insoluble fractions, as would be the case for dextran conjugates compared to their glucose counterparts. Heat treatment of the insoluble dextran fractions obtained after the Maillard reaction slightly improved surface hydrophobicity, and ability to lower surface tension due to unfolding and disaggregation most probably, but this was not the case for glucose conjugates that remained aggregated.

Therefore, on one hand, it is recommended to fractionate the complex reaction mixture for analyzing it thoroughly using specific Maillard reaction markers, instead of the very general OPA method; on the other hand, it is useful to link the chemical information to the functionality of different fractions. Based on this analysis, a comprehensive understanding of the properties in each SPI fraction can be obtained, and a rational design of e.g., food emulsions and foams using different fractions of glycated plant proteins can be achieved. In this way, effective utilization of each fraction can be achieved to minimize losses of precious materials.

Supplementary materials

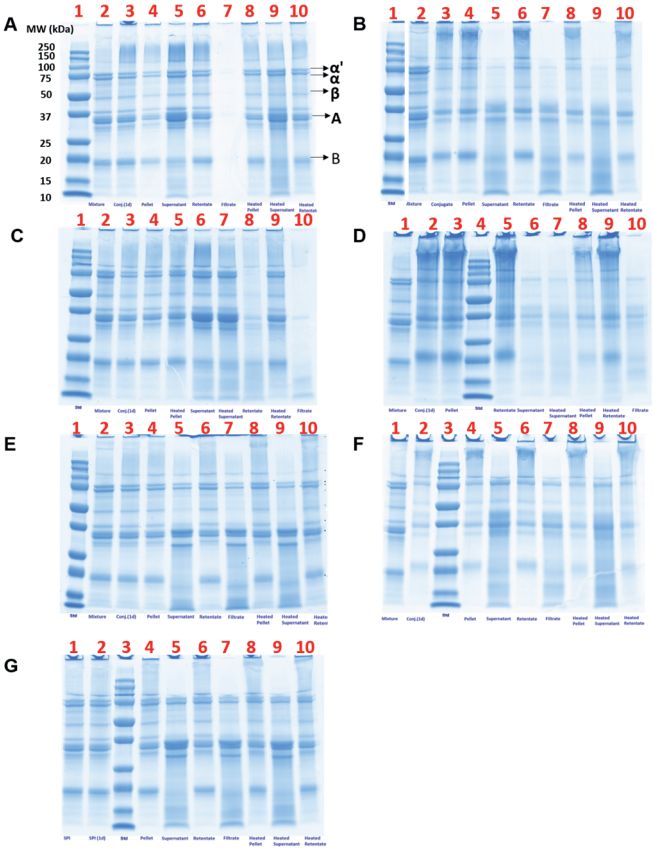

Figure S3.1. SDS-PAGE patterns (reducing conditions) for SPI-dextran (1:1) (A), SPI-glucose (1:1) (B), SPI-dextran (2:1) (C), SPI-glucose (2:1) (D), SPI-dextran (10:1) (E), SPI-glucose (10:1) (F), and SPI (G) systems. For A, B, and E, lane: 1, protein marker; 2, mixture; 3, conjugate; 4, pellet; 5, supernatant; 6, retentate; 7, filtrate; 8, heated pellet; 9, heated supernatant; 10, heated retentate. For C, lane: 1, protein marker; 2, mixture; 3, conjugate; 4, pellet; 5, heated pellet; 6, supernatant; 7, heated supernatant; 8, retentate; 9, heated retentate; 10, filtrate. For D, lane: 1, mixture; 2, conjugate; 3, pellet; 4, protein marker; 5, retentate; 6, supernatant; 7, heated supernatant; 8, heated pellet; 9, heated retentate; 10, filtrate. For F, lane: 1, mixture; 2, conjugate; 3, protein marker; 4, pellet; 5, supernatant; 6, retentate; 7, filtrate; 8, heated pellet; 9, heated supernatant; 10, heated retentate. For G, lane: 1, SPI; 2, dry heated SPI; 3, protein marker; 4, pellet; 5, supernatant; 6, retentate; 7, filtrate; 8, heated pellet; 9, heated supernatant; 10, heated retentate.

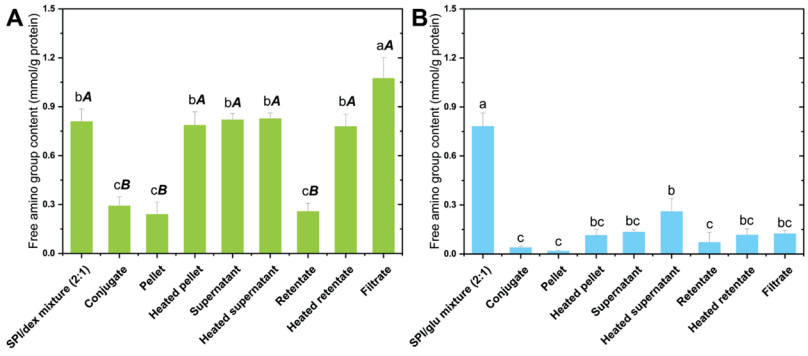

Figure S3.2. Free amino group contents in different fractions of SPI-dextran (2:1) (A) and SPI-glucose (2:1) (B) systems. The lowercase is for comparison among different fractions in the same system. The uppercase is for comparison of SPI and dextran systems within the same fraction. Different letters indicate significant differences ($P < 0.05$).

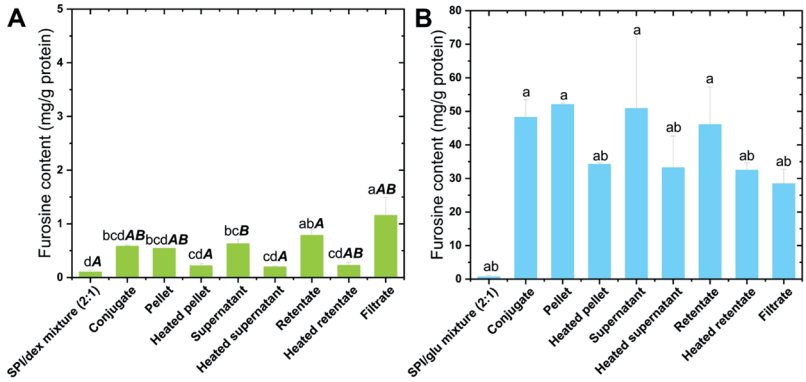

Figure S3.3. Furosine content in different fractions of SPI-dextran (2:1) (A) and SPI-glucose (2:1) (B) systems. The lowercase is for comparison among different fractions in the same system. The bold italic uppercase is for comparison of SPI and dextran systems within the same fraction. The normal uppercase is for comparison of SPI and glucose systems within the same fraction. Different letters indicate significant differences ($P < 0.05$).

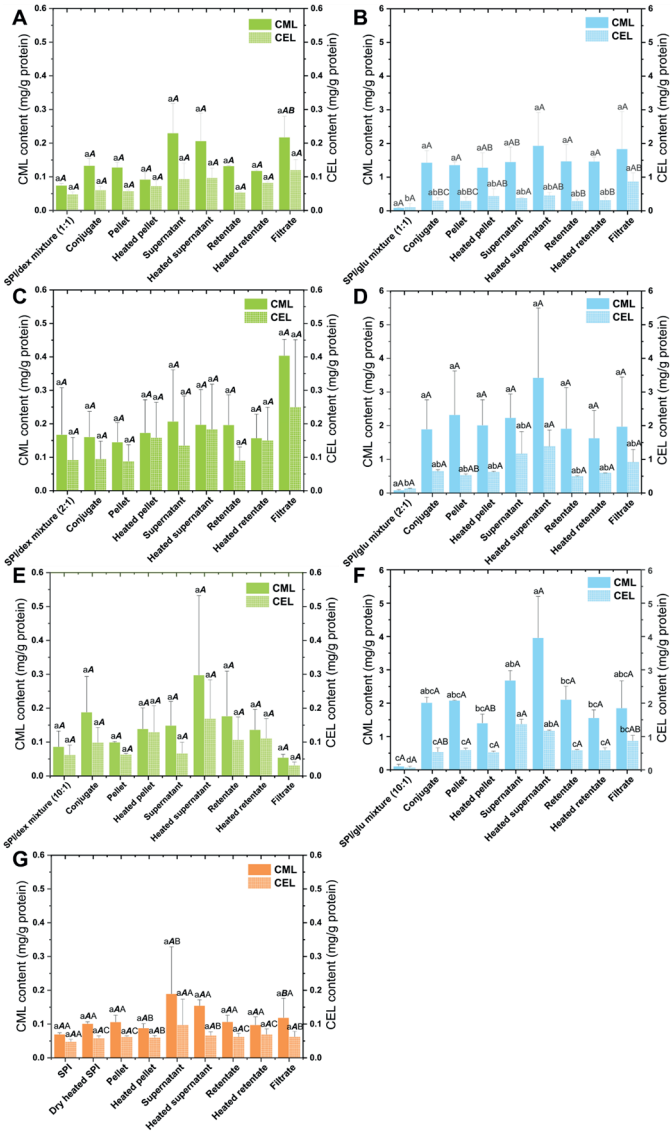

Figure S3.4. Nε-(carboxymethyl)-L-lysine (CML) and Nε-(carboxyethyl)-L-lysine (CEL) contents in different fractions of SPI-dextran (1:1) (A), SPI-glucose (1:1) (B), SPI-dextran (2:1) (C), SPI-glucose (2:1) (D), SPI-dextran (10:1) (E), SPI-glucose (10:1) (F) , and SPI (G) systems. The lowercase is for comparison among different fractions in the same system. The bold italic uppercase is for comparison of SPI and dextran systems within the same fraction. The normal uppercase is for comparison of SPI and glucose systems within the same fraction. Different letters indicate significant differences ($P < 0.05$).

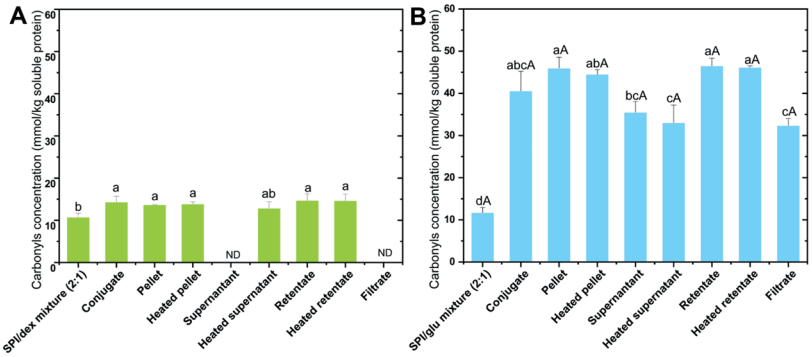

Figure S3.5. Protein-bound carbonyl contents in different fractions of SPI-dextran (2:1) (A) and SPI-glucose (2:1) (B) systems. The lowercase is for comparison among different fractions in the same system. The bold italic uppercase is for comparison of SPI and dextran systems within the same fraction. The normal uppercase is for comparison of SPI and glucose systems within the same fraction. Different letters indicate significant differences ($P < 0.05$).

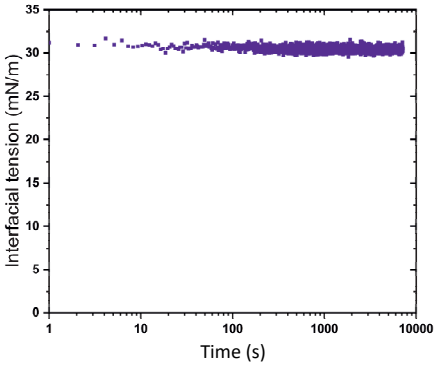

Figure S3.6. Interfacial tension of the stripped oil-water interface in the absence of protein as a function of time (log scale).

Table S3.1. HunterLab color values, color difference (ΔE), and browning index (BI) of the SPI and SPI-carbohydrate mixture powder samples and their dry heated powder samples after the first heat treatment.

Time	SPI			SPI : dextran =10:1			SPI : dextran =2:1			SPI : dextran =1:1			SPI : glucose =10:1			SPI : glucose =2:1			SPI : glucose =1:1		
	L^*	a^*	b^*	L^*	a^*	b^*	L^*	a^*	b^*	L^*	a^*	b^*	L^*	a^*	b^*	L^*	a^*	b^*	L^*	a^*	b^*
0 h	79.56 ± 5.13^{a}	0.18 ± 1.19^{a}	16.27 ± 1.66^{a}	78.13 ± 2.02^{a}	0.74 ± 0.44^{a}	16.55 ± 1.22^{a}	78.77 ± 0.97^{a}	0.60 ± 0.12^{a}	15.76 ± 0.53^{b}	80.81 ± 0.74^{a}	0.22 ± 0.19^{a}	14.33 ± 0.63^{a}	77.75 ± 2.39^{a}	0.83 ± 0.43^{b}	17.11 ± 1.79^{b}	81.03 ± 0.74^{a}	0.24 ± 0.16^{b}	13.99 ± 0.72^{b}	81.64 ± 0.29^{a}	0.10 ± 0.04^{b}	13.65 ± 0.10^{b}
24 h	79.36 ± 5.26^{a}	0.50 ± 1.20^{a}	18.13 ± 2.77^{a}	78.25 ± 2.42^{a}	0.70 ± 0.43^{a}	18.75 ± 1.60^{a}	78.09 ± 1.07^{a}	0.61 ± 0.37^{a}	17.99 ± 1.04^{a}	80.09 ± 1.32^{a}	0.37 ± 0.22^{a}	16.68 ± 1.15^{a}	74.21 ± 1.54^{a}	4.21 ± 0.65^{a}	27.79 ± 0.93^{a}	76.82 ± 0.39^{b}	2.98 ± 0.13^{a}	26.58 ± 0.28^{a}	77.09 ± 1.91^{a}	2.70 ± 0.26^{a}	25.38 ± 0.43^{a}
Color difference (ΔE)	1.90 ± 1.10^{B}			2.24 ± 0.60^{B}			2.38 ± 0.64^{B}			2.49 ± 0.71^{B}			11.76 ± 2.01^{A}			13.55 ± 0.59^{A}			12.91 ± 1.01^{A}		
Browning index (BI)	25.83 ± 7.45^{B}			27.22 ± 3.93^{B}			25.89 ± 2.40^{B}			22.93 ± 2.40^{B}			49.48 ± 3.20^{A}			43.82 ± 0.70^{A}			41.14 ± 1.76^{A}		

Different lowercase in each column and different uppercase in each row represent statistically significant difference ($P < 0.05$).

Table S3.2. Correlation matrix.

	Carbonyls	CML	CEL
Carbonyls	1.000	0.810**	0.640**
CML	0.810**	1.000	0.926**
CEL	0.640**	0.926**	1.000

($^{**}P < 0.01$)

Table S3.3. Maximum emission wavelength (λ_m) and fluorescence intensity in fluorescence spectra of different samples.

Sample	SPI		SPI : dextran = 10 : 1		SPI : glucose = 10 :1	
	Maximum emission (λ_m)	Fluorescence intensity at λ_m	Maximum emission (λ_m)	Fluorescence intensity at λ_m	Maximum emission (λ_m)	Fluorescence intensity at λ_m
SPI or SPI/carbohydrate mixture	333.0 ± 0.0	114445 ± 14284^{abA}	333.0 ± 0.0	106687 ± 7290^{bA}	333.0 ± 0.0	116323 ± 10976^{aA}
Conjugates	333.0 ± 0.0	85250 ± 12034^{abA}	333.0 ± 0.0	51088 ± 161^{cAB}	333.0 ± 0.0	49610 ± 8291^{bB}
Pellet	330.0 ± 0.0	78671 ± 23231^{bA}	330.0 ± 0.0	53579 ± 9378^{cA}	330.0 ± 0.0	45951 ± 13735^{bA}
Heated pellet	333.0 ± 0.0	137908 ± 5024^{abA}	331.5 ± 1.5	132919 ± 4507^{aA}	336.0 ± 0.0	63022 ± 5418^{bB}
Supernatant	357.5 ± 0.5	3542 ± 998^{cAB}	354.0 ± 0.0	5086 ± 83^{dA}	363.5 ± 0.5	971 ± 447^{cB}
Heated supernatant	357.5 ± 0.5	3654 ± 906^{cA}	354.0 ± 0.0	4516 ± 659^{dA}	363.5 ± 0.5	904 ± 77^{cB}
Retentate	330.5 ± 0.5	88364 ± 26998^{abA}	332.0 ± 1.0	66006 ± 1936^{cA}	330.0 ± 0.0	45270 ± 16772^{bA}
Heated retentate	332.0 ± 1.0	140439 ± 21724^{aA}	333.0 ± 0.0	120290 ± 7684^{abAB}	334.5 ± 1.5	64178 ± 6575^{bB}
Filtrate	363.5 ± 0.5	1904 ± 69^{cA}	366.0 ± 0.0	1234 ± 383^{dAB}	366.5 ± 0.5	752 ± 0^{cB}

Different lowercase in each column and different uppercase in each row represent statistically significant difference ($P < 0.05$).

4

Antioxidant potential of non-modified and glycated soy proteins in the continuous phase of oil-in-water emulsions

This chapter has been published as Feng, J., Schroën, K., Fogliano, V., & Berton-Carabin, C. (2021). Antioxidant potential of non-modified and glycated soy proteins in the continuous phase of oil-in-water emulsions. *Food Hydrocolloids*, *114*, 106564. https://doi.org/https://doi.org/10.1016/j.foodhyd.2020.106564

Abstract

Food emulsions with a high omega-3 polyunsaturated fatty acid content are desirable from a nutritional point of view. However, such products are particularly prone to lipid oxidation and have thus a limited shelf-life. The use of natural antioxidants is a promising and consumer-oriented strategy to counteract lipid oxidation. The addition of an excess of proteins to the continuous phase may be considered in that respect.

Starting emulsions were prepared with either Tween 20 (a nonionic surfactant) or whey protein isolate (WPI). They were then supplemented with non-modified or dextran-glycated soy protein isolate (SPI) added to the continuous phase. As controls, emulsions with excess WPI or unreacted SPI/dextran mixture were also prepared. The addition of these compounds did not significantly affect the physical stability of emulsions, while the lipid oxidation inhibition capacity was, starting from the highest, in the order glycated SPI mixture ≈ SPI/dextran mixture > SPI > WPI. This suggests that SPI ingredients and dextran hold potential for mitigating lipid oxidation in emulsions. The antioxidant mechanisms involved include iron-binding and free radical-scavenging activities; the former effect is predominant by preventing transition metals from approaching the oil-water interface. Furthermore, compared to WPI-stabilized emulsions, the antioxidant potential of excess proteins is boosted in Tween 20-stabilized emulsions. Interaction of surfactants with proteins could lead to a conformational change of proteins, which could increase their ability to bind molecules involved in the reaction cascade. This study shows that it is possible to tune emulsions towards greater oxidative stability by adjusting protein localization and continuous phase composition, which reduces the need for synthetic antioxidants.

4.1 Introduction

There is an increasing trend in fortifying food products with health-promoting omega-3 polyunsaturated fatty acids (EFSA Panel on Dietetic Products and Allergies (NDA), 2010). This is often challenging because these components are highly sensitive to oxidation (McClements & Decker, 2018). Lipid oxidation generates off-flavors and forms products with questionable health effects, such as lipid peroxides or malondialdehyde, and thus deteriorates the sensory and nutritional quality of foods (Addis, 1986; Villière et al., 2007). A feasible strategy to counteract lipid oxidation is to use antioxidants. Several effective synthetic antioxidants (e.g., butylated hydroxytoluene (BHT), ethylenediamine tetraacetic acid (EDTA)) have already been employed, but this is less and less desired by consumers (McClements & Decker, 2000; Pokorný, 2007). There is thus a strong incentive to use natural antioxidants (e.g., tocopherols), although their efficiency is often not optimal (Pokorný, 2007; Ragnarsson et al., 1977). Other currently dominating trends in food formulation include the clean-label trend, which strives for minimizing the use of food additives; and the rising interest in plant-derived ingredients (Berton-Carabin & Schroën, 2019).

In this framework, plant-based ingredients that are inherently part of conventional food emulsion formulation would be ideal candidates. Here, we focused on the use of proteins since they can inhibit lipid oxidation by multiple mechanisms, including scavenging free radicals, chelating transition metals, and inactivating reactive oxygen species (Elias et al., 2008). Protein antioxidant activity is affected by multiple factors, such as molecular properties, charge, and location. Some amino acids (e.g., histidine, tryptophan, methionine, and glutamic acid) can act as metal chelators and/or free-radical scavengers; depending on charge and localization of proteins, they may exhibit different effects on lipid oxidation. For instance, negatively charged proteins adsorbed at the interface may bring cationic metal ions in close proximity to lipids, which favors lipid oxidation; while those remaining in the continuous phase may bind metal ions and prevent them from approaching the interface, which retards lipid oxidation (Gumus et al., 2017). Non-adsorbed proteins present in the continuous phase of emulsions have been consistently reported to prevent or delay lipid

oxidation (Dong et al., 2011; Elias et al., 2005; Faraji et al., 2004; Gumus et al., 2017; Shi et al., 2019). For instance, whey protein isolate (WPI)-stabilized emulsions where the unadsorbed WPI was removed were less oxidatively stable than those where unadsorbed WPI was not removed (Faraji et al., 2004). Similarly, Elias and co-workers reported that β-lactoglobulin in the continuous phase of O/W emulsions, even a low concentration, could inhibit lipid oxidation. This is probably due to the free radical scavenging activity of the free cysteine and tryptophan residues in β-lactoglobulin (Elias et al., 2005).

Moreover, an interesting approach to improve protein antioxidant activity is their derivatization via the Maillard reaction (MR). The latter is a set of chemical reactions involving the condensation between amino compounds and reducing sugars that occur during heat treatment of products (Hodge, 1953). Glycated proteins have been shown to exhibit higher antioxidant activity (such as reducing power and radical scavenging activity) than initial proteins (Liu et al., 2014). The reasons for this can be (i) the electron donating ability of the exposed amino groups (e.g., tryptophan, tyrosine, valine, and phenylalanine) as a result of protein denaturation during glycation and (ii) the hydrogen donating ability of some intermediate or final MRPs (e.g., reductones and melanoidins) (Khadidja, Asma, Mahmoud, & Meriem, 2017; Q. Liu, Li, Kong, Jia, & Li, 2014; Nasrollahzadeh, Varidi, Koocheki, & Hadizadeh, 2017; Sproston & Akoh, 2016). Moreover, their use as emulsifiers has been reported to better protect lipids against oxidation compared to the original proteins, which might be attributed to their improved antioxidant capacity and/or physical barrier properties (Cermeño et al., 2019; Shi et al., 2019). Yet, the potential of glycated proteins to inhibit lipid oxidation when present in the aqueous phase of emulsions is not clear yet. For instance, Dong and co-workers observed that casein peptides glycated with glucose did not protect lipids against oxidation when present in the continuous phase of emulsions (Dong et al., 2011, 2012).

The current research aimed to assess the ability of soy protein ingredients, added to the continuous phase of pre-formed O/W emulsions, to prevent lipid oxidation. The experiments were designed to disentangle any mixed effect of the continuous phase and

interfacial protein ingredients, and to understand the potential of such ingredients as natural antioxidants. To achieve this, starting O/W emulsions stabilized by common emulsifiers (Tween 20 or whey protein isolate (WPI)) were prepared such that minimal amounts of excess emulsifier remained in the continuous phase. They were supplemented with non-modified or dextran-glycated soy protein isolate (SPI) added to the continuous phase. Emulsions with excess WPI or unreacted SPI/dextran mixture were also investigated. The emulsions' physical stability and lipid oxidation were monitored during storage.

4.2 Materials and methods

4.2.1 Materials

Soy protein isolate (SPI, 79.14 ± 0.66%, N × 5.71; SUPRO® 500E) was supplied by Solae (St Louis, MO, USA). Whey protein isolate (WPI, 88.11 ± 1.15%, N × 6.25) was obtained from Davisco (Lancy, Switzerland). Protein concentration was determined by Dumas (Interscience Flash EA 1112 series, Thermo Scientific, Breda, The Netherlands). Refined rapeseed oil was purchased from a local supermarket (Wageningen, the Netherlands) and stripped using alumina powder (Alumina N, Super I, EcoChrome™, MP Biomedicals, France) to remove impurities and tocopherols (Berton et al., 2011). The free fatty acid composition of the stripped rapeseed oil was measured according to the method described earlier (Christie, 1989), and the results is reported in **Table S4.1**. The hydroperoxide concentration and para-anisidine value of the stripped oil were 0.26 ± 0.08 meq/oil kg and 0.14 ± 0.07, respectively. For sodium dodecyl sulfate-polyacrylamide gel electrophoresis (SDS-PAGE), 12% Mini-PROTEAN® TGX™ precast gels (10 well, 30 µl/well), 2× Laemmli sample buffer (#1610737), 10× Tris/Glycine/SDS buffer (#1610772), precision plus protein™ standards (dual color), and Bio-safe™ Coomassie stain (#1610787) were obtained from Bio-Rad (Richmond, CA, USA). For lipid oxidation analysis, iron(II) sulfate heptahydrate ($FeSO_4 \cdot 7H_2O$), cumene hydroperoxide solution (80%), n-hexane, sodium chloride (NaCl), para-anisidine were purchased from Sigma-Aldrich (Saint Louis, MO, USA); hydrochloric acid (37%), acetic acid (glacial), barium chloride dihydrate ($BaCl_2 \cdot 2H_2O$), ammonium thiocyanate (NH_4SCN), 2-propanol, 1-butanol were obtained from Merck Millipore (Merck, Germany); methanol was

purchased from Actu-All Chemicals B.V. (Oss, The Netherlands). Dextran from *Leuconostoc* spp. (a branched glucan composed of linear α (1→6) linked glucose units and α (1→3) link initiated branches, MW ~70 kDa), Tween® 20, sodium phosphate dibasic (Na_2HPO_4), sodium phosphate monobasic dihydrate ($NaH_2PO_4 \cdot 2H_2O$), potassium sorbate, sodium dodecyl sulfate (SDS), 2,2-diphenyl-1-picrylhydrazyl (DPPH), L-ascorbic acid, 3-(2-pyridyl)-5,6-di(2-furyl)-1,2,4-triazine-5′,5′′-disulfonic acid disodium salt (ferene), ammonium iron(II) sulfate hexahydrate, and 2-mercaptoethanol were purchased from Sigma-Aldrich (Saint Louis, MO, USA). Ethanol (95%) was obtained from Merck Millipore (Merck, Germany). Potassium bromide and sodium acetate were supplied by VMR (Radnor, PA, USA). The chemicals used were all of at least of analytical grade. Ultrapure water prepared by a Milli-Q system (Millipore Corporation, Billerica, Massachusetts, US) was used for all the experiments unless otherwise stated.

4.2.2 Preparation of glycated soy protein isolate mixture

SPI/dextran solution was prepared by mixing 5 wt% SPI and 5 wt% dextran in a weight ratio of 1:1, following by being hydrated overnight at 4 °C. The solution was then freeze-dried. This dried sample was milled using a Fritsch ball mill (Fritsch, Oberstein, Germany) and incubated at 60 °C for 24 h in a desiccator with a relative humidity of 79% to prepare glycated SPI mixture. The obtained glycated SPI mixture were subsequently stored at -20 °C until further use.

The free amino group content (measured by the o-phthaldialdehyde method), and furosine, Nε-(carboxymethyl)-L-lysine (CML), and Nε-(carboxyethyl)-L-lysine (CEL) contents (measured by liquid chromatography/mass spectrometry) of the glycated SPI mixture were around 0.44 mol/g protein, 0.83 mg/g protein, 0.13 mg/g protein, and 0.06 mg/g protein, respectively. Those contents for the starting SPI were around 0.77 mol/g protein, 0.08 mg/g protein, 0.07 mg/g protein, and 0.05 mg/g protein, respectively. Detailed physical and chemical properties of the glycated SPI mixture (and the starting SPI) can be found in our previous work (Feng et al., 2021).

4.2.3 Preparation of O/W emulsions

A scheme of the emulsions prepared for this study is shown in **Figure 4.1**. To prepare stock emulsions, emulsifiers (Tween 20 and WPI) were separately dispersed in sodium phosphate buffer (10 mM, pH 7.0) and stirred overnight at 4 °C to ensure complete solubilization. Stock O/W emulsions were prepared by homogenizing 20 wt% rapeseed oil, 79 wt% sodium phosphate buffer (10 mM, pH 7.0) and 1 wt% emulsifier (Tween 20 or WPI) using a rotor-stator homogenizer (Ultra-turrax IKA T18 basic, Germany) operating at 11,000 rpm for 1 min, followed by further droplet size reduction with a M-110Y Microfluidizer equipped with a F12Y interaction chamber (Microfluidics, Massachusetts, USA), for five passes at 800 bar. The thermostated tank of the instrument was filled with an ice bath to minimize oxidation during the process.

Prior to adding excess protein compounds to the stock emulsion, a pre-homogenization step was applied to breakup large protein aggregates and improve dispersibility. In brief, WPI, SPI, SPI/dextran mixture (1:1, w/w) as well as glycated SPI mixture were dispersed in 10 mM sodium phosphate buffer (pH 7.0) with a concentration of 0.50 wt% and placed at 4 °C overnight for full hydration. The suspensions were then passed through a lab-scale colloid mill (IKA Magic Lab, Staufen, Germany) with a gap width of 0.32 mm (26,000 rpm, 2×1.5 min with 20 s intervals). The molecular weight distribution of the obtained samples was analyzed with SDS-PAGE (section 4.2.5).

A portion of the stock emulsions was diluted with buffer or aforementioned homogenized protein suspensions (WPI, SPI, SPI/dextran mixture or glycated SPI mixture) to achieve the final desired concentrations of 10 wt% rapeseed oil, 0.5 wt% emulsifiers (Tween 20 or WPI), and 0.25 wt% excess protein compounds. To prevent microbial growth, 0.35 wt% and 0.225 wt% of potassium sorbate were added to the Tween 20- and WPI-stabilized emulsions, respectively.

Finally, Tween 20- or WPI-based emulsions were partitioned as 2-g aliquots in capped glass tubes (KIMAX®, 16 x 125 mm) or polypropylene tubes (Eppendorf®, 15 x 120 mm),

respectively. These tubes were then rotated at 2 rpm in the dark at 40 °C for 70 h (SB3 rotator, Stuart, Staffordshire, UK).

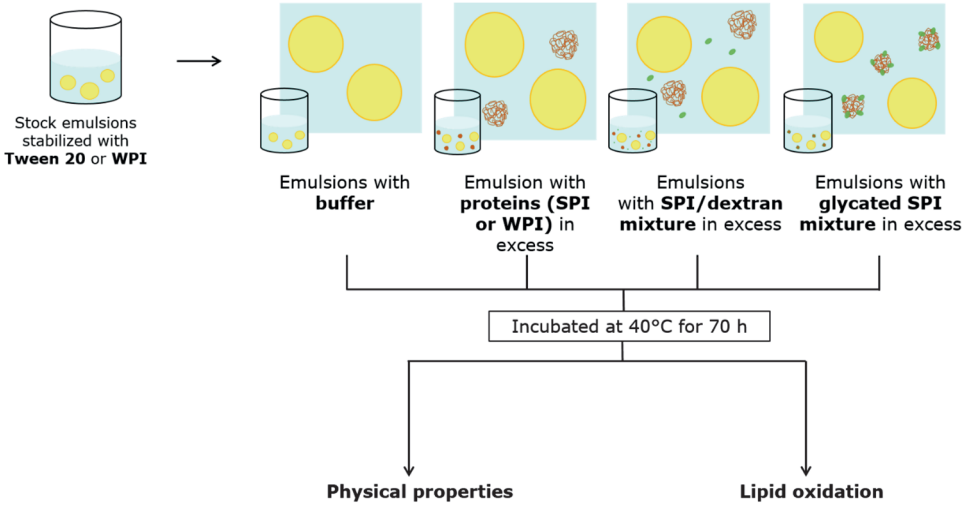

Figure 4.1. Scheme of preparation of different emulsions.

4.2.4 Collection of interface components

Collection of proteins adsorbed at the interface in the emulsions was performed according to the method described by Hinderink and co-workers (Hinderink et al., 2019). In short, fresh emulsions were centrifuged at 15,000×*g* for 1.5 h to separate the continuous phase from oil droplets. The cream phase (oil droplets) was collected, re-dispersed in 1% SDS, and centrifuged again as earlier. The interfacial proteins were displaced by SDS and therefore present in the aqueous subnatant obtained after this second centrifugation. The subnatant was then collected for protein composition analysis (section 4.2.5).

4.2.5 SDS-PAGE

Proteins present in the excess dispersions and at the interface (obtained from sections 4.2.3 and 4.2.4, respectively) were analyzed by SDS-PAGE using a Mini-PROTEANe Tetra system

(Bio-Rad, Richmond, CA, USA) under reducing conditions. Prior to analysis, the protein concentration of these samples was measured using a PierceTM BCA protein assay kit (Thermo Scientific, Rockford, IL, USA). Mixtures of 0.2 w/v% protein sample and Laemmli sample buffer (containing 5 v% β-mercaptoethanol) at a volume ratio of 1:1 were heated at 95 °C for 5 min on an Eppendorf ThermoMixer® C heating block (Eppendorf, Hamburg, Germany). Then, pre-stained protein standard (10 µL) and treated samples (20 µL) were loaded onto Mini-PROTEAN gels. Electrophoretic separation was carried out at a constant voltage of 200 V for around 30 min. Subsequently, gels were stained using Coomassie G-250 for 1 h and de-stained with ultrapure water overnight. Finally, these gels were scanned on a GS-900TM calibrated densitometer (Bio-rad, USA) and analyzed with Image Lab 5.2.1 software (Bio-Rad, USA).

4.2.6 Physical properties of emulsions

Physical characterization of emulsions was performed immediately after emulsification and after 70 h incubation.

4.2.6.1 Droplet size distribution

The droplet size distribution of emulsions was measured by static light scattering (Mastersizer 3000, Malvern Instruments, Worcestershire, UK). The refractive indices of rapeseed oil and water were set to 1.473 and 1.33, respectively. The absorption index was set to 0.01.

4.2.6.2 Light microscopy

The microstructure of emulsions was observed using an optical microscope Carl Zeiss Axio Scope A1 (Oberkochen, Germany). Before the analysis, the emulsions were gently mixed. A drop (5 µL) of sample was carefully transferred onto a glass microscopy slide and covered with a coverslip. The emulsions were observed at a magnification of 40 ×.

4.2.6.3 Droplet surface charge

The droplet surface charge of emulsions was determined using dynamic light scattering (Zetasizer Ultra, Malvern Instruments, Worcestershire, UK). Emulsions were diluted 1,000

times in sodium phosphate buffer (10 mM, pH 7.0) prior to the measurement to minimize multiple scattering effects. The samples were placed in a disposable cuvette (DTS 1080) and analyzed at 20 °C. Zeta-Potential was automatically calculated by using ZS Xplorer software according to the Smoluchowski model.

4.2.7 Lipid oxidation in emulsions

The oxidative stability of emulsions was analyzed by measuring the primary (lipid hydroperoxides) and secondary (aldehydes) reaction products over incubation.

4.2.7.1 Lipid hydroperoxides

Lipid hydroperoxides were measured according to a method adapted from Shanta and Decker (1994). First, 0.3 mL emulsion was mixed with 1.5 mL n-hexane/2-propanol (3:1, v/v). Then, this mixture was vortexed 3 x 10 s with 20 s intervals and centrifuged at 14,600 rpm for 2 min. Subsequently, 0.2 mL of the upper organic phase was added to 2.8 mL of the methanol/1-butanol (2:1, v/v), followed by reacting with 3.94 M ammonium thiocyanate/ferrous iron solution (1:1, v/v; 30 µL). The solution was vortexed and reacted for 20 min, and the absorbance measured at 510 nm using a DU 720 UV–visible spectrophotometer (Beckman Coulter, Woerden, the Netherlands). The lipid hydroperoxide concentration was calculated using a cumene hydroperoxide standard curve.

4.2.7.2 Aldehydes

Total aldehydes as measured by the para-anisidine value (pAV) were quantified using the AOCS Official Method CD 18-90 (AOCS, 1998). Briefly, 2.1 mL emulsion were mixed with 1 mL saturated sodium chloride solution and 5 mL n-hexane/2-propanol (3:1, v/v). The mixture was vortexed 3 x 10 s with 20 s intervals and centrifuged at 2,000×*g* for 8 min. The absorbance of 1 mL of the clear upper hexane layer (*Ab*) was measured at 350 nm using hexane as a blank. One milliliter of this upper layer or hexane was mixed with 0.2 mL of 2.5 g/L para-anisidine in acetic acid solution. After exactly 10 min, the absorbance (*As*) was measured at 350 nm, using hexane with para-anisidine solution as a blank. The pAV was calculated using Eq. (4.1):

$$pAV = \frac{1.2 \times As - Ab}{m} \quad (4.1)$$

where *m* is the mass of oil per milliliter hexane (g/mL).

4.2.8 Antioxidant activity of protein samples

To investigate the possible antioxidant mechanisms of the tested protein materials, their capacities for radical scavenging and iron binding were investigated.

4.2.8.1 DPPH radical scavenging activity

The DPPH radical scavenging activity of the continuous phase proteins was determined according to the methodology described by Yen & Hsieh with some modifications (Yen & Hsieh, 1995). An aliquot (1 mL) of 2.5 g/L protein-based compounds or dextran was mixed with 1 mL of 200 µM DPPH in ethanol. The mixture was vortexed vigorously and incubated in the dark at room temperature for 30 min, followed by filtration using syringe filters (PVDF, 0.45 Millipore, Billerica, MA, USA). The absorbance of the filtrate (*As*) was measured at 517 nm using ethanol as the blank. The percentage of DPPH radical scavenging activity (%) was calculated according to Eq. (4.2):

$$\text{DPPH radical scavenging activity } (\%) = \left(1 - \frac{As - Ab}{Ac}\right) \times 100\% \quad (4.2)$$

where *Ac* is the absorbance of the solution containing 1 mL of ultrapure water and 1 mL of DPPH in ethanol solution, and *Ab* is the absorbance measured for the protein-based compounds mixed with ethanol in the same ratio as used for *As*.

4.2.8.2 Iron binding capacity

Iron binding capacity was determined based on the method of Hennessy, Reid, Smith, and Thompson (1984). Protein or dextran samples (2.5 g/L) were added to known amounts of 5 g/L ferrous iron solution. The solutions were left for 24 h at 20 °C, followed by filtration using ultracentrifugation tubes (cut-off 10 kDa). Five hundred microliters of the filtrate were mixed with 0.5 mL dissociating agent (containing 0.5 M L-ascorbic acid and 1.4 M acetic acid buffer (pH 4.5); 1:1, v/v) and 0.1 mL of 6 mM ferene solution. After 5 min, the absorbance

of the mixed solutions was measured at 593 nm. The Fe^{2+} concentration was determined using a calibration curve based on ferrous sulfate hexahydrate solutions (1-10 mg/L). The amount of bound iron (µg per mg of protein) was calculated by subtraction of the amount of unbound iron to the total amount of iron added.

4.2.9 Experimental design and statistical analysis

All measurements were performed on at least two independent samples of which each was analyzed at least three times. The data reported herein are mean values ± standard deviation of all the measurements. Statistical analysis was conducted on IBM SPSS statistics 23.0.0.2 (SPSS Inc, Chicago, Illinois, USA) using student's t-test and one-way analysis of variance (ANOVA) with Tukey's post-hoc test. Differences at $P < 0.05$ were considered significant unless otherwise stated.

4.3 Results and discussion

4.3.1 *Protein composition of the continuous phase proteins*

Commercial protein isolates often contain aggregates; therefore, a pre-homogenization step was applied to improve dispersibility and hydration. The resulting size distribution and composition can be found in **Figure 4.2**. Before homogenization, the WPI solution had a monomodal size distribution with an average diameter (D[3,2]) around 0.66 µm (**Figure 4.2A**), which is considerably larger than the individual proteins present, which are typically in the 1-5 nm range (Zhang et al., 2014). This indicates that aggregates are present. The SPI solution showed a bimodal size distribution, whereas glycated SPI mixture solution had only a larger peak (**Figure 4.2A**). Upon homogenization, there was a considerable size reduction for all samples (**Figure 4.2A**). The D[3,2] values of WPI, SPI, and glycated SPI mixture decreased from 0.66, 87, and 173 µm, to 0.14, 0.089, and 0.38 µm, respectively.

The protein composition of the samples after homogenization is given in **Figure 4.2B**. WPI was mostly composed of β-lactoglobulin (β-Lg), α-lactalbumin (α-Lac), and bovine serum albumin (BSA) (**Figure 4.2B**; lane 2). SPI-based samples consisted of α, α′, and β subunits

from β-conglycinin and acidic (A) and basic (B) subunits from glycinin (**Figure 4.2B**; lanes 3-5). Moreover, a broad band with high molecular weights around 250 kDa was observed for the glycated SPI mixture (**Figure 4.2B**; red arrow), suggesting the formation of large protein aggregates as a consequence of the MR (de Oliveira et al., 2016).

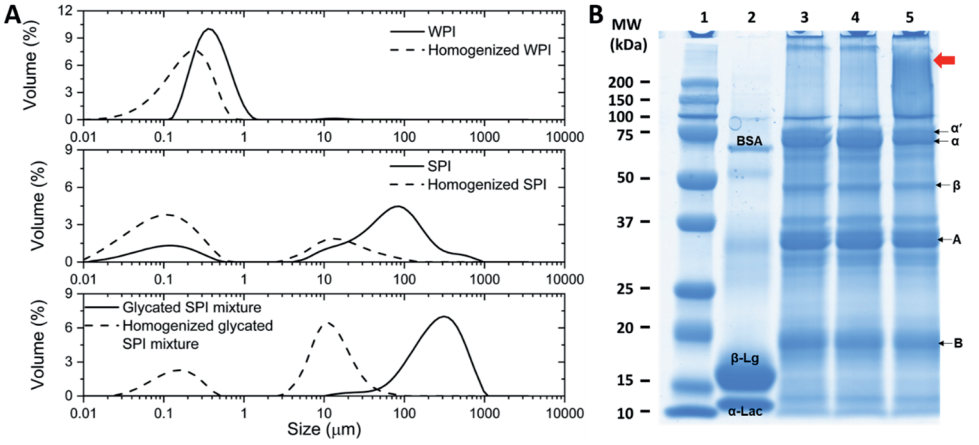

Figure 4.2. (A) Size distribution of protein suspensions before and after homogenization. (B) SDS-PAGE patterns (reducing conditions) of continuous phase protein-based compounds. Lanes: 1, protein marker; 2, homogenized WPI; 3, homogenized SPI; 4, homogenized SPI/dextran mixture; 5, homogenized glycated SPI mixture.

4.3.2 Physical properties of emulsions

4.3.2.1 Droplet size distribution

The effect of emulsifier (Tween 20 or WPI) concentration on the droplet size of the stock emulsions was preliminarily adjusted to limit the fraction of unadsorbed emulsifiers in the continuous phase, while warranting physical stability (**Figure S4.1**). Based on these adjustments, stock emulsions stabilized with 1 wt% of Tween 20 or WPI were selected to further investigate the effect of adding an excess of proteins post homogenization. Subsequently, droplet size distribution, microstructure, droplet surface charge, and lipid oxidation were monitored throughout storage.

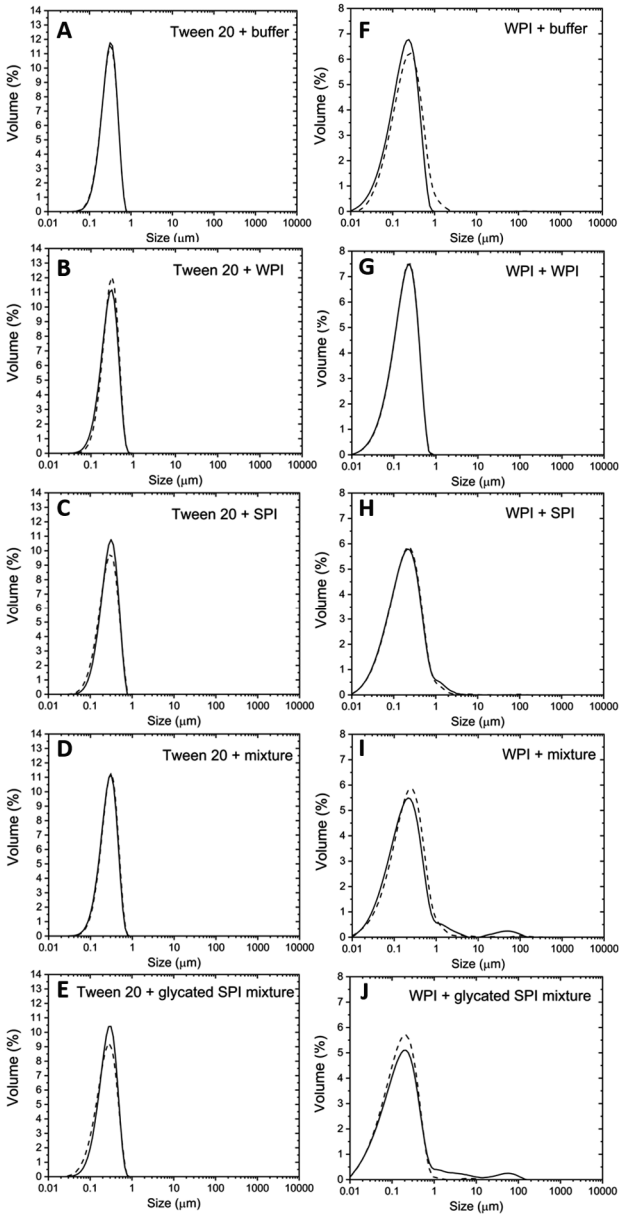

Figure 4.3. Droplet size distribution of Tween 20-stabilized emulsions (A–E) and WPI-stabilized emulsions (F–J) freshly prepared (solid line) or at the end of the incubation period (40 ◦C, 70 h) (dotted line).

All freshly prepared emulsions had a mean droplet size (D[3,2]) of 0.1–0.2 µm, with WPI-stabilized emulsions showing a slightly broader size distribution than Tween 20-stabilized ones (**Figure 4.3**). Tween 20-stabilized emulsions remained fully stable after 3 days of storage (**Figure 4.3**), whereas WPI-stabilized emulsions used in combination with SPI-based samples showed a tailed signal corresponding to particles between 1 and 100 µm (**Figure 4.3H-J**) which is probably due to the continuous phase SPI or glycated SPI mixture aggregates as discussed before (**Figure 4.2**). Nonetheless, no appreciable differences were observed for all emulsions upon storage, indicating they were physically stable. This is important to later compare lipid oxidation among different emulsifiers without a surface area bias.

4.3.2.2 Droplet surface charge

All emulsions in this study have a negative charge (**Figure 4.4**), which was expected for WPI-stabilized emulsions because the pH (7.0) was higher than the isoelectric point of whey proteins (~5.1). The reason why Tween 20-stabilized emulsions exhibited a negative surface charge is less obvious, since Tween 20 is a non-ionic surfactant. Nevertheless, similar behavior was previously found by others (Cengiz, Schroën, et al., 2019; Noon et al., 2020), which was attributed to several factors. First, hydroxyl ions (OH^-) formed by autoprotolysis of water could preferentially locate near the polar head groups of Tween 20, i.e., in the droplets' Stern layer (McClements, 2005). Second, free fatty acids present as impurities in Tween 20 or rapeseed oil could locate at the oil-water interface and are negatively charged at neutral pH (Hsu & Nacu, 2003; Waraho et al., 2011). Third, phosphate ions may also locate in the Stern layer of the Tween 20-coated droplets (Cengiz, Kahyaoglu, et al., 2019). We will not investigate this in detail, but it is important to point out that the negative charge of all Tween 20-based emulsions reduced further upon incubation, irrespective of whether excess protein was added or not. The decrease in ζ-potential at day 3 was similar in all Tween 20-stabilized emulsions, leading us to conclude that we could not distinguish any significant effect of excess proteins on top of the effects related to the 'Tween 20-base case'. The decrease in zeta-potential could be related to surface-active fatty acids that may be present in the oil, or formed upon triglyceride hydrolysis (Chen et al., 2011; St. Angelo,

1996). Alternatively, organic acids formed through lipid oxidation could cause similar effects (Chen et al., 2011; St. Angelo, 1996). In all emulsions, we observed a small reduction of pH (**Figure S4.2**) but this cannot explain the large changes in zeta-potential.

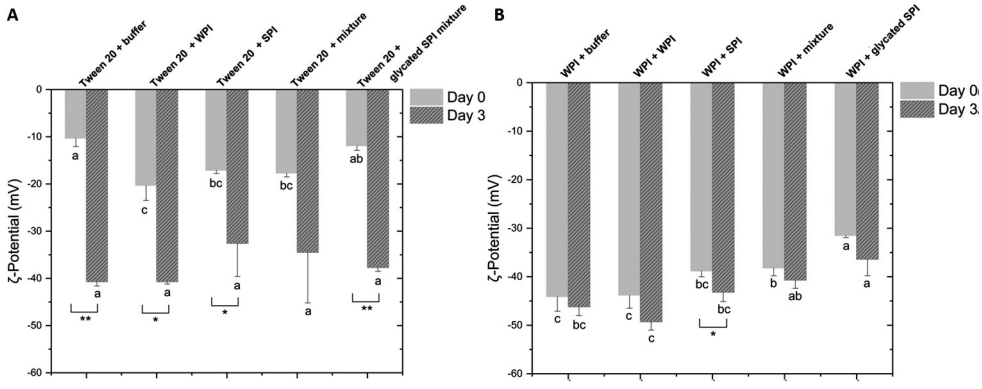

Figure 4.4. Zeta(ζ)-Potential of Tween 20-stabilized emulsions (A) and WPI-stabilized emulsions (B) before (Day 0) and after (Day 3) incubation (40 °C, 70 h). The lowercase letter is for comparison among the emulsions containing different excess protein ingredients on the same day. Different letters indicate significant differences ($P < 0.05$). Asterisks indicate a significant difference between day 0 and day 3 (* represents $P < 0.05$, and ** represents $P < 0.01$).

4.3.3 Protein composition of the oil-water interface

In general, the interfacial composition of emulsions is dominated by the emulsifiers present during emulsification (Berton-Carabin, Ropers, & Genot, 2014), although proteins added to the continuous phase may compete for adsorption to the interface, and eventually partly replace, or adsorb on top of initially adsorbed molecules (Dalgleish et al., 1991). To characterize this, the interfacial proteins were collected and analyzed with SDS-PAGE (**Figure 4.5**). The interfacial film in Tween 20-stabilized emulsions is almost protein-free (**Figure 4.5A**), which indicates that Tween 20 fully dominates the interface and prevents continuous phase proteins from adsorbing post-emulsification.

In WPI-stabilized emulsions, β-Lg and α-Lac dominated the interface, and the presence of a small proportion of BSA can be detected (**Figure 4.5B**). This observation is consistent with previous findings (Hinderink et al., 2019). Upon addition of SPI-based compounds to the continuous phase, faint bands of soy proteins (α, α′, β and A subunits) could be detected (**Figure 4.5B**; lanes 2-4), indicating that a relatively small amount of soy proteins adsorbed, or at least became bound to the interface. Moreover, smeared bands with high molecular weight could be seen when glycated protein mixture was added to the aqueous phase (**Figure 4.5B**, lane 4), implying the presence of glycated protein mixture at the interface. It is worth noting that some continuous phase proteins may be captured between the droplets in the creamed phase during the centrifugation step. However, since the same method was applied for Tween 20-stabilized emulsions where we hardly detected proteins at the interface, the amount of continuous phase proteins captured between the droplets in the cream of WPI-stabilized emulsions should be limited. We thus concluded that a limited yet existing fraction of SPI components were able to co-locate at WPI-based interfaces.

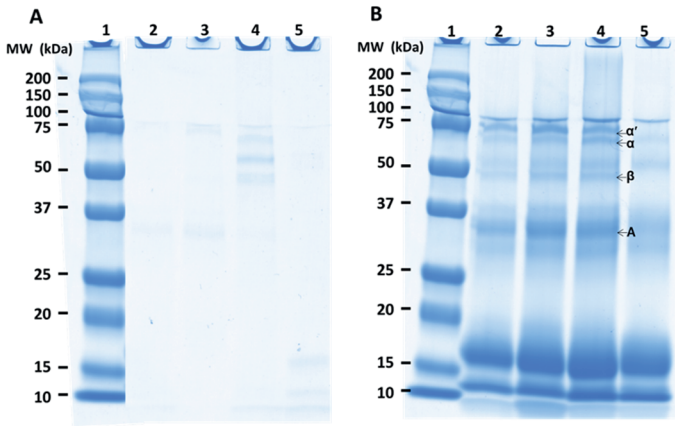

Figure 4.5. SDS-PAGE determination of the proteins present in the creamed phase of freshly prepared Tween 20-stabilized (A) and WPI-stabilized emulsions (B), with SPI (lane 2), SPI/dextran mixture (lane 3), glycated SPI mixture (lane 4) or WPI (lane 5) added to the continuous phase post-homogenization. Lanes 1: protein marker.

4.3.4 Lipid oxidation in emulsions

4.3.4.1 Antioxidant activity of continuous phase proteins

Proteins are known to act as antioxidants through multiple pathways including the scavenging of free radicals and the chelation of prooxidant transition metals. Therefore, these properties were assessed for the proteins considered in the present work. As shown in **Figure 4.6A**, WPI exhibited a significantly higher DPPH radical scavenging activity than any of the SPI-based compounds, among which no significant difference was found ($P > 0.05$). Besides, dextran showed low DPPH radical scavenging activity. The free radical scavenging ability of WPI has been related to surface-exposed sulfhydryl groups that possess hydrogen-donating abilities (Faraji et al., 2004). Compared to the starting SPI, we did not observe an enhanced antioxidant capacity of glycated protein mixture, which may be due to the limited affinity of the DPPH radicals for proteins grafted with a large carbohydrate moiety (Dean et al., 1991; Liu et al., 2014). Another possibility is related to the loss of free amino groups that can scavenge radicals or chelate irons determined by the glycation reaction (Pan et al., 2020; Ruiz-Roca et al., 2008). Tween 20 showed a low inherent ability to scavenge DPPH radicals, but boosted the scavenging ability of proteins, which may be due to the ability of Tween 20 to alter proteins conformation and therefore increase accessibility of free radicals (Donnelly et al., 1998).

WPI was able to bind less iron than SPI-based compounds ($P < 0.05$), which is in line with the results of Faraji et al. (2004). No significant differences were observed among the different SPI-based compounds (**Figure 4.6B**). The greater iron chelating ability of SPI compared to WPI could be due to the higher content of acidic amino acids (aspartic acid, glutamic acid) in SPI (Kaushik et al., 2016), since the carboxyl groups in the side chains can act as metal chelators (Sarmadi & Ismail, 2010). In addition, the higher content of histidine in SPI than in WPI (Kaushik et al., 2016) could also account for the higher iron chelating activity of SPI. In fact, two or three histidine residues are capable of chelating one divalent metal ion (Esfandi et al., 2019). Furthermore, SPI typically contains 0.12-0.35% phytic acid (a strong metal chelator), which may also contribute to the fairly high iron binding capacity

of SPI (Reddy et al., 1982). However, unlike DPPH scavenging activity, the iron binding capacities of the proteins did not change significantly after adding Tween 20 (**Figure 4.6B**). This could be because of the hydrophilic properties of the amino acids that are capable of chelating metal ions (e.g., aspartic acid, glutamic acid, and histidine). Therefore, the conformational change of proteins as a result of interacting with Tween 20 would not largely affect the metal binding capacity of proteins.

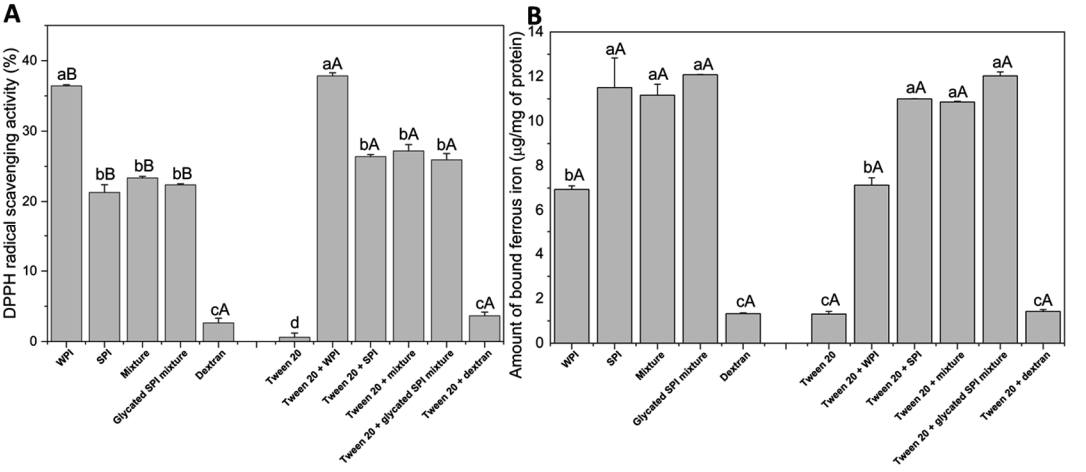

Figure 4.6. DPPH radical scavenging activity (A) and iron-chelating capacity (B) of the different protein suspensions. The lowercase letter is for comparison among the proteins. The uppercase letter is for comparison between before and after adding Tween 20. Different letters indicate significant differences ($P < 0.05$).

4.3.4.2 Lipid oxidation

Hydroperoxide concentration and para-anisidine value (pAV) were used to assess the formation of primary and secondary lipid oxidation products, respectively. Considerable differences regarding the extent of lipid oxidation were found for the various compositions (**Figures 4.7 & 4.8**).

In Tween 20-stabilized emulsions (**Figure 4.7A**), hydroperoxides developed earlier, faster and to a greater extent in the control sample (Tween 20 + buffer) than in the other Tween

20-stabilized emulsions. The presence of continuous phase protein was thus effective at inhibiting hydroperoxide formation in Tween 20-stabilized emulsions. In that respect, SPI components showed a stronger ability to prevent hydroperoxide formation than WPI. The secondary lipid oxidation products (pAV) exhibited similar tends as hydroperoxides (**Figure 4.7B**): the formation of aldehydes decreased in the order control (Tween 20 + buffer) > Tween 20 + WPI > Tween 20 + SPI-based compounds. After 3 days of storage, aldehydes were 1.3-, 6.2-, 8.2-, and 12.3-fold higher for the control emulsion than for emulsions containing WPI, SPI, SPI-dextran mixture, and glycated SPI mixture, respectively.

WPI-stabilized emulsions displayed lipid oxidation kinetics that were fairly similar to their Tween 20-stabilized counterparts (**Figure 4.8**). The control emulsions (no excess protein added) had significantly higher hydroperoxides and aldehydes concentrations than the emulsions added with WPI, which themselves had consistently higher values than SPI-added emulsions. At the end of storage, the aldehyde contents were 1.0-, 1.8-, 3.7-, and 4.2-fold higher for the control emulsion than emulsions containing excess WPI, SPI, SPI-dextran mixture, and glycated SPI mixture, respectively.

Taking in consideration that (i) the droplet size of all emulsions was stable in time, (ii) the surfactant concentration in Tween 20-stabilized emulsions was optimized to avoid excess in the continuous phase, and (iii) the WPI-stabilized emulsions had only very small amounts of SPI components located at the interface, we can conclude that the observed effects can be largely attributed to the proteins present in the continuous phase of emulsions.

The ability of proteins in the continuous phase of emulsions to protect lipids against oxidation can be attributed to their free radical scavenging and iron-binding abilities (**Figure 4.6**), as discussed before for both proteins tested herein. In the present case, where WPI is better capable of scavenging radicals, SPI has a higher iron binding capacity. When it comes to lipid oxidation in emulsions, a higher antioxidant activity was observed for added SPI-based components, i.e., proteins with relatively low DPPH scavenging activity, but high iron binding capacity. This shows that in the present systems, lipid oxidation is strongly

dependent on transition metal availability, and thus the proteins' iron chelating capacity is the most relevant property for the prevention of lipid oxidation. This capacity could inhibit the decomposition of lipid hydroperoxides by preventing transition metals from approaching the oil-water interface, where lipid oxidation primarily occurs, and/or by decreasing the activity of transition metals (Kellerby et al., 2006). In addition, according to the literature, the improved antioxidant activity of SPI may also be ascribed to the presence of isoflavones. The ring B that is at the 3-position of heterocyclic ring as well as the 5,7-dihydroxy structure in ring A in isoflavones can effectively scavenge peroxyl radicals (Pietta, 2000). Moreover, genistein (a class of isoflavone), though less effectively, could also chelate metal due to the hydroxyl groups at the C-4', C-5, and C-7 positions (Arora et al., 1998).

Maillard reaction products as emulsifiers have been reported to exhibit better protection against lipid oxidation than the corresponding non-glycated proteins (Hu et al., 2020; Hwang et al., 2011; Zha et al., 2019), which was ascribed to the antioxidant potential of some Maillard reaction products (e.g., reductone compounds) and to their ability to form a dense physical barrier at the oil-water interface. Given our experimental design, where glycated protein mixture is almost only present in the continuous phase, the former effect can be specifically assessed. In the present work, we observed a protective effect against lipid oxidation not only when adding glycated SPI, but also when adding a non-reacted mixture of SPI and dextran. This suggests that the chemical conjugation of soy proteins with dextran did not play a major role in improving the oxidative stability of the emulsion, but that the presence of dextran had in itself a protective effect (**Figures 4.7 & 4.8**). It is possible that the dextran molecules in the continuous phase slow down the mobility of pro-oxidants and thus delay lipid oxidation. For example, Shimada and co-workers found that adding polysaccharides (xanthan, pectin, guar gum, or tragacanth gum) in emulsions was able to suppress lipid oxidation (as measured with oxygen consumption) by increasing the viscosity of emulsions (Shimada et al., 1996). However, the exact mode of action of dextran would need to be further proven. Additionally, in previous work, glycated hydrolyzed β-lactoglobulin showed antioxidant activity in Tween 20-stabilized fish O/W emulsions, but it was also found that prolonged heating times (>4 h) applied to form the Maillard reaction

products led to a decrease in oxidative stability compared to the non-reacted and short-time heated hydrolyzed β-lactoglobulin-glucose mixture (Dong et al., 2012).

Interestingly, in the presence of continuous phase proteins, all Tween 20-stabilized emulsions exhibited very low lipid oxidation levels, which means that the antioxidant potential of excess proteins is boosted in surfactant-stabilized emulsions. Even if the Tween 20 concentration was optimized, there was still some Tween 20 in the continuous phase, which is expected to interact with the nonpolar segments of proteins via hydrophobic interactions, leading to partial unfolding of proteins (Dickinson & Hong, 1995; Otzen et al., 2009). To explore the possible the conformational change of proteins, FTIR spectroscopy was conducted. As can be seen form the second derivation of amide I spectra (**Figure S4.3**), SPI exhibited more α-helices (~1655 cm^{-1}) and intramolecular β-sheets (~1635 cm^{-1}) structures after the addition of Tween 20. Enrichment of α-helices in the presence of a surfactant was also observed by others (Deep & Ahluwalia, 2001; Li et al., 2006; Vermeer & Norde, 2000). The formation of this highly ordered (α-helix and intramolecular β-sheet) non-native secondary structure has been reported as a result of exposure and reorientation of the non-polar residues of proteins towards the hydrophobic materials (Herrero et al., 2011; Lee et al., 2007; Zhai et al., 2011, 2012). On the other hand, the conformational changes for WPI were less significant; there was only a slight decrease of α-helices and a slight increase of β-sheets after adding Tween 20. This may indicate that there were few interactions of proteins with Tween 20 (Lee et al., 2009). Such partially conformational changes of proteins could lead to the exposure of certain hydrophobic amino acids. Particularly, the aromatic amino acids have been reported to have antioxidant properties because of their electron-donating properties that allow for converting radicals to stable molecules (Sarmadi & Ismail, 2010). As previously described, the DPPH scavenging activity of the protein increased after mixing with Tween 20 (**Figure 4.6A**), which supports this explanation. In addition, changes in protein conformation were also described by others as markedly increasing the proteins' ability to bind lipid molecules, and notably lipid hydroperoxides (Yamamoto et al., 1996). This might also slow down the physical

propagation of lipid oxidation reactions, for which the segregation/transport of intermediate products is possibly instrumental (Laguerre et al., 2017, 2020).

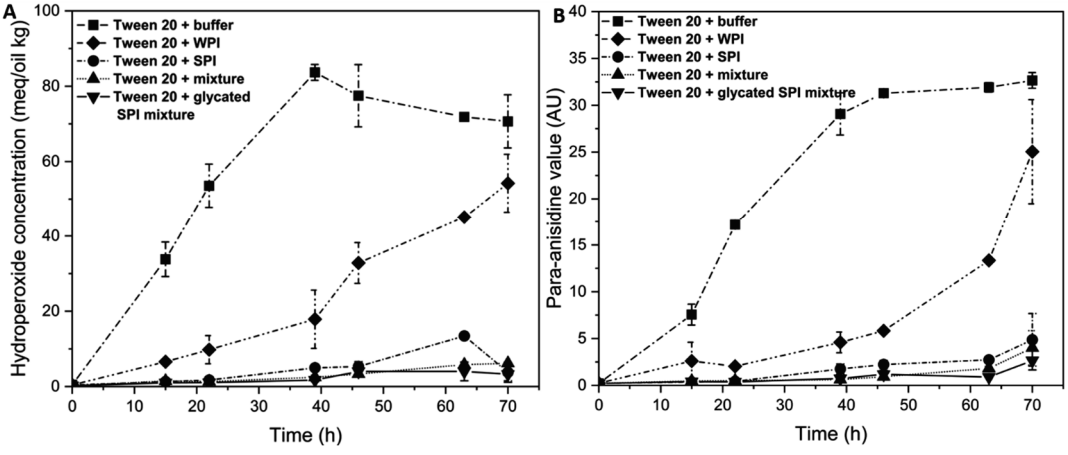

Figure 4.7. Hydroperoxide concentrations (A) and para-anisidine values (B) in Tween 20-stabilized emulsions over the incubation period (40 °C, 70 h).

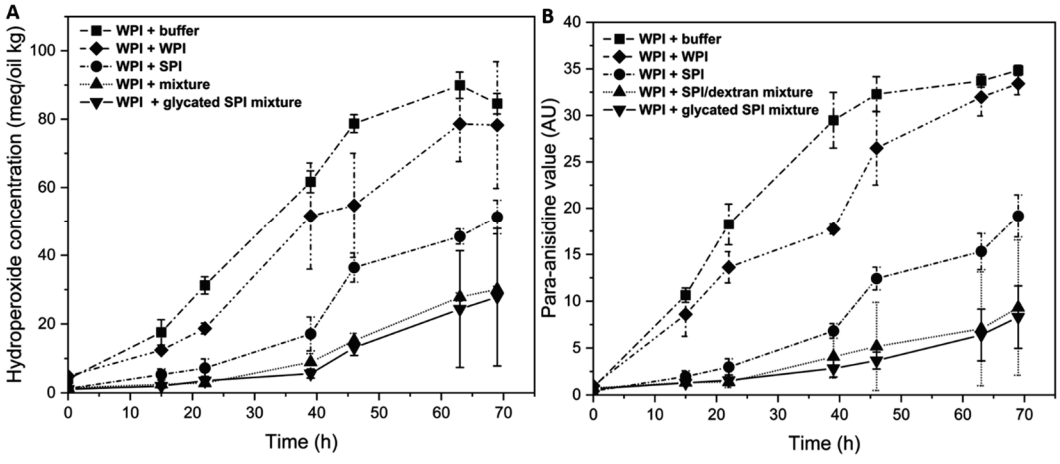

Figure 4.8. Hydroperoxide concentrations (A) and para-anisidine values (B) in WPI-stabilized emulsions over the incubation period (40 °C, 70 h).

4.4. Conclusion

The addition of WPI, SPI, SPI/dextran mixture and glycated SPI mixture to the continuous phase of emulsions stabilized by Tween 20 or WPI did not significantly affect the physical stability of emulsions. The tested continuous phase proteins are all capable of inhibiting lipid oxidation in emulsions, and the inhibition capacity was, starting from the highest, in the order glycated SPI mixture ≈ SPI/dextran mixture > SPI > WPI. Iron chelating ability was proposed as a potentially important mechanism in that respect, since metal catalyzed decomposition of hydroperoxides is a dominant oxidation pathway in emulsions. Both non-reacted SPI/dextran mixture and glycated SPI mixture showed a better protective effect against lipid oxidation than SPI. This suggests that the chemical conjugation of soy proteins with dextran did not play a major role in improving the oxidative stability of the emulsion, but that the presence of dextran had in itself a protective effect. In addition, the antioxidant potential of excess proteins is boosted in Tween 20-stabilized emulsions, as compared to WPI-stabilized emulsions. Interaction of surfactants with proteins may lead to the changes in protein conformation, which could increase the ability of proteins to bind molecules involved in the lipid oxidation reaction cascade.

Using soy proteins in the continuous phase of emulsions may therefore constitute a promising route to engineer oxidatively stable food emulsions, which could reduce or eliminate the need for artificial antioxidants. Protein glycation may potentiate this effect, although to a rather limited extent. Further research is needed to elucidate if later stage of Maillard reaction products, which are reported to have strong antioxidant activity, can also be applied for this purpose.

Supplementary material

Table S4.1. Fatty acid composition (%) of stripped rapeseed oil.

Fatty acids	Stripped rapeseed oil (%)
Myristic acid (C14:0)	0.06 ± 0.00
Palmitic acid (C16:0)	4.95 ± 0.02
Palmitoleate acid (C16:1)	0.26 ± 0.01
Stearate (C18:0)	1.47 ± 0.04
Oleate (C18:1)	63.18 ± 0.15
Linoleate (C18:2)	18.74 ± 0.07
Linolenate (C18:3)	7.37 ± 0.06
Arachidate (C20:0)	0.64 ± 0.01
Eicosenoate (C20:1)	2.31 ± 0.02
Behenate (C22:0)	0.30 ± 0.00
Erucate (C22:1)	0.54 ± 0.00
Lignocerate (C24)	0.18 ± 0.05

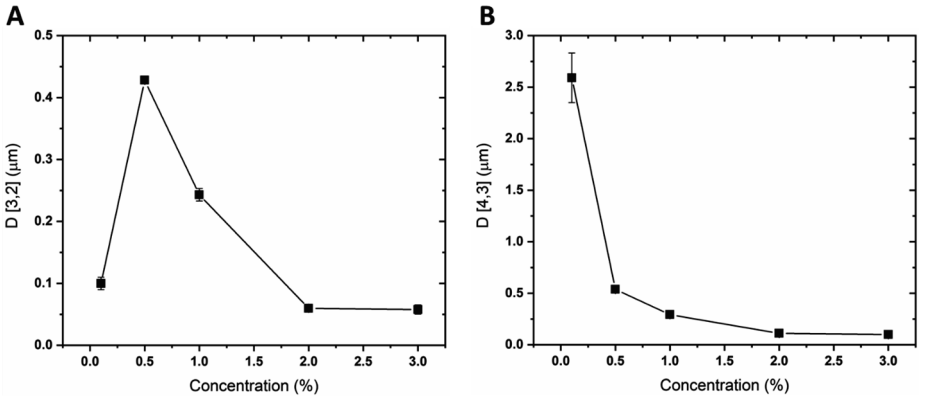

Figure S4.1. D[3,2] (A) and D[4,3] (B) of emulsions stabilized with different concentrations of Tween 20.

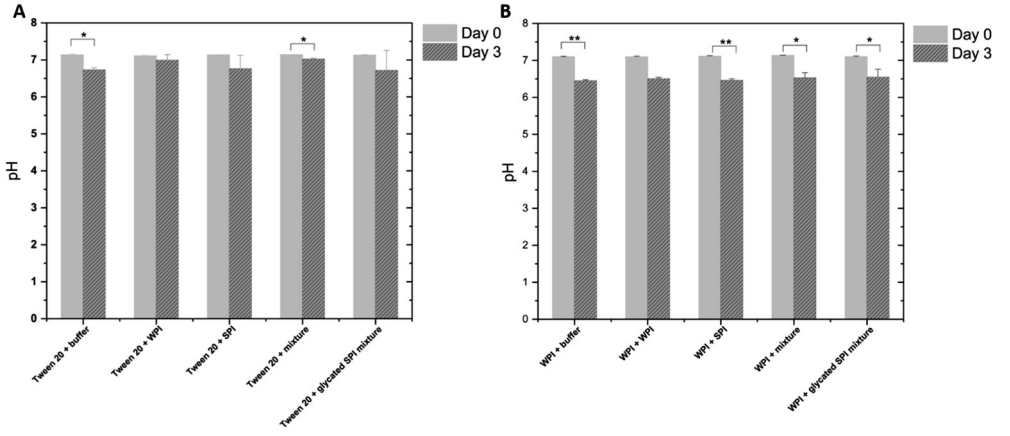

Figure S4.2. pH of Tween 20-stabilized emulsions (A) and WPI-stabilized emulsions (B) before (Day 0) and after (Day 3) incubation (40 °C, 70 h). * $P < 0.05$, ** $P < 0.01$.

Fourier transform infrared spectroscopy (FTIR) method

Protein secondary structure before and after adding Tween 20 was analyzed using Attenuated total reflectance (ATR) - Fourier transform infrared spectroscopy (FTIR) on a Tensor system (Bruker Optics, Ettlingen, Germany) and a Platiunum ATR unit. Measurements were conducted at room temperature against sodium phosphate buffer (10 mM, pH 7.0) as background and averaged over 510 scans at a resolution of 4 cm^{-1}.

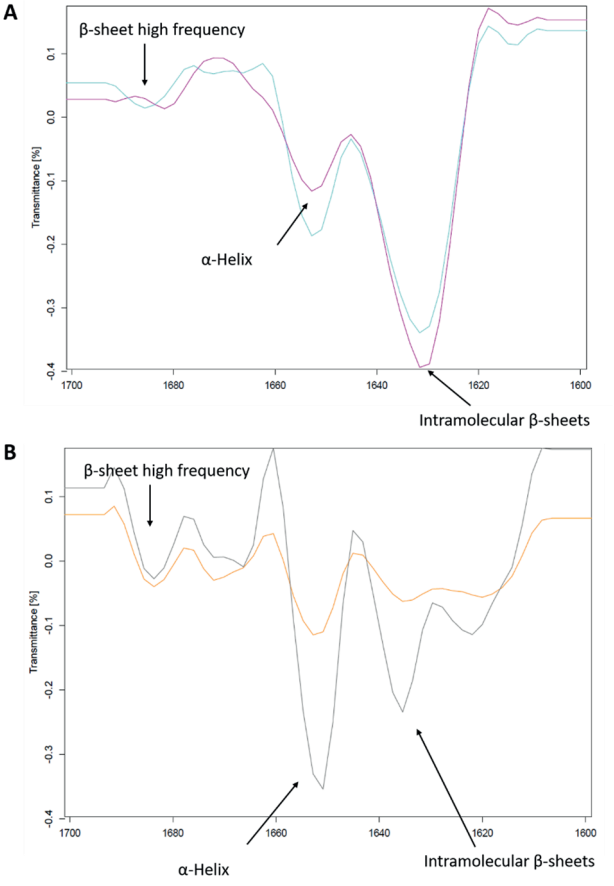

Figure S4.3. Influence of Tween 20 on the secondary structures of WPI (A) and SPI (B), as measured by the second derivation of the amide I band using ATR-FTIR. Blue: WPI; purple: WPI + Tween 20; orange: SPI; grey: SPI + Tween 20.

5

Coffee melanoidins as emulsion stabilizers

This chapter will submitted as Feng, J., Berton-Carabin, C. C., Guyot, S., Gacel, A., Fogliano, V., & Schroën, K. Coffee melanoidins as emulsion stabilizers.

Abstract

The use of conventional food stabilizers (e.g., surfactants and animal-derived proteins) is not in line with the consumers' consumers' demand for natural products. This has led to a great interest in novel emulsion stabilizers. In this paper, we explore the emulsification properties of coffee melanoidins, which are brown polymers formed during beans roasting. The physical properties and stability of oil-in-water (O/W) emulsions (10 wt% oil) stabilized with 0.25-4 wt% coffee melanoidins were investigated upon storage. Coffee melanoidins can form emulsions with a nearly monomodal size distribution. Upon 28 days of storage at room temperature, emulsions prepared with low (0.25-1 wt%) melanoidin concentrations underwent creaming, flocculation, and coalescence; emulsions prepared with high (4 wt%) melanoidin concentrations gradually transformed from a liquid-like state to a gel-like structure, whereas emulsions prepared with 2 wt% melanoidins were physically stable.

Stabilization of the emulsions is explained by both interfacial effects and an increased viscosity at high melanoidin concentrations. Surface load determination, confocal laser scanning microscopy (CLSM), and polarized light microscopy revealed that polysaccharide-rich melanoidins were able to adsorb at the droplet surface. Therefore, we conclude that coffee melanoidins act both as emulsifiers (decreasing the interfacial tension and inducing electrostatic and steric repulsion) and texture modifiers (increasing the viscosity of emulsions). This clearly shows the potential of coffee melanoidins as natural emulsion stabilizers in targeted food products.

5.1 Introduction

Emulsions are dispersed systems of two or more immiscible liquids, which make up the basic structure of a wide variety of products, such as foods, pharmaceuticals, and cosmetics. Being thermodynamically unstable, they tend to physically destabilize (e.g., gravitational separation, flocculation, and/or coalescence), finally leading to their destruction. Yet, it is possible to produce kinetically stable emulsions, by using texture modifiers or emulsifiers (McClements, 2005). Texture modifiers increase the continuous phase viscosity and thus improve emulsion stability by slowing down droplet creaming or sedimentation; examples include polysaccharides (e.g., carrageenan, xanthan gum, cellulose) and proteins (e.g., gelatin). Emulsifiers are amphiphilic compounds that can adsorb at the oil-water interface and decrease the interfacial tension; commonly used emulsifiers include surfactants, proteins, and phospholipids (Berton-Carabin & Schroën, 2015; McClements, 2005). Although surfactants and animal-derived proteins are commonly used in food emulsions, from a consumer perspective, this is becoming less and less desired given the current demand for natural and sustainable food ingredients and clean-label foods. This explains the current great interest in identifying new sources of emulsion stabilizers, notably those naturally present in foods.

Coffee is one of the most widely consumed beverages, and contains strong antioxidant compounds (Del Pino-García et al., 2012; Higdon & Frei, 2006). Roasting of coffee beans takes place at high temperatures and low water activity that favors the development of the Maillard reaction (Friedman, 1996), leading to the formation of high molecular weight, brown-colored, nitrogen-containing end-products, known as melanoidins. The major components of coffee melanoidins are polysaccharides (mainly galactomannans and arabinogalactans type II), proteins, and phenolic compounds (Bekedam et al., 2006; Borrelli et al., 2002; D'Agostina et al., 2004; Moreira et al., 2012, 2014; Nunes et al., 2012). Some of these compounds (e.g., polysaccharides and proteins) are expected to have properties that can be instrumental in stabilizing emulsions. For example, galactomannans consisting of a β-(1→4)-linked D-mannose backbone with α-D-galactose side groups are able to form highly

viscous solutions and exhibit some surface activity, leading to physically stable emulsions (Garti & Reichman, 1994; Wu et al., 2009). Arabinogalactans are often covalently linked to proteins and thus present as arabinogalactan proteins (AGPs), which are believed to predominantly determine the emulsifying property of the widely used emulsifier gum Arabic (Dickinson, 2003). Based on these insights, it is likely that coffee melanoidins have potential as emulsion stabilizers. This is strengthened by the fact that melanoidins are instrumental in stabilizing foams. D'Agostina et al. (2004) and Piazza et al. (2008) extracted a total foaming fraction from espresso coffee and separated it into two fractions based on solubility in 2-propanol/water. The soluble fraction exhibited a prevailing protein-like character and had better foamability, whereas the insoluble fraction showed a prevailing polysaccharide-like character that contributed more to the foam stability via the thickening behavior and/or the interaction with absorbed proteins at the air-water interface (D'Agostina et al., 2004; Piazza et al., 2008). The foamability of coffee melanoidins has been related to their amphiphilic nature: furan and pyrrole-like hydrophobic moieties and the negatively-charged hydrophilic moieties (Bekedam et al., 2007), whereas polysaccharides can behave as viscosity improvers to enhance foam stability (Nunes & Coimbra, 1998).

Coffee melanoidins constitute a significant part of the diet of coffee drinker (Fogliano & Morales, 2011), and they can also be used as food ingredients in the search for healthier and tasty foods. For example, coffee melanoidin-enriched bread was able to elicit satiety and modulate postprandial glycemia and other biomarkers (Walker et al., 2020). Our study aimed to explore the potential of coffee melanoidins as food ingredients to stabilize emulsions. Coffee melanoidins at the concentrations of 0.25-4 wt% were used to stabilize purified rapeseed oil-in-water (O/W) emulsions, and the physical properties of these emulsions were investigated during 28 days of storage. The results showed that these components have great potential for applications in emulsions.

5.2 Materials and methods

5.2.1 Materials

Dark roasted arabica coffee beans and refined rapeseed oil were purchased from a local supermarket (Wageningen, the Netherlands). The latter was stripped with alumina powder (Alumina N, Super I, EcoChrome™, MP Biomedicals, France) to remove surface-active impurities and tocopherols (Berton et al., 2011). Whey protein isolate (WPI, 88.11 wt%, dry basis) was supplied by Davisco (Lancy, Switzerland). D-Glucose, chlorogenic acid, calcofluor white, rhodamine B, BODIPY 505/515, sodium dodecyl sulphate (SDS), hexane, and sulfuric acid (98%) were purchased from Sigma-Aldrich (St. Louis, MO, USA). Sodium carbonate decahydrate and phenol were obtained from VWR (Radnor, PA, USA). Folin-Ciocalteu reagent and ethanol (95%) were purchased from Merck Millipore (Merck, Germany). Dichloromethane was from Actu-All Chemicals B.V. (Oss, The Netherlands). All chemicals and reagents used in this study were of analytical grade. Ultrapure water was obtained with a Millipore Milli-Q water purification system and used throughout the experiments.

5.2.2 Preparation of high molecular weight coffee melanoidins

High molecular weight coffee melanoidins were extracted from roasted coffee beans according to the procedure described by Zhang et al. (2019) with some modifications. In brief, dark roasted coffee beans (Illy®, Trieste, Italy) were ground to powder with a particle size < 0.45 mm using a Spex sample Prep 6870 cryogenic mill (Minneapolis, Minnesota, US). The powder was then defatted by extraction with dichloromethane (1:3, w/v, three times). After that, 100 g of the defatted powder were extracted with 1.2 L of water at 80℃ for 20 min. The suspension obtained was filtered through a Whatman 595 filter paper (Billerica, MA, US) under vacuum. An aliquot of the filtrate was subjected to ultrafiltration using an Amicon stirred cell (Millipore Co., MA, US) equipped with a 10 kDa nominal molecular weight cut-off regenerated cellulose membrane (Merck, Germany). The obtained retentate was filled up to 100 mL water and the ultrafiltration process was continued to eliminate the low molecular weight components. This washing step was repeated three times. The

retentate (high molecular weight fraction) that contained the coffee melanoidins was freeze-dried and stored at -20 °C.

5.2.3 Determination of carbohydrate, protein, and phenolic group contents

The total sugar content of coffee melanoidins was determined using the phenol-sulphuric acid method (Nielsen, 2010). Protein content (%, N × 5.5) was estimated using the Dumas method (Interscience Flash EA 1112 series, Thermo Scientific, Breda, The Netherlands) (Bekedam et al., 2006). Phenolic group content was measured using the Folin-Ciocalteu reagent, with chlorogenic acid as the standard (Singleton et al., 1965).

5.2.4 Adsorption kinetics

The interfacial tension between coffee melanoidins (or WPI) solution (0.01 w/v%) and stripped rapeseed oil was recorded with an automated drop volume tensiometer (Tracker, Teclis, Longessaigne, France) by analyzing the axial symmetric shape (Laplace profile) of a rising oil drop (area: 40 mm^2) in the aqueous solution using a 20-gauge needle. The interfacial tension (γ) was measured for 2 h at 20 °C, and the results were expressed as surface pressure ($\pi = \gamma_0 - \gamma$).

5.2.5 Preparation of coffee melanoidin-stabilized emulsions

Coffee melanoidins (0.25, 0.5, 1, 2, or 4 wt%) were dispersed in water and stirred overnight at 4 °C to ensure complete hydration. Coarse emulsions were prepared by homogenizing 90 wt% of the aqueous phase containing coffee melanoidins and 10 wt% of stripped rapeseed oil using a rotor-stator homogenizer (Ultra-turrax IKA T18 basic, Germany) at 11,000 rpm for 1 min. Final emulsions were prepared by passing the coarse emulsions through an M-110Y Microfluidizer (800 bar, 5 cycles) equipped with a F12Y interaction chamber (Microfluidics, Massachusetts, USA). The emulsions were partitioned as 3-g aliquots in polypropylene tubes (Eppendorf®,15 x 120 mm) and stored at room temperature (~ 20℃) for 28 days. To prepared 4 wt% homogenized melanoidin solution, 4 wt% coffee melanoidins (without the addition of oil) were homogenized via a rotor-stator homogenizer and Microfluidizer in the same conditions as used for the emulsion preparation.

5.2.6 Physical stability of coffee melanoidin-stabilized emulsions

The droplet size distribution, surface charge, and microstructural changes of emulsions were monitored over the storage time (at 0, 7, 14, 21, and 28 days) at room temperature (~ 20℃).

Droplet size distribution. The droplet size distribution of emulsions was determined by static light scattering using a Mastersizer 3000 (Malvern Instruments Ltd., Worcestershire, UK) at 20 ℃. The emulsions were diluted in water and stirred at 1400 rpm to prevent multiple scattering effects. The refractive index was set to 1.473 for rapeseed oil and 1.33 for water. The absorption index was set to 0.01.

Light microscopy. The microstructural changes of emulsions were monitored via an optical microscope (Carl Zeiss Axio Scope A1, Oberkochen, Germany). Emulsions were gently mixed prior to the observation. A drop of emulsions was then placed on a glass microscopy slide and covered with a cover slip. The microscopic images were taken using an objective magnification of 40 ×. Some images were taken using a polarized light filter.

Viscosity. An Anton Paar rheometer (MCR502, Anton Paar GmbH, Graz, Austria) was used to determine the dynamic viscosity of the samples at 20 °C. For 0.25–2 wt% melanoidin-stabilized emulsions and 4 wt% homogenized melanoidin solution, a concentric cylinder system (DG 26.7, diameter: 26.662 mm, internal diameter: 24.655 mm, length: 40.000 mm) was used. For 4 wt% melanoidin-stabilized emulsions, a plate-plate geometry (PP-25/P2, diameter: 25 mm) was used.

Droplet surface charge. The droplet surface charge (zeta-potential, mV) of emulsions was measured by dynamic light scattering using a Zetasizer Ultra (Malvern Instruments LTD., Worcestershire, UK) in a disposable cuvette (DTS 1080) at 20 °C. Prior to the measurement, all emulsions were diluted 1000 times in water to minimize multiple scattering effects. The optical property settings were the same as those used for the droplet size distribution measurement. Zeta-potential was calculated using the Smoluchowski model (ZS Xplorer software).

5.2.7 Surface load

The surface load of the coffee melanoidin-stabilized emulsions was determined via two methods: (i) unadsorbed melanoidins in the continuous phase, and (ii) adsorbed melanoidins in the creamed phase. Prior to the surface load analysis, calibration curves to determine coffee melanoidin concentration were obtained by recording the absorption spectra (200 – 600 nm) of melanoidins (0.01 – 0.1 g/L) dispersed in water or 1 wt% SDS solution using a DU 720 UV–visible spectrophotometer (Beckman Coulter, Woerden, the Netherlands).

Emulsions were centrifuged at 15,000×*g* for 1 h to separate the continuous phase and the creamed phase. To determine the surface load via the continuous phase, the continuous phase was collected by piercing a hole in the bottom of the centrifuge tubes. The concentration was determined according to calibration curves for melanoidins dispersed in water, and the surface load Γ_s (mg/m^2) was calculated according to Eq. (5.1):

$$\Gamma_s = \frac{C_a d_{3,2}}{6\varphi} \tag{5.1}$$

where C_a (kg/m^3 water phase) corresponds to the concentration adsorbed coffee melanoidins, which was calculated by subtracting the concentration in the continuous phase from the concentration of the melanoidin solution used for emulsion preparation, $d_{3,2}$ (m) is the Sauter mean diameter of the fresh emulsions, and φ is the oil volume fraction.

To determine the surface load via the creamed phase, the concentration of the adsorbed coffee melanoidins and the oil content in the creamed phase were measured. The creamed phase obtained after centrifugation was collected and re-dispersed in water and centrifuged again as described earlier to remove any unadsorbed coffee melanoidins that may have been trapped between the oil droplets in the creamed phase after the first centrifugation. The resulting washed creamed phase was collected. An aliquot (0.2 g) of creamed phase was mixed with 3 g of water and 15 g of extraction solvent (hexane:isopropanol, 3:1, v/v). The mixture was then vortexed for 3 × 1 min and mixed in a

rotator for 1 h, followed by centrifugation (3000×*g*, 5 min). The upper phase (hexane and oil) was collected and placed in the fume hood until the hexane evaporated, and the amount of oil remaining was weighed. Another aliquot of creamed phase was dispersed in a 1 wt% SDS solution and centrifuged at 15,000×*g* for 1 h. The adsorbed coffee melanoidins were displaced by SDS to the aqueous subnatant. The concentration of coffee melanoidins was then determined using the calibration curves for melanoidins dispersed in 1 wt% SDS. This value of C_a can directly be used in Eq. 5.1 to calculate the surface load Γ_s (mg/m^2).

5.2.8 Confocal laser scanning microscopy (CLSM)

Confocal laser scanning microscopy (CLSM) (Carl Zeiss, Jena, Germany) was used to further visualize the interfacial composition of the emulsion droplets. Proteins, polysaccharides, and lipids were fluorescently labelled with rhodamine B (10 µL/mL of sample, 1 mg/mL in water), calcofluor white (5 µL/mL of sample, 2 mg/mL in water), and BODIPY (10 µL/mL of sample, 1 mg/mL in ethanol), respectively. A small quantity of these emulsions was placed on a confocal microscope slide and gently covered with a cover slip. The excitation/emission wavelengths of rhodamine B, calcofluor white, and BODIPY were set at 543/580 nm, 405/450 nm, and 488/518 nm, respectively. Images of 512 × 512 pixels were obtained using a 100× oil immersion objective.

5.2.9 Statistical analysis

All experiments were carried out at least in triplicate on samples that were prepared in duplicate in independent experiments. The results were reported as mean values ± standard deviations. The statistical analyses were carried out using one-way analysis of variance (ANOVA) using IBM SPSS statistics 23.0.0.2 (SPSS Inc, Chicago, Illinois, USA) with $P < 0.05$ being considered as significantly different.

5.3 Results and discussion

5.3.1 Characterization of coffee melanoidins

Absorption spectra. UV–visible absorption spectra were recorded to confirm the extraction of melanoidins from coffee brews (**Figure S5.1**). The spectrum showed two absorption maxima at 280 and 325 nm and minor absorbance from 400 nm onward. This is in agreement with spectra reported previously (Bekedam et al., 2006): absorption at 280 nm has been linked to proteins, caffeine, chlorogenic acids, and caffeic acid in the melanoidins, whereas absorption at 325 nm was mainly attributed to chlorogenic acid and caffeic acid (Bekedam et al., 2006; Lopes et al., 2016). Melanoidins have been reported to have a unique absorption signature at 405 and 420 nm, which was suggested to correspond to the core structure (405 nm) and the chromophore groups of melanoidins (420 nm) (Del Pino-García et al., 2012; Silván et al., 2010). To estimate the relative content of these compounds and compare the results to those of other research, the specific extinction coefficient (K_{mix}) at 280, 325, 405 and 420 nm was calculated based on the Lambert-Beer law (**Table S5.1)**. The relative amounts of melanoidins ($K_{mix\ 405nm}$), proteins ($K_{mix\ 280nm}$), and chlorogenic acid ($K_{mix\ 280,\ 325nm}$) were in line with the results reported previously (Bekedam et al., 2006, 2007).

Chemical composition. The composition of coffee melanoidins is ~70% carbohydrates, 12% protein, and 13% phenolics as shown in **Table S5.2**. The total carbohydrate content was consistent with the results reported by others (Bekedam et al., 2006; Tagliazucchi & Verzelloni, 2014). Mannose, galactose as well as arabinose are the most abundant sugars, indicating that galactomannans (~69%) and arabinogalactans (~28%) are the main polysaccharides in coffee melanoidins (Bekedam et al., 2006; Nunes & Coimbra, 2001). The protein content of 12% is similar to the results of Nunes & Coimbra (2001), although it is good to point out that the Dumas method may result in overestimation, since other non-protein nitrogen such as caffeine and trigonelline can also be detected. The phenolic group content (13%) is in line with Bekedam et al. (2006), who reported 15% of phenolic groups, confirming that phenolic groups are also largely incorporated into melanoidins.

Surface activity. The surface pressure generated by melanoidins was measured at the rapeseed oil-water interface and compared with that obtained with whey protein isolate (WPI), a commonly used emulsifier. There was a rapid increase in surface pressure in the first 400 s, followed by a slower increase for both components, albeit that the surface pressure is higher (both initially and after 2 hours of interfacial film aging) for whey protein isolate (**Figure 5.1**).

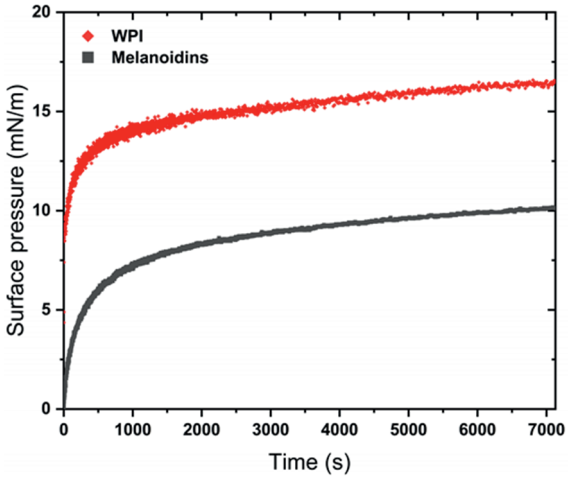

Figure 5.1. Surface pressure of WPI and coffee melanoidins at a concentration of 0.01 w/v% in water at 20℃.

Whey proteins are known to adsorb at the oil-water interface where they are next subjected to conformational rearrangements (Schröder et al., 2017). Regarding melanoidins, their surface activity might be due to the presence of amphipathic proteins, e.g., arabinogalactan proteins or galactomannans. Arabinogalactan proteins from green coffee beans have been shown to increase the surface tension at air-water interface to ~22 mN/m, and they could easily adsorb at the interface to form a film (Redgwell et al., 2005). Wu et al. (2009) and Garti & Reichman (1994) found that galactomannans were able to reduce both the surface and interfacial tensions. After diffusing and adsorbing at the interface, the galactomannans could undergo a conformational change at the interface with a hydrophobic part anchoring to the oil phase and other parts extending to the water phase (Garti & Reichman, 1994).

Particle size distribution and light microscopy. The homogenization process used for emulsion preparation (section 5.3.2) is expected to alter the particle size and possibly the charge (zeta potential) of coffee melanoidins dispersed in water. Therefore, this was investigated first. The initial particle size distribution of the dispersions was dominated by large aggregates/molecules in the micron range (≥ 10 µm) (**Figure 5.2A**) with undefined shapes (**Figure 5.2C1**). Upon homogenization, the particle size decreased considerably (**Figure 5.2 A&C2**), suggesting that the homogenization process causes disaggregation or disruption of melanoidins.

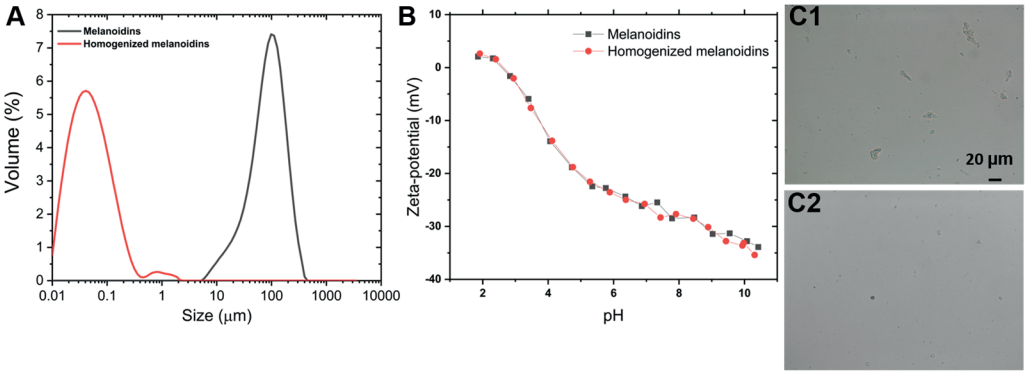

Figure 5.2. Particle size distribution (A) and zeta-potential (B) of coffee melanoidins and homogenized coffee melanoidins dispersed in water, and microscopic pictures of these dispersions (C1, C2, respectively).

Zeta-potential. For both the original and homogenized melanoidin dispersions, the plots of the zeta-potential as function of pH overlap (**Figure 5.2 B**). The isoelectric point was around 2.5, close to the values reported for melanoidins prepared from glycine and glucose (Migo et al., 1997). At pH higher than 2.5, melanoidins were negatively charged, becoming more negative as pH increased (**Figure 5.2 B**), probably due to the presence of ferulic acid or caffeic acid moieties from chlorogenic acids (CGA) and uronic acids from arabinogalactans (Bekedam et al., 2008). At pH lower than 2.5, coffee melanoidins were slightly positively charged, probably because of the amino groups from proteins (Bekedam et al., 2008; Migo et al., 1997).

5.3.2 Characterization of coffee melanoidin-stabilized emulsions

5.3.2.1 Emulsion appearance

Dispersions of coffee melanoidins in water with concentrations ranging from 0.25 to 4 wt% were used to prepare emulsions. Initially, all the emulsions had a brown, opaque, and homogeneous appearance (**Figure 5.3**, inserts in A1-E1). All the fresh emulsions were fluid-like but were more viscous at increasing melanoidin concentration.

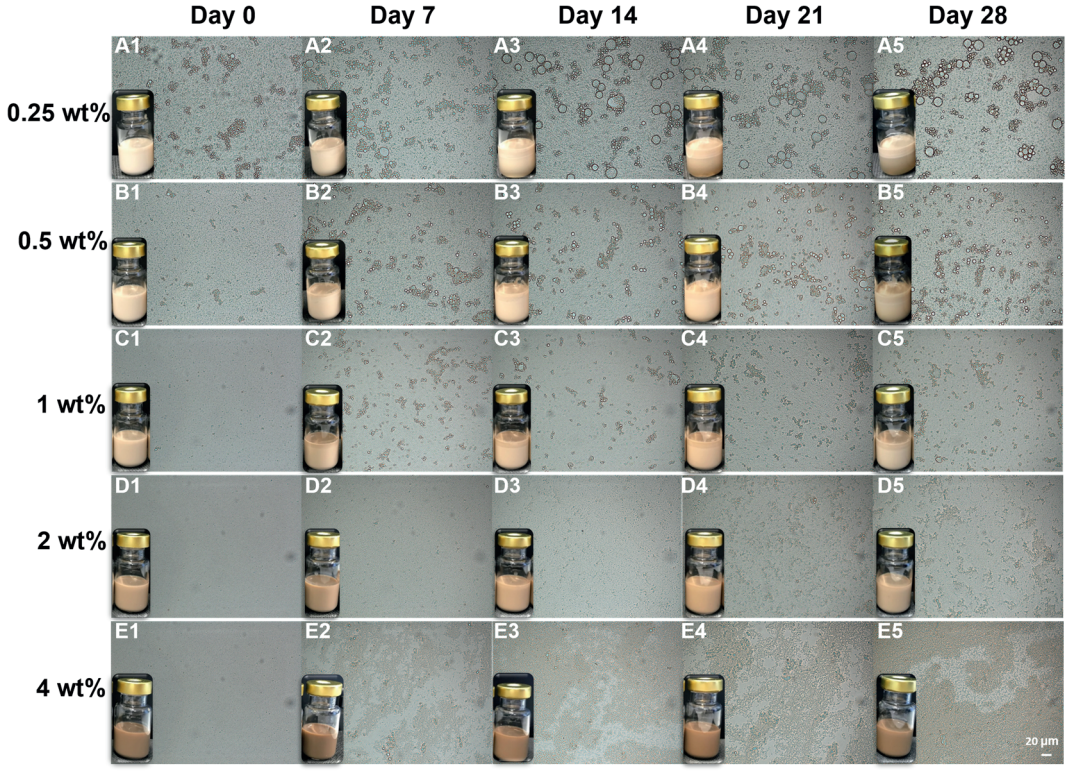

Figure 5.3. Microscopic pictures of emulsions stabilized with 0.25 (A), 0.5 (B), 1 (C), 2 (D), and 4 wt% (E) coffee melanoidins stored at room temperature for 0 (1), 7 (2), 14 (3), 21 (4), and 28 days (5). All images are at the same magnification (scale bar - shown on panel E5 - is 20 µm). Inserts are macroscopic images of the emulsions.

After 7 days of storage at room temperature, a visible creamed layer formed in emulsions containing 0.25 - 1 wt% melanoidins (**Figure 5.3**, inserts of A2-C2), whereas the emulsions containing 2 and 4 wt% melanoidins showed a homogeneous appearance (**Figure 5.3**, inserts of D2-E2). In addition, the 4 wt% melanoidin-stabilized emulsions transformed from a liquid-like state to a gel-like appearance (**Figure 5.4**, insert E). However, the emulsion gel was not strong and could easily be disrupted by agitation. Creaming rate is proportional to the square of the droplet size, and therefore creaming was expected for emulsions containing a low amount of melanoidins in which large droplets are present and the continuous phase has low viscosity (discussed further in sections 5.3.2.2 and 5.3.2.3). In the emulsions with higher continuous phase viscosity, the creaming rate is accordingly lower, and it may be reduced to zero if a weak gel is present.

After 28 days of storage, the creamed layer of the 0.25 wt% melanoidin-stabilized emulsions became more distinct, and the bottom serum layer became less opaque (**Figure 5.3**, insets of A5). For the other emulsions, no significant change in appearance was observed after day 7. It is worth noting that no oil layer was formed (no oiling off) in all emulsions during storage.

5.3.2.2 Droplet size distribution and emulsion morphology

At day zero, all emulsions exhibited a nearly monomodal size distribution, with sometimes a minor tail (**Figure 5.4**, black curves). With increasing melanoidin concentration, the most prominent peak shifted to lower values resulting in a decrease in $d_{3,2}$ from 0.42 µm to 0.06 µm (**Figure 5.4**).

For 0.25 wt% melanoidin-based emulsions, some droplets were loosely connected (**Figure 5.3A1**); whereas for 0.5 wt% melanoidin-based emulsions, slight flocculation was observed (**Figure 5.3B1**). At these relatively low concentrations, the amount of melanoidins at the interface is probably not sufficient to cover the surface of all oil droplets, resulting in bridging flocculation (with melanoidins shared between droplets), and possibly coalescence (Berton-Carabin et al., 2018; Guzey & McClements, 2006). At 0.5 wt% melanoidin concentrations and higher, the emulsions became microscopically homogeneous (**Figure**

5.3C1-E1). After 7 days of storage, emulsions containing 0.25 and 0.5 wt% melanoidins experienced more flocculation and coalescence, and those containing 1 wt% melanoidins also started to flocculate (**Figure 5.3A2-C2**). This is reflected in the occurrence of a small shoulder/peak in **Figure5. 4**. At longer storage times, a second peak appeared at larger sizes, that continued to increase in time, whereas the contribution of the smaller droplets decreased in these emulsions (**Figure 5.4A-C**), leading to further destabilization.

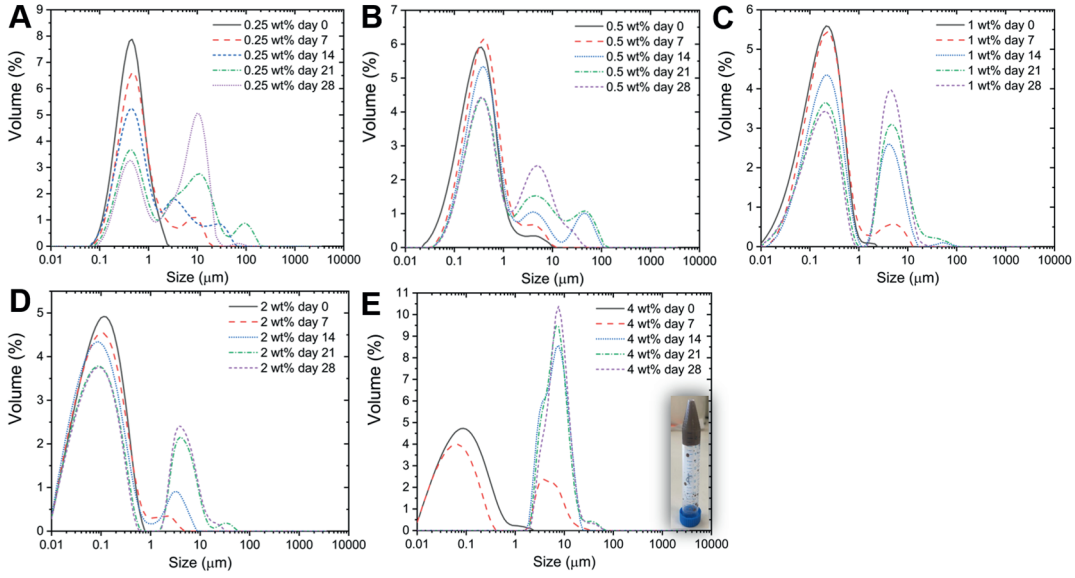

Figure 5.4. Droplet size distribution of emulsions stabilized with 0.25 (A), 0.5 (B), 1 (C), 2 (D), and 4 wt% (E) of coffee melanoidins. Insert in panel E, the gelled emulsion after 7 days of storage.

Emulsions stabilized with 2 wt% melanoidins were more stable than other emulsions. The droplet size distribution was rather constant for 2 weeks, exhibiting a monomodal distribution with a small tail (**Figure 5.4D**). After 3 weeks of storage, a second peak ranging from 1 to 100 μm appeared as a result of flocculation (**Figure 5.3D4-D5**), which remained unchanged until the end of the experiments (**Figure 5.4D**). In 4 wt% melanoidin-stabilized emulsions, a network-like structure was formed (**Figure 5.3E2**) and a large-sized peak

appeared (**Figure 5.4E**) after 7 days of storage, which dramatically increased with time, whereas the original small peak disappeared (**Figure 5.4E**). As mentioned and also illustrated by the upside-down tube in **Figure 5.4E**, 4 wt% melanoidin-stabilized emulsions gradually formed gel-like structures upon storage. Also others have found the formation of gel-like structures at high amounts of galactomannans (Garti et al., 1997; Wu et al., 2009). In the next section dedicated to viscosity, it is investigated whether the gel formation is due to the melanoidins as such, or to their interaction with the oil droplets.

5.3.2.3 Viscosity

We determined the apparent viscosity of the homogenized melanoidin solution with the highest concentration (4 wt%), and of all emulsions as a function of shear (**Figure 5.5**). The viscosity profile of the 4 wt% homogenized melanoidin solution was constant and similar to that measured for the 0.25 wt% melanoidin-stabilized emulsion. The viscosity of emulsions with >0.25 wt% melanoidins increased with melanoidin concentration and decreased with increasing shear rate, showing typical shear thinning behavior that was more pronounced at higher melanoidin concentrations. This indicates that network formation involves melanoidins and droplets, and does not occur in a concentrated pure melanoidin dispersion. Data also showed that a threshold concentration of melanoidins is needed for network formation to take place in the O/W emulsions.

The shear-thinning behavior of the emulsions can be attributed to the disintegration of the network involving droplets and melanoidins, and realignment of the droplets upon shearing, resulting in a decrease in the resistance to flow (Ye et al., 2016; Ali Al-Maqtari et al., 2021). For the emulsion with 4 wt% melanoidins, the network was strong (section 5.3.2.2), forming a gelled structure with high viscosity (**Figure 5.5**). It is interesting to note that melanoidins and oil droplets (with low dispersed fraction, 10 wt%) did not give a high viscosity on their own. Instead, the presence of large amounts of melanoidins in the continuous phase may induce depletion attraction between the droplets that thus form a gel-like network (Dickinson, 2003). Huang et al. (2019) reported that insoluble soybean fiber (ISF, 0.4 wt%) was able to improve the stability of low-concentration soy protein isolate (0.4 wt%)

emulsions (10 wt% soybean oil) via the formation of flocculated droplets and the gel-like network. Similarly, the apparent viscosity of ISF suspension (1 wt%, prepared using a rotor-stator at 10,000 rpm for 2 min) was low and constant (~3 mPa·s) with the increase of shear rate from 0 to 100 s^{-1} (Chen et al., 2019).

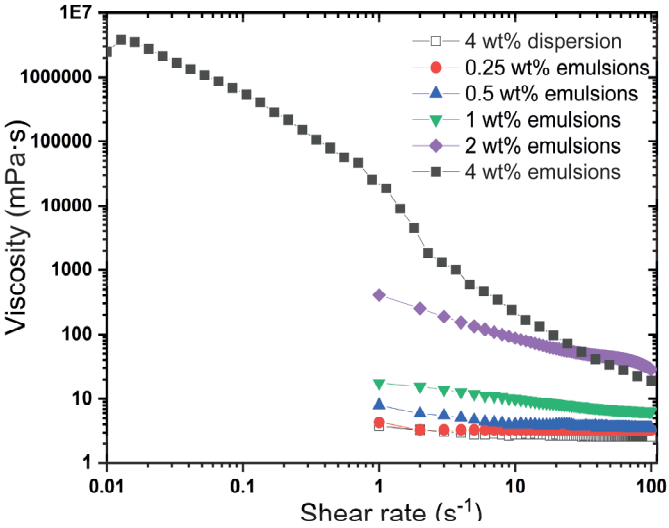

Figure 5.5. Apparent viscosity as a function of applied shear rate of the 4 wt% homogenized melanoidin solution (hollow) and of O/W emulsions (10 wt% oil) stabilized with 0.25 - 4 wt% melanoidins (solid).

5.3.2.4 Surface charge of emulsion droplets

The surface charge of the oil droplets was assessed by measuring the zeta-potential (**Figure 5.6**). All emulsions had a negative surface charge. The zeta-potential increased from -48 mV to -38 mV (**Figure 5.6**), going from melanoidin concentration 0.25 to 4 wt%, and the pH value decreased from 7 to 5.5 (**Figure S5.2**). These zeta-potentials were much higher than those measured in a pure melanoidins solution (**Figure 5.2**), which may be due to the presence of charged groups at the droplet surface or due to the rearrangement of melanoidins at the interface leading to the exposure of negatively charged groups. For each emulsion, no significant change in zeta-potential was observed upon 28 days of storage ($P > 0.05$).

In general, electrostatic repulsion between droplets is considered substantial enough to ensure emulsion stability when the magnitude of zeta-potential is greater than 30 mV (Dukhin & Goetz, 1998), which all our emulsions had (**Figure 5.6**). However, our 0.25 wt% melanoidin-stabilized emulsion (-48 mV) was not physically stable, indicating that also other destabilizing factors were playing a role.

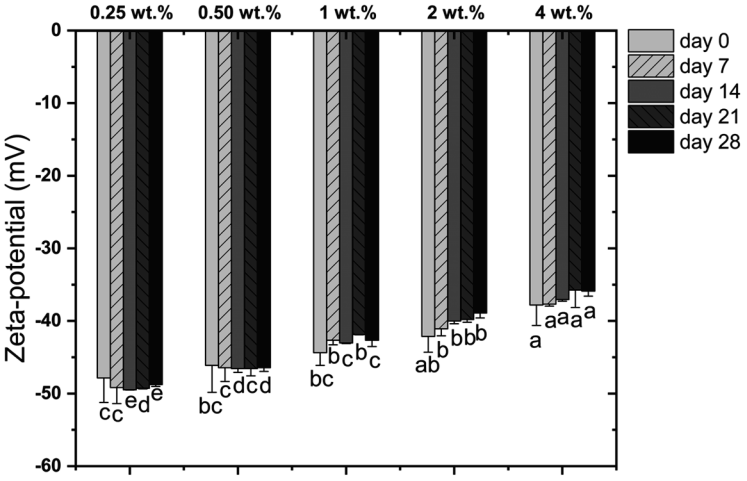

Figure 5.6. Zeta-potential of the coffee melanoidin-stabilized emulsion droplets. Small letters are for comparison among the emulsions with different melanoidin concentrations on the same day. Different letters indicate significant differences ($P < 0.05$).

5.3.2.5 Surface load

The surface load of the fresh emulsions was estimated via either the creamed phase or the continuous phase of the emulsions (**Figure 5.7**). For both methods, the surface load slightly decreased and then increased with increasing the melanoidin concentration. The continuous phase method (**Figure 5.7B**) gave higher surface loads than the creamed phase method (**Figure 5.7A**), which is in agreement with the investigations of Hinderink et al. (2021) for pea protein-stabilized emulsions. The continuous phase method is widely used but precipitated components are not accounted for appropriately, leading to overestimation of the surface load. Therefore, the creamed phase method was considered as a more reliable method for our systems.

The surface load of the melanoidin-stabilized emulsions ranged from 0.3 to 0.6 mg/m^2 (**Figure 5.7A**), which is relatively low compared to protein-stabilized emulsions (generally around 1-3 mg/m^2) but similar to values found for other polysaccharide-stabilized emulsions (e.g., 0.4 - 0.9 mg/m^2: Mikkonen et al., 2016). These results hint that polysaccharide-rich fractions from coffee melanoidins might be more likely to accumulate at the oil-water surface, a hypothesis which was further investigated by CLSM.

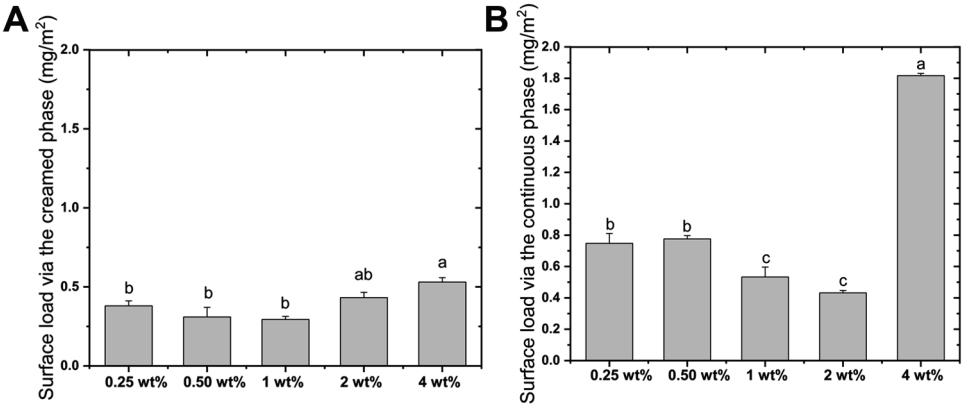

Figure 5.7. Surface load of the coffee melanoidin-stabilized emulsions measured via the creamed phase (A) or the continuous phase (B).

5.3.2.6 Confocal laser scanning microscope (CLSM) and polarized light microscope

As emulsions with large enough droplets are needed to give insightful images in CLSM, fresh emulsions stabilized with 0.25 wt% melanoidins were chosen for this study (i.e., the system with the largest droplets) (**Figure 5.8**). Most of the oil droplets (labelled in red) were connected with each other in clusters, which confirms the light microscopy results (**Figure 5.3**). Polysaccharides (labelled in green) encircled the oil droplets (**Figure 5.8 A&B**), whereas proteins (labelled in teal) were mainly detected in the continuous phase (**Figure 5.8C**), suggesting that polysaccharide-rich fractions from the melanoidins were predominantly present at the interface. To confirm this finding, 1 wt% melanoidin-stabilized coarse emulsions (prepared via rotor-stator homogenization only) were also prepared and investigated, and similar results were found (**Figure S5.3**). Other studies also found that in

polysaccharide-rich samples, the protein component did not play a significant role in stabilizing emulsions (Garti & Reichman, 1994; Mikkonen et al., 2009; Wu et al., 2009). Garti & Reichman (1994) even found that purified guar gum (protein content reduced to 0.8 wt%) had higher surface activity than the original gum, and they suggested that the protein fraction may not be surface-active.

When observing the emulsions with polarized light microscopy (Figure 5.8 D-E), both emulsions showed distinctive rings on the oil droplets, and that could be related to accumulation of galactomannan fractions at the oil-water interface, as was observed for other galactomannans-stabilized emulsions (Garti & Reichman, 1993, 1994).

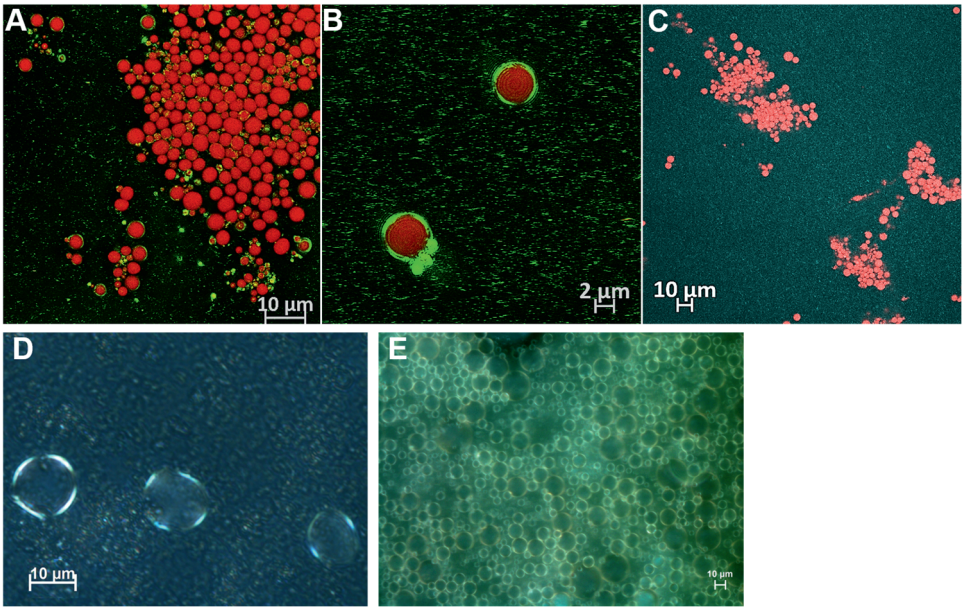

Figure 5.8. Confocal micrographs of emulsions stabilized with 0.25 wt% coffee melanoidins (A-C). Green color represents polysaccharides (stained by calcofluor white), teal color represents proteins (stained by Rhodamine B), and red color represents oil (stained by BODIPY). Polarized light microscopy images of emulsions prepared by (D) high pressure homogenization, using 0.25 wt% melanoidins, or (E) rotor-stator homogenization, using 1 wt% melanoidins.

5.4 Conclusion

This work demonstrates that naturally-occurring coffee melanoidins are capable of stabilizing O/W emulsions without the need of other stabilizers. Fresh emulsions stabilized with 0.25-4 wt% melanoidins, prepared by high pressure homogenization had a brown, opaque, and homogeneous appearance with a nearly monomodal size distribution. Upon 28 days of storage at room temperature (~20 ℃), emulsions stabilized with 0.25-1 wt% melanoidins underwent creaming and showed some droplet flocculation and possibly coalescence. The emulsion stabilized by 2 wt% melanoidins showed high physical stability, and the one prepared with 4 wt% melanoidins gradually transformed from liquid-like to gel-like state due to network formation between droplets and melanoidins.

Coffee melanoidins can reduce the oil-water interfacial tension, induce electrostatic repulsion between emulsion droplets, and may form a weak network that contribute to emulsion stability. In particular, the polysaccharide-rich fractions from the melanoidins are present at the interface, at the expense of the protein-rich fractions, as deduced by CLSM and polarized light microscopy. This study showed that coffee melanoidins exhibit great potential to formulate clean label food-grade emulsions. Further work is directed toward the capability of coffee melanoidins to act as dual-function ingredients (i.e., emulsifiers with antioxidant properties to also improve the oxidative stability of emulsions).

Supplementary materials

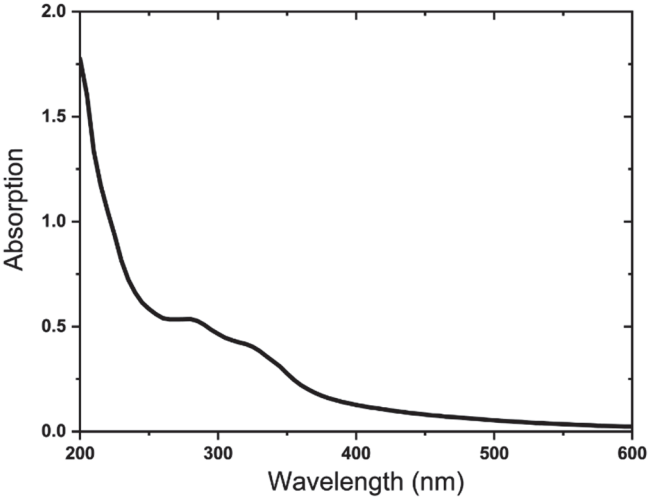

Figure S5.1. Absorption spectrum of coffee melanoidins in water (0.01 w/v%).

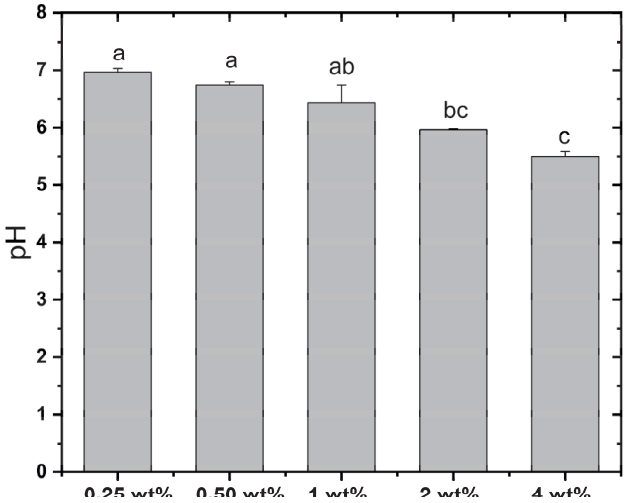

Figure S5.2. pH of the coffee melanoidin-stabilized emulsions with different melanoidin concentrations.

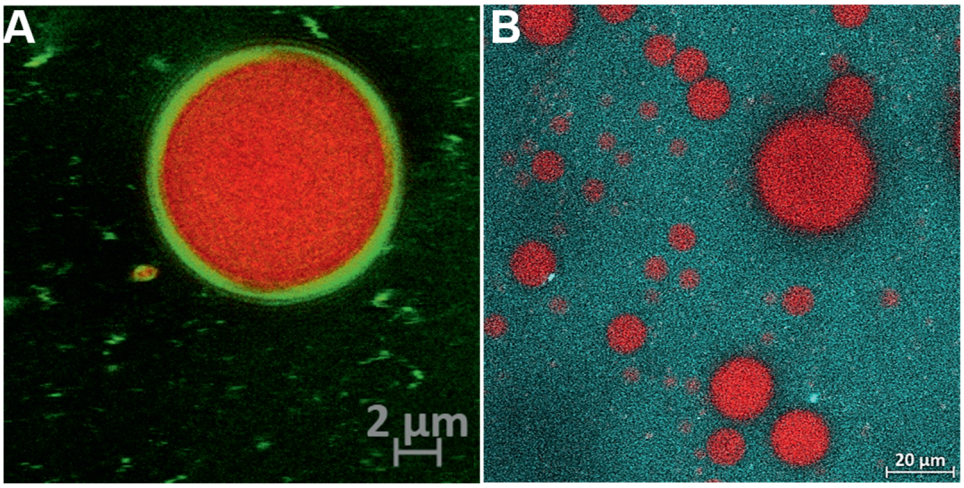

Figure S5.3. Confocal micrographs of coffee melanoidin (1 wt%)-stabilized emulsions prepared by rotor-stator homogenization (11,000 rpm for 1 min). Green color represents polysaccharides (stained by calcofluor white), teal color represents proteins (stained by Rhodamine B), and red color represents oil (stained by BODIPY).

Table S5.1. Specific extinction coefficients (K_{mix}) of coffee melanoidins in water.

Sample	$K_{mix\ 280nm}$ (L·cm^{-1}·g^{-1})	$K_{mix\ 325nm}$ (L·cm^{-1}·g^{-1})	$K_{mix\ 405nm}$ (L·cm^{-1}·g^{-1})	$K_{mix\ 420nm}$ (L·cm^{-1}·g^{-1})
Coffee melanoidins	5.29 ± 0.10	3.99 ± 0.07	1.20 ± 0.01	1.06 ± 0

Table S5.2. Chemical composition of coffee melanoidins.

Sample	Carbohydrates (%)	Proteins (%)	Phenolic groups (%)
Coffee melanoidins	70.82 ± 3.63	12.18 ± 1.37	13.38 ± 1.38

6

Physical and oxidative stabilization of oil-in-water emulsions by roasted coffee fractions: Interface- and continuous phase-related effects

This chapter will submitted as Feng, J., Schroën, K., Guyot, S., Gacel, A., Fogliano, V., & Berton-Carabin, C. C. Physical and oxidative stabilization of oil-in-water emulsions by roasted coffee fractions: Interface- and continuous phase-related effects.

Abstract

Food emulsions fortified with health-promoting polyunsaturated fatty acids are highly relevant from a nutritional perspective; however, such products are particularly prone to lipid oxidation, resulting in quality deterioration. In the current work, this is mitigated by the use of natural antioxidants occurring in coffee. Coffee fractions with different molecular weights were extracted from roasted coffee beans using hot water. We found that these components were positioned either at the interface or in the continuous phase of emulsions where they contributed to emulsion stability via different pathways.

Coffee brew as a whole, and its high molecular weight fraction (HMWF), were able to form emulsions with good physical stability and excellent oxidative stability. When added post homogenization to the continuous phase of protein-stabilized emulsions, all coffee fractions were able to slow down lipid oxidation considerably without significantly affecting the physical stability of emulsions, though HMWF were more effective in retarding lipid oxidation than whole coffee brew and the low molecular weight fraction (LMWF) of coffee brew. This is caused by various effects, such as the antioxidant properties (metal chelating and radical scavenging activities) of coffee extracts, the partitioning of components in the emulsions, and the nature and amount of the phenolic compounds.

These outcomes show that coffee extracts can be used effectively as multifunctional stabilizers in dispersed systems leading to emulsion products with high chemical and physical stability. The fact that these components act as natural antioxidants gives them great potential for applications in food products.

6.1 Introduction

It is nowadays well-recognized that higher amounts of ω-3 polyunsaturated fatty acids should be targeted to contribute to healthier diets (Morzelle et al., 2020). As a result, the food industry strives for developing ω-3-rich products, but that is far from trivial. The presence of several double bonds makes ω-3 polyunsaturated fatty acids vulnerable to oxidation, which results in quality deterioration in foods (e.g., undesirable changes in flavor, nutritional quality, and shelf life) (McClements & Decker, 2018; Villière et al., 2007). A strategy to counteract lipid oxidation is through the addition of antioxidants, and ideally, these should be natural antioxidants that are preferred by consumers (Rasheed & Fathima Abdul Azeez, 2019). Synthetic antioxidants, such as butylated hydroxytoluene (BHT) and butylated hydroxyanisole (BHA) are known to be highly effective, and currently, the search is on for natural alternatives that are just as effective.

Coffee is a rich source of compounds with potent antioxidant activity, which is modulated by the coffee bean roasting process (Parliment, 2000). During roasting, on the one hand, natural phenolic compounds (predominantly chlorogenic acids, CGAs) present in the green coffee beans undergo chemical reactions such as isomerization, degradation, and/or oxidation, leading to a reduction of their antioxidant activity (Panusa et al., 2013), whereas on the other hand, additional antioxidant activity may be created through Maillard reaction product formation. In particular, melanoidins that are generated during roasting of coffee beans at high temperatures and low water activity (Del Pino-García et al., 2012; Delgado-Andrade & Morales, 2005) could be of interest due to their antioxidant potential. In addition, some volatile heterocyclic compounds (furans, pyrroles, and maltol) formed during roasting have also been reported as potential antioxidants (Yanagimoto et al., 2004). The antioxidant mechanisms of coffee components were reported to be mainly related to their ability to break the radical chain reaction cascade by hydrogen donation and to chelate metal ions (Delgado-Andrade et al., 2005; Echavarría et al., 2012; Mesías & Delgado-Andrade, 2017).

Coffee fractions may contribute in various ways to the overall antioxidant activity of coffee. The high antioxidant activity of the high molecular weight fraction (HMWF) from coffee brew was attributed to melanoidins to which low molecular weight compounds (e.g., phenolic compounds) were bound (Coelho et al., 2014; Delgado-Andrade et al., 2005; Moreira et al., 2012). The low molecular weight fraction (LMWF) from coffee brew is in itself rich in phenolic compounds that constitute 70% of the overall antioxidant capacity (Verzelloni et al., 2011), and the remaining effects are expected to be caused by volatile heterocyclic compounds (Perrone et al., 2012). Although the antioxidant activity (e.g., metal chelating and radical scavenging activities) of coffee fractions has been widely reported, their ability to inhibit lipid oxidation in food systems (e.g., emulsions) has not been investigated. Unfortunately, the antioxidant activity is not always a good predictor of their efficacy as antioxidants in foods (Decker et al., 2017). This could be due to the complexity of food systems where antioxidants can be partitioned at different locations, and therefore their properties (reactivity) may vary depending on the nature of the environments present (e.g., interactions with other components).

As mentioned, the effect of chemically active components on lipid oxidation in emulsions largely depends on their localization (i.e., in the oil phase, aqueous phase, or at the interface). It is widely admitted that lipid oxidation initiates at the oil-water interface (Berton-Carabin et al., 2014). Adsorbed emulsifiers with antioxidant potential (interfacial antioxidants) may therefore promote good oxidative stability of emulsified lipids through various mechanisms, such as free radical scavenging, transition metal chelating, and secondary oxidation product binding (McClements & Decker, 2018). On the other hand, localization away from the interface may make antioxidants less effective in mitigating the previously mentioned effects, but may still contribute through other mechanisms, e.g., binding of metal ions, therewith delaying initiation of lipid oxidation (McClements & Decker, 2018). In fact, there is a large proportion of emulsifiers remaining in the continuous phases, and thus the contribution of these non-adsorbed emulsifiers (in particular, proteins) to retard lipid oxidation could be substantial (Berton-Carabin et al., 2014).

We recently reported the ability of the high molecular weight fraction from coffee brew to physically stabilize oil-in-water (O/W) emulsions, with the polysaccharide-rich fraction predominantly present at the interface (**Chapter 5**). Considering their emulsifying properties and well-known antioxidant activity, one can assume that certain coffee fractions could act as antioxidant emulsifiers. The current research was therefore aimed to assess the efficiency of different coffee fractions, either present at the interface or in the continuous phase, to stabilize O/W emulsions, with a particular emphasis on their ability to inhibit lipid oxidation. To achieve this, different coffee fractions (coffee brew, HMWF, non-defatted HMWF, and LMWF) were extracted from dark roasted arabica coffee beans. Then, they were either used to make rapeseed oil-in-water (O/W) emulsions, or added to the continuous phase of whey protein isolate (WPI)-stabilized emulsions (with minimal excess WPI remaining in the continuous phase). The physical and oxidative stability of these emulsions were monitored during storage at 40℃.

6.2 Materials and methods

6.2.1 Materials

Dark roasted arabica coffee beans and rapeseed oil were obtained from a local supermarket (Wageningen, the Netherlands). Rapeseed oil was stripped with alumina powder (Alumina N, Super I, EcoChrome™, MP Biomedicals, France) to remove the surface-active impurities and tocopherols (Berton et al., 2011). Whey protein isolate (WPI, 88.11 ± 1.15 wt%, N × 6.25) was obtained from Davisco (Lancy, Switzerland). L-ascorbic acid, 1,1-diphenyl-2-picryl-hydrazyl (DPPH), 3-(2-pyridyl)-5,6-di(2-furyl)-1,2,4-triazine-5',5''-disulfonic acid disodium salt (ferene), iron(II) sulfate heptahydrate ($FeSO_4 \cdot 7H_2O$), chlorogenic acid (#C3878), caffeic acid, p-coumaric, cumene hydroperoxide solution (80%), sodium chloride (NaCl), para-anisidine and n-hexane were purchased from Sigma-Aldrich (Saint Louis, MO, USA). Glacial acetic acid, hydrochloric acid (37%), 2-propanol, 1-butanol ethanol, ethylenediaminetetraacetic acid (EDTA), barium chloride dihydrate ($BaCl_2 \cdot 2H_2O$), ammonium thiocyanate (NH_4SCN), and sodium hydroxide (NaOH) were obtained from

Merck Millipore (Merck, Germany). Acetonitrile and methanol were purchased from Carlo Erba Reagents (Val de Reuil, France). Dichloromethane was obtained from Actu-All Chemicals B.V. (Oss, The Netherlands). Sodium acetate trihydrate was purchased from VMR (Radnor, PA, USA). Ferulic acid was obtained from Extrasynthèse (Genay, France). All solvents were of at least of analytical grade. Ultrapure water was obtained from a Millipore Milli-Q water purification system (Millipore Corporation, Billerica, MA, USA) and used for all experiments.

6.2.2 Preparation of coffee brew

Roasted coffee beans were ground using a Spex sample Prep 6870 cryogenic mill (Minneapolis, Minnesota, US) to pass through a 0.425 mm sieve. The ground coffee was defatted using dichloromethane (1:3, w/v) three times. Coffee brew was prepared by adding 100 g of the defatted ground coffee to 1200 mL of water at 80℃ for 20 min, followed by filtering through a filter paper (Whatman 595, Billerica, MA, US). Part of the filtrate was freeze-dried and stored at -20 °C before use, and the other part of the filtrate was used for further isolation (section 6.2.3).

6.2.3 Isolation of high molecular weight fraction (HMWF), low molecular weight fraction (LMWF), and non-defatted HMWF from coffee brew

An aliquot of the coffee brew obtained above was subjected to ultrafiltration (10 kDa, Amicon® stirred cell, Millipore Co., MA, US). The filtrate was collected and is referred to as low molecular weight fraction (LMWF). To the retentate, 100 mL water was added during three washing steps, which thus became the high molecular weight fraction (HMWF). The HMWF was lyophilized and stored at -20 °C. Non-defatted HMWF was prepared similarly as HMWF, except for the defatting step with dichloromethane that was not included.

6.2.4 Carbohydrate, protein, and phenolic group contents

The total sugar content of different coffee fractions (coffee brew, HMWF, non-defatted HMWF, and LMWF) was measured using the phenol-sulphuric acid method (Nielsen, 2010). Nitrogen content was determined using the Dumas method (Interscience Flash EA 1112 series, Thermo Scientific, Breda, The Netherlands), and protein content was estimated using

a nitrogen to protein factor of 5.5 (Bekedam et al., 2006). Phenolic group content was evaluated with the Folin-Ciocalteu reagent, using chlorogenic acid as the standard (Singleton et al., 1965).

6.2.5 Analysis of unbound phenolic compounds by liquid chromatography coupled with diode array detection and mass spectrometry (LC-DAD-MS)

Methanol suspensions (for coffee brew and HMWFs) or dilutions (for LMWF) of the coffee fractions were sonicated for 30 min, then diluted 2-fold with acidified water (0.1 v% formic acid), filtrated on 0.45 µm PTFE filters and finally injected (2 µL) onto the LC-DAD-MS system. Separations were performed on a reverse-phase Purospher STAR Hibar HR RP18 end-capped column (150 mm × 2.1 mm, 3 µm, thermostated at 30 °C, Supelco, Bellefonte, PA, USA) in a LC system that is composed of a solvent degasser (SCM1000, Thermo scientific, Wathman, MA, USA), a binary high-pressure pump (1100 series, Agilent Technologies, Santa Clara, CA, USA) and a Surveyor autosampler thermostated at 4 °C (Thermo Scientific), and equipped with a UV-visible photodiode array detector (UV6000 LP, Thermo Scientific) and an ion trap mass spectrometer with electrospray ionization source (LCQ Deca, Thermo Scientific). The separation of phenolic compounds was performed using a gradient mixture of A (0.1 v% formic acid in water) and B (0.1 v% formic acid in acetonitrile) at a flow rate of 0.2 mL/min. The linear gradient elution steps were: 0–3 min, 3% B; 3–21 min, 7% B; 21–27 min, 13% B; 27–41 min, 20% B; 41–51 min, 45% B; 51–53 min, 90% B; 53–56 min, 90% B, followed by washing and reconditioning of the column. UV-visible detection was performed in the 240–600 nm range. MS spectra were acquired in full scan mode with negative ionization mode on m/z 50–2000 range. The source parameters were set as follows: spray voltage, 4.2 kV; capillary voltage, -41 V; sheath gas, 66 arbitrary units; auxiliary gas, 10 arbitrary units; capillary temperature: 250 °C. The phenolic compounds were identified by comparison of their retention times, UV−vis spectra, and mass spectra with those of the standards, and quantified using the UV-visible spectra based on the external standards for each class of phenolic compounds. Data were analyzed using Xcalibur software (Thermo Scientific).

6.2.6 Analysis of covalently bound phenolic compounds

The covalently bound phenolic compounds were released by alkaline saponification of HMWF, non-defatted HMWF, and coffee brew according to the method described by Zhang et al., (2019) with some modifications. Briefly, 45 mg of sample was dissolved in 3 mL of 2 M NaOH solution containing 20 mM EDTA and 2 w/v% ascorbic acid. After incubation at 30 °C for 1 h, the mixture was adjusted to pH 3.0 with 5 M HCl. The mixture was stored at 4 °C for 2 h, followed by centrifugation at 4000*g* and 4 °C for 10 min. The supernatant was diluted by two with methanol, filtered with a 0.45 µm PTPE filter and injected (2 µL) into the LC-DAD-MS system for analysis as described in section 6.2.5.

6.2.7 Interfacial activity

The interfacial tension between the stripped rapeseed oil and different coffee fractions in water (0.01 w/v%) was measured with an automated drop volume tensiometer (Tracker, Teclis, Longessaigne, France). A rising oil drop (area: 40 mm^2 made with a 20-gauge needle) was immersed in an aqueous with the component of interest. The interfacial tension (γ) was calculated based on the shape of the droplet using the Laplace equation and measured for 7200 s at 20 ℃. The results were expressed as surface pressure ($\pi = \gamma_0 - \gamma$), with γ_0 the interfacial tension between oil and water without any coffee fraction.

6.2.8 Antioxidant properties

1,1-Diphenyl-2-picryl-hydrazyl (DPPH) radical scavenging activity of coffee fractions was determined according to the method described by Yen & Hsieh (1995) with a few modifications. Briefly, 1 mL of fresh DPPH solution (200 µM in ethanol) was added to 1 mL of 0.01 w/v% WPI or coffee fraction suspension/solution in water. The mixture was shaken at 20℃ in the dark for 30 min (Eppendorf ThermoMixer® C, Eppendorf, Hamburg, Germany). The absorbance of the reaction mixture (A_s: 1 mL ethanol, 1 mL sample with 0.01 w/v% component) was determined at 517 nm using ethanol as the blank. The scavenged percent of DPPH radicals (%) was calculated according to Eq. (6.1).

$$\text{DPPH radical scavenging activity } (\%) = \left(1 - \frac{A_S - A_b}{A_c}\right) \times 100\% \quad (6.1)$$

where A_b is the absorbance of the mixture of ethanol (1 mL) and sample (1 mL, 0.01 w/v%), and A_c is the absorbance of the mixture of DPPH solution (1 mL) and water (1 mL).

Iron-chelating capacity was determined using a modified version of (Hennessy et al., 1984). In brief, 1 mL of 0.01 w/v% WPI or coffee fraction was mixed with a known amount of ferrous iron (1 mL). The mixture was vortexed and left at 20 °C for 24 h, and then separated using an ultrafiltration-centrifugation tube with a membrane (cut-off 10 kDa). The filtrate obtained (0.5 mL) was added to 1 mL of dissociating agent (containing 0.5 mL of 0.5 M L-ascorbic acid and 0.5 mL of 1.4 M acetic acid buffer (pH 4.5)) and 0.1 mL of 6 mM ferene solution. After 5 min, the absorbance was measured at 593 nm. The quantity of bound iron (μg per mg of the sample) was calculated using a mass balance between unbound Fe^{2+} in the filtrate and the initial Fe^{2+} content.

6.2.9 Emulsion preparation

A coarse O/W emulsion containing 10 wt% stripped rapeseed oil and 90 wt% aqueous phase (with 2 wt% coffee fractions or WPI) was prepared using a rotor-stator homogenizer (Ultra-turrax IKA T18 basic, Germany) at 11,000 rpm for 1 min. A M-110Y Microfluidizer (equipped with a F12Y interaction chamber, Microfluidics, Massachusetts, USA) was used to further break down the coarse oil droplets to fine droplets with five passes at 800 bar. Potassium sorbate (0.2 wt%) was added to emulsions to prevent microbial spoilage. Emulsions (2 g aliquots) were partitioned in polypropylene tubes (Eppendorf®,15 x 120 mm), which were then incubated in the dark at 40℃ for 7 days under rotative agitation at 2 rpm (SB3 rotator, Stuart, Staffordshire, UK).

Addition of components. Stock WPI (1 wt%)-stabilized emulsions (20 wt% rapeseed oil) were prepared as previously described (Feng et al., 2021). Coffee fractions suspensions, WPI solution, or water were added to the stock emulsions to achieve final concentrations of 0.5 wt% emulsifier, 10 wt% oil, and 0.125-2 w/v% excess compounds (coffee fractions or WPI) in the continuous phase. To prevent microbial growth, 0.2 wt% of potassium sorbate was added. These emulsions were incubated under the same conditions as described above.

6.2.10 Physical properties of emulsions

The physical properties of emulsions were measured immediately after emulsification and at the end of incubation at 40℃.

The droplet size distribution was determined by static light scattering using a particle size analyzer (Mastersizer 3000, Malvern Instruments Ltd., Worcestershire, UK). The optical parameters were a dispersed phase refractive index of 1.473, a droplet absorbance of 0.01, and a continuous phase refractive index of 1.33.

Light microscopy (Carl Zeiss Axio Scope A1, Oberkochen, Germany) was used to capture the emulsion microstructure. One droplet of the emulsion was placed on a microscopic slide and covered with a coverslip. Images were taken at a magnification of 40 ×.

Surface charge was measured through zeta-potential using a dynamic light scattering instrument (Zetasizer Ultra, Malvern Instruments Ltd., Worcestershire, UK). Emulsions were diluted 1000-fold in water to prevent multiple scattering. The optical parameters were the same as those used for the droplet size distribution measurement. Measurements were performed at 20 °C.

6.2.11 Lipid oxidation

Lipid oxidation of emulsions was evaluated by determining the primary (lipid hydroperoxides) and secondary (aldehydes) oxidation products throughout the incubation period.

Lipid hydroperoxides were measured according to a method reported by Shanta & Decker (1994) with some modifications. In short, 0.3 g of emulsion was mixed with 1.5 mL of n-hexane/2-propanol (3:1, v/v). The mixture was vortexed 3 times for 10 s each, with 20 s intervals, followed by centrifugation at 14600 rpm for 2 min. Then, 0.2 mL of the upper organic phase was mixed with a 2.8 mL of methanol/1-butanol (2:1, v/v) and 30 µL of thiocyanate/ferrous iron solution (1:1, v/v). After 20 min, the absorbance of the sample was measured at 510 nm using a DU 720 UV–visible spectrophotometer (Beckman Coulter,

Woerden, the Netherlands). The lipid hydroperoxide concentration was calculated using a cumene hydroperoxide standard curve.

Aldehydes were measured through the para-anisidine value (*pAV*) according to the AOCS Official Method CD 18-90 (AOCS, 1998). In brief, 2 g of emulsion was mixed with 5 mL of n-hexane/2-propanol (3:1, v/v) and 1 mL of saturated sodium chloride solution. The mixture was vortexed 3 times for 10s with 20 s intervals and centrifuged at 4000 rpm for 8 min. The absorbance of the upper hexane layer (A_b) was measured at 350 nm using hexane as a blank. Then, 1 mL of this hexane phase was mixed with 0.2 mL of para-anisidine solution (0.25 w/v% in acetic acid). After 10 min, the absorbance (A_s) was measured at 350 nm using hexane with para-anisidine solution as a blank. The *pAV* (arbitrary units) was calculated according to Eq. (6.2):

$$pAV = \frac{1.2 \times A_s - A_b}{m} \quad (6.2)$$

where m is the mass (g) of oil per mL hexane.

6.2.12 Statistical analysis

All analyses were carried out in triplicate on at least two independent samples, and data were reported as mean values ± standard deviation. Significance of the results ($p < 0.05$) was determined by one-way analysis of variance (ANOVA) with Tukey's post-hoc test using IBM SPSS statistics software 23.0.0.2 (SPSS Inc, Chicago, Illinois, USA).

6.3 Results and discussion

6.3.1 Characterization of coffee fractions

6.3.1.1 Chemical composition

The carbohydrate, protein, and phenolic contents of different coffee fractions are listed in **Table 6.1**. The carbohydrate contents of the coffee brew, HMWF, and LMWF were around 38, 70, and 16 wt%, respectively, which are within the range of values reported in literature

(Bekedam et al., 2006; Bekedam, Loots, et al., 2008; Lopes et al., 2016; Oosterveld et al., 2003; Tagliazucchi & Verzelloni, 2014). The majority of the carbohydrates from coffee brew ended up in HMWF (**Table 6.1**), indicating that coffee brew carbohydrates are mostly polysaccharides with a minor fraction of simple sugars and oligosaccharides. Mannose, galactose, and arabinose are the most abundant sugar residues in HMWF, which suggests that these are the main constituents of polysaccharides in coffee brew and HMWF (Bekedam et al., 2006; Nunes & Coimbra, 2001). During coffee roasting, these polysaccharides undergo structural changes (e.g., depolymerization, debranching, isomerization, and polymerization) and are involved in melanoidin formation (Moreira et al., 2014; Simões et al., 2019). The most abundant sugars in LMWF were reported to be mannose and galactose (Ludwig, Clifford, et al., 2014).

The protein contents of the coffee brew, HMWF, and LMWF are 17, 12, and 22 wt%, respectively (**Table 6.1**), which is in line with other studies (Bekedam et al., 2006; Bekedam, Roos, et al., 2008). Proteins in green coffee beans undergo denaturation, depolymerization, and Maillard reactions during roasting, resulting in compositional and structural changes and integration into the polymeric structure of melanoidins (Wei & Tanokura, 2015).

Coffee brew, HMWF, and LMWF contain ~20, 17, and 32 wt% of phenolic compounds, respectively (**Table 6.1**), which is in line with the findings of Bekedam et al. (2006). Potentially, these proportions are overestimated because of interferences with non-polyphenolic materials, in particular proteins, in the Folin-Ciocalteu assay. Therefore, phenolic compounds in their free and bound forms were also analyzed by HPLC-DAD-MS. Free phenolic compounds in coffee brew and LMWF were directly analyzed in aqueous methanol whereas bound phenolics in HMWF and defatted HMWF were analyzed after alkaline hydrolysis (**Table 6.2**). The main phenolic compounds in coffee fractions were chlorogenic acids (CGAs), amongst which the caffeoylquinic acids (CQAs) were present in much higher amounts than feruloylquinic acids (FQAs) and dicaffeoylquinic acids (diCQAs), which is in agreement with Ludwig, Mena, et al. (2014). As shown in **Table 6.2** (detailed data can be found in **Table S6.1**), free CQAs, FQAs, diCQAs, and CQLs were detected in coffee

brew and its LMWF, which is consistent with the findings from previous research (Bekedam, Roos, et al., 2008). In contrast, no free CGAs were found in HMWFs; during coffee bean roasting, a part of the CGAs are degraded into phenol derivatives and bound to melanoidins' backbones (Bekedam, Schols, et al., 2008; Coelho et al., 2014; Silván et al., 2010), which cannot pass the ultrafiltration membrane. Thus, covalently bound CGAs were measured after the saponification of HMWFs coffee fractions. For these fractions, the release of caffeic (CA), ferulic (FA), and *p*-coumaric (*pc*oum) acids were observed (**Table 6.2**), suggesting the incorporation of CQAs, diCQAs, FQAs, caffeoylferuloylquinic acids (CFQAs), and *p*-coumaroylquinic acids (*p*CoQAs) into melanoidins (Perrone et al., 2012).

Non-defatted HMWF was prepared to investigate if the defatting step affected the composition of HMWF. As shown in **Table 6.1**, this does not seem to be the case since non-defatted HMWF has a similar amount of carbohydrates, phenolic compounds, and proteins compared to the HMWF.

Table 6.1. Composition of coffee fractions*

Sample	Carbohydrates (wt%)	Phenolic compounds (wt%)**	Proteins (wt%)
Coffee brew	37.77 ± 0.64^{b}	20.31 ± 1.02^{b}	17.30 ± 1.25^{ab}
HMWF	70.82 ± 3.63^{a}	16.94 ± 0.76^{bc}	12.18 ± 1.37^{b}
Non-defatted HMWF	72.85 ± 1.17^{a}	15.89 ± 1.08^{c}	10.92 ± 0.12^{b}
LMWF	16.40 ± 0.50^{c}	32.30 ± 1.30^{a}	22.29 ± 4.07^{a}

* Different letters indicate significant differences (P < 0.05) between samples for each component.

** Chlorogenic acid (CGA) was used as a reference phenolic compound.

Table 6.2. Unbound and covalently bound phenolic compounds of coffee fractions (g/100g)

	Unbound phenolic compounds		Covalently bound phenolic compounds	
	Coffee brew	**LMWF**	**HMWF**	**Non-defatted HMWF**
total CQAs	2.94 ± 0.14	5.50 ± 0.09	nd	nd
total FQAs	0.83 ± 0.05	1.69 ± 0.02	nd	nd
total diCQAs	0.04 ± 0.00	0.07 ± 0.00	nd	nd
total CQLs	0.42 ±0.03	0.86 ± 0.07	nd	nd
CA	nd	nd	0.44 ± 0.01	0.43 ± 0.02
FA	nd	nd	0.10 ± 0.00	0.10 ± 0.00
***pc*oum**	nd	nd	0.01 ± 0.00	0.01 ± 0.00

nd: not detected; +/- values correspond to standard deviation (n=3).

6.3.1.2 Interfacial activity

The interfacial activity of coffee fractions was determined by their time-dependent capacity to increase the surface pressure at the oil-water interface and was compared with that of WPI, a commonly used emulsifier. As shown in **Figure 6.1**, all samples showed a rapid increase in the surface pressure within the first 400 s, followed by a slower increase. However, the surface pressure values obtained with WPI were always higher than those obtained with the coffee fractions. Comparing the coffee fractions, HMWF and non-defatted HMWF led to a higher surface pressure than LMWF, while the surface pressure obtained with coffee brew fell in between those obtained with HMWF and LMWF (**Figure 6.1**), as expected.

Whey proteins are known to rapidly diffuse and adsorb at the oil-water interface, thus lowering interfacial tension, and in later stages also re-arranging and forming surface films (Schröder et al., 2017). HMWF contains amphipathic proteins (e.g., arabinogalactan proteins) as part of the melanoidins and these components are also surface-active (Redgwell et al., 2005). The majority of compounds in the LMWF are highly polar, and this

may imply that surface activity is relatively low, as may be concluded from **Figure 6.1**. The lower surface activity of coffee brew compared to HMWF is a logical combination of the effects found for HMWF and LMWF.

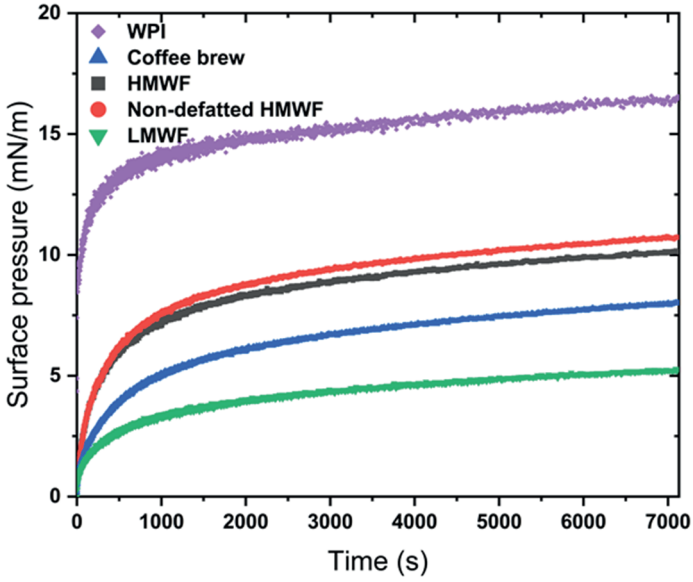

Figure 6.1. Surface pressure of WPI and coffee fractions (0.01 w/v%) as a function of time, at the stripped oil-water interface, at 20 ℃. For clarity, one representative curve is shown for each sample, but similar results were obtained on independent triplicates.

6.3.2 Coffee fractions at the interface of emulsions

6.3.2.1 Physical properties of emulsions

HMWF from coffee brew (melanoidins) used at concentrations ranging from 0.25 to 4 wt% was previously found to be able to physically stabilize O/W emulsions, amongst which the 2 wt% melanoidin-stabilized emulsions showed the highest physical stability (**Chapter 5**). Here, we tested all coffee fractions at a concentration of 2 wt% for emulsion preparation and evaluated their effect on droplet size distribution, microstructure, droplet surface charge, and later also lipid oxidation was monitored throughout storage. WPI (2 wt%)-stabilized emulsions were used as reference emulsions.

With the exception of emulsions stabilized with LMWF that underwent creaming and subsequent oiling off shortly after homogenization, all other freshly prepared emulsions exhibited a nearly monomodal size distribution with a mean droplet size ($d_{3,2}$) of ~0.1 µm (**Figure 6.2**). The coffee brew-stabilized emulsions showed a small peak at larger sizes due to slight flocculation and coalescence (**Figures 6.2B & S6.1**). Upon 7 days of storage at 40℃, WPI-stabilized emulsions remained fully stable (**Figure 6.2A**), and non-defatted HMWF-stabilized emulsions remained mostly stable even though a minor tail in the size distribution appeared between 1 and 3 µm (**Figure 6.2D**). Multimodal size distributions were observed in emulsions stabilized with coffee brew and HMWF (**Figure 6.2 B&C**), which was probably caused by flocculation and coalescence of droplets (**Figure S6.1**). Nevertheless, no oiling off was detected in all emulsions.

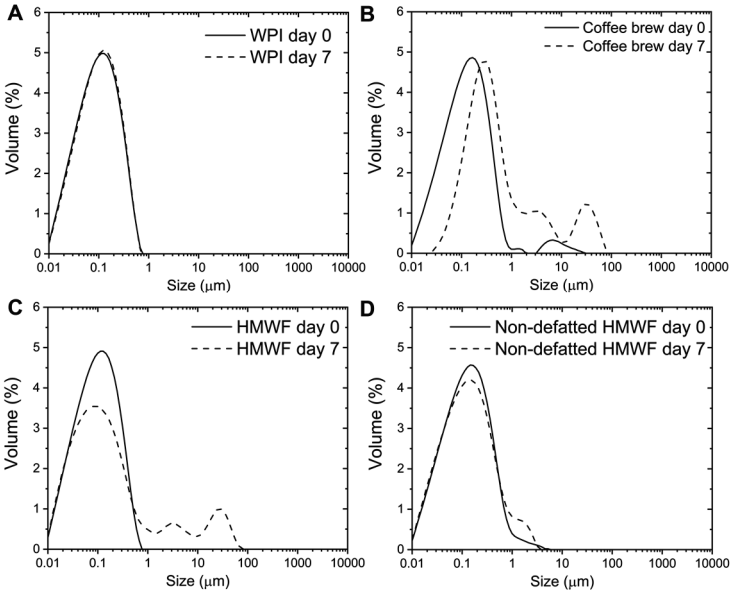

Figure 6.2. Droplet size distribution of emulsions stabilized with WPI (A), coffee brew (B), HMWF (C), and non-defatted HMWF (D) freshly prepared (solid line) or after 7 days at 40℃ (2) (dotted line). For all emulsions, the concentration of the emulsifying ingredient was 2 wt%. For clarity, one representative curve is shown for each sample, but similar results were obtained on independent triplicates.

The zeta-potential (**Figure 6.3**) was measured, and all freshly prepared emulsions had a negative charge at around -40 mV, which was expected because both WPI and coffee melanoidins are negatively charged at pH higher than the isoelectric point (~5.1 and ~2.5, respectively). At the end of storage, the emulsions still had a considerable net charge, with significant changes noted (except for coffee brew-stabilized emulsions, **Figure 6.3**). The decrease in zeta-potential for WPI-stabilized emulsions might be related to the surface-active fatty acids that may be formed upon lipid hydrolysis, or organic acids generated as a result of lipid oxidation, or degradation of positively charged amino groups (Chen et al., 2011; St. Angelo, 1996; Tian et al., 2021). In addition, this decrease could also be related to the conformational rearrangements of the whey proteins at the interface, which may lead to an exposure of negatively charged amino groups. The increase in zeta-potential for coffee fraction-stabilized emulsions is most probably the result of a small decrease in pH which reduces the net charge, and this may also favor aggregation of oil droplets (**Figures 6.2 & S6.1**).

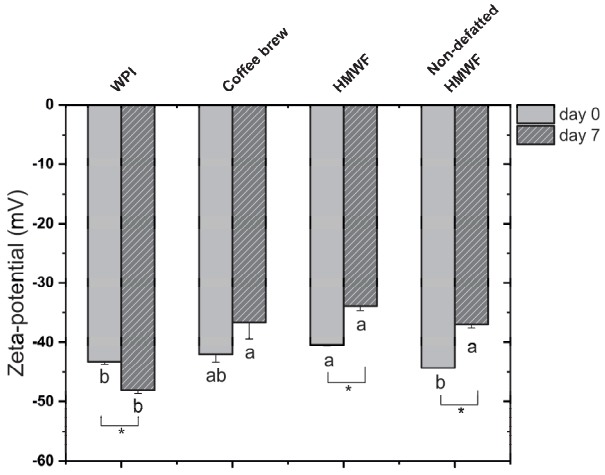

Figure 6.3. Zeta-potential of the emulsions freshly prepared or after 7 days at 40 °C. The lowercase letter is for comparison among different emulsions. Different letters indicate significant differences ($P < 0.05$). Asterisks indicate a significant difference for the same sample between day 0 and day 7.

6.3.2.2 Antioxidant activity of coffee fractions

Coffee components may affect oxidative reactions through various mechanisms including scavenging of free radicals and binding of metal ions. Therefore, before analyzing the lipid oxidation in emulsions, the antioxidant properties of coffee fractions were assessed and compared with those of WPI. As can be seen in **Figure 6.4A**, WPI exhibited a significantly lower DPPH radical scavenging activity than any of the coffee fractions, amongst which non-defatted HMWF showed the lowest activity. With respect to the iron-chelating activity, all coffee fractions were able to bind more iron than WPI (**Figure 6.4B**), with LMWF having a significantly higher capacity than the other fractions (**Figure 6.4B**).

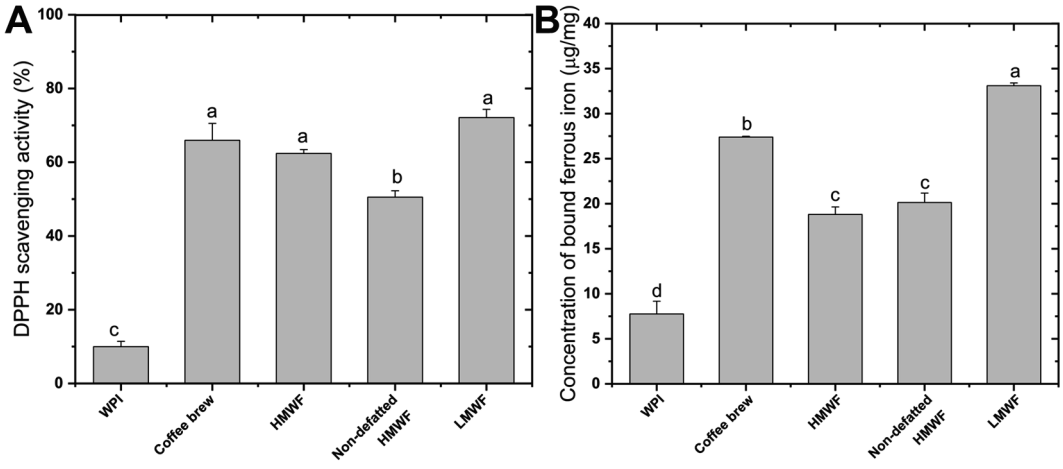

Figure 6.4. DPPH radical scavenging activity (A) and iron-chelating capacity (B) of WPI and different coffee fractions. The lowercase letter is for comparison among the samples. Different letters indicate significant differences ($P < 0.05$).

For WPI, it has been suggested that the sulfhydryl groups located on the surface of the molecules have hydrogen-donating ability (Faraji et al., 2004), whereas the carboxyl groups of acidic amino acids (aspartic acid, glutamic acid) might account for metal-chelating ability (Kaushik et al., 2016). The antioxidant properties of the HMWF are probably due to the melanoidins that contain CGAs. The presence of reductons, enaminol, and o-hydroxyl groups in phenolic compounds might explain the strong radical scavenging activity (Borrelli

et al., 2002), whereas the catechol moieties from incorporated phenolic compounds and the ketone and/or hydroxyl groups of pyranone or pyridone might act as metal chelators (Kim et al., 2020; Wang et al., 2011). LMWF is rich in unbound phenolic compounds, especially those with catechol moieties (e.g., CQAs, section 3.1) which are effective free radical acceptors and metal chelators (Samsonowicz et al., 2019; Troup et al., 2015; Verzelloni et al., 2011). In addition, the volatile heterocyclic compounds (e.g., pyrrols, furans, and thiophenes) and hydroxybenzenes (e.g., ethylcathecol and pyrogallol) in LMWF may contribute to over antioxidant activity (Perrone et al., 2012).

6.3.2.3 Lipid oxidation in emulsions

Hydroperoxide concentration (**Figure 6.5A**) and para-anisidine value (pAV) (**Figure 6.5B**) were used to characterize lipid oxidation in emulsions. WPI-stabilized emulsions showed a rapid initial increase in hydroperoxides, followed by a gradual increase until the end of storage (**Figure 6.5A**). Similarly, the pAV of WPI-stabilized emulsions rapidly increased within 1 day of storage, after which it remained constant for the rest of the storage period (**Figure 6.5B**). In contrast, the hydroperoxide concentration and pAV of emulsions stabilized by coffee fractions were very low during the accelerated storage at 40℃ (**Figure 6.5 A&B**; a magnification is therefore shown in **Figure 6.5 a&b**), indicating that coffee fractions (coffee brew, HMWF, and non-defatted HMWF) were highly effective in preventing oxidation of emulsified lipids.

The strong ability of coffee fractions to protect lipids from oxidation can be related to their relatively high antioxidant activity (compared to WPI, section 6.3.2.2) and their interfacial localization. During storage, trace amounts of pre-existing lipid hydroperoxides (LOOH) located at the oil-water interface would decompose into alkoxy radicals ($LO^{\bullet}$) or peroxyl radicals ($LOO^{\bullet}$) (Laguerre et al., 2020). Some compounds from the adsorbed coffee fractions (e.g., phenolic compounds and melanoidins, as discussed in section 6.3.2.2) might act as chain-breaking electron donors, which could readily transfer hydrogen atoms to scavenge $LO^{\bullet}$ and $LOO^{\bullet}$, thereby inhibiting lipid oxidation (Morales & Jiménez-Pérez, 2004; Pérez-Martínez et al., 2010). On the other hand, coffee fractions have metal binding capacity

(**Figure 6.4B**), which prevents metals from initiating radical formation and decomposing surface-active LOOH. Both relatively high radical scavenging and iron binding capacities seem to be logical explanations for the effectiveness of coffee fractions, whereas the much lower values for WPI emulsions point in the opposite direction.

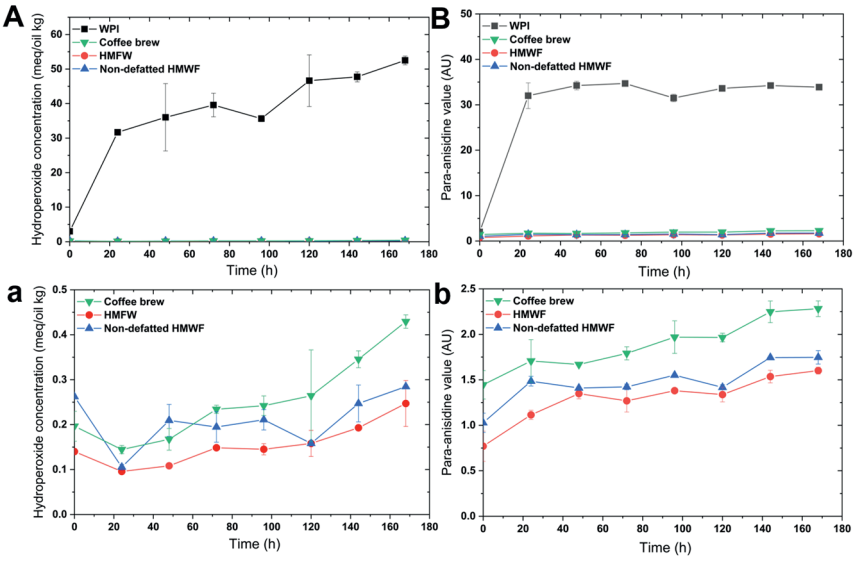

Figure 6.5. Hydroperoxide concentrations (left column) and para-anisidine values (right column) in different emulsions over the incubation period (40 °C, 7 days). Top row: all emulsions; bottom row: coffee fraction-stabilized emulsions (bottom row graphs show a magnification on low values of oxidation markers; please note the difference in Y-axis scales between panels A/a and panels B/b).

Next to the role of the adsorbed fractions, components present in the continuous phase may also play an important role in lipid oxidation (Berton-Carabin et al., 2014). For example, melanoidins may trap transition metals and free radicals in the continuous phase, and thus prevent these aqueous pro-oxidants from getting into contact with labile unsaturated lipids in the droplets. To distinguish between these effects, excess coffee material was added to the continuous phase of preliminary prepared emulsions, and both physical and oxidative stability were monitored.

6.3.3 Added coffee materials to the continuous phase of emulsions

6.3.3.1. Influence of HMWF concentrations on the stability of emulsions

Stock WPI-stabilized emulsions were prepared with minimal amounts of unadsorbed WPI remaining in the continuous phase (Feng et al., 2021), and HMWF suspensions with concentrations ranging from 0 to 2 w/v% were added to the emulsion after homogenization. Physical stability and lipid oxidation were monitored during storage at 40℃ for 4 days.

All emulsions with added HMWF exhibited bimodal size distributions (**Figure 6.6**): the peak ranging from 0.01 to 1 µm probably corresponds to the emulsion droplets, the second peak to aggregated HMWF in the continuous phase. This is supported by (i) the similar particle size distribution of the HMWF dispersion (**Figure 6.6A**, red curve) and (ii) the increased intensity of the second peak as HMWF concentration increased (**Figure 6.6**). No appreciable changes in droplet size and microstructure were observed for all emulsions upon storage (**Figure 6.6 & S6.2**), suggesting these emulsions were physically stable.

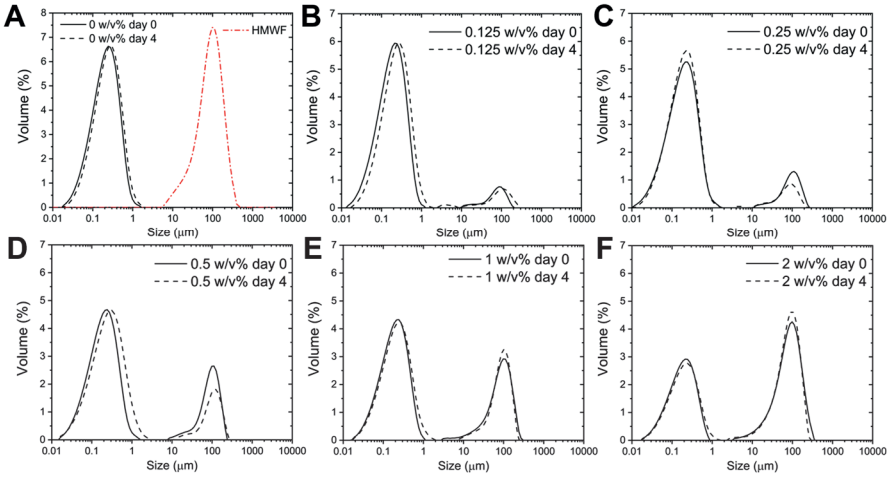

Figure 6.6. Droplet size distribution of WPI-stabilized emulsions stabilized with 0 (A), 0.125 (B), 0.25 (C), 0.5 (D), 1 (E), and 2 (F) w/v% HMW coffee melanoidins added to the emulsion post-homogenization. For clarity, one representative curve is shown for each sample, but similar results were obtained on independent triplicates.

As can be seen in **Figure 6.7**, emulsion droplets had a slightly more negative surface charge when the HMWF concentration increased, which may be due to some exchange taking place at the interface, leading to more negatively charged 'compounds' from HMWF, such as uronic acids from arabinogalactans and ferulic acid or caffeic acid moieties from CGAs incorporated at the interface (Bekedam, Schols, et al., 2008). The decrease in zeta-potential over time (**Figure 6.7**) can be similarly explained as before by the formation of fatty acids or organic acids, or degradation of the positively charged amino groups, or the conformational rearrangements of the whey proteins (section 6.3.2.1).

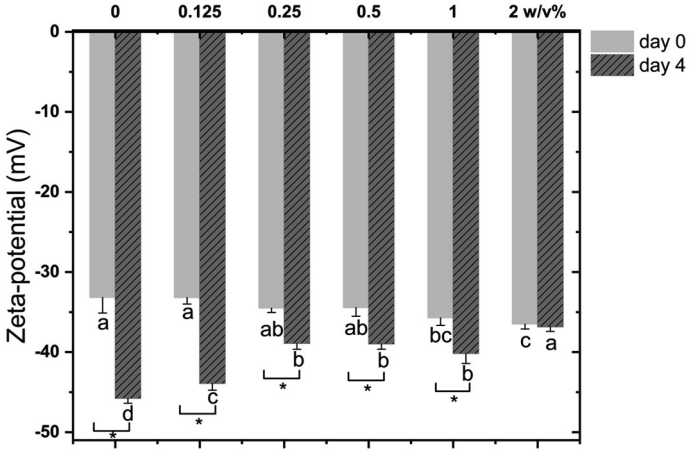

Figure 6.7. Zeta-potential of the WPI-stabilized emulsions supplemented with 0-2 w/v% of HMWF freshly prepared or at the end of the incubation period (40 °C, 4 days).

With respect to lipid oxidation, hydroperoxides and aldehydes developed earlier, faster and to a much greater extent in the control emulsion (0 w/v% HMWF) than in the other emulsions (supplemented with 0.125 – 2 w/v% HMWF) (**Figure 6.8**), in which oxidation products were formed according to the amount of HMWF added. It is actually challenging to compare the effects, since the difference between the curves is highly time-dependent (as would be expected for cascaded reactions like lipid oxidation). When taking the final concentrations measured, the aldehyde contents were 3.6-, 5.2-, 9.3-, 23- and 31-fold higher for the control emulsion than emulsions to which HMWF was added at 0.125, 0.25,

0.5, 1, and 2 w/v%, respectively. What is more important to point out is that HMWF was highly efficient even at very low concentrations used in the continuous phase. Most probably, the free radical scavenging and iron-binding abilities (**Figure 6.4A and B**) are instrumental in creating such positive effects, as also discussed before (Kellerby et al., 2006).

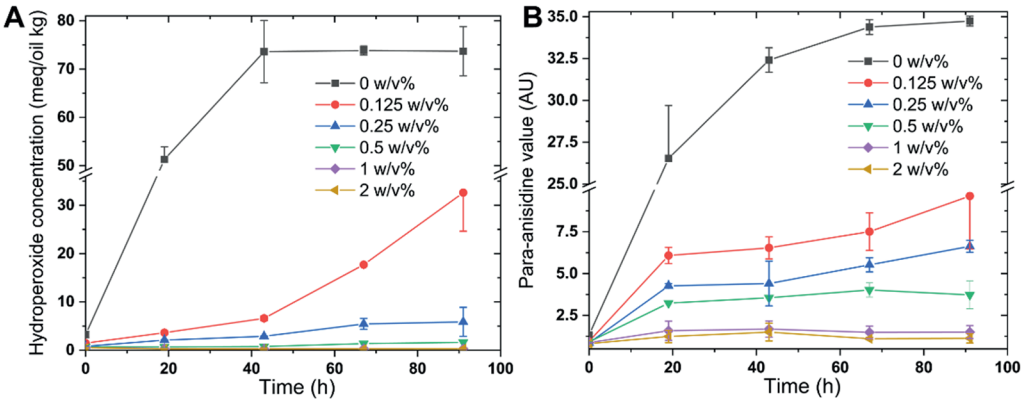

Figure 6.8. Hydroperoxide concentrations (A) and para-anisidine values (B) in WPI-stabilized emulsions supplemented with 0-2 w/v% of HMWF, over the incubation period (40 °C, 4 days).

6.3.3.2. Influence of coffee fractions on the stability of emulsions

In the last experiment, the different coffee fractions were added to whey protein-stabilized emulsions, post homogenization, to test their capacity to inhibit lipid oxidation at a concentration of 0.25 w/v%. Again, no appreciable differences in the physical properties (droplet size distribution, microstructures, and zeta-potentials) were observed for all emulsions (**Figure S6.3 - S6.5**).

With respect to lipid oxidation (**Figure 6.9**), the presence of added compounds improved the oxidative stability of emulsions, although WPI was considerably less effective than coffee brew and LMWF, which themselves were less effective than both HMWFs. After 4 days of storage, the aldehyde concentration was 1.0-, 2.0-, 2.2-, 5.2-, and 5.5-fold higher for

the control emulsion than for emulsions containing excess WPI, LMWF, coffee brew, HMWF, and non-defatted HMWF (**Figure 6.9B**). The order of appearance is not in line with radical scavenging and iron-chelating activities (**Figure 6.4**); as a matter of fact, LMWF is highest in both, but does not perform best in the prevention of lipid oxidation. The mobility and localization of the components in the emulsion systems are probably the keys to understanding this. In order to be effective, the antioxidants would need to be placed at the interface to prevent the initiation of lipid oxidation. Overall, HMWF components may be more likely to bind to the interface than their low molecular weight counterparts (Ćosović et al., 2010), as seems to be confirmed by the surface pressure measurements (**Figure 6.1**); In addition, assuming they may locate at the interface, adsorbed HMWFs would be less mobile and thus could be more efficient to prevent lipid oxidation by conferring their antioxidant moieties a more substantial residence time at the interface, as compared to low molecular weight molecules (Schröder et al., 2020). Besides, as discussed in **section 6.3.1.1**, unbound phenolic compounds were recovered in LMWF, and covalently bound phenolic compounds were found in HMWF. Unbound phenolic compounds themselves might be oxidized by oxygen and transition metals during the storage at 40°C, whereas bound phenolic compounds may be protected against oxygen by the large moieties (e.g., melanoidin backbones) they are bound to (Xu et al., 2018). In addition, as compared to HMWF, LMWF and coffee brew had higher phenolic contents (**Table 6.1 and 6.2**), which may result in a higher amount of phenolic compound-bound Fe^{3+} (Perron & Brumaghim, 2009) and higher reducing power that reduces Fe^{3+} to Fe^{2+} in emulsions (Tian, Yang, et al., 2021; Timoshnikov et al., 2020), thereby promoting the formation of free radicals and the decomposition of hydroperoxides. Furthermore, the total antioxidant effect of coffee fractions can be due to hydrophilic as well as hydrophobic compounds (Liang & Kitts, 2014), and thus, depending on the polarity of the media, different compounds might be responsible for the tested antioxidant effect. This implies that antioxidants having a high response in the iron-chelating or DPPH assay may have a low response in the emulsion systems due to partitioning effects. Furthermore, it has been suggested that higher phenolic content (**Table 6.1**) may cause an increase in the amount of associated iron, which may

accelerate lipid oxidation (Tian et al., 2021). And obviously, there could still be numerous other components at work, resulting in synergism or antagonism of antioxidants (Hwang et al., 2019). In spite of this, our finds clearly point to the great potential of coffee fractions to control oxidation in emulsion, either as a main emulsifier, or as an add-on to the emulsion after its preparation.

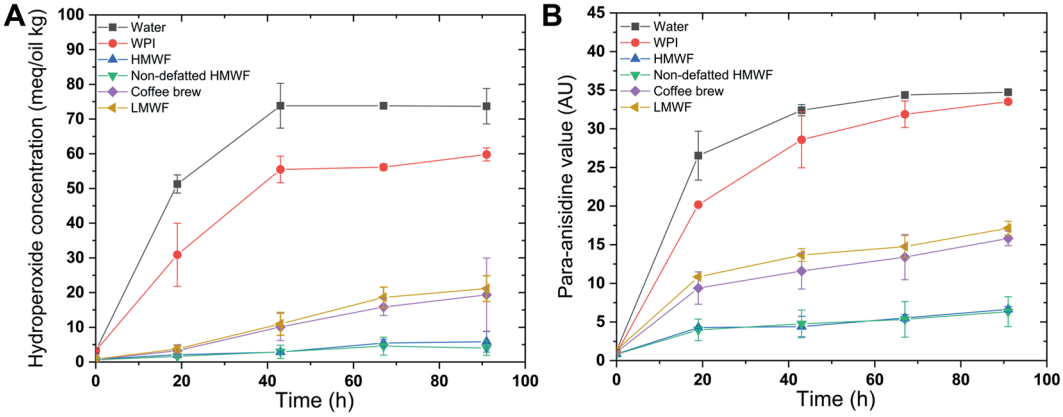

Figure 6.9. Hydroperoxide concentrations (A) and para-anisidine values (B) in WPI-stabilized emulsions over the incubation period (40 °C, 4 days).

6.4 Conclusions

This work demonstrates the great potential of various coffee fractions in the preparation of emulsions that are physically as well as oxidatively stable. We explored using various fractions as emulsifiers, and as add-ons post emulsification. Especially the high molecular weight fraction is able to form emulsions with a nearly monomodal size distribution, and keep emulsions chemically stable at 40 °C for 7 days. When added to the emulsion post homogenization, all coffee fractions were able to slow down lipid oxidation considerably without significantly affecting the physical stability of emulsions, though both HMWFs were more effective in retarding lipid oxidation than coffee brew and LMWF.

It is expected that a number of effects, such as the antioxidant properties (metal chelating and radical scavenging activities) of coffee fractions, the partitioning of antioxidant components in the emulsions and the phenolic compounds profile, are responsible for the overall effects that we found. Fractionation into different coffee fractions improves the techno-functional properties of coffee. Especially from a practical perspective, the high molecular weight fraction has a less pronounced coffee flavor than coffee and therefore can be a more versatile ingredient than coffee as such. This research showed that coffee ingredients could act as multifunctional stabilizers with a wide potential for application in dispersed systems (e.g., emulsions) as used in foods, pharmaceutics, and cosmetics. Future work is directed toward understanding the contribution of individual components to the antioxidant activity of coffee fractions.

Supplementary materials

Table S6.1. Detailed unbound and covalently bound phenolic compounds of coffee fractions (g/100g).

RT (min)	λmax (nm)	$[M-H]^-$	Compounds	Unbound phenolic compounds		Covalently bound phenolic compounds	
				Coffee brew	LMWF	HMWF	Non-defatted HMWF
11.06	320	353	**CQA isomer**	0.11 ± 0.01	0.21 ± 0.00	nd	nd
12.98	320	353	**CQA isomer**	0.62 ± 0.04	1.22 ± 0.00	nd	nd
16.83	320	353	**CQA isomer**	0.23 ± 0.02	0.39 ± 0.02	nd	nd
17.40	320	353	**CQA isomer**	0.09 ± 0.01	0.18 ± 0.00	nd	nd
19.18	320	353	**5CQA**	0.99 ± 0.04	2.06 ± 0.07	nd	nd
20.15	326	367	**FQA isomer**	0.69 ± 0.04	1.43 ± 0.01	nd	nd
20.15	320	353	**CQA isomer**	0.69 ± 0.03	1.44 ± 0.00	nd	nd
22.50	320	179	**CA**	nd	nd	0.44 ± 0.01	0.43 ± 0.02
22.83	320	335	**CQL isomer**	0.03 ± 0.01	0.06 ± 0.00	nd	nd
23.03	320	353	**CQA isomer**	0.03 ± 0.00	nd	nd	nd
28.85	320	353	**CQA isomer**	0.19 ± 0.01	nd	nd	nd
29.60	326	367	**FQA isomer**	0.14 ± 0.01	0.26 ± 0.00	nd	nd
30.70	320	335	**CQL isomer**	0.04 ± 0.00	0.08 ± 0.01	nd	nd
31.13	320	335	**CQL isomer**	0.24 ± 0.02	0.45 ± 0.04	nd	nd
31.60	310	163	***p*coum**	nd	nd	0.01 ± 0.00	0.01 ± 0.00
33.71	320	335	**CQL isomer**	0.11 ± 0.01	0.27 ± 0.03	nd	nd
37.30	320	193	**FA**	nd	nd	0.10 ± 0.00	0.10 ± 0.00
46.51	320	515	**diCQA**	0.04 ± 0.00	0.07 ± 0.00	nd	nd

RT: retention time; nd: not detected; +/- values correspond to standard deviation (n=3).

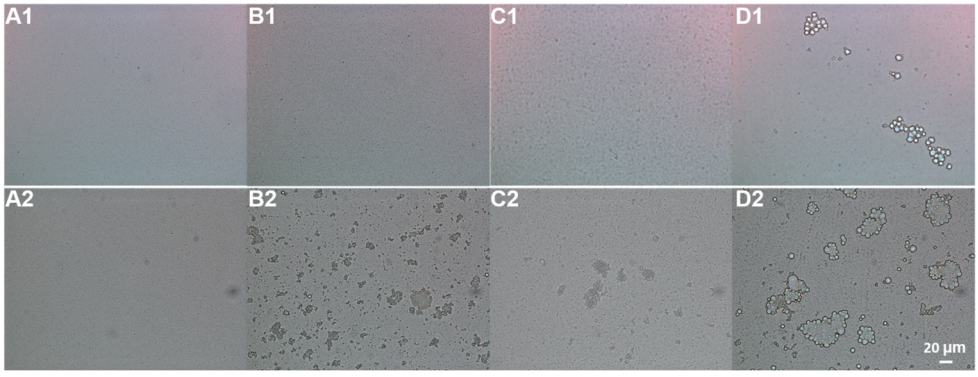

Figure S6.1. Microscopic pictures of emulsions stabilized with WPI (A), coffee brew (B), HMWF (C), and non-defatted HMWF (D) freshly prepared (1) or after 7 days at 40℃ (2).

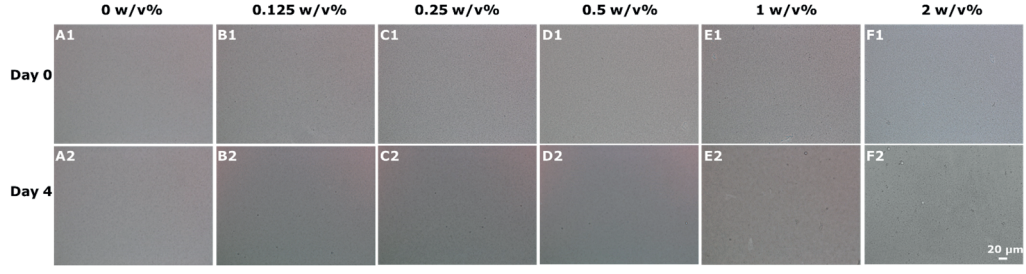

Figure S6.2. Microscopic pictures of WPI-stabilized emulsions with 0 (A), 0.125 (B), 0.25 (C), 0.5 (D), 1 (E), and 2 (F) w/v% of HMWF added to the continuous phase freshly prepared (1) or at the end (2) of the incubation period (40℃, 4 days).

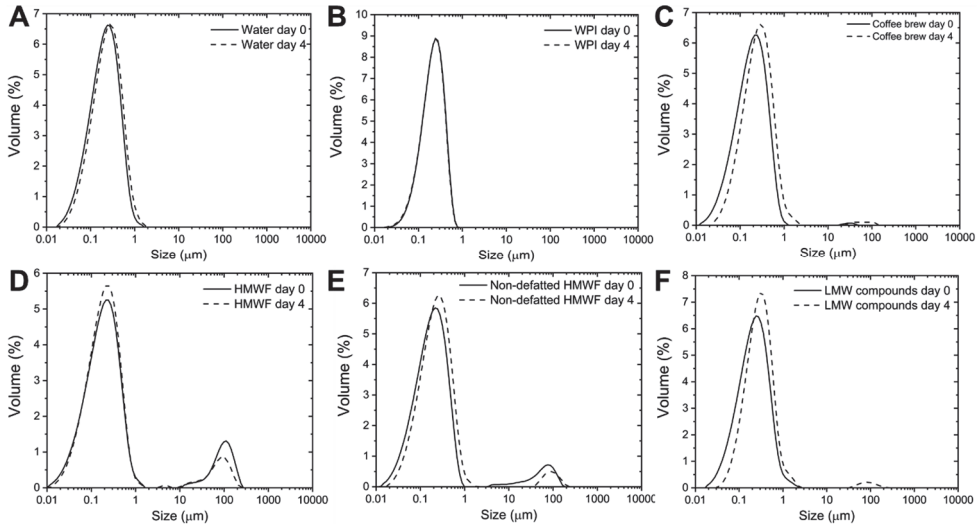

Figure S6.3. Droplet size distribution of WPI-stabilized emulsions with water (A), WPI (B), coffee brew (C), HMWF (D), Non-defatted HMWF (E), and LMWF (F) added to the continuous phase post-homogenization. For clarity, one representative curve is shown for each sample, but similar results were obtained on independent triplicates.

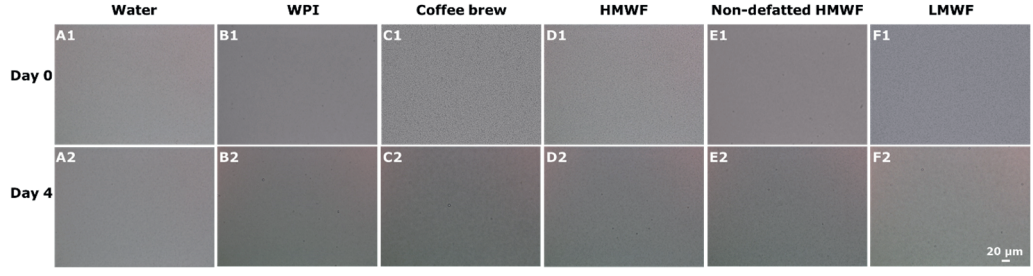

Figure S6.4. Microscopic pictures of WPI-stabilized emulsions with water (A), WPI (B), coffee brew (C), HMWF (D), Non-defatted HMWF (E), and LMWF (F) added to the continuous phase freshly prepared (1) or at the end (2) of the incubation period (40℃, 4 days).

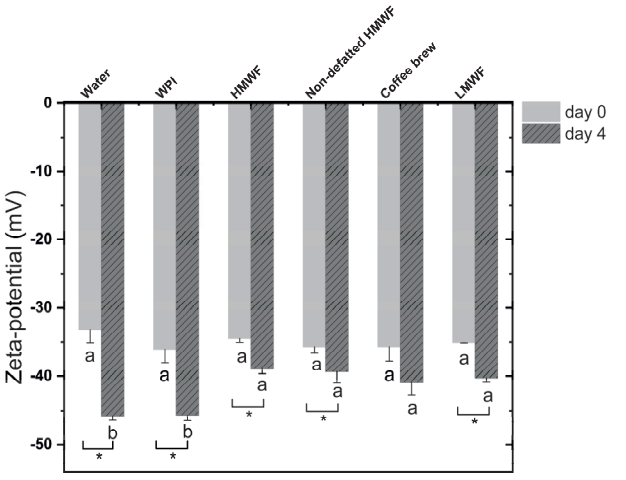

Figure S6.5. Zeta-potential of the WPI-stabilized emulsions freshly prepared or at the end of the incubation period (40℃, 4 days).

7

General discussion

7.1. Introduction

This thesis focused on the ability of Maillard reaction products (MRPs) that were either prepared from model systems or present in foods, to physically and oxidatively stabilize food emulsions. In **Chapter 2**, we summarized literature with respect to interfacial and antioxidant properties, on the basis of which we identified MRPs from model systems and extracted from food products as two feasible sources for components with dual functionality.

MRPs were first prepared from soy proteins and carbohydrates, and the physicochemical properties of various glycated soy proteins were characterized, which led to a comprehensive understanding of components (**Chapter 3**). Glycation of soy proteins with dextran led to a substantial increase in the furosine content, but not Nε-(carboxymethyl)-L-lysine (CML) and Nε-(carboxyethyl)-L-lysine (CEL) contents, indicating that these glycated proteins are mainly early-stage MRPs. Glycating soy proteins with glucose, on the other hand, significantly increased these contents, showing that the Maillard reaction (MR) processed to a more advanced stage. In addition to the compositional changes, thermal treatment during the MR also altered the tertiary protein structures and thus the hydrophobicity of soy proteins. The interfacial properties can be related to the latter, with dextran conjugates showing higher activity than glucose counterparts.

The potential of the early stage MRPs (glycated soy proteins with dextran) obtained in **Chapter 3**, when present in the continuous phase, to protect emulsified lipids against oxidation was investigated in **Chapter 4**. These MRPs were capable of inhibiting lipid oxidation while maintaining the physical stability of emulsions, although the antioxidant activity of these MRPs was only slightly higher than that of the non-glycated soy proteins. This is a good sign since early-stage MRPs can be induced during some food processing steps, and thus contribute to overall antioxidant activity.

Next, we considered MRPs inherently present in foods. Final stage MRPs melanoidins were extracted from dark roasted coffee beans and used as interfacial stabilizers (**Chapter 5**).

Coffee melanoidins were able to reduce the oil-water interfacial tension, induce electrostatic repulsion between emulsion droplets, and may form a weak network in the continuous phase that contributes to emulsion stability when used at a high enough concentration. In addition, we investigated the dual functionality of various coffee fractions in emulsions (**Chapter 6**). Coffee brew and its high molecular fractions with strong metal and radical scavenging activity were able to locate at the interface and therefore act as efficient interfacial antioxidants. When present in the continuous phase of pre-formed emulsions, all coffee fractions (coffee brew, its high- and low-molecular-weight fractions) can greatly retard lipid oxidation, possibly due to the presence of strong antioxidants, including melanoidins, phenolic compounds, heterocyclic compounds, and hydroxybenzenes, etc.

Combining the findings from this thesis with those of others, here in **Chapter 7**, we try to sum up the elements required at various scales (e.g., from molecular composition, droplet properties, to system stability) to thus design of food emulsions.

This work has shown that MRPs are able to contribute both to the physical and oxidative stability of emulsions, and to both effects, they may contribute when present at the interface (e.g., layer formation, metal chelation, and radical binding activity) and in the continuous phase (network formation, metal chelation, and radical binding activity). The various effects are discussed in the next sections and put into the wider perspective of stable emulsion design that complies with current consumer demands.

7.2 What should ideal emulsions look like?

From different points of view, target emulsions would have different desired attributes. Consumers may find food emulsions desired if the products are healthy, nutritional, natural, “clean-label” and have pleasurable sensory quality, and of course, low price. Food manufacturers would aim for competing for market share and therefore would ensure that emulsions have appropriate physicochemical attributes, stability, safety, and high

profitability. In the current social context, emulsions should be made in such a way that they contribute to a sustainable future. This implies that food professionals should develop emulsions with sustainable formulation (e.g., renewable sources) and production (e.g., gentle and energy-efficient processing conditions).

The soy-protein MRPs and coffee melanoidins are of plant origin and would be more sustainable than currently used animal-based proteins, and would appear as of natural origin on labels. Therewith our components of interest comply with requirements in a multi-faceted way.

To provide dual-functionalities (i.e., emulsification and antioxidant activities) in emulsions, both purposely produced and extracted MRPs can be used. They hold in common that they exhibit surface activity, although the adsorption of MRPs at the oil-water interface could be slow due to their high molecular weight and the presence of supramolecular structures. By glycating proteins with carbohydrates in model systems, the amphiphilicity of reaction products can be tuned by controlling reaction conditions carefully (e.g., type of carbohydrate, heating time, and temperature) (Livney, 2012), and thus improve their interfacial properties. For melanoidins, control over the reaction is much harder to achieve, given the multitude of reactions taking place before reaching the late stages of the Maillard reaction. Furthermore, it is expected that various components may form particles with dual wettability that contribute to interfacial stabilization. This may be instrumental in sustainability since Pickering emulsions can be formed by using a moderately low energy input (Roy-Perreault et al., 2005).

After nesting in the interface, components may undergo conformational changes and form an interfacial film that resists the destabilization of the emulsified oil droplets. Protein moieties from glycated soy proteins are able to rearrange and reorient at the interface and form a viscoelastic layer, and this also holds for galactomannan and arabinogalactan proteins from coffee melanoidins. These compounds are able to provide emulsions with physical stability mainly through steric and/or electrostatic repulsion.

Interestingly, all MRPs exhibit antioxidant activity (e.g., metal chelating and radical scavenging abilities). Although this antioxidant activity cannot always predict or directly correlate to the actual ability to prevent lipid oxidation (section 7.4), all MRPs contributed to the oxidative stability of emulsions, with final stage MRPs exerting stronger effects than early and intermediate stage MRPs, as also found by Aljahdali & Carbonero (2019).

From the thesis, it is clear that two routes can be followed to obtain dual-functional emulsifiers (i.e., production from base ingredients or extracting from food, and both have their pros and cons. For instance, preparing ingredients on purpose gives higher control over the compounds formed and their properties, leading to higher reproducibility, and standardization. Extraction from foods holds less reproducibility, may require extensive screening, and be more costly, but fits better within the naturalness requirements (Berton-Carabin et al., 2021).

The role of continuous phase emulsifiers

In general, it is accepted that antioxidant emulsifiers when present at the interface are more efficient in lowering lipid oxidation than those that remain in the continuous phase. However, the importance of the latter should not be neglected as elaborated for both our MRPs of interest. In literature, it has been suggested that surface-active lipid hydroperoxides might transfer from one droplet to another through the continuous phase via diffusion, collision-exchange-separation, and/or micelle-assisted transfer, thus propagating oxidation (Laguerre et al., 2017). Unadsorbed antioxidant emulsifiers may be able to retard the propagation of lipid oxidation by decomposing hydroperoxides into non-radical products, and chelation of transition metals in the continuous phase. Furthermore, the surplus of emulsion stabilizers that remains in the continuous phase may contribute to the physical stability of emulsions. Certain types of conjugated polysaccharides may be able to serve as thickening agents or gelling agents to reduce creaming, and the rate at which the film between droplets thins, thus preventing coalescence. Besides, high amounts of galactomannans from coffee melanoidins in the continuous phase improve the physical

stability (gravitational separation and coalescence stability) of emulsions through network formation as shown in **Chapter 5**.

7.3 Food oil-in-water (O/W) emulsion design

Notwithstanding that many factors affecting the physicochemical properties and stability of emulsions have been identified, the design of emulsions is still not a simple task, mainly due to the inherent complexity of emulsion systems and the lack of consistent models and databases. This holds even more for the less defined components that we extracted from coffee, and that typically occur in plant-derived ingredients (Berton-Carabin & Schroën, 2019). An approach to make more sense out of these myriad options is through a multiscale strategy consisting of molecular, microscopic, and macroscopic levels. Here we propose two schemes, i.e., "bottom-up" (from molecular to macroscopic level) and "top-down" (from macroscopic to molecular level) approach, for food O/W emulsion design (**Figure 7.1**).

7.3.1 "Top-down" approach

The "top-down" design is a stepwise design that breaks down a system into sub-systems, and is more desirable when quantifiable parameters, databases or models are available. Quantifiable product characteristics at macro-scale may be appearance, viscosity, and physical and chemical stability (Taifouris et al., 2020), which needs to be translated to emulsion properties at the microscopic scale, and later to the molecular scale and energy input, by using e.g., available engineering equations and databases (Serna et al., 2021). After selecting the candidate formulations and processing conditions, they can be experimentally verified. The effectiveness of this method is clearly related to the completeness and quality of the information in the data- and knowledge bases, which should be continuously enriched.

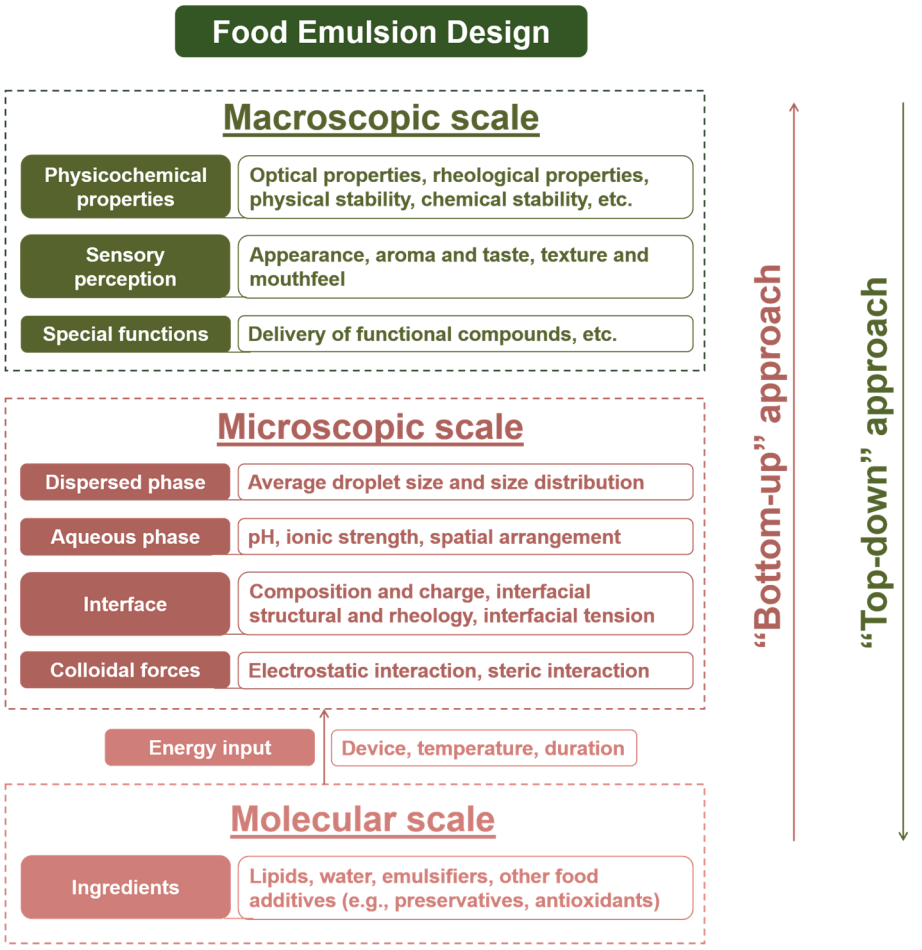

Figure 7.1. Design of food O/W emulsions through a multiscale strategy including top-down and bottom-up approaches.

7.3.2 *"Bottom-up" approach*

The principle of the "bottom-up" approach is to convert raw materials and energy into desired final products that can be used to stabilize emulsions. The actual preparation of the emulsion is normally done through a trial-and-error approach, i.e., searching for formulations that meet targeted performance. Furthermore, consumer needs also need to be considered (Mattei et al., 2012).

In an ideal world, the characteristics of molecules (e.g., structures, composition, size, charge, polarity, surface properties, and other functionalities) have been analyzed and put in a database. What is currently common practice is that once the ingredients with the most advantageous characteristics are selected, a design of experiments is carried out to investigate how the ingredients (e.g., compositions, concentrations), emulsification process (e.g., homogenization device, time), and environments (e.g., pH, ionic strength) affect emulsion properties, such as rheology, and appearance. It is clear that this is a laborious, expensive, and material-consuming way of working. However, it is good to point out that the droplet size (and thus the physical stability) of emulsions could be predicted if the flow conditions (homogenizing process) are set and the interfacial tension at similar time scales as droplet formation is known (Schroën et al., 2020). The latter might be measured using microfluidic devices, which has recently gained much attention, since droplet formation (product formulation) and droplet coalescence (product stability) can be studied in one energy-efficient device.

A case study – melanoidin-stabilized emulsions

The coffee melanoidin-stabilized emulsions in **Chapters 5 and 6** are now used to illustrate the "bottom-up" emulsion design strategy (**Figure 7.2**).

Problem definition. Designing O/W food emulsions with physical and oxidative stability and that comply with consumer preferences (natural ingredients).

Ingredient identification. Emulsifiers that contribute both to physical and oxidative stability. Melanoidins from natural sources (e.g., coffee, cocoa, beer, and vinegar) have strong antioxidant effect {Formatting Citation} and some are (e.g., from coffee) surface-active (D'Agostina et al., 2004; Da Fonseca Selgas Martins et al., 2014; Piazza et al., 2008). Rapeseed oil that is high in ω-3 fatty acids was chosen as an oil that is inexpensive and healthy, and able to help in elucidating effects on oxidation. Concentrations and emulsifying conditions were set based on experimental experience.

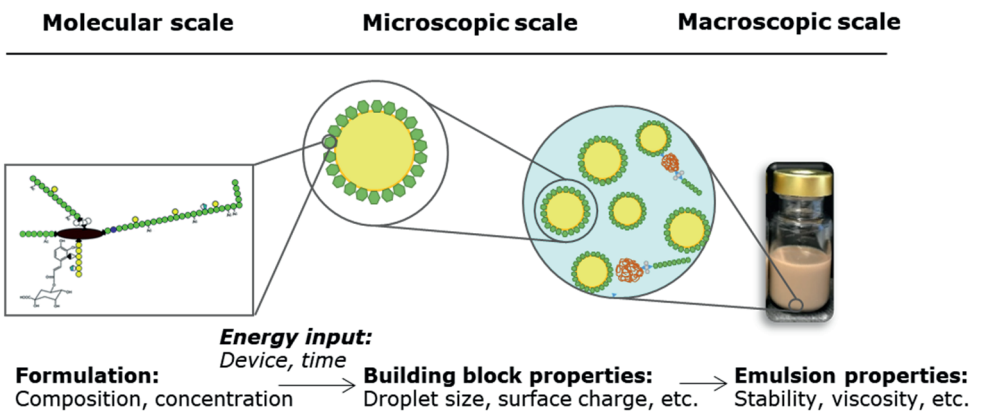

Figure 7.2. A "bottom-up" multiscale strategy to design coffee melanoidin-stabilized emulsions.

Properties at the microscopic scale. The droplet size and its distribution, surface charge, etc., were measured as a function of melanoidin concentration (**Figure 7.3**), and together with microscopic observations showing aggregated oil droplets in emulsions with either low (0.25 - 1 wt%) or high melanoidin (4 wt%) concentration, this led to the identification of 2 wt% of coffee melanoidins as desired for stable emulsion preparation.

Properties at the macroscopic scale. The formulation with 2 wt% melanoidins could keep emulsions physically stable for one month at room temperature and chemically stable under accelerated storage conditions (40 °C for at least 7 days).

It is clear that considerable effort has gone into facilitating knowledge-based design when using bottom-up and top-down approaches, and thus, rational design of food emulsion products can be made less costly, time- and resource-consuming.

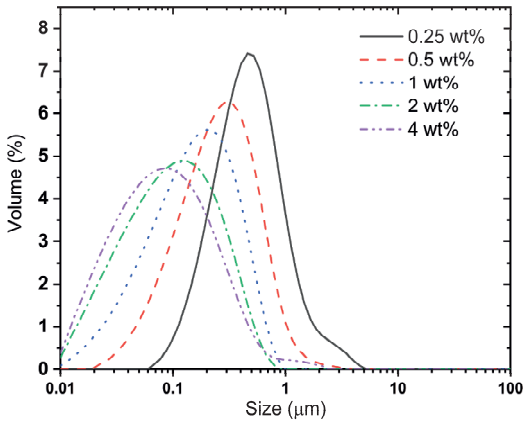

Figure 7.3. Droplet size distribution of fresh emulsions stabilized with 0.25-4 wt% coffee melanoidins.

7.4 Methodological considerations

In this thesis, the antioxidant capacity of MRPs towards unsaturated lipids was evaluated both indirectly in single-phase systems, and directly in an O/W emulsion. The indirect method, which measures the ability of a substance to scavenge a stable artificial free radical or chelate a transition metal in the absence of an oxidizable substrate, is a widely used method (Laguerre et al., 2007), which is simple, fast, cheap, and allows direct comparisons of results between labs. However, the results obtained via the indirect method do not necessarily reflect the actual antioxidant behavior in a two-phase system as an emulsion, given the different solubility and chemical reactivity of substrates in different media, and different localization of the substrates, as discussed in **Chapters 2, 4, and 6**. Although the direct method is good for fast screening and assessing the involved antioxidant mechanism(s), an emulsion experiment would always need to be carried out to confirm this. In this study, we chose two of the most used spectrophotometric analyses, the hydroperoxide content and the para-anisidine value (pAV), to measure the primary and secondary oxidation products. They are simple, reliable, moderately sensitive, and do not require expensive equipment. However, the accuracy of the results largely relies on the fat

extraction step, because when this step is not done efficiently or consistently, it could introduce errors in the determination of oxidation (Daoud et al., 2019). It has recently been found in our lab that fat extraction using n-hexane/2-propanol might not be able to completely extract lipids from oxidized protein-stabilized O/W emulsions. In this case, an improved fat extraction method or alternative analytical technique might be needed. For instance, attenuated total reflectance-Fourier transform infrared (ATR-FTIR) combined with chemometrics tools, which does not require any sample preparation step (non-destructive) and is rapid, accurate, and sensitive, might be an alternative method (Abeyrathne et al., 2021; Daoud et al., 2019; Zhang et al., 2021). In addition, ^{1}H NMR method is able to provide an accurate fingerprint of samples and thus is also a convenient and fast tool to simultaneously quantify primary and secondary oxidation products with high sensitivity (Barriuso et al., 2013; Merkx et al., 2018).

To evaluate the extent of the MR in model systems in **Chapter 3**, we first evaluated the degree of glycation by quantifying the free amino group contents before and after the glycation via the commonly used o-phthalaldehyde (OPA) method. However, we observed an apparent loss in free amino groups in soy proteins (without carbohydrate) upon thermal heating. This implies that access to free amino groups may be hindered in protein aggregates, and thus prevented from reacting with the reagents, leading to an overestimation of the degree of glycation. Therefore, to better understand the systems, we measured the content of different MR markers, including furosine, CML, and CEL, by using the stable isotope dilution assay coupled with liquid chromatography tandem mass spectrometry. Compared to the OPA method, this analytical approach is more accurate and sensitive, allowing a comprehensive understanding of different stages of MR. Furthermore, lysine content can also be measured using this approach (Troise et al., 2015), thereby calculating the degree of glycation more accurately.

7.5 Concluding remarks

Plant-based ingredients have gained great interest in sustainable food formulation in the last decade. In line with this, we have demonstrated the promising potential of plant-derived MRPs as antioxidant emulsifiers in emulsions. This thesis, therefore, has generated knowledge not only on new functional ingredients but also on their application in specific food products in which they can exhibit a dual functionality that we expect to be relevant for industrial applications (e.g., plant-based dairy products, baked goods, etc.). We think that the identification of novel functional ingredients from especially food by-products (e.g., melanoidins from spent coffee grounds) can be instrumental in contributing to sustainable food design.

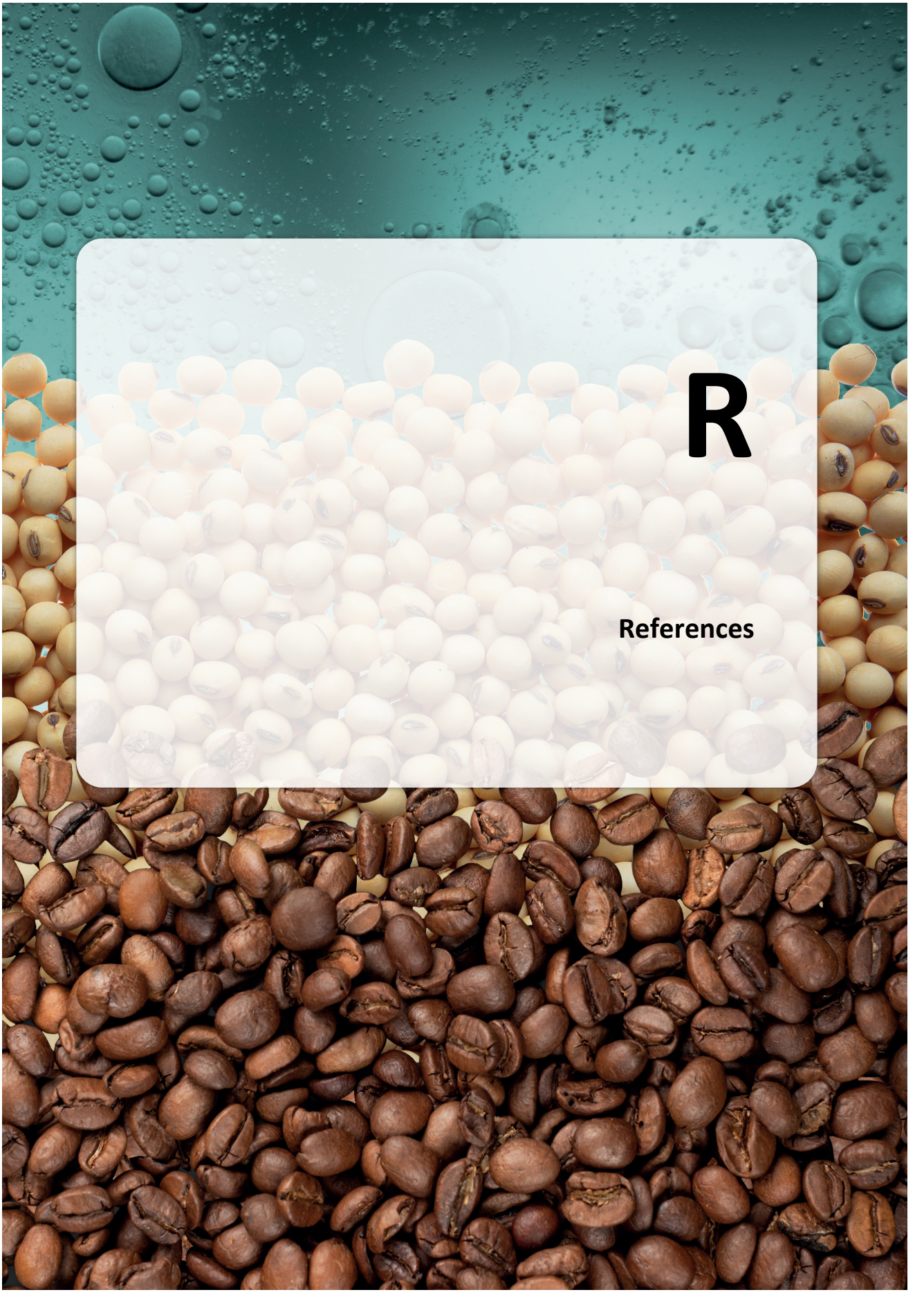

R

References

References

Abeyrathne, E.D.N.S., Nam, K., Ahn, D.U., 2021. Analytical methods for lipid oxidation and antioxidant capacity in food systems. Antioxidants 10, 1–19.

Addis, P.B., 1986. Occurrence of lipid oxidation products in foods. Food Chem. Toxicol. 24, 1021–1030. https://doi.org/10.1016/0278-6915(86)90283-8

Akagawa, M., Sasaki, T., Suyama, K., 2002. Oxidative deamination of lysine residue in plasma protein of diabetic rats: Novel mechanism via the Maillard reaction. Eur. J. Biochem. 269, 5451–5458. https://doi.org/10.1046/j.1432-1033.2002.03243.x

Akhtar, M., Ding, R., 2017. Covalently cross-linked proteins & polysaccharides : Formation , characterisation and potential applications. Curr. Opin. Colloid Interface Sci. 28, 31–36. https://doi.org/10.1016/j.cocis.2017.01.002

Al-Hakkak, J., Al-Hakkak, F., 2010. Functional egg white–pectin conjugates prepared by controlled Maillard reaction. J. Food Eng. 100, 152–159. https://doi.org/https://doi.org/10.1016/j.jfoodeng.2010.03.040

Ali Al-Maqtari, Q., Ghaleb, A.D.S., Ali Mahdi, A., Al-Ansi, W., Essam Noman, A., Wei, M., Aladeeb, A., Yao, W., 2021. Stabilization of water-in-oil emulsion of pulicaria jaubertii extract by ultrasonication: Fabrication, characterization, and storage stability. Food Chem. 350, 129249. https://doi.org/10.1016/j.foodchem.2021.129249

Aljahdali, N., Carbonero, F., 2019. Impact of Maillard reaction products on nutrition and health : Current knowledge and need to understand their fate in the human digestive system. Crit. Rev. Food Sci. Nutr. 0, 1–14. https://doi.org/10.1080/10408398.2017.1378865

Anese, M., Nicoli, M.C., Massini, R., Lerici, C.R., 1999. Effects of drying processing on the Maillard reaction in pasta. Food Res. Int. 32, 193–199. https://doi.org/10.1016/S0963-9969(99)00076-9

Antony, S.M., Han, I.Y., Rieck, J.R., Dawson, P.L., 2000. Antioxidative effect of Maillard reaction products formed from honey at different reaction times. J. Agric. Food Chem. 48, 3985–3989. https://doi.org/10.1021/jf000305x

AOCS, 1998. p-Anisidine value - Official method CD 18-90, in: Official Methods and Recommended Practices of the American Oil Chemists. AOCS Press, Champaign (USA).

Arora, A., Nair, M.G., Strasburg, G.M., 1998. Antioxidant activities of isoflavones and their biological metabolites in a liposomal system. Arch. Biochem. Biophys. 356, 133–141. https://doi.org/10.1006/abbi.1998.0783

Barriuso, B., Astiasarán, I., Ansorena, D., 2013. A review of analytical methods measuring lipid oxidation status in foods: A challenging task. Eur. Food Res. Technol. 236, 1–15. https://doi.org/10.1007/s00217-012-1866-9

Bekedam, E.K., 2008. Coffee brew melanoidins. Struct. Funct. Prop. Brown-Colored Coffee Compd. 2–15.

Bekedam, E.K., De Laat, M.P.F.C., Schols, H.A., Van Boekel, M.A.J.S., Smit, G., 2007. Arabinogalactan proteins are incorporated in negatively charged coffee brew melanoidins. J. Agric. Food Chem. 55, 761–768. https://doi.org/10.1021/jf063010d

Bekedam, E.K., Loots, M.J., Schols, H.A., Van Boekel, M.A.J.S., Smit, G., 2008a. Roasting effects on formation mechanisms of coffee brew melanoidins. J. Agric. Food Chem. 56, 7138–7145. https://doi.org/10.1021/jf800999a

Bekedam, E.K., Roos, E., Schols, H.A., Van Boekel, M.A.J.S., Smit, G., 2008b. Low molecular weight melanoidins in coffee brew. J. Agric. Food Chem. 56, 4060–4067. https://doi.org/10.1021/jf8001894

Bekedam, E.K., Schols, H.A., Van Boekel, M.A.J.S., Smit, G., 2008c. Incorporation of chlorogenic acids in coffee brew melanoidins. J. Agric. Food Chem. 56, 2055–2063. https://doi.org/10.1021/jf073157k

Bekedam, E.K., Schols, H.A., Van Boekel, M.A.J.S., Smit, G., 2006. High molecular weight melanoidins from coffee brew. J. Agric. Food Chem. 54, 7658–7666. https://doi.org/10.1021/jf0615449

Berton-Carabin, C., Schröder, A., Schroën, K., Laguerre, M., 2021. Lipid oxidation in Pickering emulsions, Omega-3 Delivery Systems. Elsevier Inc. https://doi.org/10.1016/b978-0-12-821391-9.00011-9

Berton-Carabin, C., Schroën, K., 2019. Towards new food emulsions: designing the interface and beyond. Curr. Opin. Food Sci. 27, 74–81. https://doi.org/10.1016/j.cofs.2019.06.006

Berton-Carabin, C.C., Ropers, M.H., Genot, C., 2014. Lipid oxidation in oil-in-water emulsions: Involvement of the interfacial layer. Compr. Rev. Food Sci. Food Saf. 13, 945–977. https://doi.org/10.1111/1541-4337.12097

Berton-Carabin, C.C., Sagis, L., Schroën, K., 2018. Formation, structure, and functionality of interfacial layers in food emulsions. Annu. Rev. Food Sci. Technol. 9, 551–587. https://doi.org/10.1146/annurev-food-030117-012405

Berton-Carabin, C.C., Schroën, K., 2015. Pickering emulsions for food applications: Background, trends, and challenges. Annu. Rev. Food Sci. Technol. 6, 263–297. https://doi.org/10.1146/annurev-food-081114-110822

Berton, C., Genot, C., Ropers, M., 2011. Quantification of unadsorbed protein and surfactant emulsifiers in oil-in-water emulsions. J. Colloid Interface Sci. 354, 739–748. https://doi.org/10.1016/j.jcis.2010.11.055

Beverung, C.J., Radke, C.J., Blanch, H.W., 1999. Protein adsorption at the oil/water interface: characterization of adsorption kinetics by dynamic interfacial tension measurements. Biophys. Chem. 81, 59–80. https://doi.org/https://doi.org/10.1016/S0301-4622(99)00082-4

Bi, B., Yang, H., Fang, Y., Nishinari, K., Phillips, G.O., 2017. Characterization and emulsifying properties of b -lactoglobulin-gum Acacia Seyal conjugates prepared via the Maillard reaction. Food Chem. 214, 614–621. https://doi.org/10.1016/j.foodchem.2016.07.112

Boostani, S., Aminlari, M., Moosavi-nasab, M., Niakosari, M., Mesbahi, G., 2017. Fabrication and characterisation of soy protein isolate-grafted dextran biopolymer: A novel ingredient in spray-dried soy beverage formulation. Int. J. Biol. Macromol. 102, 297–307. https://doi.org/10.1016/j.ijbiomac.2017.04.019

Borrelli, R.C., Visconti, A., Mennella, C., Anese, M., Fogliano, V., 2002. Chemical characterization and antioxidant properties of coffee melanoidins. J. Agric. Food Chem. 50, 6527–6533. https://doi.org/10.1021/jf025686o

Browdy, A.A., Harris, N.D., 1997. Whey improves oxidative stability of soybean oil. J. Food Sci. 62, 348–350. https://doi.org/10.1111/j.1365-2621.1997.tb03998.x

Calligaris, S., Manzocco, L., Anese, M., Nicoli, M.C., 2004. Effect of heat-treatment on the antioxidant and pro-oxidant activity of milk. Int. Dairy J. 14, 421–427. https://doi.org/10.1016/j.idairyj.2003.10.001

Cämmerer, B., Jalyschko, W., Kroh, L.W., 2002. Intact carbohydrate structures as part of the melanoidin skeleton. J. Agric. Food Chem. 50, 2083–2087. https://doi.org/10.1021/jf011106w

Cämmerer, B., Kroh, L.W., 1995. Investigation of the influence of reaction conditions on the elementary composition of melanoidins. Food Chem. 53, 55–59. https://doi.org/10.1016/0308-8146(95)95786-6

Cengiz, A., Kahyaoglu, T., Schröen, K., Berton-Carabin, C., 2019a. Oxidative stability of emulsions fortified with iron: The role of liposomal phospholipids. J. Sci. Food Agric. 99, 2957–2965. https://doi.org/10.1002/jsfa.9509

Cengiz, A., Schroën, K., Berton-Carabin, C., 2019b. Lipid oxidation in emulsions fortified with iron-loaded alginate beads. Foods 8. https://doi.org/10.3390/foods8090361

Cermeño, M., Felix, M., Connolly, A., Brennan, E., Co, B., Ryan, E., Fitzgerald, R.J., 2019. Role of carbohydrate conjugation on the emulsification and antioxidant properties of intact and hydrolysed whey protein concentrate. Food Hydrocoll. 88, 170–179. https://doi.org/10.1016/j.foodhyd.2018.09.030

Chaiyasit, W., Elias, R.J., McClements, D.J., Decker, E.A., 2007. Role of physical structures in bulk oils on lipid oxidation. Crit. Rev. Food Sci. Nutr. 47, 299–317. https://doi.org/10.1080/10408390600754248

Cheetangdee, N., Fukada, K., 2014. Emulsifying activity of bovine β-lactoglobulin conjugated with hexoses through the Maillard reaction. Colloids Surfaces A Physicochem. Eng. Asp. 450, 148–155. https://doi.org/10.1016/j.colsurfa.2014.03.026

Chen, B., Cai, Y., Liu, T., Huang, L., Deng, X., Zhao, Q., Zhao, M., 2019. Improvements in physicochemical and emulsifying properties of insoluble soybean fiber by physical-chemical treatments. Food Hydrocoll. 93, 167–175. https://doi.org/10.1016/j.foodhyd.2019.01.058

Chen, B., Mcclements, D.J., Decker, E.A., 2011. Minor components in food oils: A critical review of their roles on lipid oxidation chemistry in bulk oils and emulsions. Crit. Rev. Food Sci. Nutr. 51, 901–916. https://doi.org/10.1080/10408398.2011.606379

Chen, H., Jin, Y., Ding, X., Wu, F., Bashari, M., Chen, F., Cui, Z., Xu, X., 2014. Improved the emulsion stability of phosvitin from hen egg yolk against different pH by the covalent attachment with dextran. Food Hydrocoll. 39, 104–112. https://doi.org/10.1016/j.foodhyd.2013.12.031

Chen, H., Qiu, S., Gan, J., Liu, Y., Zhu, Q., Yin, L., 2016. New insights into the functionality of protein to the emulsifying properties of sugar beet pectin. Food Hydrocoll. 57, 262–270. https://doi.org/10.1016/j.foodhyd.2016.02.005

Chen, L., Chen, J., Wu, K., Yu, L., 2016. Improved low pH emulsification properties of glycated peanut protein isolate by ultrasound Maillard reaction. J. Agric. Food Chem. 64, 5531–5538. https://doi.org/10.1021/acs.jafc.6b00989

Christie, W.W., 1989. Gas chromatography and lipids: A practical guide. The Oily Press, Ayr, Scotland.

Coelho, C., Ribeiro, M., Cruz, A.C.S., Domingues, M.R.M., Coimbra, M.A., Bunzel, M., Nunes, F.M., 2014. Nature of phenolic compounds in coffee melanoidins. J. Agric. Food Chem. 62, 7843–7853. https://doi.org/10.1021/jf501510d

Consoli, L., Dias, R.A.O., Rabelo, R.S., Furtado, G.F., Sussulini, A., Cunha, R.L., Dupas, M., 2018. Sodium caseinate-corn starch hydrolysates conjugates obtained through the Maillard reaction as stabilizing agents in resveratrol-loaded emulsions. Food Hydrocoll. 84, 458–472. https://doi.org/10.1016/j.foodhyd.2018.06.017

Contreras-Calderón, J., Guerra-Hernández, E., García-Villanova, B., 2008. Indicators of non-enzymatic browning in the evaluation of heat damage of ingredient proteins used in manufactured infant formulas. Eur. Food Res. Technol. 227, 117–124. https://doi.org/10.1007/s00217-007-0700-2

Corzo-martínez, M., Carrera, C., Moreno, F.J., Rodríguez, J.M., Villamiel, M., 2012. Interfacial and foaming properties of bovine b -lactoglobulin : Galactose Maillard conjugates. Food Hydrocoll. 27, 438–447. https://doi.org/10.1016/j.foodhyd.2011.11.003

Corzo-Martínez, M., Soria, A.C., Villamiel, M., Olano, A., Harte, F.M., Moreno, F.J., 2011. Effect of glycation on sodium caseinate-stabilized emulsions obtained by ultrasound. J. Dairy Sci. 94, 51–58. https://doi.org/10.3168/jds.2010-3551

Ćosović, B., Vojvodić, V., Bošković, N., Plavšić, M., Lee, C., 2010. Characterization of natural and synthetic humic substances (melanoidins) by chemical composition and adsorption measurements. Org. Geochem. 41, 200–205. https://doi.org/10.1016/j.orggeochem.2009.10.002

D'Agostina, A., Boschin, G., Bacchini, F., Arnoldi, A., 2004. Investigations on the high molecular weight foaming fractions of espresso coffee. J. Agric. Food Chem. 52, 7118–7125. https://doi.org/10.1021/jf049013c

Da Fonseca Selgas Martins, S.I., van der Hijden, H.T.W., Ihechere, E., Vreeker, R., 2014. Method of preparing an emulsifying agent and emulsifying agent so obtained. EP2774496A1.

Dalgleish, D.G., Euston, S.E., Hunt, J.A., Dickinson, E., 1991. Competitive adsorption of β-lactoglobulin in mixed protein emulsions. Food Polym. Gels Colloids 485–489. https://doi.org/10.1533/9781845698331.1.485

Daoud, S., Bou-maroun, E., Dujourdy, L., Waschatko, G., Billecke, N., Cayot, P., 2019. Fast and direct analysis of oxidation levels of oil-in-water emulsions using ATR-FTIR. Food Chem. 293, 307–314. https://doi.org/10.1016/j.foodchem.2019.05.005

Darewicz, M., Dziuba, J., 2001. The effect of glycosylation on emulsifying and structural properties of bovine β-casein. Nahrung - Food 45, 15–20. https://doi.org/10.1002/1521-3803(20010101)45:1<15::AID-FOOD15>3.0.CO;2-Y

Davidek, T., Davidek, J., 2004. Chemistry of the Maillard reaction in foods, in: Tomasik, P. (Ed.), Chemical and Functional Properties of Food Saccharides. CRC Press, London, pp. 278–301.

Davidov-Pardo, G., Joye, I.J., Espinal-Ruiz, M., McClements, D.J., 2015. Effect of Maillard conjugates on the physical stability of Zein nanoparticles prepared by liquid antisolvent coprecipitation. J. Agric. Food Chem. 63, 8510–8518. https://doi.org/10.1021/acs.jafc.5b02699

de Oliveira, F.C., Coimbra, J.S. dos R., de Oliveira, E.B., Zuñiga, A.D.G., Rojas, E.E.G., 2016. Food protein-polysaccharide conjugates obtained via the Maillard reaction: A Review. Crit. Rev. Food Sci. Nutr. 56, 1108–1125. https://doi.org/10.1080/10408398.2012.755669

Dean, R.T., Hunt, J. V., Grant, A.J., Yamamoto, Y., Niki, E., 1991. Free radical damage to proteins: The influence of the relative localization of radical generation, antioxidants, and target proteins. Free Radic. Biol. Med. 11, 161–168. https://doi.org/10.1016/0891-5849(91)90167-2

Decker, E.A., McClements, D.J., Bourlieu-Lacanal, C., Durand, E., Figueroa-Espinoza, M.C., Lecomte, J., Villeneuve, P., 2017. Hurdles in predicting antioxidant efficacy in oil-in-water emulsions. Trends Food Sci. Technol. 67, 183–194. https://doi.org/10.1016/j.tifs.2017.07.001

Decker, E.A., Warner, K., Richards, M.P., Shahidi, F., 2005. Measuring antioxidant effectiveness in food. J. Agric. Food Chem. 53, 4303–4310. https://doi.org/10.1021/jf058012x

Decourcelle, N., Sabourin, C., Dauer, G., Guérard, F., 2010. Effect of the Maillard reaction with xylose on the emulsifying properties of a shrimp hydrolysate (Pandalus borealis). Food Res. Int. 43, 2155–2160. https://doi.org/10.1016/j.foodres.2010.07.026

Deep, S., Ahluwalia, J.C., 2001. Interaction of bovine serum albumin with anionic surfactants. Phys. Chem. Chem. Phys. 3, 4583–4591. https://doi.org/10.1016/j.jcis.2010.03.017

Del Pino-García, R., González-Sanjosé, M.L., Rivero-Pérez, M.D., Muñiz, P., 2012. Influence of the degree of roasting on the antioxidant capacity and genoprotective effect of instant coffee: Contribution of the melanoidin fraction. J. Agric. Food Chem. 60, 10530–10539. https://doi.org/10.1021/jf302747v

Delahaije, R.J.B.M., Gruppen, H., Van Nieuwenhuijzen, N.H., Giuseppin, M.L.F., Wierenga, P.A., 2013. Effect of glycation on the flocculation behavior of protein-stabilized oil-in-water emulsions. Langmuir 29, 15201–15208. https://doi.org/10.1021/la403504f

Delgado-Andrade, C., Fogliano, V., 2018. Dietary advanced glycosylation end-products (dages) and melanoidins formed through Maillard reaction: Physiological consequences of their intake. Annu. Rev. Food Sci. Technol. 9, null. https://doi.org/10.1146/annurev-food-030117-012441

Delgado-Andrade, C., Morales, F.J., 2005. Unraveling the contribution of melanoidins to the antioxidant activity of coffee brews. J. Agric. Food Chem. 53, 1403–1407. https://doi.org/10.1021/jf048500p

Delgado-Andrade, C., Rufián-Henares, J.A., Morales, F.J., 2005. Assessing the antioxidant activity of melanoidins from coffee brews by different antioxidant methods. J. Agric. Food Chem. 53, 7832–7836. https://doi.org/10.1021/jf0512353

Deng, L., 2021. Current progress in the utilization of soy-based emulsifiers in. Foods 10, 1354.

Diah, A., Vermeir, L., Martins, J., Meulenaer, B. De, Meeren, P. Van Der, 2016. Improved heat stability of protein solutions and O / W emulsions upon dry heat treatment of whey protein isolate in the presence of low-methoxyl pectin. Colloids Surfaces A Physicochem. Eng. Asp. 510, 93–103. https://doi.org/10.1016/j.colsurfa.2016.05.034

Dickinson, E., 2003. Hydrocolloids at interfaces and the influence on the properties of dispersed systems. Food Hydrocoll. 17, 25–39. https://doi.org/10.1016/S0268-005X(01)00120-5

Dickinson, E., Hong, S.T., 1995. Influence of water-soluble nonionic emulsifier on the rheology of heat-set protein-stabilized emulsion gels. J. Agric. Food Chem. 43, 2560–2566. https://doi.org/10.1021/jf00058a002

Diftis, N., Kiosseoglou, V., 2006a. Stability against heat-induced aggregation of emulsions prepared with a dry-heated soy protein isolate-dextran mixture. Food Hydrocoll. 20, 787–792. https://doi.org/10.1016/j.foodhyd.2005.07.010

Diftis, N., Kiosseoglou, V., 2006b. Physicochemical properties of dry-heated soy protein isolate-dextran mixtures. Food Chem. 96, 228–233. https://doi.org/10.1016/j.foodchem.2005.02.036

Diftis, N.G., Biliaderis, C.G., Kiosseoglou, V.D., 2005. Rheological properties and stability of model salad dressing emulsions prepared with a dry-heated soybean protein isolate-dextran mixture. Food Hydrocoll. 19, 1025–1031. https://doi.org/10.1016/j.foodhyd.2005.01.003

Ding, R., Valicka, E., Akhtar, M., Ettelaie, R., 2017. Insignificant impact of the presence of lactose impurity on formation and colloid stabilising properties of whey protein – maltodextrin conjugates prepared via Maillard reactions. Food Struct. 12, 43–53. https://doi.org/10.1016/j.foostr.2017.02.004

Dong, S., Panya, A., Zeng, M., Chen, B., McClements, D.J., Decker, E.A., 2012. Characteristics and antioxidant activity of hydrolyzed β-lactoglobulin-glucose Maillard reaction products. Food Res. Int. 46, 55–61. https://doi.org/10.1016/j.foodres.2011.11.022

Dong, S., Wei, B., Chen, B., McClements, D.J., Decker, E.A., 2011. Chemical and antioxidant properties of casein peptide and its glucose Maillard reaction products in fish oil-in-water emulsions. J. Agric. Food Chem. 59, 13311–13317. https://doi.org/10.1021/jf203778z

Donnelly, J.L., Decker, E.A., McClements, D.J., 1998. Iron-Catalyzed Oxidation of Menhaden Oil as Affected by Emulsifiers. J. Food Sci. 63, 997–1000. https://doi.org/10.1111/j.1365-2621.1998.tb15841.x

Drapala, K.P., Auty, M.A.E., Mulvihill, D.M., Mahony, J.A.O., 2016. Improving thermal stability of hydrolysed whey protein-based infant formula emulsions by protein –

carbohydrate conjugation. Food Res. Int. 88, 42–51. https://doi.org/10.1016/j.foodres.2016.01.028

Du, Y., Shi, S., Jiang, Y., Xiong, H., Woo, M.W., Zhao, Q., Bai, C., Zhou, Q., Sun, W., 2013. Physicochemical properties and emulsion stabilization of rice dreg glutelin conjugated with κ-carrageenan through Maillard reaction. J. Sci. Food Agric. 93, 125–133. https://doi.org/10.1002/jsfa.5739

Dukhin, A.S., Goetz, P.J., 1998. Characterization of aggregation phenomena by means of acoustic and electroacoustic spectroscopy. Colloids Surfaces A Physicochem. Eng. Asp. 144, 49–58. https://doi.org/10.1016/S0927-7757(98)00565-2

Dunlap, C.A., Côté, G.L., 2005. β-Lactoglobulin-dextran conjugates: Effect of polysaccharide size on emulsion stability. J. Agric. Food Chem. 53, 419–423. https://doi.org/10.1021/jf049180c

Duque-Estrada, P., Kyriakopoulou, K., de Groot, W., van der Goot, A.J., Berton-Carabin, C.C., 2020. Oxidative stability of soy proteins: From ground soybeans to structured products. Food Chem. 318, 126499. https://doi.org/10.1016/j.foodchem.2020.126499

Echavarría, A.P., Pagán, J., Ibarz, A., 2012. Melanoidins formed by Maillard reaction in food and their biological activity. Food Eng. Rev. 4, 203–223. https://doi.org/10.1007/s12393-012-9057-9

EFSA, 2015. Acrylamide in food. EFSA Explains Risk Assessment. 2015 4.

EFSA, 2012. Scientific Opinion on the re-evaluation of butylated hydroxytoluene BHT (E 321) as a food additive. EFSA J. 10, 1–43. https://doi.org/10.2903/j.efsa.2012.2588

EFSA, 2004. Opinion of the scientific panel on food additives, flavourings, processing aids and materials in contact with food on a request from the commission related to tertiary-butylhydroquinone (TBHQ). EFSA J. 84, 1–50. https://doi.org/10.2903/j.efsa.2007.315

EFSA Panel on Dietetic Products and Allergies (NDA), N., 2010. Scientific opinion on dietary reference values for fats, including saturated fatty acids, polyunsaturated fatty acids, monounsaturated fatty acids, trans fatty acids, and cholesterol. EFSA J. 8, 1461. https://doi.org/10.2903/j.efsa.2010.1461

Ekin, C., Davidov-pardo, G., Julian, D., 2016. Lutein-enriched emulsion-based delivery systems : Impact of Maillard conjugation on physicochemical stability and gastrointestinal fate. Food Hydrocoll. 60, 38–49. https://doi.org/10.1016/j.foodhyd.2016.03.021

Elias, R.J., Kellerby, S.S., Decker, E.A., 2008. Antioxidant activity of proteins and peptides. Crit. Rev. Food Sci. Nutr. 48, 430–441. https://doi.org/10.1080/10408390701425615

Elias, R.J., McClements, D.J., Decker, E.A., 2005. Antioxidant activity of cysteine, tryptophan, and methionine residues in continuous phase β-lactoglobulin in oil-in-water emulsions. J. Agric. Food Chem. 53, 10248–10253. https://doi.org/10.1021/jf0521698

Erbersdobler, H.F., Somoza, V., 2007. Forty years of furosine - Forty years of using Maillard reaction products as indicators of the nutritional quality of foods. Mol. Nutr. Food Res. 51, 423–430. https://doi.org/10.1002/mnfr.200600154

Esfandi, R., Walters, M.E., Tsopmo, A., 2019. Antioxidant properties and potential mechanisms of hydrolyzed proteins and peptides from cereals. Heliyon 5, e01538. https://doi.org/10.1016/j.heliyon.2019.e01538

Estévez, M., 2011. Protein carbonyls in meat systems: A review. Meat Sci. 89, 259–279. https://doi.org/10.1016/j.meatsci.2011.04.025

Fan, Y., Yi, J., Zhang, Y., Yokoyama, W., 2018. Fabrication of curcumin-loaded bovine serum albumin (BSA)-dextran nanoparticles and the cellular antioxidant activity. Food Chem. 239, 1210–1218. https://doi.org/10.1016/j.foodchem.2017.07.075

Faraji, H., McClements, D.J., Decker, E.A., 2004. Role of continuous phase protein on the oxidative stability of fish oil-in-water emulsions. J. Agric. Food Chem. 52, 4558–4564. https://doi.org/10.1021/jf035346i

Farmer, E.H., Bloomfield, G.F., Sundralingam, A., Sutton, D.A., 1942. The course and mechanism of autoöxidation reactions in olefinic and polyolefinic substances, including rubber. Rubber Chem. Technol. 15, 756–764. https://doi.org/10.5254/1.3543161

Feng, J.-L., Qi, J.-R., Yin, S.-W., Wang, J.-M., Guo, J., Weng, J.-Y., Liu, Q.-R., Yang, X.-Q., 2015. Fabrication and characterization of stable soy β-conglycinin-dextran core-shell nanogels prepared via a self-assembly approach at the isoelectric point. J. Agric. Food Chem. 63. https://doi.org/10.1021/acs.jafc.5b01778

Feng, J., Berton-Carabin, C.C., Ataç Mogol, B., Schroën, K., Fogliano, V., 2021a. Glycation of soy proteins leads to a range of fractions with various supramolecular assemblies and surface activities. Food Chem. 343. https://doi.org/10.1016/j.foodchem.2020.128556

Feng, J., Schroën, K., Fogliano, V., Berton-Carabin, C., 2021b. Antioxidant potential of non-modified and glycated soy proteins in the continuous phase of oil-in-water emulsions.

Food Hydrocoll. 114, 106564.
https://doi.org/https://doi.org/10.1016/j.foodhyd.2020.106564

Fiore, A., Troise, A.D., Mogol, A., Roullier, V., Gourdon, A., El, S., Jian, M., Aytu, B., Go, V., Fogliano, V., 2012. Chloride in Cookies.

Frankel, E.N., 1980. Lipid oxidation. Prog. Lipid Res. 19, 1–22.

Friedman, M., 1996. Food browning and its prevention: An overview. J. Agric. Food Chem. 44. https://doi.org/10.1021/jf950394r

Garti, N., Madar, Z., Aserin, A., Sternheim, B., 1997. Fenugreek galactomannans as food emulsifiers. LWT - Food Sci. Technol. 30, 305–311. https://doi.org/10.1006/fstl.1996.0179

Garti, N., Reichman, D., 1994. Surface properties and emulsification activity of galactomannans. Food Hydrocoll. 8, 155–173. https://doi.org/10.1016/S0268-005X(09)80041-6

Garti, N., Reichman, D., 1993. Food structure hydrocolloids as food emulsifiers and stabilizers. Food Struct. 12, 411–426.

Genot, C., Kabri, T.H., Meynier, A., 2013. Stabilization of omega-3 oils and enriched foods using emulsifiers. Food Enrich. with Omega-3 Fat. Acids.
https://doi.org/10.1533/9780857098863.2.150

Gheysen, L., Dejonghe, C., Bernaerts, T., Van Loey, A., De Cooman, L., Foubert, I., 2019. Measuring primary lipid oxidation in food products enriched with colored microalgae. Food Anal. Methods 12, 2150–2160. https://doi.org/10.1007/s12161-019-01561-0

Giroux, H.J., Houde, J., Britten, M., 2010. Use of heated milk protein-sugar blends as antioxidant in dairy beverages enriched with linseed oil. LWT - Food Sci. Technol. 43, 1373–1378. https://doi.org/10.1016/j.lwt.2010.05.001

Gniechwitz, D., Reichardt, N., Ralph, J., Blaut, M., Steinhart, H., Bunzel, M., 2008. Isolation and characterisation of a coffee melanoidin fraction. J. Sci. Food Agric. 88, 2153–2160. https://doi.org/10.1002/jsfa.3327

Golkar, A., Nasirpour, A., Keramat, J., Desobry, S., 2015. Emulsifying properties of angum gum (amygdalus scoparia spach) conjugated to β -lactoglobulin through Maillard-type reaction. Int. J. Food Prop. 18, 2042–2055.
https://doi.org/10.1080/10942912.2014.962040

Gomyo, T., Horikoshi, M., 1976. On the interaction of melanoidin with metallic ions. Agric. Biol. Chem. 40, 33–40. https://doi.org/10.1080/00021369.1976.10862003

Gu, F., Kim, J.M., Hayat, K., Xia, S., Feng, B., Zhang, X., 2009. Characteristics and antioxidant activity of ultrafiltrated Maillard reaction products from a casein-glucose model system. Food Chem. 117, 48–54. https://doi.org/10.1016/j.foodchem.2009.03.074

Gu, F.L., Kim, J.M., Abbas, S., Zhang, X.M., Xia, S.Q., Chen, Z.X., 2010. Structure and antioxidant activity of high molecular weight Maillard reaction products from casein-glucose. Food Chem. 120, 505–511. https://doi.org/10.1016/j.foodchem.2009.10.044

Gu, L., Peng, N., Chang, C., McClements, D.J., Su, Y., Yang, Y., 2017. Fabrication of surface-active antioxidant food biopolymers: Conjugation of catechin polymers to egg white proteins. Food Biophys. 12, 198–210. https://doi.org/10.1007/s11483-017-9476-5

Gumus, C.E., Decker, E.A., McClements, D.J., 2017. Impact of legume protein type and location on lipid oxidation in fish oil-in-water emulsions: Lentil, pea, and faba bean proteins. Food Res. Int. 100, 175–185. https://doi.org/10.1016/j.foodres.2017.08.029

Guo, X., Xiong, Y.L., 2013. Characteristics and functional properties of buckwheat protein-sugar Schiff base complexes. LWT - Food Sci. Technol. 51, 397–404. https://doi.org/10.1016/j.lwt.2012.12.003

Guo, Xiaobing, Guo, Xiaoming, Yu, S., Kong, F., 2018. Influences of the different chemical components of sugar beet pectin on the emulsifying performance of conjugates formed between sugar beet pectin and whey protein isolate. Food Hydrocoll. 82, 1–10. https://doi.org/10.1016/j.foodhyd.2018.03.032

Guzey, D., McClements, D.J., 2006. Formation, stability and properties of multilayer emulsions for application in the food industry. Adv. Colloid Interface Sci. 128–130, 227–248. https://doi.org/10.1016/j.cis.2006.11.021

Hamdani, A.M., Wani, I.A., Bhat, N.A., Siddiqi, R.A., 2018. Effect of guar gum conjugation on functional, antioxidant and antimicrobial activity of egg white lysozyme. Food Chem. 240, 1201–1209. https://doi.org/10.1016/j.foodchem.2017.08.060

Han, L., Li, L., Li, B., Zhao, D., Li, Y., Xu, Z., Liu, G., 2013. Hydroxyl radical induced by lipid in Maillard reaction model system promotes diet-derived Nε-carboxymethyllysine formation. Food Chem. Toxicol. 60, 536–541. https://doi.org/10.1016/j.fct.2013.07.081

Han, M.M., Yi, Y., Wang, H.X., Huang, F., 2017. Investigation of the Maillard reaction between polysaccharides and proteins from longan pulp and the improvement in activities. Molecules 22, 5–8. https://doi.org/10.3390/molecules22060938

Haskard, C.A., Li-Chan, E.C.Y., 1998. Hydrophobicity of bovine serum albumin and ovalbumin determined using uncharged (PRODAN) and anionic (ANS -) fluorescent probes. J. Agric. Food Chem. 46, 2671–2677. https://doi.org/10.1021/jf970876y

Hayase, F., Usui, T., Watanabe, H., 2006. Chemistry and some biological effects of model melanoidins and pigments as Maillard intermediates. Mol. Nutr. Food Res. 50, 1171–1179. https://doi.org/10.1002/mnfr.200600078

Hellwig, M., Henle, T., 2010. Formyline, a new glycation compound from the reaction of lysine and 3-deoxypentosone. Eur. Food Res. Technol. 230, 903–914. https://doi.org/10.1007/s00217-010-1237-3

Hennessy, D.J., Reid, G.R., Smith, F.E., Thompson, S.L., 1984. Ferene — a new spectrophotometric reagent for iron. Can. J. Chem. 62, 721–724. https://doi.org/10.1139/v84-121

Hernández, H.L.H., Santos, I.J.B., Oliveira, E.B. de, Teófilo, R.F., Soares, N. de F.F., Coimbra, J.S. dos R., 2020. Nanostructured conjugates from tara gum and α-lactalbumin. Part 1. Structural characterization. Int. J. Biol. Macromol. 153, 995–1004. https://doi.org/https://doi.org/10.1016/j.ijbiomac.2019.10.229

Herrero, A.M., Carmona, P., Pintado, T., Jiménez-Colmenero, F., Ruíz-Capillas, C., 2011. Infrared spectroscopic analysis of structural features and interactions in olive oil-in-water emulsions stabilized with soy protein. Food Res. Int. 44, 360–366. https://doi.org/10.1016/j.foodres.2010.10.006

Hidalgo, F.J., Zamora, R., 2017. Food Processing Antioxidants, 1st ed, Advances in Food and Nutrition Research. Elsevier Inc. https://doi.org/10.1016/bs.afnr.2016.10.002

Higdon, J. V., Frei, B., 2006. Coffee and health: A review of recent human research. Crit. Rev. Food Sci. Nutr. 46, 101–123. https://doi.org/10.1080/10408390500400009

Hinderink, E.B.A., Münch, K., Sagis, L., Schroën, K., Berton-Carabin, C.C., 2019. Synergistic stabilisation of emulsions by blends of dairy and soluble pea proteins: Contribution of the interfacial composition. Food Hydrocoll. 97, 105206. https://doi.org/10.1016/j.foodhyd.2019.105206

Hinderink, E.B.A., Sagis, L., Schroën, K., Berton-Carabin, C.C., 2021. Sequential adsorption and interfacial displacement in emulsions stabilized with plant-dairy protein blends. J. Colloid Interface Sci. 583, 704–713. https://doi.org/10.1016/j.jcis.2020.09.066

Hinderink, E.B.A., Sagis, L., Schroën, K., Berton-Carabin, C.C., 2020. Behavior of plant-dairy protein blends at air-water and oil-water interfaces. Colloids Surfaces B Biointerfaces 192, 111015. https://doi.org/10.1016/j.colsurfb.2020.111015

Hodge, J.E., 1953. Dehydrated foods, chemistry of browning reactions in model systems. J. Agric. Food Chem. 1, 928–943. https://doi.org/10.1021/jf60015a004

Hofmann, T., 1998a. 4-Alkylidene-2-imino-5-[4-alkylidene-5-oxo-1,3-imidazol-2-inyl] azamethylidene-1,3-imidazolidine - A novel colored substructure in melanoidins formed by Maillard reactions of bound arginine with glyoxal and furan-2-carboxaldehyde. J. Agric. Food Chem. 46, 3896–3901. https://doi.org/10.1021/jf980396m

Hofmann, T., 1998b. Studies on melanoidin-type colorants generated from the Maillard reaction of protein-bound lysine and furan-2-carboxaldehyde - Chemical characterisation of a red coloured domaine. Zeitschrift fur Leb. -Untersuchung und -forsch. 206, 251–258. https://doi.org/10.1007/s002170050253

Hofmann, T., 1998c. Studies on the relationship between molecular weight and the color potency of fractions obtained by thermal treatment of glucose/amino acid and glucose/protein solutions by using ultracentrifugation and color dilution techniques. J. Agric. Food Chem. 46, 3891–3895. https://doi.org/10.1021/jf980397e

Hou, C., Wu, S., Xia, Y., Phillips, G.O., Cui, S.W., 2017. A novel emulsifier prepared from Acacia seyal polysaccharide through Maillard reaction with casein peptides. Food Hydrocoll. 69, 236–241. https://doi.org/10.1016/j.foodhyd.2017.01.038

Hsu, J.P., Nacu, A., 2003. Behavior of soybean oil-in-water emulsion stabilized by nonionic surfactant. J. Colloid Interface Sci. 259, 374–381. https://doi.org/10.1016/S0021-9797(02)00207-2

Hu, B., Wang, K., Han, L., Zhou, B., Yang, J., Li, S., 2020. Pomegranate seed oil stabilized with ovalbumin glycated by inulin: Physicochemical stability and oxidative stability. Food Hydrocoll. 102, 105602. https://doi.org/10.1016/j.foodhyd.2019.105602

Huang, L., Cai, Y., Liu, T., Zhao, X., Chen, B., Long, Z., Zhao, M., Deng, X., Zhao, Q., 2019. Stability of emulsion stabilized by low-concentration soybean protein isolate: Effects of

insoluble soybean fiber. Food Hydrocoll. 97, 105232. https://doi.org/10.1016/j.foodhyd.2019.105232

Hwang, H.S., Winkler-Moser, J.K., Kim, Y., Liu, S.X., 2019. Antioxidant activity of spent coffee ground extracts toward soybean oil and fish oil. Eur. J. Lipid Sci. Technol. 121, 1–12. https://doi.org/10.1002/ejlt.201800372

Hwang, I.G., Kim, H.Y., Woo, K.S., Lee, J., Jeong, H.S., 2011. Biological activities of Maillard reaction products (MRPs) in a sugar-amino acid model system. Food Chem. 126, 221–227. https://doi.org/10.1016/j.foodchem.2010.10.103

Ide, N., Lau, B.H.S., Ryu, K., Matsuura, H., Itakura, Y., 1999. Antioxidant effects of fructosyl arginine, a Maillard reaction product in aged garlic extract. J. Nutr. Biochem. 10, 372–376. https://doi.org/10.1016/S0955-2863(99)00021-2

Jacobsen, C., García-Moreno, P.J., Yesiltas, B., Sørensen, A.-D.M., 2021. Lipid oxidation and traditional methods for evaluation. Omega-3 Deliv. Syst. 183–200. https://doi.org/10.1016/b978-0-12-821391-9.00009-0

Jacobsen, C., Horn, F.F., Nielsen, N.S., 2013. Enrichment of emulsified foods with omega-3 fatty acids, Food Enrichment with Omega-3 Fatty Acids. Woodhead Publishing Limited. https://doi.org/10.1533/9780857098863.3.336

Jacobsen, C., Let, M.B., Nielsen, N.S., Meyer, A.S., 2008. Antioxidant strategies for preventing oxidative flavour deterioration of foods enriched with n-3 polyunsaturated lipids: a comparative evaluation. Trends Food Sci. Technol. 19, 76–93. https://doi.org/10.1016/j.tifs.2007.08.001

Jin, B., Zhou, X., Li, X., Lin, W., Chen, G., Qiu, R., 2016. Self-assembled modified soy protein/dextran nanogel induced by ultrasonication as a delivery vehicle for riboflavin. Molecules 21. https://doi.org/10.3390/molecules21030282

Jung, W.K., Park, P.J., Ahn, C.B., Je, J.Y., 2014. Preparation and antioxidant potential of maillard reaction products from (MRPs) chitooligomer. Food Chem. 145, 173–178. https://doi.org/10.1016/j.foodchem.2013.08.042

Karbasi, M., Madadlou, A., 2018. Interface-related attributes of the Maillard reaction-born glycoproteins. Crit. Rev. Food Sci. Nutr. 58, 1595–1603. https://doi.org/10.1080/10408398.2016.1270894

Karnjanapratum, S., Benjakul, S., O'Brien, N., 2017. Production of antioxidative maillard reaction products from gelatin hydrolysate of unicorn leatherjacket skin. J. Aquat. Food Prod. Technol. 26, 148–162. https://doi.org/10.1080/10498850.2015.1113221

Kasran, M., Cui, S.W., Goff, H.D., 2013a. Emulsifying properties of soy whey protein isolate-fenugreek gum conjugates in oil-in-water emulsion model system. Food Hydrocoll. 30, 691–697. https://doi.org/10.1016/j.foodhyd.2012.09.002

Kasran, M., Cui, S.W., Goff, H.D., 2013b. Covalent attachment of fenugreek gum to soy whey protein isolate through natural Maillard reaction for improved emulsion stability. Food Hydrocoll. 30, 552–558. https://doi.org/10.1016/j.foodhyd.2012.08.004

Kato, A., Murata, K., Kobayashi, K., 1988. Preparation and characterization of ovalbumin-dextran conjugate having excellent emulsifying properties. J. Agric. Food Chem. 36, 421–425. https://doi.org/10.1021/jf00081a005

Kato, A., Sasaki, Y., Furuta, R., Kobayashi, K., 1990. Functional protein-polysaccharide conjugate prepared by controlled dry-heating of ovalbumin-dextran mixtures. Agric. Biol. Chem. 54, 107–112. https://doi.org/10.1080/00021369.1990.10869907

Kaushik, P., Dowling, K., McKnight, S., Barrow, C.J., Wang, B., Adhikari, B., 2016. Preparation, characterization and functional properties of flax seed protein isolate. Food Chem. 197, 212–220. https://doi.org/10.1016/j.foodchem.2015.09.106

Keerati-u-rai, M., Miriani, M., Iametti, S., Bonomi, F., Corredig, M., 2012. Structural changes of soy proteins at the oil-water interface studied by fluorescence spectroscopy. Colloids Surfaces B Biointerfaces 93, 41–48. https://doi.org/10.1016/j.colsurfb.2011.12.002

Kellerby, S.S., McClements, D.J., Decker, E.A., 2006. Role of proteins in oil-in-water emulsions on the stability of lipid hydroperoxides. J. Agric. Food Chem. 54, 7879–7884. https://doi.org/10.1021/jf061340s

Khadidja, L., Asma, C., Mahmoud, B., Meriem, E., 2017. Alginate/gelatin crosslinked system through Maillard reaction: preparation, characterization and biological properties. Polym. Bull. 74, 4899–4919. https://doi.org/10.1007/s00289-017-1997-z

Kim, H.J., Choi, S.J., Shin, W.S., Moon, T.W., 2003. Emulsifying properties of bovine serum albumin-galactomannan conjugates. J. Agric. Food Chem. 51, 1049–1056. https://doi.org/10.1021/jf020698v

Kim, J.S., 2013. Antioxidant activity of Maillard reaction products derived from aqueous and ethanolic glucose-glycine and its oligomer solutions. Food Sci. Biotechnol. 22, 39–46. https://doi.org/10.1007/s10068-013-0006-z

Kim, J.Y., Kim, S., Han, S., Han, S.Y., Passos, C.P., Seo, J., Lee, H., Kang, E.K., Mano, J.F., Coimbra, M.A., Park, J.H., Choi, I.S., 2020. Coffee melanoidin-based multipurpose film formation: Application to single-cell nanoencapsulation. ChemNanoMat 6, 379–385. https://doi.org/https://doi.org/10.1002/cnma.202000004

Kroh, L.W., Fiedler, T., Wagner, J., 2008. α-Dicarbonyl compounds - Key intermediates for the formation of carbohydrate-based melanoidins. Ann. N. Y. Acad. Sci. 1126, 210–215. https://doi.org/10.1196/annals.1433.058

Laguerre, M., Bily, A., Roller, M., Birtić, S., 2017. Mass Transport Phenomena in Lipid Oxidation and Antioxidation. Annu. Rev. Food Sci. Technol. 8, 391–411. https://doi.org/10.1146/annurev-food-030216-025812

Laguerre, M., Lecomte, J., Villeneuve, P., 2007. Evaluation of the ability of antioxidants to counteract lipid oxidation: Existing methods, new trends and challenges. Prog. Lipid Res. 46, 244–282. https://doi.org/10.1016/j.plipres.2007.05.002

Laguerre, M., Tenon, M., Bily, A., Birtić, S., 2020. Toward a spatiotemporal model of oxidation in lipid dispersions: A hypothesis-driven review. Eur. J. Lipid Sci. Technol. 122, 1–10. https://doi.org/10.1002/ejlt.201900209

Langner, E., Rzeski, W., 2014. Biological properties of melanoidins: A review. Int. J. Food Prop. 17, 344–353. https://doi.org/10.1080/10942912.2011.631253

Lee, K.G., Shibamoto, T., 2002. Toxicology and antioxidant activities of non-enzymatic browning reaction products: Review. Food Rev. Int. 18, 151–175. https://doi.org/10.1081/FRI-120014356

Lee, S.H., Lefèvre, T., Subirade, M., Paquin, P., 2009. Effects of ultra-high pressure homogenization on the properties and structure of interfacial protein layer in whey protein-stabilized emulsion. Food Chem. 113, 191–195. https://doi.org/10.1016/j.foodchem.2008.07.067

Lee, S.H., Lefèvre, T., Subirade, M., Paquin, P., 2007. Changes and roles of secondary structures of whey protein for the formation of protein membrane at soy oil/water interface under high-pressure homogenization. J. Agric. Food Chem. 55, 10924–10931. https://doi.org/10.1021/jf0726076

Lee, Y.Y., Tang, T.K., Phuah, E.T., Alitheen, N.B.M., Tan, C.P., Lai, O.M., 2017. New functionalities of Maillard reaction products as emulsifiers and encapsulating agents, and the processing parameters: a brief review. J. Sci. Food Agric. 97, 1379–1385. https://doi.org/10.1002/jsfa.8124

Lesmes, U., McClements, D.J., 2012. Controlling lipid digestibility: Response of lipid droplets coated by beta-lactoglobulin-dextran Maillard conjugates to simulated gastrointestinal conditions. Food Hydrocoll. 26, 221–230. https://doi.org/10.1016/j.foodhyd.2011.05.011

Li, C., Wang, J., Shi, J., Huang, X., Peng, Q., Xueb, F., 2015. Encapsulation of tomato oleoresin using soy protein isolate-gum aracia conjugates as emulsifier and coating materials. Food Hydrocoll. 45, 301–308. https://doi.org/10.1016/j.foodhyd.2014.11.022

Li, J., Yu, S., Yao, P., Jiang, M., 2008. Lysozyme−dextran core−shell nanogels prepared via a green process. Langmuir 24, 3486–3492. https://doi.org/10.1021/la702785b

Li, R., Cui, Q., Wang, G., Liu, J., Chen, S., Wang, Xiaodan, Wang, Xibo, Jiang, L., 2019a. Relationship between surface functional properties and flexibility of soy protein isolate-glucose conjugates. Food Hydrocoll. 95, 349–357. https://doi.org/10.1016/j.foodhyd.2019.04.030

Li, R., Wang, Xibo, Liu, J., Cui, Q., Wang, Xiaodan, Chen, S., Jiang, L., 2019b. Relationship between molecular flexibility and emulsifying properties of soy protein isolate-glucose conjugates. J. Agric. Food Chem. 67, 4089–4097. https://doi.org/10.1021/acs.jafc.8b06713

Li, W., Zhao, H., He, Z., Zeng, M., Qin, F., Chen, J., 2016. Modification of soy protein hydrolysates by Maillard reaction : Effects of carbohydrate chain length on structural and interfacial properties 138, 70–77.

Li, Y., Wang, X., Wang, Y., 2006. Comparative studies on interactions of bovine serum albumin with cationic gemini and single-chain surfactants. J. Phys. Chem. B 110, 8499–8505. https://doi.org/10.1021/jp060532n

Liang, N., Kitts, D.D., 2014. Antioxidant property of coffee components: Assessment of methods that define mechanism of action. Molecules 19, 19180–19208. https://doi.org/10.3390/molecules191119180

Lin, C., Toto, C., Were, L., 2015. Antioxidant effectiveness of ground roasted coffee in raw ground top round beef with added sodium chloride. LWT - Food Sci. Technol. 60, 29–35. https://doi.org/10.1016/j.lwt.2014.08.010

Lin, L.H., Chen, K.M., Liu, H.J., Chu, H.C., Kuo, T.C., Hwang, M.C., Wang, C.F., 2012. Preparation and surface activities of modified gelatin-glucose conjugates. Colloids Surfaces A Physicochem. Eng. Asp. 408, 97–103. https://doi.org/10.1016/j.colsurfa.2012.05.036

Lin, Q., Li, M., Xiong, L., Qiu, L., Bian, X., Sun, C., Sun, Q., 2019. Characterization and antioxidant activity of short linear glucan – lysine nanoparticles prepared by Maillard reaction. Food Hydrocoll. 92, 86–93. https://doi.org/10.1016/j.foodhyd.2019.01.054

Liu, G., Xiong, Y.L., Butterfield, D.A., 2000. Properties of oxidized myofibrils and whey- and soy-protein isolates. J. Food Sci. 65, 811–818.

Liu, J., Gan, J., Yu, Y., Zhu, S., Yin, L., Cheng, Y., 2016. Effect of laboratory-scale decoction on the antioxidative activity of Zhenjiang Aromatic Vinegar: The contribution of melanoidins. J. Funct. Foods 21, 75–86. https://doi.org/10.1016/j.jff.2015.11.041

Liu, L., Zhao, Q., Liu, T., Zhao, M., 2011. Dynamic surface pressure and dilatational viscoelasticity of sodium caseinate/xanthan gum mixtures at the oil-water interface. Food Hydrocoll. 25, 921–927. https://doi.org/10.1016/j.foodhyd.2010.08.023

Liu, Q., Li, J., Kong, B., Jia, N., Li, P., 2014a. Antioxidant capacity of maillard reaction products formed by a porcine plasma protein hydrolysate-sugar model system as related to chemical characteristics. Food Sci. Biotechnol. 23, 33–41. https://doi.org/10.1007/s10068-014-0005-8

Liu, Q., Li, J., Kong, B., Li, P., Xia, X., 2014b. Physicochemical and antioxidant properties of Maillard reaction products formed by heating whey protein isolate and reducing sugars. Int. J. Dairy Technol. 67, 220–228. https://doi.org/10.1111/1471-0307.12110

Livney, Y.D., 2012. Biopolymeric amphiphiles and their assemblies as functional food ingredients and nutraceutical delivery systems, Encapsulation Technologies and Delivery Systems for Food Ingredients and Nutraceuticals. Elsevier Masson SAS. https://doi.org/10.1533/9780857095909.3.252

Lopes, G.R., Ferreira, A.S., Pinto, M., Passos, C.P., Coelho, E., Rodrigues, C., Figueira, C., Rocha, S.M., Nunes, F.M., Coimbra, M.A., 2016. Carbohydrate content, dietary fibre and melanoidins: Composition of espresso from single-dose coffee capsules. Food Res. Int. 89, 989–996. https://doi.org/10.1016/j.foodres.2016.01.018

Lorenzo, J.M., Munekata, P.E.S., Baldin, J.C., Franco, D., Domínguez, R., Trindade, M.A., Tindade, M., 2017. The use of natural antioxidants to replace chemical antioxidants in foods, in: Strategies for Obtaining Healthier Foods. pp. 205–228.

Lu, X., Huang, Q., 2020. Nano/submicrometer milled red rice particles-stabilized Pickering Emulsions and their antioxidative properties. J. Agric. Food Chem. 68, 292–300. https://doi.org/10.1021/acs.jafc.9b04827

Ludwig, I.A., Clifford, M.N., Lean, M.E.J., Ashihara, H., Crozier, A., 2014a. Coffee: Biochemistry and potential impact on health. Food Funct. 5, 1695–1717. https://doi.org/10.1039/c4fo00042k

Ludwig, I.A., Mena, P., Calani, L., Cid, C., Del Rio, D., Lean, M.E.J., Crozier, A., 2014b. Variations in caffeine and chlorogenic acid contents of coffees: What are we drinking? Food Funct. 5, 1718–1726. https://doi.org/10.1039/c4fo00290c

Lund, M.N., Heinonen, M., Baron, C.P., Estévez, M., 2011. Protein oxidation in muscle foods: A review. Mol. Nutr. Food Res. 55, 83–95. https://doi.org/10.1002/mnfr.201000453

Lusk, L.T., Cronan, C.L., Chicoye, E., Goldstein, H., Lusk, L.T., Cronan, C.L., Chicoye, E., A, H.G., 1987. A surface-active fraction isolated from beer. J. Am. Soc. Brew. Chem. 45. https://doi.org/10.1094/asbcj-45-0091

Lusk, L.T., Goldstein, H., Ryder, D., 1995. Independent role of beer proteins, melanoidins and polysaccharides in foam formation. J. Am. Soc. Brew. Chem. 53, 93–103. https://doi.org/10.1094/asbcj-53-0093

Maillard, L.C., 1912. Action des acides aminés sur les sucres: formation des mélanoïdines par voie methodique. Comptes Rendus l'Académie Des Sci. 154, 66–68.

Manzocco, L., Calligaris, S., Mastrocola, D., Nicoli, M.C., Lerici, C.R., 2000. Review of non-enzymatic browning and antioxidant capacity in processed foods. Trends Food Sci. Technol. 11, 340–346. https://doi.org/10.1016/S0924-2244(01)00014-0

Martinez-Gomez, A., Caballero, I., Blanco, C.A., 2020. Phenols and melanoidins as natural antioxidants in beer. Structure, reactivity and antioxidant activity. Biomolecules 10. https://doi.org/10.3390/biom10030400

Martins, S.I.F.S., Jongen, W.M.F., Boekel, M.A.J.S. Van, 2001. A review of Maillard reaction in food and implications to kinetic modelling. Trends Food Sci. Technol. 11, 364–373. https://doi.org/10.1515/9783110973976.218

Mattei, M., Kontogeorgis, G.M., Gani, R., 2012. A systematic methodology for design of emulsion based chemical products, in: Karimi, I.A., Srinivasan, R.B.T.-C.A.C.E. (Eds.), 11

International Symposium on Process Systems Engineering. Elsevier, pp. 220–224. https://doi.org/https://doi.org/10.1016/B978-0-444-59507-2.50036-6

McClements, D.J., 2015. Food emulsions: Principles, practices, and techniques, 3rd ed. Boca Raton: CRC Press. https://doi.org/10.1201/b18868-8

McClements, D.J., 2005. Food emulsions: Principles, practices, and techniques, Boca Raton: CRC Press. Boca Raton: CRC Press.

McClements, D.J., Decker, E., 2018. Interfacial antioxidants: A Review of natural and synthetic emulsifiers and coemulsifiers that can inhibit lipid oxidation. J. Agric. Food Chem. 66, 20–25. https://doi.org/10.1021/acs.jafc.7b05066

McClements, D.J., Decker, E.A., 2000. Lipid oxidation in oil-in-water emulsions: Impact of molecular environment on chemical reactions in heterogeneous food systems. J. Food Sci. 65, 1270–1282. https://doi.org/10.1111/j.1365-2621.2000.tb10596.x

Medrano, A., Abirached, C., Moyna, P., Panizzolo, L., Añón, M.C., 2012. The effect of glycation on oil-water emulsion properties of β-lactoglobulin. LWT - Food Sci. Technol. 45, 253–260. https://doi.org/10.1016/j.lwt.2011.06.017

Meng, J., Kang, T.T., Wang, H.F., Zhao, B. Bin, Lu, R.R., 2018. Physicochemical properties of casein-dextran nanoparticles prepared by controlled dry and wet heating. Int. J. Biol. Macromol. 107, 2604–2610. https://doi.org/10.1016/j.ijbiomac.2017.10.140

Merkx, D.W.H., Hong, G.T.S., Ermacora, A., Van Duynhoven, J.P.M., 2018. Rapid quantitative profiling of lipid oxidation products in a food emulsion by 1H NMR. Anal. Chem. 90, 4863–4870. https://doi.org/10.1021/acs.analchem.8b00380

Mesías, M., Delgado-Andrade, C., 2017. Melanoidins as a potential functional food ingredient. Curr. Opin. Food Sci. 14, 37–42. https://doi.org/10.1016/j.cofs.2017.01.007

Michalska, A., Amigo-Benavent, M., Zielinski, H., del Castillo, M.D., 2008. Effect of bread making on formation of Maillard reaction products contributing to the overall antioxidant activity of rye bread. J. Cereal Sci. 48, 123–132. https://doi.org/10.1016/j.jcs.2007.08.012

Migo, V.P., Del Rosario, E.J., Matsumura, M., 1997. Flocculation of melanoidins induced by inorganic ions. J. Ferment. Bioeng. 83, 287–291. https://doi.org/10.1016/S0922-338X(97)80994-4

Mikkonen, K.S., Tenkanen, M., Cooke, P., Xu, C., Rita, H., Willför, S., Holmbom, B., Hicks, K.B., Yadav, M.P., 2009. Mannans as stabilizers of oil-in-water beverage emulsions. LWT - Food Sci. Technol. 42, 849–855. https://doi.org/10.1016/j.lwt.2008.11.010

Mikkonen, K.S., Xu, C., Berton-Carabin, C., Schroën, K., 2016. Spruce galactoglucomannans in rapeseed oil-in-water emulsions: Efficient stabilization performance and structural partitioning. Food Hydrocoll. 52, 615–624. https://doi.org/10.1016/j.foodhyd.2015.08.009

Miralles, B., Martínez-Rodríguez, A., Santiago, A., van de Lagemaat, J., Heras, A., 2007. The occurrence of a Maillard-type protein-polysaccharide reaction between β-lactoglobulin and chitosan. Food Chem. https://doi.org/10.1016/j.foodchem.2005.11.009

Mohamed, M. O., & Morris, H. A. (1988). Effects of enzyme modified soy protein on rennet-induced reconstituted nonfat dry milk coagulum properties. *Journal of Food Science*, *53*(3), 798–804. https://doi.org/10.1111/j.1365-2621.1988.tb08958.x

Morales, F.J., Babbel, M.B., 2002. Melanoidins exert a weak antiradical activity in watery fluids. J. Agric. Food Chem. 50, 4657–4661. https://doi.org/10.1021/jf0255230

Morales, F.J., Fernández-Fraguas, C., Jiménez-Pérez, S., 2005. Iron-binding ability of melanoidins from food and model systems. Food Chem. 90, 821–827. https://doi.org/10.1016/j.foodchem.2004.05.030

Morales, F.J., Jiménez-Pérez, S., 2004. Peroxyl radical scavenging activity of melanoidins in aqueous systems. Eur. Food Res. Technol. 218, 515–520. https://doi.org/10.1007/s00217-004-0896-3

Moreira, A.S.P., Coimbra, M.A., Nunes, F.M., Domingues, M.R.M., 2013. Roasting-induced changes in arabinotriose, a model of coffee arabinogalactan side chains. Food Chem. 138, 2291–2299. https://doi.org/10.1016/j.foodchem.2012.11.130

Moreira, A.S.P., Coimbra, M.A., Nunes, F.M., Passos, C.P., Santos, S.A.O., Silvestre, A.J.D., Silva, A.M.N., Rangel, M., Domingues, M.R.M., 2015. Chlorogenic acid-arabinose hybrid domains in coffee melanoidins: Evidences from a model system. Food Chem. 185, 135–144. https://doi.org/10.1016/j.foodchem.2015.03.086

Moreira, A.S.P., Nunes, F.M., Domingues, M.R., Coimbra, M.A., 2012. Coffee melanoidins: Structures, mechanisms of formation and potential health impacts. Food Funct. 3, 903–915. https://doi.org/10.1039/c2fo30048f

Moreira, A.S.P., Nunes, F.M., Domingues, M.R.M., Coimbra, M.A., 2014a. Galactomannans in coffee. Coffee Heal. Dis. Prev. 173–183. https://doi.org/10.1016/B978-0-12-409517-5.00019-X

Moreira, A.S.P., Nunes, F.M., Simões, C., Maciel, E., Domingues, P., Domingues, M.R.M., Coimbra, M.A., 2017. Transglycosylation reactions, a main mechanism of phenolics incorporation in coffee melanoidins: Inhibition by Maillard reaction. Food Chem. 227, 422–431. https://doi.org/10.1016/j.foodchem.2017.01.107

Moreira, A.S.P., Simões, J., Pereira, A.T., Passos, C.P., Nunes, F.M., Domingues, M.R.M., Coimbra, M.A., 2014b. Transglycosylation reactions between galactomannans and arabinogalactans during dry thermal treatment. Carbohydr. Polym. 112, 48–55. https://doi.org/10.1016/j.carbpol.2014.05.031

Morzelle, M.C., Watkins, B.A., Li, Y., Hennig, B., Toborek, M., 2020. Dietary lipids and health. Bailey's Ind. Oil Fat Prod. 1–27. https://doi.org/10.1002/047167849x.bio025.pub2

Mu, L., Zhao, H., Zhao, M., Cui, C., Liu, L., 2011. Physicochemical properties of soy protein isolates-acacia gum conjugates. Czech J. Food Sci. 29, 129–136. https://doi.org/10.1007/s11665-017-2547-4

Mulcahy, E.M., Fargier-Lagrange, M., Mulvihill, D.M., O'Mahony, J.A., 2017. Characterisation of heat-induced protein aggregation in whey protein isolate and the influence of aggregation on the availability of amino groups as measured by the ortho-phthaldialdehyde (OPA) and trinitrobenzenesulfonic acid (TNBS) methods. Food Chem. 229, 66–74. https://doi.org/10.1016/j.foodchem.2017.01.155

Namiki, M., 1988. Chemistry of maillard reactions: Recent studies on the browning reaction mechanism and the development of antioxidants and mutagens. Adv. Food Res. 32, 115–184. https://doi.org/10.1016/S0065-2628(08)60287-6

Nasrollahzadeh, F., Varidi, M., Koocheki, A., Hadizadeh, F., 2017. Effect of microwave and conventional heating on structural, functional and antioxidant properties of bovine serum albumin-maltodextrin conjugates through Maillard reaction. Food Res. Int. 100, 289–297. https://doi.org/10.1016/j.foodres.2017.08.030

Nesterenko, A., Alric, I., Silvestre, F., Durrieu, V., 2013. Vegetable proteins in microencapsulation: A review of recent interventions and their effectiveness. Ind. Crops Prod. 42, 469–479. https://doi.org/10.1016/j.indcrop.2012.06.035

Nielsen, P.M., Petersen, D., Dambmann, C., 2001. Improved method for determining food protein degree of hydrolysis. J. Food Sci. 66, 642–646. https://doi.org/10.1111/j.1365-2621.2001.tb04614.x

Nielsen, S.S., 2010. Phenol-sulfuric acid method for total carbohydrates, in: Nielsen, S.S. (Ed.), Food Analysis Laboratory Manual. Springer US, Boston, MA, pp. 47–53. https://doi.org/10.1007/978-1-4419-1463-7_6

Noon, J., Mills, T.B., Norton, I.T., 2020. The use of natural antioxidants to combat lipid oxidation in O/W emulsions. J. Food Eng. 281, 110006. https://doi.org/10.1016/j.jfoodeng.2020.110006

Nooshkam, M., Varidi, M., 2020. Maillard conjugate-based delivery systems for the encapsulation, protection, and controlled release of nutraceuticals and food bioactive ingredients: A review. Food Hydrocoll. 100, 105389. https://doi.org/10.1016/j.foodhyd.2019.105389

Nooshkam, M., Varidi, M., Bashash, M., 2019. The Maillard reaction products as food-born antioxidant and antibrowning agents in model and real food systems. Food Chem. 275, 644–660. https://doi.org/10.1016/j.foodchem.2018.09.083

Nooshkam, M., Varidi, M., Verma, D.K., 2020. Functional and biological properties of Maillard conjugates and their potential application in medical and food: A review. Food Res. Int. 131, 109003. https://doi.org/10.1016/j.foodres.2020.109003

Nuchi, C.D., Hernandez, P., McClements, J.J., Decker, E.A., 2002. Ability of lipid hydroperoxides to partition into surfactant micelles and alter lipid oxidation rates in emulsions. J. Agric. Food Chem. 50, 5445–5449. https://doi.org/10.1021/jf020095j

Nunes, F.M., Coimbra, M.A., 2010. Role of hydroxycinnamates in coffee melanoidin formation. Phytochem. Rev. 9, 171–185. https://doi.org/10.1007/s11101-009-9151-7

Nunes, F.M., Coimbra, M.A., 2001. Chemical characterization of the high molecular weight material extracted with hot water from green and roasted arabica coffee. J. Agric. Food Chem. 49, 1773–1782. https://doi.org/10.1021/jf0012953

Nunes, F.M., Coimbra, M.A., 1998. Influence of polysaccharide composition in foam stability of espresso coffee. Carbohydr. Polym. 37, 283–285. https://doi.org/10.1016/S0144-8617(98)00072-1

Nunes, F.M., Cruz, A.C.S., Coimbra, M.A., 2012. Insight into the mechanism of coffee melanoidin formation using modified “in Bean” models. J. Agric. Food Chem. 60, 8710–8719. https://doi.org/10.1021/jf301527e

O’Brien, J., Morrissey, P.A., 1997. Metal ion complexation by products of the Maillard reaction. Food Chem. 58, 17–27. https://doi.org/10.1016/S0308-8146(96)00162-8

O’Brien, J., Morrissey, P.A., 1989. Nutritional and toxicological aspects of the maillard browning reaction in foods. Crit. Rev. Food Sci. Nutr. 28, 211–248. https://doi.org/10.1080/10408398909527499

O’Mahony, J.A., Drapala, K.P., Mulcahy, E.M., Mulvihill, D.M., 2018. Whey protein−carbohydrate conjugates, Whey Proteins. Elsevier Inc. https://doi.org/10.1016/b978-0-12-812124-5.00008-4

O’Regan, J., Mulvihill, D.M., 2009. Preparation, characterisation and selected functional properties of sodium caseinate–maltodextrin conjugates. Food Chem. 115, 1257–1267. https://doi.org/https://doi.org/10.1016/j.foodchem.2009.01.045

Oliver, C.M., Melton, L.D., Stanley, R.A., 2006. Creating proteins with novel functionality via the maillard reaction: A review. Crit. Rev. Food Sci. Nutr. 46, 337–350. https://doi.org/10.1080/10408690590957250

Oosterveld, A., Harmsen, J.S., Voragen, A.G.J., Schols, H.A., 2003. Extraction and characterization of polysaccharides from green and roasted Coffea arabica beans. Carbohydr. Polym. 52, 285–296. https://doi.org/10.1016/S0144-8617(02)00296-5

Otzen, D.E., Sehgal, P., Westh, P., 2009. α-Lactalbumin is unfolded by all classes of surfactants but by different mechanisms. J. Colloid Interface Sci. 329, 273–283. https://doi.org/https://doi.org/10.1016/j.jcis.2008.10.021

Pan, Y., Wu, Z., Xie, Q.T., Li, X.M., Meng, R., Zhang, B., Jin, Z.Y., 2020. Insight into the stabilization mechanism of emulsions stabilized by Maillard conjugates: Protein hydrolysates-dextrin with different degree of polymerization. Food Hydrocoll. 99, 105347. https://doi.org/10.1016/j.foodhyd.2019.105347

Panusa, A., Zuorro, A., Lavecchia, R., Marrosu, G., Petrucci, R., 2013. Recovery of natural antioxidants from spent coffee grounds. J. Agric. Food Chem. 61, 4162–4168. https://doi.org/10.1021/jf4005719

Parliment, T.H., 2000. An overview of coffee roasting. ACS Symp. Ser. 754, 188–201. https://doi.org/10.1021/bk-2000-0754.ch020

Patrignani, M., Rinaldi, G.J., Lupano, C.E., 2016. In vivo effects of Maillard reaction products derived from biscuits. Food Chem. 196, 204–210. https://doi.org/10.1016/j.foodchem.2015.09.038

Pawar, A.B., Caggioni, M., Hartel, R.W., Spicer, P.T., 2012. Arrested coalescence of viscoelastic droplets with internal microstructure. Faraday Discuss. 158, 341. https://doi.org/10.1039/c2fd20029e

Pérez-Martínez, M., Caemmerer, B., De Peña, M.P., Concepción, C., Kroh, L.W., 2010. Influence of brewing method and acidity regulators on the antioxidant capacity of coffee brews. J. Agric. Food Chem. 58, 2958–2965. https://doi.org/10.1021/jf9037375

Perrechil, F.A., Santana, R.C., Lima, D.B., Polastro, M.Z., Cunha, R.L., 2014. Emulsifying properties of maillard conjugates produced from sodium caseinate and locust bean gum. Brazilian J. Chem. Eng. 31, 429–438. https://doi.org/10.1590/0104-6632.20140312s00002328

Perrone, D., Farah, A., Donangelo, C.M., 2012. Influence of coffee roasting on the incorporation of phenolic compounds into melanoidins and their relationship with antioxidant activity of the brew. J. Agric. Food Chem. 60, 4265–4275. https://doi.org/10.1021/jf205388x

Piazza, L., Gigli, J., Bulbarello, A., 2008. Interfacial rheology study of espresso coffee foam structure and properties. J. Food Eng. 84, 420–429. https://doi.org/10.1016/j.jfoodeng.2007.06.001

Pietta, P.G., 2000. Flavonoids as antioxidants. J. Nat. Prod. 63, 1035–1042. https://doi.org/10.1021/np9904509

Pipe, C.J., Gehin-Delval, C., Mora, F., Vieira, J.B., Husson, J., 2014. Emulsifier system. WO 2014/102230 Al.

Pirestani, S., Nasirpour, A., Keramat, J., Desobry, S., 2017. Effect of glycosylation with gum Arabic by Maillard reaction in a liquid system on the emulsifying properties of canola protein isolate. Carbohydr. Polym. 157, 1620–1627. https://doi.org/10.1016/j.carbpol.2016.11.044

Pokorný, J., 2007. Are natural antioxidants better - and safer - Than synthetic antioxidants? Eur. J. Lipid Sci. Technol. 109, 629–642. https://doi.org/10.1002/ejlt.200700064

Ponginebbi, L., Nawar, W.W., Chinachoti, P., 1999. Oxidation of linoleic acid in emulsions: Effect of substrate, emulsifier, and sugar concentration. JAOCS, J. Am. Oil Chem. Soc. 76, 131–138. https://doi.org/10.1007/s11746-999-0059-6

Qi, P.X., Xiao, Y., Wickham, E.D., 2017. Changes in physical , chemical and functional properties of whey protein isolate (WPI) and sugar beet pectin (SBP) conjugates formed by controlled dry-heating. Food Hydrocoll. 69, 86–96. https://doi.org/10.1016/j.foodhyd.2017.01.032

Quiroz-Reyes, C.N., Fogliano, V., 2018. Design cocoa processing towards healthy cocoa products: The role of phenolics and melanoidins. J. Funct. Foods 45, 480–490. https://doi.org/10.1016/j.jff.2018.04.031

Ragnarsson, J.O., Leick, D., Labuza, T.P., 1977. Accelerated temperature study of antioxidants. J. Food Sci. 42, 1536–1539. https://doi.org/10.1111/j.1365-2621.1977.tb08419.x

Rangsansarid, J., Cheetangdee, N., Kinoshita, N., Fukuda, K., 2008. Bovine serum albumin-sugar conjugates through the Maillard reaction effects on interfacial behavior and emulsifying ability. J. Oleo Sci. 57, 539–547.

Rasheed, A., Fathima Abdul Azeez, R., 2019. A review on natural antioxidants. Tradit. Complement. Med. https://doi.org/10.5772/intechopen.82636

Reddy, N.R., Sathe, S.K., Salunkhe, D.K., 1982. Phytates in legumes and cereals, Advances in Food Research. https://doi.org/10.1016/S0065-2628(08)60110-X

Redgwell, R.J., Schmitt, C., Beaulieu, M., Curti, D., 2005. Hydrocolloids from coffee: Physicochemical and functional properties of an arabinogalactan-protein fraction from green beans. Food Hydrocoll. 19, 1005–1015. https://doi.org/10.1016/j.foodhyd.2004.12.010

Regan, J.O., Mulvihill, D.M., 2013. Preparation, characterisation and selected functional properties of hydrolysed sodium caseinate-maltodextrin conjugate. Int. J. Dairy Technol. 66, 333–345. https://doi.org/10.1111/1471-0307.12052

Riisom, T., Sims, R.J., Fioriti, J.A., 1980. Effect of amino acids on the autoxidation of safflower oil in emulsions. J. Am. Oil Chem. Soc. 57, 354–359. https://doi.org/10.1007/BF02662057

Romero, A.M., Doval, M.M., Sturla, M.A., Judis, M.A., 2005. Antioxidant behaviour of products resulting from beef sarcoplasmic proteins-malondialdehyde reaction. Eur. J. Lipid Sci. Technol. 107, 903–911. https://doi.org/10.1002/ejlt.200501196

Roy-Perreault, A., Kueper, B.H., Rawson, J., 2005. Formation and stability of polychlorinated biphenyl Pickering emulsions. J. Contam. Hydrol. 77, 17–39. https://doi.org/10.1016/j.jconhyd.2004.11.001

Rufián-Henares, J.A., Morales, F.J., 2007. Effect of in vitro enzymatic digestion on antioxidant activity of coffee melanoidins and fractions. J. Agric. Food Chem. 55, 10016–10021. https://doi.org/10.1021/jf0718291

Ruiz-Roca, B., Navarro, M.P., Seiquer, I., 2008. Antioxidant properties and metal chelating activity of glucose-lysine heated mixtures: Relationships with mineral absorption across caco-2 cell monolayers. J. Agric. Food Chem. 56, 9056–9063. https://doi.org/10.1021/jf801718h

Ryu, K., Ide, N., Matsuura, H., Itakura, Y., 2001. Nα-(1-Deoxy-D-fructos-1-yl)-L-arginine, an antioxidant compound identified in aged garlic extract. J. Nutr. 131, 972S-976S. https://doi.org/10.1093/jn/131.3.972S

Sabik, H., Achouri, A., Alfaro, M., Pelletier, M., Belanger, D., Britten, M., Fustier, P., 2014. Study of chemical stability of lemon oil components in sodium caseinate-lactose glycoconjugate-stabilized oil-in-water emulsions using solid-phase microextraction-gas chromatography. Food Funct. 5, 1495–1505. https://doi.org/10.1039/c4fo00016a

Sarmadi, B.H., Ismail, A., 2010. Antioxidative peptides from food proteins: A review. peptides 31, 1949–1956. https://doi.org/10.1016/j.peptides.2010.06.020

Schaich, K.M., 2020a. Toxicity of lipid oxidation products consumed in the diet, Bailey's Industrial Oil and Fat Products. https://doi.org/10.1002/047167849x.bio116

Schaich, K.M., 2020b. Lipid oxidation: New perspectives on an old reaction, Bailey's Industrial Oil and Fat Products. https://doi.org/10.1002/047167849x.bio067.pub2

Schaich, K.M., 2013. Challenges in elucidating lipid oxidation mechanisms: When, where, and how do products arise?, Lipid oxidation: Challenges in food systems. AOCS Press. https://doi.org/10.1016/B978-0-9830791-6-3.50004-7

Schmidt, U.S., Pietsch, V.L., Rentschler, C., Kurz, T., Endreß, H.U., Schuchmann, H.P., 2016. Influence of the degree of esterification on the emulsifying performance of conjugates formed between whey protein isolate and citrus pectin. Food Hydrocoll. 56, 1–8. https://doi.org/10.1016/j.foodhyd.2015.11.015

Schröder, A., Berton-Carabin, C., Venema, P., Cornacchia, L., 2017. Interfacial properties of whey protein and whey protein hydrolysates and their influence on O/W emulsion stability. Food Hydrocoll. 73, 129–140. https://doi.org/10.1016/j.foodhyd.2017.06.001

Schröder, A., Laguerre, M., Sprakel, J., Schroën, K., Berton-Carabin, C.C., 2020. Pickering particles as interfacial reservoirs of antioxidants. J. Colloid Interface Sci. 575, 489–498. https://doi.org/10.1016/j.jcis.2020.04.069

Schröder, A., Laguerre, M., Tenon, M., Schroën, K., Berton-Carabin, C.C., 2021. Natural particles can armor emulsions against lipid oxidation and coalescence. Food Chem. 347. https://doi.org/10.1016/j.foodchem.2021.129003

Schroën, K., de Ruiter, J., Berton-Carabin, C., 2020. The importance of interfacial tension in emulsification: Connecting scaling relations used in large scale preparation with microfluidic measurement methods. ChemEngineering 4, 1–22. https://doi.org/10.3390/chemengineering4040063

Sedaghat Doost, A., Nikbakht Nasrabadi, M., Wu, J., A'yun, Q., Van der Meeren, P., 2019. Maillard conjugation as an approach to improve whey proteins functionality: A review of conventional and novel preparation techniques. Trends Food Sci. Technol. 91, 1–11. https://doi.org/10.1016/j.tifs.2019.06.011

Seo, S., Karboune, S., Archelas, A., 2014. Production and characterisation of potato patatin-galactose, galactooligosaccharides, and galactan conjugates of great potential as functional ingredients. Food Chem. 158, 480–489. https://doi.org/10.1016/j.foodchem.2014.02.141

Serna, J., Narvaez Rincon, P.C., Falk, V., Boly, V., Camargo, M., 2021. A methodology for emulsion design based on emulsion science and expert knowledge. Part 1: Conceptual approach. Ind. Eng. Chem. Res. 60, 3210–3227. https://doi.org/10.1021/acs.iecr.0c04942

Serpen, A., Gökmen, V., 2009. Evaluation of the Maillard reaction in potato crisps by acrylamide, antioxidant capacity and color. J. Food Compos. Anal. 22, 589–595. https://doi.org/10.1016/j.jfca.2008.11.003

Shaheen, S., Shorbagi, M., Lorenzo, J.M., Farag, M.A., 2021. Dissecting dietary melanoidins: formation mechanisms, gut interactions and functional properties. Crit. Rev. Food Sci. Nutr. 0, 1–18. https://doi.org/10.1080/10408398.2021.1937509

Shanta, N.C., Decker, E.A., 1994. Iron-based spectrophotometric methods for determination of peroxide values of food lipids. J. AOAC Int. 77, 421–424.

Shao, Y., Tang, C.H., 2014. Characteristics and oxidative stability of soy protein-stabilized oil-in-water emulsions: Influence of ionic strength and heat pretreatment. Food Hydrocoll. 37, 149–158. https://doi.org/10.1016/j.foodhyd.2013.10.030

Shekarforoush, E., Mirhosseini, H., Islam, Z., 2016. Soy protein – gum karaya conjugate : Emulsifying activity and rheological behavior in aqueous system and oil in water emulsion. JAOCS, J. Am. Oil Chem. Soc. 93, 1–10. https://doi.org/10.1007/s11746-015-2751-z

Shen, L., Tang, C.H., 2012. Microfluidization as a potential technique to modify surface properties of soy protein isolate. Food Res. Int. 48, 108–118. https://doi.org/10.1016/j.foodres.2012.03.006

Shen, Z., Bhail, S., Sanguansri, L., Augustin, M.A., 2014. Improving the oxidative stability of krill oil-in-water emulsions. JAOCS, J. Am. Oil Chem. Soc. 91, 1347–1354. https://doi.org/10.1007/s11746-014-2489-z

Shewry, P.R., 1995. Plant storage proteins. Biol. Rev. 70, 375–426. https://doi.org/10.1111/j.1469-185x.1995.tb01195.x

Shi, Y., Liang, R., Chen, L., Liu, H., Go, H.D., Ma, J., 2019. The antioxidant mechanism of Maillard reaction products in oil-in-water emulsion system. Food Hydrocoll. 87, 582–592. https://doi.org/10.1016/j.foodhyd.2018.08.039

Shimada, K., Okada, H., Matsuo, K., Yoshioka, S., 1996. Involvement of chelating action and viscosity in the antioxidative effect of xanthan in an oil/water emulsion. Biosci. Biotechnol. Biochem. 60, 125–127. https://doi.org/10.1271/bbb.60.125

Silván, J.M., Assar, S.H., Srey, C., Dolores Del Castillo, M., Ames, J.M., 2011. Control of the Maillard reaction by ferulic acid. Food Chem. 128, 208–213. https://doi.org/10.1016/j.foodchem.2011.03.047

Silván, J.M., Morales, F.J., Saura-Calixto, F., 2010. Conceptual study on maillardized dietary fiber in coffee. J. Agric. Food Chem. 58, 12244–12249. https://doi.org/10.1021/jf102489u

Silván, J.M., van de Lagemaat, J., Olano, A., del Castillo, M.D., 2006. Analysis and biological properties of amino acid derivates formed by Maillard reaction in foods. J. Pharm. Biomed. Anal. 41, 1543–1551. https://doi.org/10.1016/j.jpba.2006.04.004

Simões, J., Moreira, A.S.P., Passos, C.P., Nunes, F.M., Domingues, M.R.M., Coimbra, M.A., 2019. CHAPTER 19 Polysaccharides and other carbohydrates, in: Coffee: Production, Quality and Chemistry. The Royal Society of Chemistry, pp. 445–457. https://doi.org/10.1039/9781782622437-00445

Singleton, V.L., Rossi, J.A., Jr, J., 1965. Colorimetry of total phenolics with phosphomolybdic-phosphotungstic acid reagents. Am. J. Enol. Vitic. 16, 144–158.

Smith, G.A., Friedman, M., 1984. Effect of carbohydrates and heat on the amino acid composition and chemically available lysine content of casein. J. Food Sci. 49, 817–820. https://doi.org/10.1111/j.1365-2621.1984.tb13219.x

Spotti, M.J., Loyeau, P.A., Marangón, A., Noir, H., Rubiolo, A.C., Carrara, C.R., 2019. Influence of Maillard reaction extent on acid induced gels of whey proteins and dextrans. Food Hydrocoll. 91, 224–231. https://doi.org/https://doi.org/10.1016/j.foodhyd.2019.01.020

Sproston, M.J., Akoh, C.C., 2016. Antioxidative effects of a glucose-cysteine maillard reaction product on the oxidative stability of a structured lipid in a complex food emulsion. J. Food Sci. 81, C2923–C2931. https://doi.org/10.1111/1750-3841.13541

St. Angelo, A.J., 1996. Lipid oxidation in foods, Critical Reviews in Food Science and Nutrition. https://doi.org/10.1080/10408399609527723

Summa, C., McCourt, J., Cämmerer, B., Fiala, A., Probst, M., Kun, S., Anklam, E., Wagner, K.-H., 2008. Radical scavenging activity, anti-bacterial and mutagenic effects of cocoa bean Maillard Reaction products with degree of roasting. Mol. Nutr. Food Res. 52, 342–351. https://doi.org/10.1002/mnfr.200700403

Sun, Y.E., Wang, W.D., Chen, H.W., Li, C., 2011. Autoxidation of unsaturated lipids in food emulsion. Crit. Rev. Food Sci. Nutr. 51, 453–466. https://doi.org/10.1080/10408391003672086

Tagliazucchi, D., Verzelloni, E., 2014. Relationship between the chemical composition and the biological activities of food melanoidins. Food Sci. Biotechnol. 23, 561–568. https://doi.org/10.1007/s10068-014-0077-5

Tagliazucchi, D., Verzelloni, E., Conte, A., 2010. Contribution of melanoidins to the antioxidant activity of traditional balsamic vinegar during aging. J. Food Biochem. 34, 1061–1078.

Taifouris, M., Martín, M., Martínez, A., Esquejo, N., 2020. Challenges in the design of formulated products: multiscale process and product design. Curr. Opin. Chem. Eng. 27, 1–9. https://doi.org/https://doi.org/10.1016/j.coche.2019.10.001

Tamnak, S., Mirhosseini, H., Ping, C., Mohd, H., Muhammad, K., 2016. Physicochemical properties , rheological behavior and morphology of pectin-pea protein isolate mixtures and conjugates in aqueous system and oil in water emulsion. Food Hydrocoll. 56, 405–416. https://doi.org/10.1016/j.foodhyd.2015.12.033

Tao, F., Jiang, H., Chen, W., Zhang, Y., Pan, J., Jiang, J., Jia, Z., 2018. Covalent modification of soy protein isolate by (−)-epigallocatechin-3-gallate: Effects on structural and emulsifying properties. J. Sci. Food Agric. 98, 5683–5689. https://doi.org/10.1002/jsfa.9114

Thanh, V.H., Shibasaki, K., 1978. Major proteins of soybean seeds. reconstitution of β-conglycinin from its subunits. J. Agric. Food Chem. 26, 695–698. https://doi.org/10.1021/jf60217a027

Tian, L., Kejing, Y., Zhang, S., Yi, J., Zhu, Z., Decker, E.A., McClements, D.J., 2021. Impact of tea polyphenols on the stability of oil-in-water emulsions coated by whey proteins. Food Chem. 343, 128448. https://doi.org/10.1016/j.foodchem.2020.128448

Tressl, R., Wondark, G.T., Krüger, R.P., Rewicki, D., 1998a. New melanoidin-like Maillard polymers from 2-deoxypentoses. J. Agric. Food Chem. 46, 104–110. https://doi.org/10.1021/jf970657c

Tressl, R., Wondrak, G.T., Garbe, L.A., Krüger, R.P., Rewicki, D., 1998b. Pentoses and hexoses as sources of new melanoidin-like Maillard polymers. J. Agric. Food Chem. 46, 1765–1776. https://doi.org/10.1021/jf970973r

Trnková, L., Dršata, J., Boušová, I., 2015. Oxidation as an important factor of protein damage: Implications for Maillard reaction. J. Biosci. 40, 419–439. https://doi.org/10.1007/s12038-015-9523-7

Troise, A.D., Fiore, A., Wiltafsky, M., Fogliano, V., 2015. Quantification of Nε-(2-Furoylmethyl)-l-lysine (furosine), Nε-(Carboxymethyl)-l-lysine (CML), Nε-(Carboxyethyl)-l-lysine (CEL) and total lysine through stable isotope dilution assay and tandem mass spectrometry. Food Chem. 188, 357–364. https://doi.org/https://doi.org/10.1016/j.foodchem.2015.04.137

Troise, A.D., Fogliano, V., 2013. Reactants encapsulation and Maillard Reaction. Trends Food Sci. Technol. 33, 63–74. https://doi.org/10.1016/j.tifs.2013.07.002

Troup, G.J., Navarini, L., Liverani, F.S., Drew, S.C., 2015. Stable radical content and anti-radical activity of roasted arabica coffee: From in-tact bean to coffee brew. PLoS One 10, 10–16. https://doi.org/10.1371/journal.pone.0122834

Uluata, S., Durmaz, G., Julian McClements, D., Decker, E.A., 2021. Comparing DPPP fluorescence and UV based methods to assess oxidation degree of krill oil-in-water emulsions. Food Chem. 339, 127898. https://doi.org/10.1016/j.foodchem.2020.127898

Vermeer, A.W.P., Norde, W., 2000. The influence of the binding of low molecular weight surfactants on the thermal stability and secondary structure of IgG. Colloids Surfaces A Physicochem. Eng. Asp. 161, 139–150. https://doi.org/10.1016/S0927-7757(99)00332-5

Verzelloni, E., Tagliazucchi, D., Del Rio, D., Calani, L., Conte, A., 2011. Antiglycative and antioxidative properties of coffee fractions. Food Chem. 124, 1430–1435. https://doi.org/10.1016/j.foodchem.2010.07.103

Vhangani, L.N., Wyk, J. Van, 2016. Antioxidant activity of Maillard reaction products (MRPs) in a lipid-rich model system. Food Chem. 208, 301–308. https://doi.org/10.1016/j.foodchem.2016.03.100

Viau, M., Genot, C., Ribourg, L., Meynier, A., 2016. Amounts of the reactive aldehydes, malonaldehyde, 4-hydroxy-2-hexenal, and 4-hydroxy-2-nonenal in fresh and oxidized edible oils do not necessary reflect their peroxide and anisidine values. Eur. J. Lipid Sci. Technol. 118, 435–444. https://doi.org/10.1002/ejlt.201500103

Villaverde, A., Estévez, M., 2013. Carbonylation of myofibrillar proteins through the Maillard pathway: Effect of reducing sugars and reaction temperature. J. Agric. Food Chem. 61, 3140–3147. https://doi.org/10.1021/jf305451p

Villière, A., Rousseau, F., Brossard, C., Genot, C., 2007. Sensory evaluation of the odour of a sunflower oil emulsion throughout oxidation. Eur. J. Lipid Sci. Technol. 109, 38–48. https://doi.org/10.1002/ejlt.200600084

Villiere, A., Viau, M., Bronnec, I., Moreau, N., Genot, C., 2005. Oxidative stability of bovine serum albumin- and sodium caseinate-stabilized emulsions depends on metal availability. J. Agric. Food Chem. 53, 1514–1520. https://doi.org/10.1021/jf0486951

Vivian, J.T., Callis, P.R., 2001. Mechanisms of tryptophan fluorescence shifts in proteins. Biophys. J. 80, 2093–2109. https://doi.org/10.1016/S0006-3495(01)76183-8

Walker, J.M., Mennella, I., Ferracane, R., Tagliamonte, S., Holik, A.K., Hölz, K., Somoza, M.M., Somoza, V., Fogliano, V., Vitaglione, P., 2020. Melanoidins from coffee and bread differently influence energy intake: A randomized controlled trial of food intake and gut-brain axis response. J. Funct. Foods 72. https://doi.org/10.1016/j.jff.2020.104063

Wang, C., Li, J., Li, X., Chang, C., Zhang, M., Gu, L., Su, Y., Yang, Y., 2019. Emulsifying properties of glycation or glycation-heat modified egg white protein. Food Res. Int. 119, 227–235. https://doi.org/10.1016/j.foodres.2019.01.047

Wang, C., Liu, Z., Xu, G., Yin, B., Yao, P., 2016. BSA-dextran emulsion for protection and oral delivery of curcumin. Food Hydrocoll. 61, 11–19. https://doi.org/10.1016/j.foodhyd.2016.04.037

Wang, H.Y., Qian, H., Yao, W.R., 2011. Melanoidins produced by the Maillard reaction: Structure and biological activity. Food Chem. 128, 573–584. https://doi.org/10.1016/j.foodchem.2011.03.075

Wang, L., Wu, M., Liu, H., 2017. Emulsifying and physicochemical properties of soy hull hemicelluloses-soy protein isolate conjugates. Carbohydr. Polym. 163, 181–190. https://doi.org/10.1016/j.carbpol.2017.01.069

Wang, P.-P., Wang, W.-D., Chen, C., Fu, X., Liu, R.-H., 2020. Effect of Fructus Mori. bioactive polysaccharide conjugation on improving functional and antioxidant activity of whey protein. Int. J. Biol. Macromol. 148, 761–767. https://doi.org/10.1016/j.ijbiomac.2020.01.195

Wang, Q., Ismail, B., 2012. Effect of Maillard-induced glycosylation on the nutritional quality, solubility, thermal stability and molecular configuration of whey proteinv. Int. Dairy J. 25, 112–122. https://doi.org/10.1016/j.idairyj.2012.02.009

Wang, W.Q., Bao, Y.H., Chen, Y., 2013. Characteristics and antioxidant activity of water-soluble Maillard reaction products from interactions in a whey protein isolate and sugars system. Food Chem. 139, 355–361. https://doi.org/10.1016/j.foodchem.2013.01.072

Wang, X., Xiong, Y.L., 2016. Oxidative polyaldehyde production : A novel approach to the conjugation of dextran with soy peptides for improved emulsifying properties. J. Food Sci. Technol. 53, 3215–3224. https://doi.org/10.1007/s13197-016-2296-7

Wang, Y., Gan, J., Li, Y., Nirasawa, S., Cheng, Y., 2019. Conformation and emulsifying properties of deamidated wheat gluten-maltodextrin/citrus pectin conjugates and their abilities to stabilize β-carotene emulsions. Food Hydrocoll. 87, 129–141. https://doi.org/https://doi.org/10.1016/j.foodhyd.2018.07.050

Wang, Z., Zhang, Z., Li, S., Zhang, X., Xia, M., Xia, T., Wang, M., 2021. Formation mechanisms and characterisation of the typical polymers in melanoidins from vinegar, coffee and model experiments. Food Chem. 355, 129444. https://doi.org/10.1016/j.foodchem.2021.129444

Waraho, T., Mcclements, D.J., Decker, E.A., 2011. Mechanisms of lipid oxidation in food dispersions. Trends Food Sci. Technol. 22, 3–13. https://doi.org/10.1016/j.tifs.2010.11.003

Wefers, D., Bindereif, B., Karbstein, H.P., Van Der Schaaf, U.S., 2018. Whey protein-pectin conjugates: Linking the improved emulsifying properties to molecular and physico-chemical characteristics. Food Hydrocoll. 85, 257–266. https://doi.org/10.1016/j.foodhyd.2018.06.030

Wei, F., Tanokura, M., 2015. Chemical changes in the components of coffee beans during roasting, coffee in health and disease prevention. Elsevier Inc. https://doi.org/10.1016/B978-0-12-409517-5.00010-3

Weng, J., Qi, J., Yin, S., Wang, J., Guo, J., Feng, J., Liu, Q., Zhu, J., Yang, X., 2016. Fractionation and characterization of soy β-conglycinin-dextran conjugates via macromolecular crowding environment and dry heating. Food Chem. 196. https://doi.org/10.1016/j.foodchem.2015.10.072

Wijewickreme, A.N., Kitts, D.D., 1997. Influence of reaction conditions on the oxidative behavior of model Maillard reaction products. J. Agric. Food Chem. 45, 4571–4576. https://doi.org/10.1021/jf970040v

Wong, B.T., Day, L., Augustin, M.A., 2011. Deamidated wheat protein-dextran Maillard conjugates: Effect of size and location of polysaccharide conjugated on steric stabilization of emulsions at acidic pH. Food Hydrocoll. 25, 1424–1432. https://doi.org/10.1016/j.foodhyd.2011.01.017

Wooster, T.J., Augustin, M.A., 2007. The emulsion flocculation stability of protein-carbohydrate diblock copolymers. J. Colloid Interface Sci. 313, 665–675. https://doi.org/10.1016/j.jcis.2007.04.054

Wooster, T.J., Augustin, M.A., 2006. β-Lactoglobulin–dextran Maillard conjugates: Their effect on interfacial thickness and emulsion stability. J. Colloid Interface Sci. 303, 564–572. https://doi.org/https://doi.org/10.1016/j.jcis.2006.07.081

Wu, Y., Cui, W., Eskin, N.A.M., Goff, H.D., 2009. An investigation of four commercial galactomannans on their emulsion and rheological properties. Food Res. Int. 42, 1141–1146. https://doi.org/10.1016/j.foodres.2009.05.015

Xiao, J., Li, C., Huang, Q., 2015. Kafirin nanoparticle-stabilized Pickering emulsions as oral delivery vehicles: physicochemical stability and in vitro digestion profile. J. Agric. Food Chem. 63, 10263–10270. https://doi.org/10.1021/acs.jafc.5b04385

Xu, D., Wang, X., Jiang, J., Yuan, F., Gao, Y., 2012. Impact of whey protein - Beet pectin conjugation on the physicochemical stability of β-carotene emulsions. Food Hydrocoll. 28, 258–266. https://doi.org/10.1016/j.foodhyd.2012.01.002

Xu, D., Yuan, F., Gao, Y., McClements, D.J., Decker, E.A., 2013. Influence of pH, metal chelator, free radical scavenger and interfacial characteristics on the oxidative stability of β-carotene in conjugated whey protein-pectin stabilised emulsion. Food Chem. 139, 1098–1104. https://doi.org/10.1016/j.foodchem.2013.02.027

Xu, K., Yao, P., 2009. Stable oil-in-water emulsions prepared from soy protein-dextran conjugates. Langmuir 25, 9714–9720. https://doi.org/10.1021/la900960g

Xu, M., Jin, Z., Peckrul, A., Chen, B., 2018. Pulse seed germination improves antioxidative activity of phenolic compounds in stripped soybean oil-in-water emulsions. Food Chem. 250, 140–147. https://doi.org/10.1016/j.foodchem.2018.01.049

Xu, Q., Tao, W., Ao, Z., 2007. Antioxidant activity of vinegar melanoidins. Food Chem. 102, 841–849. https://doi.org/10.1016/j.foodchem.2006.06.013

Yadav, M.P., Parris, N., Johnston, D.B., Onwulata, C.I., Hicks, K.B., 2010. Corn fiber gum and milk protein conjugates with improved emulsion stability. Carbohydr. Polym. 81, 476–483. https://doi.org/10.1016/j.carbpol.2010.03.003

Yamamoto, Y., Kato, E., Ando, A., 1996. Increased antioxidative activity of ovalbumin by heat treating in an emulsion of linoleic acid. Biosci. Biotechnol. Biochem. 60, 1430–1433. https://doi.org/10.1271/bbb.60.1430

Yanagimoto, K., Ochi, H., Lee, K.G., Shibamoto, T., 2004. Antioxidative activities of fractions obtained from brewed coffee. J. Agric. Food Chem. 52, 592–596. https://doi.org/10.1021/jf030317t

Yang, Y., Cui, S., Gong, J., Miller, S.S., Wang, Q., Hua, Y., 2015a. Stability of citral in oil-in-water emulsions protected by a soy protein–polysaccharide Maillard reaction product. Food Res. Int. 69, 357–363. https://doi.org/10.1016/j.foodres.2015.01.006

Yang, Y., Cui, S.W., Gong, J., Guo, Q., Wang, Q., Hua, Y., 2015b. A soy protein-polysaccharides Maillard reaction product enhanced the physical stability of oil-in-water emulsions containing citral. Food Hydrocoll. 48, 155–164. https://doi.org/10.1016/j.foodhyd.2015.02.004

Yaylayan, V.A., 2003. Recent advances in the chemistry of strecker degradation and amadori rearrangement: Implications to aroma and color formation. Food Sci. Technol. Res. 9, 1–6. https://doi.org/10.3136/fstr.9.1

Yaylayan, V.A., Keyhani, A., 2000. Origin of carbohydrate degradation products in L-alanine/D- [13C]glucose model systems. J. Agric. Food Chem. 48, 2415–2419. https://doi.org/10.1021/jf000004n

Ye, F., Miao, M., Cui, S.W., Jiang, B., Jin, Z., Li, X., 2016. Characterisations of oil-in-water Pickering emulsion stabilized hydrophobic phytoglycogen nanoparticles. Food Hydrocoll. 76, 78–87. https://doi.org/10.1016/j.foodhyd.2017.05.003

Yen, G. -C, Hsieh, P. -P, 1995. Antioxidative activity and scavenging effects on active oxygen of xylose-lysine maillard reaction products. J. Sci. Food Agric. 67, 415–420. https://doi.org/10.1002/jsfa.2740670320

Yi, J., Liu, Y., Zhang, Y., Gao, L., 2018. Fabrication of resveratrol-loaded whey protein–dextran colloidal complex for the stabilization and delivery of β-carotene emulsions. J. Agric. Food Chem. 66, 9481–9489. https://doi.org/10.1021/acs.jafc.8b02973

Yin, B., Wang, C., Liu, Z., Yao, P., 2017. Peptide-polysaccharide conjugates with adjustable hydrophilicity / hydrophobicity as green and pH sensitive emulsifiers. Food Hydrocoll. 63, 120–129. https://doi.org/10.1016/j.foodhyd.2016.08.028

Yu, J., Wang, G., Wang, Xibo, Xu, Y., Chen, S., Wang, Xiaodan, Jiang, L., 2018. Improving the freeze-thaw stability of soy protein emulsions via combing limited hydrolysis and Maillard-induced glycation. LWT - Food Sci. Technol. 91, 63–69. https://doi.org/10.1016/j.lwt.2018.01.031

Zha, F., Dong, S., Rao, J., Chen, B., 2019a. Pea protein isolate-gum Arabic Maillard conjugates improves physical and oxidative stability of oil-in-water emulsions. Food Chem. 285, 130–138. https://doi.org/10.1016/j.foodchem.2019.01.151

Zha, F., Yang, Z., Rao, J., Chen, B., 2019b. Gum arabic-mediated synthesis of glyco-pea protein hydrolysate via Maillard reaction improves solubility, flavor profile, and functionality of plant protein. J. Agric. Food Chem. 67, 10195–10206. https://doi.org/10.1021/acs.jafc.9b04099

Zhai, J., Hoffmann, S. V, Day, L., Lee, T.-H., Augustin, M.A., Aguilar, M.-I., Wooster, T.J.W., 2012. Conformational changes of α-lactalbumin adsorbed at oil–water interfaces: Interplay between protein structure and emulsion stability. Langmuir 28, 2357–2367.

Zhai, J., Wooster, T.J., Hoffmann, S. V., Lee, T.H., Augustin, M.A., Aguilar, M.I., 2011. Structural rearrangement of β-lactoglobulin at different oil-water interfaces and its effect on emulsion stability. Langmuir 27, 9227–9236. https://doi.org/10.1021/la201483y

Zhang, B., Guo, X., Zhu, K., Peng, W., Zhou, H., 2015. Improvement of emulsifying properties of oat protein isolate – dextran conjugates by glycation. Carbohydr. Polym. 127, 168–175. https://doi.org/10.1016/j.carbpol.2015.03.072

Zhang, H., Zhang, Hui, Troise, A.D., Fogliano, V., 2019. Melanoidins from coffee, cocoa, and bread are able to scavenge α-dicarbonyl compounds under simulated physiological conditions. J. Agric. Food Chem. 67, 10921–10929. https://doi.org/10.1021/acs.jafc.9b03744

Zhang, J., Wu, N., Lan, T., Yang, X., 2013. Improvement in emulsifying properties of soy protein isolate by conjugation with maltodextrin using high-temperature, short-time dry-heating Maillard reaction. Int. J. Food Sci. Technol. 49, 460–467. https://doi.org/10.1111/ijfs.12323

Zhang, J.B., Wu, N.N., Yang, X.Q., He, X.T., Wang, L.J., 2012. Improvement of emulsifying properties of Maillard reaction products from β-conglycinin and dextran using controlled enzymatic hydrolysis. Food Hydrocoll. https://doi.org/10.1016/j.foodhyd.2012.01.006

Zhang, N., Li, Y., Wen, S., Sun, Y., Chen, J., Gao, Y., Sagymbek, A., Yu, X., 2021. Analytical methods for determining the peroxide value of edible oils: A mini-review. Food Chem. 358, 129834. https://doi.org/10.1016/j.foodchem.2021.129834

Zhang, Q., Li, L., Lan, Q., Li, M., Wu, D., Chen, H., Liu, Y., Lin, D., Qin, W., Zhang, Z., Liu, J., Yang, W., 2019. Protein glycosylation: A promising way to modify the functional properties and extend the application in food system. Crit. Rev. Food Sci. Nutr. 59, 2506–2533. https://doi.org/10.1080/10408398.2018.1507995

Zhang, S., Hsieh, F.H., Vardhanabhuti, B., 2014. Acid-induced gelation properties of heated whey protein-pectin soluble complex (Part I): Effect of initial pH. Food Hydrocoll. 36, 76–84. https://doi.org/10.1016/j.foodhyd.2013.07.029

Zhang, W., Ray, C., Poojary, M.M., Jansson, T., Olsen, K., Lund, M.N., 2019. Inhibition of Maillard reactions by replacing galactose with galacto-oligosaccharides in casein model systems. J. Agric. Food Chem. 67, 875–886. https://doi.org/10.1021/acs.jafc.8b05565

Zhang, Y., Tan, C., Abbas, S., Eric, K., Zhang, X., Xia, S., Jia, C., 2014. The effect of soy protein structural modification on emulsion properties and oxidative stability of fish oil microcapsules. Colloids Surfaces B Biointerfaces 120, 63–70. https://doi.org/10.1016/j.colsurfb.2014.05.006

Zhang, Z., Wang, X., Yu, J., Chen, S., Ge, H., Jiang, L., 2017. Freeze-thaw stability of oil-in-water emulsions stabilized by soy protein isolate-dextran conjugates. LWT - Food Sci. Technol. 78, 241–249. https://doi.org/10.1016/j.lwt.2016.12.051

S

Summary

Summary

Oil-in-water (O/W) emulsions, where oil droplets are dispersed in an aqueous phase, often experience various physical and chemical destabilization phenomena, which compromise the quality and shelf life of the final products. To achieve acceptable shelf life, emulsifiers (e.g., surfactants and animal proteins) and synthetic antioxidants (e.g., ethylenediaminetetraacetic acid and butylated hydroxyanisole) are currently used.

However, over the past decade, sustainable and natural food ingredients have become preferred options. This has been a strong incentive for the present work, which has aimed at identifying the potential of biobased Maillard reaction products (MRPs) to both physically and chemically stabilize emulsions. With this aim, in **Chapter 2**, we provided an overview of existing literature on the interfacial and antioxidant properties of MRPs. On the basis of this, we hypothesized that preparing MRPs in model systems and extracting MRPs from food products would be two feasible routes to study their dual-function properties.

Chapters 3 and 4 were designed to study the MRPs prepared in model systems. In **Chapter 3**, we characterized the chemical and structural features of various Maillard reaction fractions prepared from soy protein isolate (SPI) and carbohydrates (dextran or glucose). The free amino group content as measured with o-phthalaldehyde (OPA) method was modulated by both protein glycation and conformational changes. Thus, other Maillard reaction (MR) markers were used. Conjugation of soy proteins with glucose led to more furosine, Nε-(carboxymethyl)-L-lysine, Nε-(carboxyethyl)-L-lysine, and protein-bound carbonyl formation, which indicates that the Maillard reaction progressed further with glucose than dextran. The surface activity was found to be related to the surface hydrophobicity, with SPI-dextran conjugates showing higher activity than SPI-glucose conjugates, and water-soluble fractions showing higher activity than insoluble fractions. Based on this analysis, a comprehensive understanding of the physicochemical properties in each fraction could be obtained.

In **Chapter 4**, we further assessed the ability of initial stage MRPs (SPI-dextran conjugates) to prevent lipid oxidation, when added to the continuous phase of pre-formed stock emulsions. As controls, whey protein isolate (WPI), SPI, or unreacted SPI/dextran mixture were also added to the stock emulsions. The addition of these protein-based compounds increased the oxidative stability of emulsions without significantly affecting the physical stability of emulsions. The antioxidant capacity in emulsions was, starting from the highest: glycated soy proteins $\approx$ SPI/dextran mixture > SPI > WPI. This implies that the presence of soy proteins and dextran had in itself a protective effect. The findings from this chapter show that it is possible to engineer oxidatively stable emulsions by adding protein-based compounds in the continuous phase, which could therefore reduce the need for synthetic antioxidants.

Chapters 5 and 6 were designed to study MRPs extracted from food (dark roasted coffee). **Chapter 5** aimed to explore the potential of melanoidins (high molecular weight fractions of the coffee brew) to physically stabilize emulsions. Therefore, coffee melanoidin were used to prepare emulsions that have a light brown, opaque, and homogeneous appearance with a nearly monomodal size distribution. Upon storage at room temperature for 28 days, emulsions with low (0.25-1 wt.%) melanoidin concentrations were subject to physical destabilization (including creaming, flocculation, and coalescence); emulsions with high (4 wt.%) melanoidin concentration gradually transformed from a liquid-like state to a gel-like structure; emulsions with 2 wt.% melanoidins remained liquid-like and were the most physically stable. It was shown by confocal laser scanning microscopy, polarized light microscopy, and surface load determination that the polysaccharide-rich fractions from the melanoidins were present at the interface. This study shows the promising potential of coffee melanoidins as sustainable physical stabilizers of emulsions.

In **Chapter 6**, we investigated the dual functionality (i.e., the ability to act both as emulsion stabilizers and antioxidants) of coffee melanoidin fractions with different molecular weights. When used as emulsifiers, coffee brew and (non-defatted) high molecular weight fraction (HMWF) of coffee brew were able to form emulsions that are both physically and oxidatively

stable. When added to the continuous phase of the stock WPI-stabilized emulsions, all coffee fractions (coffee brew, its HMWF and low molecular weight fraction (LMWF)) were able to slow down lipid oxidation considerably without significantly changing the physical stability of the stock emulsions. However, HMWFs were more effective in retarding lipid oxidation than coffee brew and LMWF, which might be the overall result of various effects, including the partitioning of antioxidant components in the emulsions, free and bound phenolic compounds, and synergism or antagonism of antioxidants. This chapter shows that coffee ingredients can serve as dual-functional stabilizers in emulsions.

Finally, in **Chapter 7**, we discussed the main findings of this thesis and proposed a multiscale approach (consisting of molecular, microscopic, and macroscopic scale) to achieve the design of food emulsions from first principles, which includes “bottom-up” and “top-down” schemes.

Appendices

Acknowledgements

About the author

List of publications

Overview of completed training activities

Acknowledgements

Finally, my PhD journey has almost reached an end. This journey would not have been possible without the invaluable support from so many outstanding people.

First and foremost, I would like to express my gratitude to my supervisors: Vincenzo, Karin, and Claire. Vincenzo, I still remember the moment you responded to my first email within a few minutes where you showed your dedication to work; the moment you drew some emoji faces on the notebook to express your thoughts during our first meeting where you showed your sense of humor. Thank you for your scientific advice and guidance, humorous conversation, and for encouraging me to think out of the box. Karin, I am so lucky that you could be part of my supervisor team after the first year. Even though your schedule is always full, you always join our weekly meetings, respond promptly to my emails, and keep me on track. I am grateful for your diligence, commitment, and humor, which really helped me a lot, especially during tough times. Claire, I am really happy that you could be my supervisor. You can easily get my points when I express my thoughts in a vague way; you always shared interesting articles with me; you can always find out some overlooked mistakes in the manuscripts. I have learned a lot from your kindness, dedication to work, ways of thinking, and experimental design. Thank you!

I would also like to thank the people that I have collaborated with. Burçe, thank you for the collaboration in the glycated soy protein papers. I am grateful that you shared your laboratory experience and your knowledge with me. You always have a big smile on your face and I really enjoyed working with you. Julia, many thanks for your help with the FTIR measurement and analysis. Sylvain and Agnès, thank you for the collaboration in the coffee melanoidin papers. Sylvain, you are so kind and knowledgeable that you explained knowledge about phenolic compounds from basic. Agnès, you are so kind to perform the phenolic compound analysis for samples even though you were very busy. It is a pity that I could not visit INRAE due to the Corona situation. Hope we can meet in person in the future.

I am particularly grateful for the assistance and support from the technicians and secretaries at FQD and FPE. Erik, thank you for your prompt technical support and your help with the CLSM analysis. Frans, Maurice, Jos, and Wouter, thank you for your instructions on different devices and assistance with some analysis. Geert, thank you for assisting me with the LC-MS and GC-MS analysis. Xandra, thank you for ordering chemicals for me. Kim, Corine, Ilona, and Marjan, thank you for dealing with administrative work that makes my life much easier.

I would like to acknowledge all my MSc and BSc students: Praksha, Pelle, Tasha, Berdet, Xiaojia, Tania, Yikfee, and Hadi. Thank you for your efforts and contributions to this project.

To my colleagues and friends at FQD and FPE, it is nice to get to know you; I have really enjoyed the time here. Anja, Emma, Katharina, Sten, and Alime, thank you for sharing your interests in emulsions and helping me a lot in the labs. Patrícia, thank you for sharing your knowledge about protein oxidation and being my lab buddy at weekends. Edoardo, thank you for the useful suggestions for analyzing results. Thank you also to Alim, Ana, Annelies, Fabiola, Ita, Kasper, Matthijs, Mohammad, Mostafa, Pieter, Sirinan, Teresa for all the nice conversation. I would also like to thank my Chinese friends in Wageningen. 王荔 (三弟)，邢沁洽(奶奶)，颜静(静姐)，感谢在那段艰难的日子里互相鼓励与支持。张浩(二弟)和陈琳天翔(四弟)，感谢你们的美食，一起聚餐唱 K 吹牛的日子太美好了。陈瑶，感谢我们一起在实验室看综艺，一起去旅行。邓博心，感谢你跟我一起讨论我们的生活与未来，感谢你愿意当我的门神。于宏威和方亮，我们的冰岛之旅很难忘呢！阚丽娇，王之珺，熊玲，郭兵兵，张春月，刘要卫，刘嘉宁，呼延宗尧，黄展，杨飞龙，解雅晶，韩晴，唐佳颖，彭郁，邓若璇，贾婉青，张露，朱思聪，邓磊，曾哲，蔡慧芳，夏文杰，程喆，纪磊，周锡龙，吕治宏和刘萧，很庆幸能在异国他乡与你们相识，你们的陪伴让这段漫长的旅程变得丰富多彩！

Twan, bedankt dat je altijd bij me bent. Ik ben dankbaar voor je liefde, begrip, aanmoediging en onvoorwaardelijke steun. Ik wens je heel veel succes in de toekomst!

Last but not the least, I would like to thank my family. 感谢爸爸妈妈和妹妹，始终作为我坚强的后盾，给予我无尽的关心与支持，你们永远是我内心温暖的港湾！

- 冯纪璐 (Jilu Feng) 26-01-2022 Wageningen

About the author

Jilu Feng was born on 8 May 1992 in Guangzhou, China. In 2010, she started her study of Food Science and Technology at South China University of Technology and obtained her bachelor degree in 2014. In the same year, Jilu continued her master program at the Engineering Research Center of Starch and Vegetable Protein Processing Ministry of Education at South China University of Technology, under the supervision of Prof. Junru Qi. For her master thesis, she focused on the fabrication and characterization of soy protein-dextran nanogels prepared via the Maillard reaction and self-assembly approach. In 2018, Jilu continued working as a PhD candidate at the Laboratory of Food Quality and Design group and the Laboratory of Food Process Engineering group at Wageningen University and Research. During this research, she worked on using Maillard reaction products to stabilize food emulsions, and the results of this research are described in this thesis.

Contact: jilu.feng@outlook.com

List of publications

This thesis

Feng, J., Berton-Carabin, C. C., Fogliano, V., & Schroën, K. (2022). Maillard reaction products as functional components in oil-in-water emulsions: A review highlighting interfacial and antioxidant properties. *Trends in Food Science & Technology*, 121, 129–141. DOI: 10.1016/j.tifs.2022.02.008

Feng, J., Berton-Carabin, C. C., Ataç Mogol, B., Schroën, K., & Fogliano, V. (2021). Glycation of soy proteins leads to a range of fractions with various supramolecular assemblies and surface activities. *Food Chemistry*, 343, 128556. DOI: 10.1016/j.foodchem.2020.128556

Feng, J., Schroën, K., Fogliano, V., & Berton-Carabin, C. (2021). Antioxidant potential of non-modified and glycated soy proteins in the continuous phase of oil-in-water emulsions. *Food Hydrocolloids*, 114, 106564. DOI: 10.1016/j.foodhyd.2020.106564

Feng, J., Berton-Carabin, C. C., Guyot, S., Gacel, A., Fogliano, V., & Schroën, K. Coffee melanoidins as emulsion stabilizers. *In preparation.*

Feng, J., Schroën, K., Guyot, S., Gacel, A., Fogliano, V., & Berton-Carabin, C. C. Physical and oxidative stabilization of oil-in-water emulsions by roasted coffee fractions: Interface- and continuous phase-related effects. *In preparation.*

Other work

Feng, J.-L., Qi, J.-R., Yin, S.-W., Wang, J.-M., Guo, J., Weng, J.-Y., Liu, Q.-R., & Yang, X.-Q. (2015). Fabrication and characterization of stable soy β-conglycinin-dextran core-shell nanogels prepared via a self-assembly approach at the isoelectric point. *Journal of Agricultural and Food Chemistry*, 63(26). DOI: 10.1021/acs.jafc.5b01778

Feng, J., Qi, J., & Liu, Q. (2016). Fabrication of soy protein isolate-soluble soy polysaccharide core-shell nanogels via Maillard reaction and self-assembly. *Gaodeng Xuexiao Huaxue Xuebao/Chemical Journal of Chinese Universities*, 37(11). DOI: 10.7503/cjcu20160364

Feng, J., Qi, J., Weng, J., Liu, Q., Cao, J., & Cheng, M. (2016). Preparation and characterization of soy β-conglycinin-dextran nanogels based on Maillard reaction. *Huagong Xuebao/CIESC Journal*, 67(9). DOI: 10.11949/j.issn.0438-1157.20160046

Liu, X., **Feng, J.**, & Tao, Y. (2021). Application of Industry 5.0 on Fruit and Vegetables Processing. In *The Prospect of Industry 5.0 in Biomanufacturing* (pp. 211-228). CRC Press.

Cheng, M., Qi, J.-R., **Feng, J.-L.**, Cao, J., Wang, J.-M., & Yang, X.-Q. (2018). Pea soluble polysaccharides obtained from two enzyme-assisted extraction methods and their application as acidified milk drinks stabilizers. *Food Research International*, 109. DOI: 10.1016/j.foodres.2018.04.056

Liu, Q.-R., Qi, J.-R., Yin, S.-W., Wang, J.-M., Guo, J., **Feng, J.-L.**, Cheng, M., Cao, J., & Yang, X.-Q. (2017). Preparation and stabilizing behavior of octenyl succinic esters of soybean soluble polysaccharide in acidified milk beverages. *Food Hydrocolloids*, 63. DOI: 10.1016/j.foodhyd.2016.09.020

Liu, Q.-R., Qi, J.-R., Yin, S.-W., Wang, J.-M., Guo, J., **Feng, J.-L.**, Cheng, M., Cao, J., Weng, J.-Y., & Yang, X.-Q. (2016). The influence of heat treatment on acid-tolerant emulsions prepared from acid soluble soy protein and soy soluble polysaccharide complexes. *Food Research International*, 89. DOI: 10.1016/j.foodres.2016.07.001

Weng, J., Qi, J., Yin, S., Wang, J., Guo, J., **Feng, J.**, Liu, Q., Zhu, J., & Yang, X. (2016). Fractionation and characterization of soy β-conglycinin-dextran conjugates via macromolecular crowding environment and dry heating. *Food Chemistry*, 196. DOI: 10.1016/j.foodchem.2015.10.072

Overview of completed training activities

Discipline specific activities

Courses

Sensory Perception & Food Preference: The role of context	VLAG, Wageningen, NL	2018
Reaction kinetics in food science	VLAG, Wageningen, NL	2018
Summer Course Glycosciences	VLAG, Wageningen, NL	2018
Food proteins: functionality, modifications and analysis	VLAG, Wageningen, NL	2018
Chemometrics (Multivariate Statistics)	VLAG, Wageningen, NL	2019
VLAG Online Lectures	VLAG, Wageningen, NL	2020
Healthy Food Design	VLAG, Wageningen, NL	2021

Conferences

3rd Young AGErs Symposium	Wageningen, NL	2018
Edible soft matter	Le Mans, FR	2019
2nd Food Chemistry conference[a]	Seville, ES	2019
33rd EFFoST conference[b]	Rotterdam, NL	2019
15th Plant-Based Foods & Proteins Summit North America	Online	2020
2020 AOCS Annual Meeting & Expo	Online	2020
95th ACS colloid and surface science symposium	Online	2021
4th Food structure and functionality symposium[a]	Online	2021

General courses

Scientific Artwork – Vector graphics and images	WUR library, Wageningen, NL	2018
Infographics and Iconography	WUR library, Wageningen, NL	2018
Introduction to R	VLAG, Wageningen, NL	2018
PhD Workshop Carousel	WGS, Wageningen, NL	2018
Applied statistics	VLAG, Wageningen, NL	2018
Adobe InDesign Essential Training	WUR library, Wageningen, NL	2018
VLAG PhD week	VLAG, Baarlo, NL	2018
Scientific Writing	Wageningen in'to Languages, Wageningen, NL	2019

Optional courses and activities FPE

Preparation of research proposal	Wageningen, NL	2018
Group meetings on project progress and colloquia	Wageningen, NL	2018-2021
Micro team meetings	Wageningen, NL	2021

[a] Poster presentation; [b] Oral presentation.

VLAG: Advanced Studies in Food Technology, Agrobiotechnology, Nutrition and Health Sciences; WGS: Wageningen Graduate Schools; WUR: Wageningen University & Research.

NL: the Netherlands; FR: France; ES: Spain.

The research described in this thesis was financially supported by the Chinese Scholarship Council.

Financial support from Wageningen University for printing this thesis is gratefully acknowledged.

Cover design by Ron Zijlmans and Jilu Feng

Printed by ProefschriftMaken.nl